1. INTRODUCTION

1.1 Background

There are different processes, interactions and activities that affect the climate on Earth, such as external processes (e.g. variability in solar output, earth's rotation around the sun, volcanic activity), ocean-atmosphere processes (e.g. the El Niño-Southern Oscillation), human activities (e.g. deforestation, atmospheric pollution) and climatic fluctuations (inter-annual variability) (Maidment, 1992; WMO/UNESCO, 1997). The major energy source of the Earth is solar radiation and this energy plays an important role in the global hydrological cycle on Earth. About 25 to 75% of the solar radiation that reaches the Earth (343 Watt/m^2) is absorbed by land, open fresh surface water resources and oceans. This part of the solar energy causes evaporation of open waters and evapotranspiration from plants, which finally affects the water balance of water resources systems on the Earth's surface. The rest is absorbed, scattered and reflected by greenhouses gases, aerosols and clouds. A schematic of the Earth-Atmospheric system is shown in Figure 1.1.

The atmosphere is for more than 98% composed of nitrogen (N_2) and oxygen (O_2), followed by clouds, greenhouse gases and aerosols. Some greenhouse gases are water vapour (H_2O), carbon dioxide (CO_2), methane (CH_4), ozone (O_3), nitrous oxide (N_2O), halocarbons (CFC's) and some aerosols are ozone and sulphate. Only the greenhouse gases hold the heat between the Earth's surface and the troposphere (about 0-10 km above Earth's surface) and cause heating of the atmosphere ("greenhouse effect"). In this way, the average temperature of the atmosphere is kept around -19^oC and the average Earth's mean surface temperature is kept around 14^oC.

In the last 100 years, the amount of greenhouse gas emissions into the atmosphere has drastically increased, compared to the removal from the atmosphere. Water vapour is responsible for about 36-70% of the greenhouse effect, followed by carbon dioxide. As water vapour can not directly be influenced by anthropogenic emissions of water vapour and this increase can also not have been caused by respiration of vegetation and forest, and ocean-atmosphere exchange, it is believed that the large CO_2 emissions come from burning of fossil fuels (57%) (e.g. coal, fuel oil or natural gas), and mineral and metal production (e.g. cement, iron, steel), followed by land use changes and forestry (19%) (e.g. expansion of agriculture and deforestation). Figure 1.2 shows the greenhouse gas emissions in year 2000.

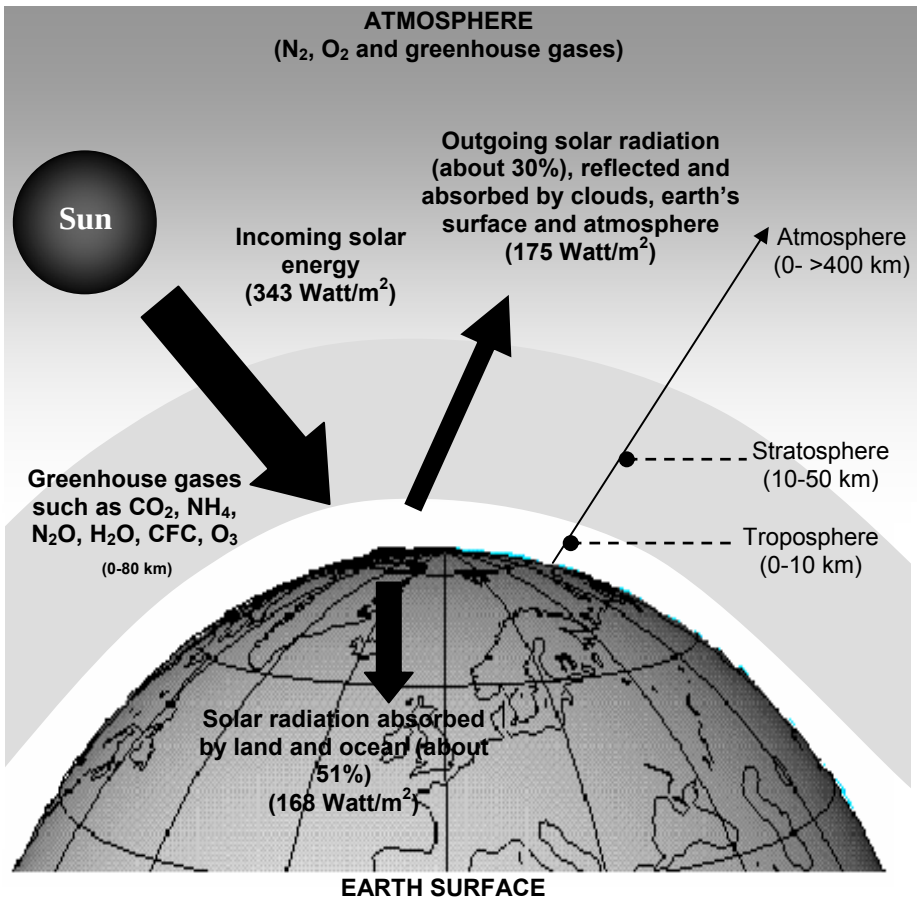

Figure 1.1: Simplified Earth-Atmospheric climate system.

Emissions of methane (14%) come from fossil fuels, domestic and animal waste, biomass burning and rice cultivation, emissions of nitrous oxide (9%) come from fertilizers in agriculture, cattle feed lots, chemical industries and biomass burning, and chlorine and bromine sources gas (CFCs, HFC's) emissions come from refrigeration systems, fire suppression systems and manufacturing processes (NEAA, 2007). Warming of ocean water may also cause high CO_2 emissions, especially during El Niño evens, as it causes little terrestrial uptake of CO_2.

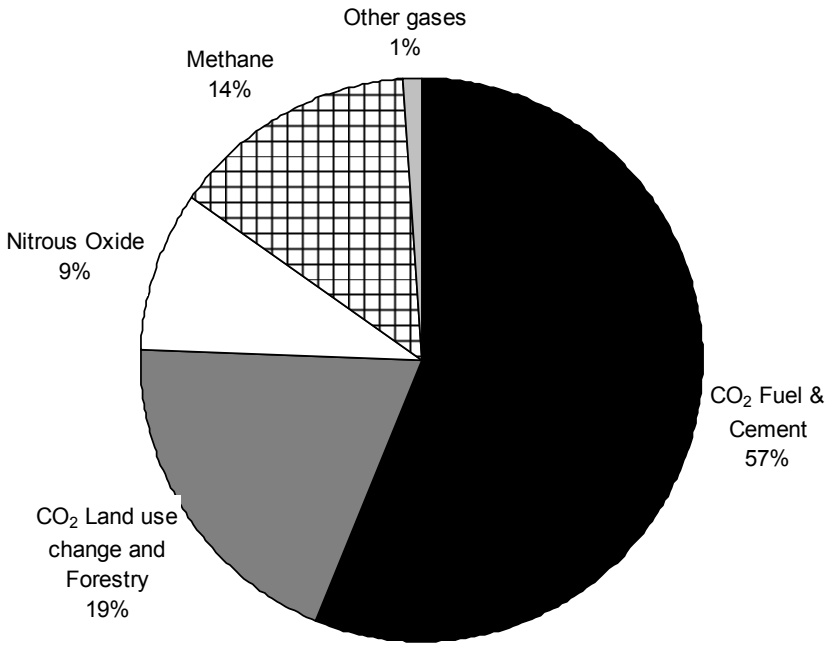

Figure 1.2: Greenhouse gas CO_2 equivalent emissions in year 2000 (Retrieved March 26, 2007 from www.epa.gov/climatechange/emissions/).

Table 1.1 shows the estimated world values for greenhouse gas emissions for two periods: 1750/1800 and 2005. These values show indeed that the most important greenhouse gases, such as carbon dioxide, increased with 32% in 2005 since 1750/1800. The significant increase in greenhouse gases can be explained by the increased industrialization and increased human consumption of food due to population growth, especially since the 1970s. Figure 1.3 shows graphically the historical (1850/1950/1990, 2000) and projected values up to 2100 for the world population, land use (cropland and forest) and energy use (coal, oil, gas, nuclear, biomass and other renewable energy). This figure shows that since 1950, the world's population has increased from 2,522 million to 6,143 million in 2000 (144%) and fossil fuel use consumption has increased from 21 ExaJoule to 130 ExaJoule in 2000 (520%). During the same period, the world cement production increased from 132,992 kilo tons to 1,443,691 kilo tons (about 1000%) and livestock increased from $2,256,485.10^3$ to $4,309,525.10^3$ in 2000 (91%) (NEAA, 2007).

Table 1.1: Estimated world values of some major greenhouse gases concentrations for the years 1750/1800 and 1998/2005 (McMichael, 1996; IPCC, 2001; Maidment, 1992).

Concentration	Carbon dioxide (CO_2) (ppbv) **)	Methane (CH_4) (ppbv)	Nitrous oxide (N_2O) (ppbv)	Halo-carbons (CFC-11) (ppbv)	Perfluoro-methane (CF_4) (ppbv)
Year 1750/1800	0.280	770	270	0	40,000
Year 1998	-	-	-	268,000	80,000
Year 2005	0.379	1,774	319	-	-
(% increase)	(32%)	(130%)	(18%)	-	(50%)
Atmospheric lifetime (years) *)	50-450	12	120	45,000	50,000
Factor (times CO_2 concentration)	1	0.05	0.003	0.000123	-

*) Lifetime (L) refers to how long it takes to restore the atmosphere system to equilibrium caused by a small increase of the gas in the atmosphere

**) X ppbv = X molecules of a greenhouse gas per billion (10^9) molecules of dry air (volume)

It has also been reported that between 1960 and 2005, about 10% of the world's tropical rainforest was destroyed (Retrieved March 26, 2007 from http://en.wikipedia.org/wiki/Categorie:Climate_change and www.fao.org/forestry/). This tremendous increase in greenhouse gas emissions in the atmosphere has resulted in a warming trend of the global mean surface temperature on Earth (land and sea surface temperature). This trend is shown in Figure 1.4. The 10 warmest years appear to be between 1995 and 2005, with 2005 as the warmest year followed by 2002 and 1998 (IPCC, 2007). This figure shows that from 1900 to date, three periods may be distinguished in the global air temperature: a rise in the period 1910-1940 (rate of about 0.5^{o}C/30 years), a leveling off in the period 1940-1980 and a rise again from 1976 to date (rate of about 0.46^{o}C/25 years). Since 1970, the mean temperature has increased about 0.76^{o}C reference to 1850-1899. The "relative stable temperature" during 1940-1970 is believed to be caused by the cooling influence of sulphate aerosols emissions from fossil fuel combustion and volcanic eruptions, together with the natural climate variability and also the increase in glaciers (short ice age) (Meehl et al., 2004; Retrieved March 26, 2007 from http://en.wikipedia.org/wiki/Categorie:Climate_change).

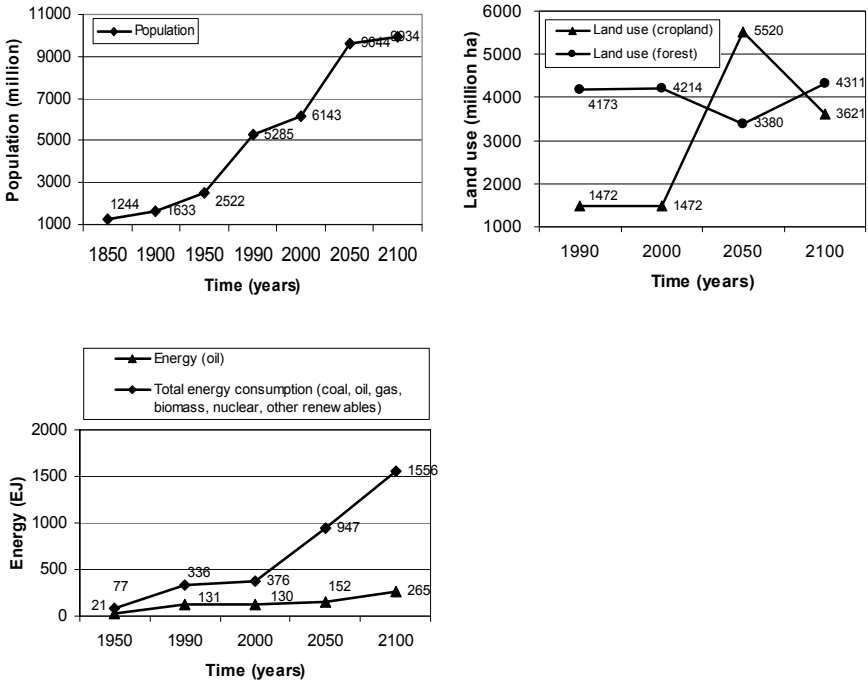

Figure 1.3: World values for population, land use and energy, using IPCC SRES Emissions Scenarios and based on the MINICAM model (Retrieved March 16, 2007 from www.sres.ciesin.org and www.mnp.nl/hyde/).

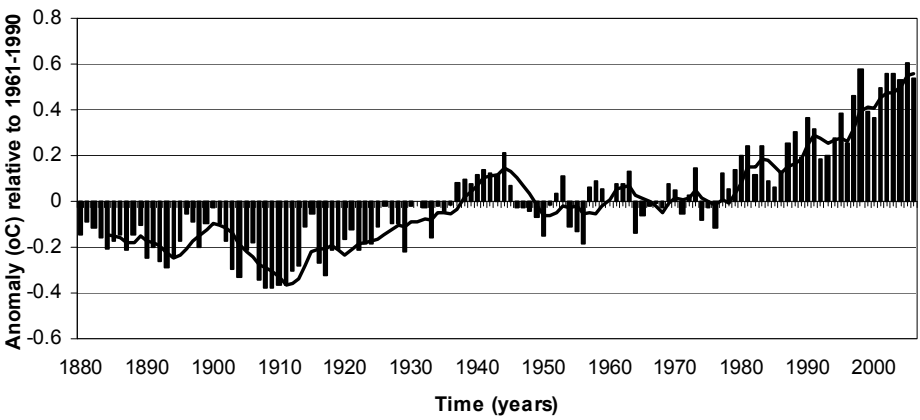

Figure 1.4: Global mean temperature over land and ocean from 1880-2006 (Retrieved March 27, 2007 from www.ncdc.noaa.gov/oa/climate/research/anomalies/anomalies.html).

This means that the increase in CO_2 should not always be related to the increase in temperature. The emitted gases absorb solar energy. It was shown that the eruption of mount Pinatubo in 1991 caused a decrease in the global temperature of about 0.5°C during that year. Most of the volcanic eruptions took place between 1880-1920 and 1960-1991.

The warming on Earth is however not equal. In the tropics (30°N-30°S) the temperature (1860-2000) increased with about 0.16°C, compared to 1961-1990, which is much lower than in the northern hemisphere (north of 30°) and the southern hemisphere (south of 30°), where the temperature increased with about 0.6°C and 0.2°C, respectively (WMO, 2001). This difference may be explained by the fact that most greenhouse gases are released in industrialized countries in the northern hemisphere and the significant ozone depletion trend over the Antarctica region and Arctic region since the 1980s. In the Guiana Shield region (0°-9°N, 54°-62°W), which Suriname is a part of, the annual average air temperature increased with 1°C (1900-2000) (IPCC, 2001; Watson et al., undated). In the eastern parts of Nord and South America, northern Europe and northern and central Asia, precipitation has increased, while in southern Africa, parts of southern Asia and the Sahel precipitation has decreased. In the tropics (30°N-30°S) an increase in precipitation of about 0.2% to 0.3% per 10 years is observed and in the Guiana Shield region, the average annual rainfall increased with about 2% (1900-1994) (IPCC, 2001).

The increase in the global mean surface temperature has also been accompanied by the rise of the mean sea level. The mean sea level has risen with about 10 to 15 cm since 1900. The changes in temperature and sea level including precipitation have already threatened human life on Earth, but also the environment, ecosystems, biodiversity, fresh water resources, agriculture, fisheries, forestry, human health and low-lying coastal lands (Dooge and Kuusisto, 1998; Hassel and Miller, 1999; McMichael A., et al., 1996). Besides the other sources, freshwater resources are the most vital for human life and economic needs (e.g. drinking water, irrigation water), but also for ecosystems. They are easily accessible from rivers, swamps and reservoirs. Freshwater is generally defined as water with a chloride concentration lower than 250 mg Cl^-/1 (Groen, 2002). However, only 2.5% of the total global water on Earth (about $1{,}386.10^6$ km^3) is freshwater and the rest (97.5%) is saltwater. From the freshwater amount, only 0.3% is found in rivers, reservoirs, and lakes. About 0.9% is found in swamp water, soil moisture and permafrost, 29.9 % is found in groundwater and the majority (68.9%) is found in glaciers and snow cover in the Antarctic, the Arctic and in the mountainous regions (Maidment, 1992). The distribution of freshwater on Earth is controlled by the hydrological cycle, which together with climate

processes, causes a non-uniform distribution of precipitation over the Earth's surface including fresh water.

In the recent decades, the changes in climate and precipitation have affected the world's freshwater resources and availability, either by floods or droughts (Keeling and Whorf, 2004; Mastny, 2000; Tamara et al., 1999; WMO/UNESCO, 1997). Floods or droughts are known to cause significant negative economic, environmental, and social impacts. Since 1960 the number of flood events have increased worldwide from about 10 to more than 225 per year due to intense rainy seasons, stronger storms and shifts in rainfall. Since the mid-1970s, droughts have been increasing. They are also widespread such as in tropical Asia, Africa, Middle Eastern, Central America and the Caribbean, due to reduced precipitation and changes in wind patterns accompanied by the El Niño events (Retrieved April 16, 2007 from www.em-dat.net). Freshwater resources for drinking water supply and food production are already becoming scarce in North and East Africa, and the Middle East, and might, besides population growth, excessive use of freshwater resources, saltwater intrusion in coastal groundwater aquifers, pollution from waste, changes in land use, lack of capital, awareness and technology, also be enhanced by future changes in the Earth's climate (Retrieved, June 15, 2005 from http://www.itt.com/waterbook/scarcity.asp). The number of hurricanes in the Atlantic ocean (with wind speeds above 56 m/s) has also increased between 1980 and 1990, and well up to 35%, due to the increase in sea surface temperatures (SSTs). A recent example is hurricane Katrina (2005), which was the 6^{th} strongest Atlantic hurricane up to now (highest SST recorded in Atlantic ocean) and which caused enormous floods and other economic damages in the Bahamas, Cuba and Gulf coast of the United States of America (New Orleans). The estimated damage in this area was about US$ 84.10^6.

Besides the long term changes in global climate, the global atmospheric circulation processes such as the El Niño-Southern Oscillation, the Tropical Atlantic Variability, the north Atlantic Oscillation and the Pacific Oscillation are also responsible for large anomalies in the Earth's climate (Berlage, 1957; Giannini et al., 2000; Marshall et al., 2001; Martis et al., 2002; Rajagopolan et al., 1997; Robertson and Mechoso, 2002; Villwock, 1998; Wang, 2001, 2005). These anomalies are mainly influenced by the sea surface temperature and may result in extremely high and longer rainfall than normal (causing floods) or in extremely low or no rainfall during longer periods than normal (causing droughts) or even heat waves. Such conditions may lead to different social, economic and environmental damage and may be even losses of lives (Ambrizzi et al., 2005, Rasmussen et al., 2005).

Up till now, the CO_2 concentrations, which are measured at Mauna Loa (Hawaii), are still increasing. In 2006, the CO_2 concentration was 20% (375 ppm) higher than in 1959 (Tans, 2007). This shows that the 1997-Kyoto Protocol may not yet has its success. This protocol aims at especially the developed and industrialized countries, reducing emission of greenhouses gases (mainly CO_2, CH_4, N_2O) by at least 5% by the period 2008-2012 compared to 1990 levels. During the last climate conference in Vienna, 158 countries (mainly industrialized countries) agreed to reduce greenhouses gas emissions with 25-40% by 2020 compared to 1990 values. The Intergovernmental Panel on Climate Change (IPCC) has however reported that even if this limit is reached, the world climate will continue to change due to the life time of the greenhouse gases in the atmosphere (Table 1.1). It is expected that the CO_2 concentrations will by doubled by 2100.

A large number of global climate models have calculated that under these conditions, the global mean surface temperature will increase with about 1.1 to 6.4^{o}C by 2090-2099, reference to 1980-1999 and that the mean sea level will rise between 0.18 and 0.59 m depending on the Special Emission Scenarios of the IPCC (SRES). In the Guiana Shield region, an alternation in the annual rainfall is estimated between -10% and 10% by 2100, compared to 1990 values and the mean surface temperature will increase by 2.5^{o}C to 3.5^{o}C by 2100, relative to 1990 values (IPCC, 2001). The mean sea level is expected to increase along the Guiana coast with about 30 cm to 50 cm by 2090 (Met Office-The Hadley Center, 2003). The IPCC also indicated that precipitation will increase more in the northern and southern hemisphere and decrease in the tropical region. Heavy precipitation events are expected to become more frequent and hurricanes more intense (in relation to sea surface temperature increase) (IPCC, 2007). Such changes are projected to affect different components of the climate system such as the atmospheric circulation, biosphere, land surface and the hydrological cycle, and may result in dramatic impacts on Earth (e.g. floods, droughts, storms). The different components are schematically shown in Figure 1.5.

It is believed that if these climate changes continue or increase, components of Suriname's climate system will also be impacted. Because of the many aspects and complexities involved in analyzing climate change impacts on different climate systems, but more because of the fact that freshwater is fundamental to human life and is already becoming a serious threat in some countries in the world, this study will therefore mainly focus on precipitation and temperature changes, and the impact on fresh water resources in Suriname.

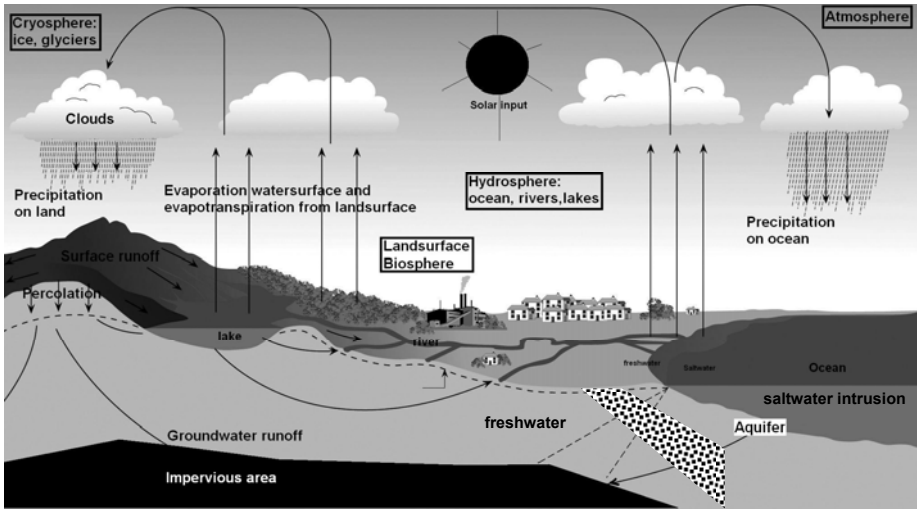

Figure 1.5: Schematic view of the components of the global climate system (rectangular-bold) including the hydrological cycle (after Maidment, 1992; after Rientjes and Boekelman, 1998; Retrieved May 12, 2005 from www.grida.no/climate/ipcc_tar/wg1/040.htm#fig11).

1.2 Problem definition

Suriname is located in the northern part of South America (1.5-6^{o}N, 54-58^{o}W) and has a tropical wet climate. The average annual temperature is about 26.8^{o}C, the annual precipitation is about 2100 mm (1961-1985) and the average annual evaporation is about 1750 mm (1961-1968). The relative humidity is around 80% and the sunshine about 58%. Figure 1.6a shows the monthly temperature and Figure 1.6b the annual temperature series at station Cultuurtuin for the period 1971-1999. A linear regression of the annual temperature during 1971-1999 shows that the annual temperature has increased by about 0.8^{o}C. Figure 1.7a shows the monthly precipitation and Figure 1.7b shows the annual precipitation series at the same station, but for the period 1900-1999. From Figure 1.7a it may be deduced that the monthly rainfall distribution throughout the year is not equal. This is mainly caused by the Intertropical Convergence Zone (ITCZ). The ITCZ causes four seasons in Suriname.

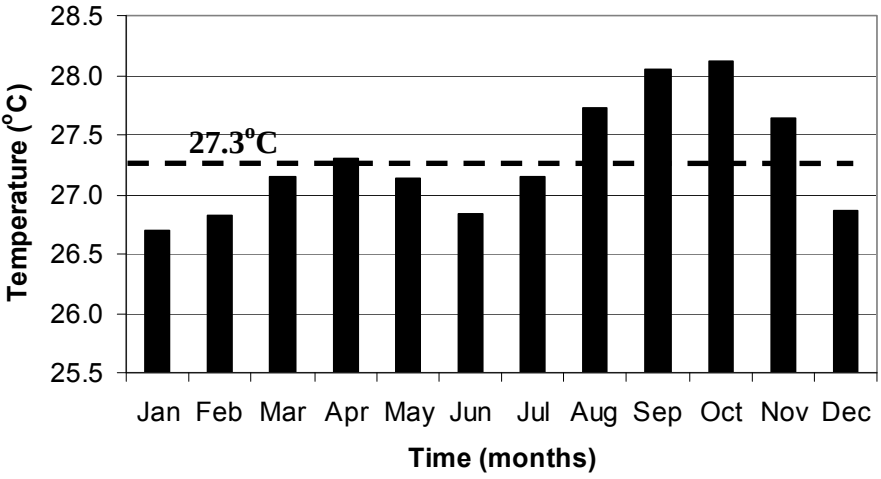

(a)

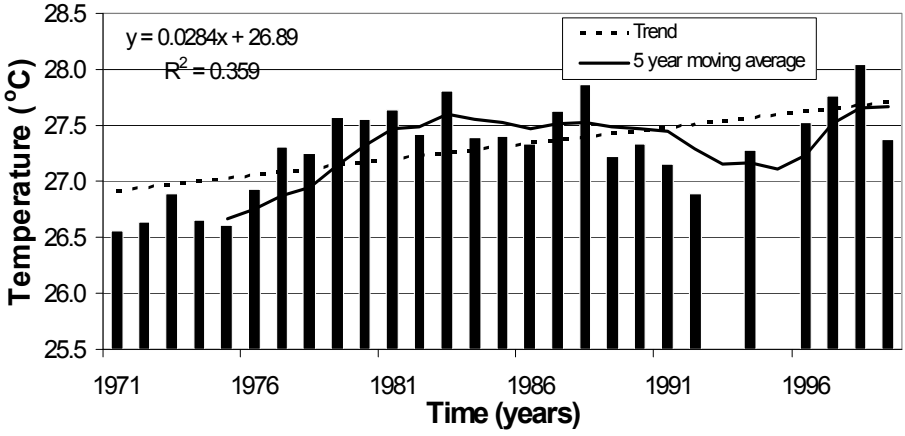

(b)

Figure 1.6: (a) Long-term monthly temperature and (b) the annual temperature at station Cultuurtuin (1971-1999).

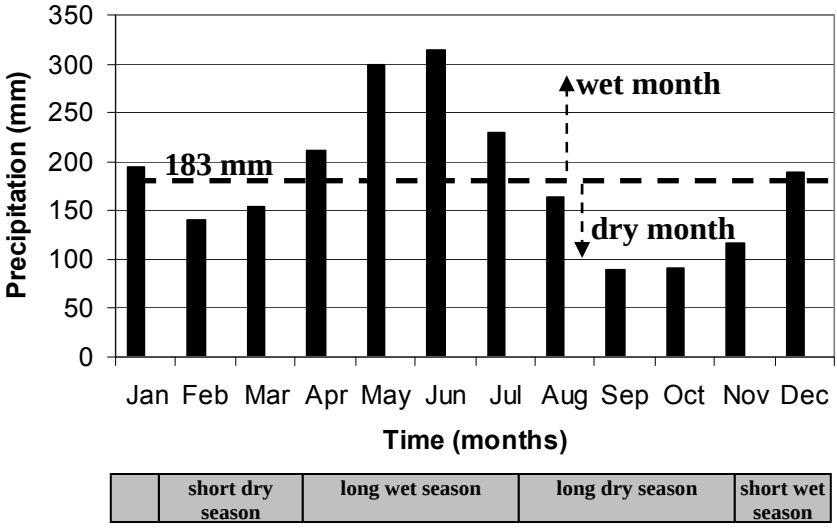

(a)

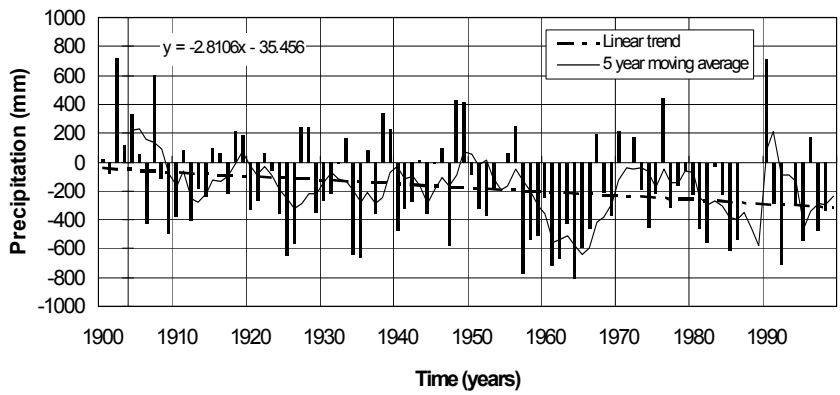

(b)

Figure 1.7: (a) Long-term monthly precipitation and (b) the annual precipitation at station Cultuurtuin (1900-1999).

The short wet season accounts for about 18% of the annual rainfall, the long wet season for about 56% of the annual rainfall, the short dry season for about 13% of the annual rainfall and the long dry season for about 13% of the annual rainfall (Emanuels, 1968). Linear trend analysis shows that the annual rainfall has decreased by 14% (about 300 mm) since 1900.

In addition to the changes in climate on a global scale, precipitation is also influenced by various dynamic processes on inter-decadal and inter-annual scale, such as the Pacific El Niño Southern Oscillation and the Tropical Atlantic Variability (Gianninni et al., 2000; Rasmussen and Wallace, 1983; Rajagopolan et al., undated). This can be noticed in Figure 1.7b, the high temporal variability in precipitation. Some of these processes are schematically shown in Figure 1.8. It is also shown that the spatial distribution of rainfall (Figure 1.9) is also not equally distributed throughout Suriname. Together with the high temporal variation in precipitation and the different oceanic-atmospheric processes, this makes it difficult to identify a clear rainfall pattern in Suriname.

The precipitation distribution is also responsible for the amount and variation in freshwater resources in Suriname. Although little is known about historical changes in Suriname's climate, Figures 1.6b and 1.7b show that perhaps global climate change may also have affected our climate. Short-term climate variation has also affected Suriname's climate. In August 1997-February 1998, the El Niño event caused rainfall much below normal in West-Suriname, while the neighboring countries Guyana and northern Brazil experienced severe and prolonged droughts. This led to rice-production losses, fish-production losses in coastal swamps and damage to road-infrastructure (Hammond and Ter Steege, 1998; Mol et al., 2000). In September 2004, hurricane Ivan caused floods in northern Suriname, but also the Caribbean region such as in Grenada, Jamaica, Cuba, and in Florida. The heavy and prolonged rainfall in May-June 2006 caused flooding in the interior of Suriname, affecting about 25,000 people, and causing a damage of more than SRD 111.10^6 or US$ 26.10^6. The heavy winds in September 2006, which originated from a tropical depression in the Atlantic ocean, caused damage to roofing of houses along the northern part of Suriname. Different literature sources have reported more extreme events (floods and droughts) in the past in Suriname (Geijskens, 1943; Hollande, N., personal communication, October 1, 2004; Houben and Molenaar, undated; Moksi Magazine, 2006; Mol et al., 2000; Scheltz, E., personal communication, September 5, 2004; United, 2006; Webster and Roebuck, 2001).

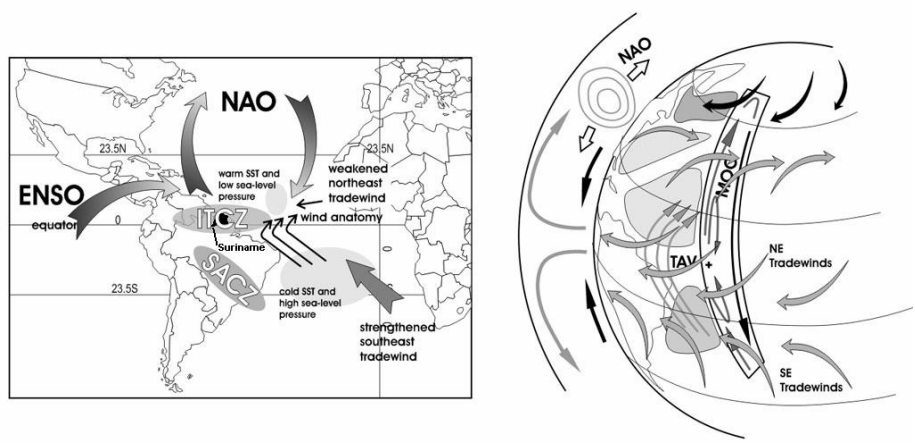

Figure 1.8: A schematic of the oceanic-atmospheric processes that influence the climate of Suriname: the North Atlantic Oscillation (NAO), the Tropical Atlantic Variability (TAV), the Intertropical Convergence Zone (ITCZ), the South Atlantic Convergence Zone (SACZ), the Pacific El Niño-Southern Oscillation (ENSO). The Pacific ENSO (through the Walker and the Hadley circulation) and the NAO (through Hadley circulation) influence the sea surface temperature anomalies (SSTAs) north of the equator (after Marshall et al., 2001; Robertson and Mechoso, 2002; after Wang, 2001).

Since 1900, at least 12 significant dry periods (drought) have been experienced in Suriname and at least 13 significant wet periods (floods). Most of these events have resulted in different hydrological and accompanying economic, social en environmental damage in Suriname. River water level observations (1960-2004) have also shown that the mean coastal-river water level along the coast of Suriname has increased with about 10 to 20 cm. Linear extrapolation of these data indicates that by 2100, the water level might increase with about 50 cm. A study by Naipal and Amatali (1999a) has shown that if the sea level rises with 1 m, this will result in flooding of 3,890 km^2 of the coastal area of Suriname and an estimated damage of US$ 30.10^9. This is due to the fact that most of the economic activities, industries, agricultural lands, infrastructure, freshwater resources, coastal ecosystems, human settlements are located in this area. The coastal part of Suriname is thus most vulnerable to climate change in, particular sea level rise.

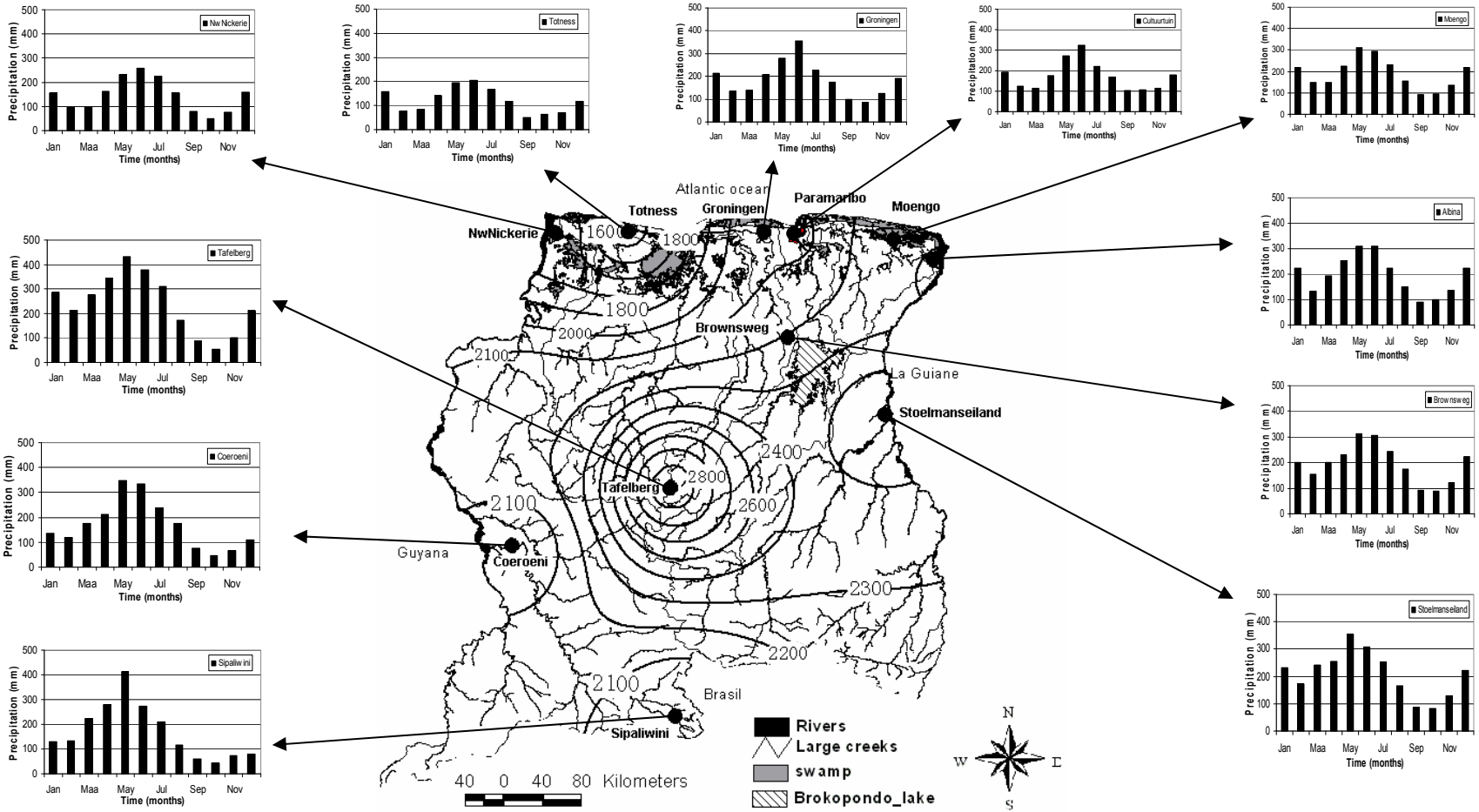

Figure 1.9: Contour map of annual precipitation totals (mm) and the monthly precipitation totals (mm) per station during a 25-year period (1961-1985) in Suriname. The small black circles indicate the meteorological stations used for constructing the isolines.

Global climate change may have impacts on more climate system components and sectors in Suriname, as shown in Figure 1.10. This schematic shows that an increase in precipitation and sea level will most negatively affect resources in the northern part of Suriname (agriculture, fisheries, industries, ecosystems, freshwater resources), while changes in precipitation will more likely affect sectors in the interior of Suriname (e.g. hydropower, agriculture, fisheries, land use, vegetation).

Both surface and groundwater resources in river basins may change due to changes in precipitation and evaporation. From Figure 1.10 it is clear that it is important to identify the historical climate changes and to quantify them. If these events are going to increase under global climate change conditions, it is also important to estimate the future changes in precipitation and freshwater resources in Suriname.

Suriname contains a large amount of renewable fresh water resources (about 479,000 m^3 available freshwater per capita per year) and has been classified as the 6th country in the world[1] abounding in water. Most of the fresh water in Suriname is found in rivers, swamps/lagoons, reservoirs and aquifers. Figure 1.11 shows the main fresh-brackish swamps/lagoons including rivers in the northern part of Suriname. The annual average renewable river discharge is about 4800 m^3/s (only rivers), from which less than 6% is used for different socio-economic sectors in the coastal area of Suriname, such as agriculture, aquaculture, hydropower, industrial and household purposes. The rest of the fresh water flows directly to the Atlantic ocean. The main rivers are shown in Figure 1.9 and some of their characteristics are listed in Table 1.2. Groundwater is the primary source of water for potable purposes in the coastal area of Suriname. Only about 0.2% of these groundwater resources is exploited (about 140,000 m^3/day) (Tsai Meu Chong, personal communication, June 8, 2004). The coastal area contains renewable groundwater resources (unconfined aquifers), where recharge is directly determined by rainfall (through the Savannah Belt), and non-renewable groundwater resources (confined aquifers).

Figure 1.12 shows a typical section of the groundwater aquifers in the coastal area of Suriname. The recharge in the Savannah Belt varies between 200 to 500 mm/year (Groen, 2002). In the coastal area close to the Savannah Belt, the lifetime of groundwater is found to be close to 1000-2000 years, while the lifetime of groundwater in the most northern part of Suriname (the young coastal plain) is found to be close to 13,000-20,000 years, compared to year 2000 (WMO/UNDP/Gov of Suriname, 1972). The largest amount of the fresh groundwater resources is present in West-Suriname (Figure 1.11).

[1] Based on a water poverty index (WPI) developed by the United Kingdom (U.K.)

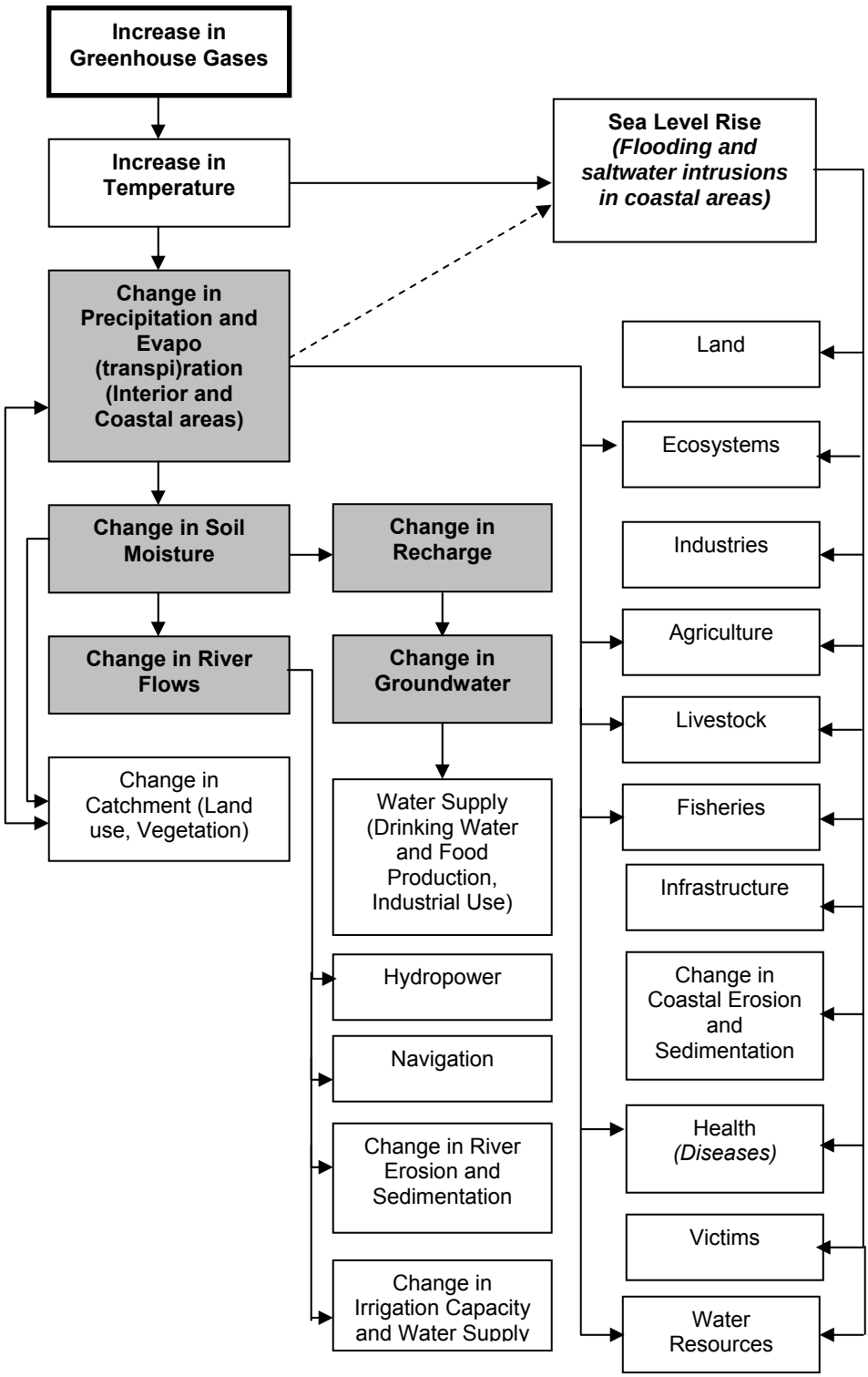

Figure 1.10: Conceptual model of the effects of greenhouse gases on the global hydrological cycle and possible impacts in Suriname. The grey boxes are components of the hydrological cycle and the white boxes are sectors of human-economic impact (after Maidment, 1992; after Yusoff et al., 2000).

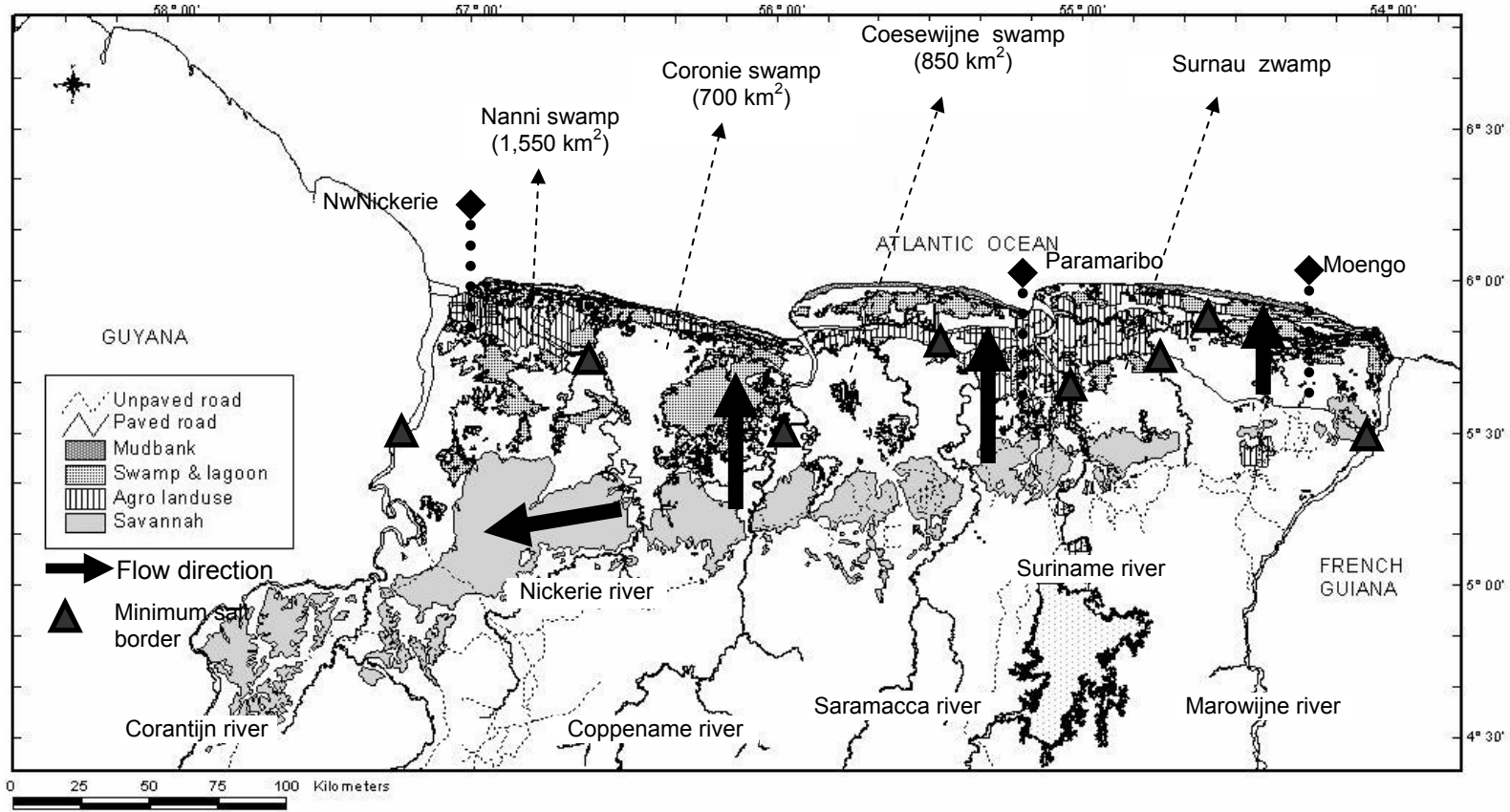

Figure 1.11: Water resources systems and idealized groundwater flow direction in the northern part of Suriname, and most of the economic sectors in this area.

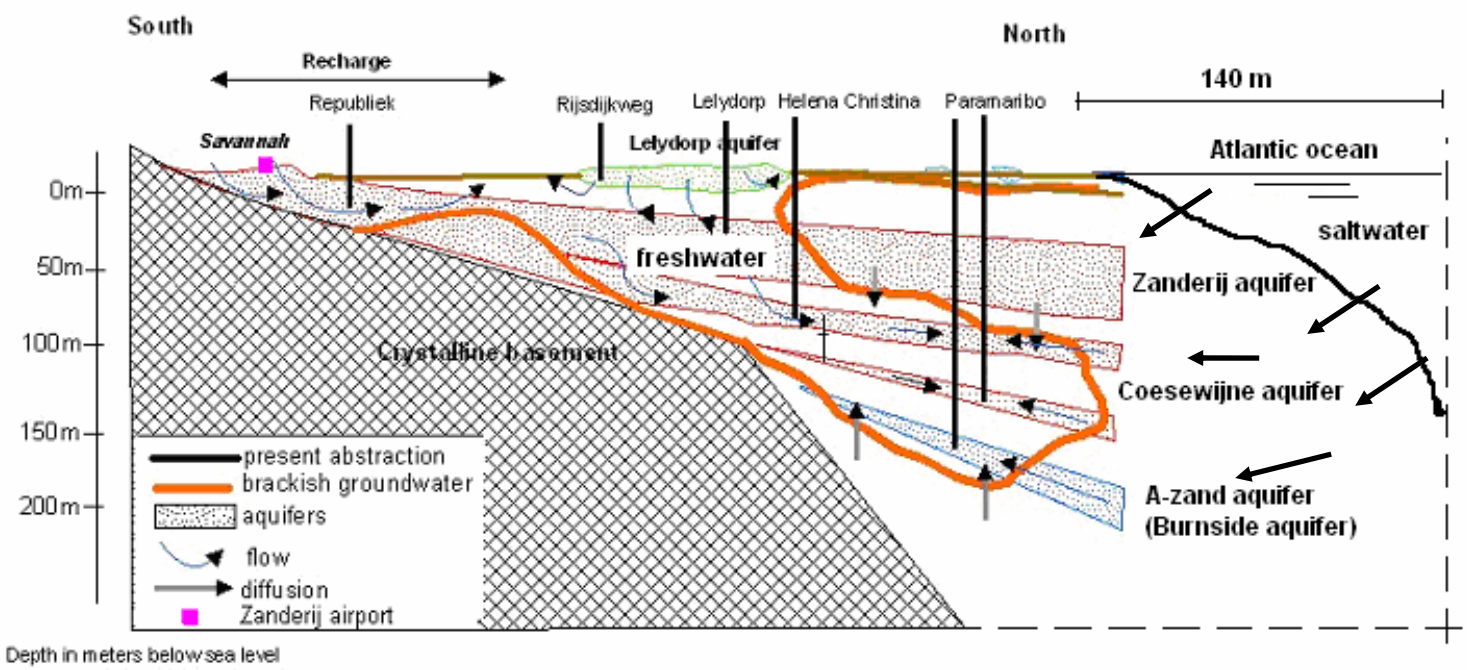

Figure 1.12: Idealized north-south section of the aquifers in Paramaribo (Suriname) with groundwater flow directions and brackish water intrusion (after WHO/UNDP/Gov of Suriname, 1972; after Groen, 1998).

Table 1.2: Characteristics of the seven main rivers of Suriname (Naipal et al., 1999a).

River[*)]	Total Catchment area [**)] (km^2)	Annual Average Discharge (m^3/s)	Maximum Discharge (m^3/s)	Minimum Discharge (m^3/s)	Min SWI[***)] (km)	Max SWI (km)
1. Corantijn	67,600	1,570	7,070	41	40	82
2. Nickerie	10,100	178	880	2	28	105
3. Coppename	21,700	500	2,200	6	31	83-95
4. Saramacca	9,000	225	1,260	5	37	89
5. Suriname	16,500	426	1,800	220 [****)]	54	90
6. Commewijne	6,600	120	215	-	-	-
7. Marowijne	68,700	1,780	6,160	48	37	59

*) There are no river measurements for the Coastal Plain available
**) Estimated value based till river mouth
***) Minimum saltwater intrusion limit (Min SIL) from river mouth (wet season). Limit used 200-300 mg Cl/l; the zero point is taken at the river mouth where the depth reaches 15m below low water spring. Maximum saltwater intrusion (Max SIL) from limit river mouth (dry season)
****) River discharge due to regulation of the hydropower dam at Afobakka

Up till now little has been reported about climate change in Suriname. The main reason has probably to do with the poor and outdated meteorological and hydrological data in Suriname, due to poor climate monitoring. On policy field, the Government of Suriname has signed some conventions related to climate change, which can be used as a basis for reducing negative impacts of global climate change on Suriname. Some of the conventions are the United National Convention on Climate Change - UNFCCC (October 14, 1997), the Vienna Convention on the protection of the Ozone layer (October 14, 1997), the Montreal Protocol on substances that deplete the Ozone layer (October 14, 1997), the UN Convention to Combat Desertification (June 1, 2000), the UN Convention on Biological Diversity (January 12, 1996), the Convention on Wetlands - RAMSAR (March 18, 1985) and the Kyoto Protocol (December, 2006).

Although Suriname produces negligible amounts of greenhouse gases (carbon dioxide = 39,874 Gg or 3,984 CO_2 equivalent, CH_4 = 45 Gg of 1,035 CO_2 equivalent, N_2O = 0.02 Gg for 1994-2003) compared to the world emissions, it will be the global changes in climate that will impact components of Suriname's climate system (Nimos, 2005). The energy sector accounts for about 49% of the greenhouse gas emissions, the agricultural sector for about 19%, land use change and forestry for about 31% and other sectors for about 1%. Meanwhile, the Ministry of Labor, Technological Development and Environment (ATM) and the National Institute for Environment and Development (NIMOS) started in 2005 with the second phase of the Netherlands Climate Change Studies Assistance Program in Suriname. This study will develop and specify identified adaptation measures in the context of climate change and analyse their possible effects and feasibility, with emphasis on vulnerable zones.

In 2005 NIMOS also started with an awareness programme in Suriname to inform the community about the causes and effects of climate change for Suriname. However, none of these studies have studied and analysed hydro-climatic observations in Suriname and the impact of global climate change on Suriname's climate and fresh water resources. Only surface water systems will be analysed in this study because of the short residence time of water resources in rivers (a few days), compared to groundwater resources in aquifers with residence time in the order of months to 10,000 years.

1.3 Objectives of the research

The main objective of this research work is to analyse the impacts of future climate change and climate variability on the water resources in Suriname. The specific objectives of this research are:

- To provide a review of methods/techniques and models to analyse climate change and climate variability (chapter 2)
- To investigate which climate processes mainly influence precipitation and river discharges in Suriname (chapter 3, 4, 5)
- To investigate if there are significant changes (trend, shift) in historical precipitation, temperature and river discharges (chapter 3, 5)
- To develop climate scenarios and estimate the future changes in precipitation and temperature under global climate change conditions (chapter 6)
- To analyse the effects of future climate change on water resources in the Upper-Suriname river basin (chapter 7)

1.4 Study area

The climate analyses will be performed throughout Suriname (about 163,820 km^2) and will be based on selected stations. The effects of future climate change on water resources will be studied in the Upper-Suriname river basin (7,750 km^2). A river basin is chosen, because it contains almost all the components of the hydrological cycle. This case study area has been chosen because of its importance for hydropower generation in Suriname and the availability of meteorological, hydrological, physical and other socio-economic data in this area. Most inhabitants in the interior of Suriname live in this basin in about 55 villages (12,355 persons) (Retrieved, June 5, 2004 from http://www.statistics-suriname.org/cen-index.html). This study area is also part of one of the world's largest nature reserve, more in particular the Central Suriname Nature Reserve (1.10^6 ha). The territory of Suriname and the case study area are shown in Figure 1.13a and 1.13b respectively.

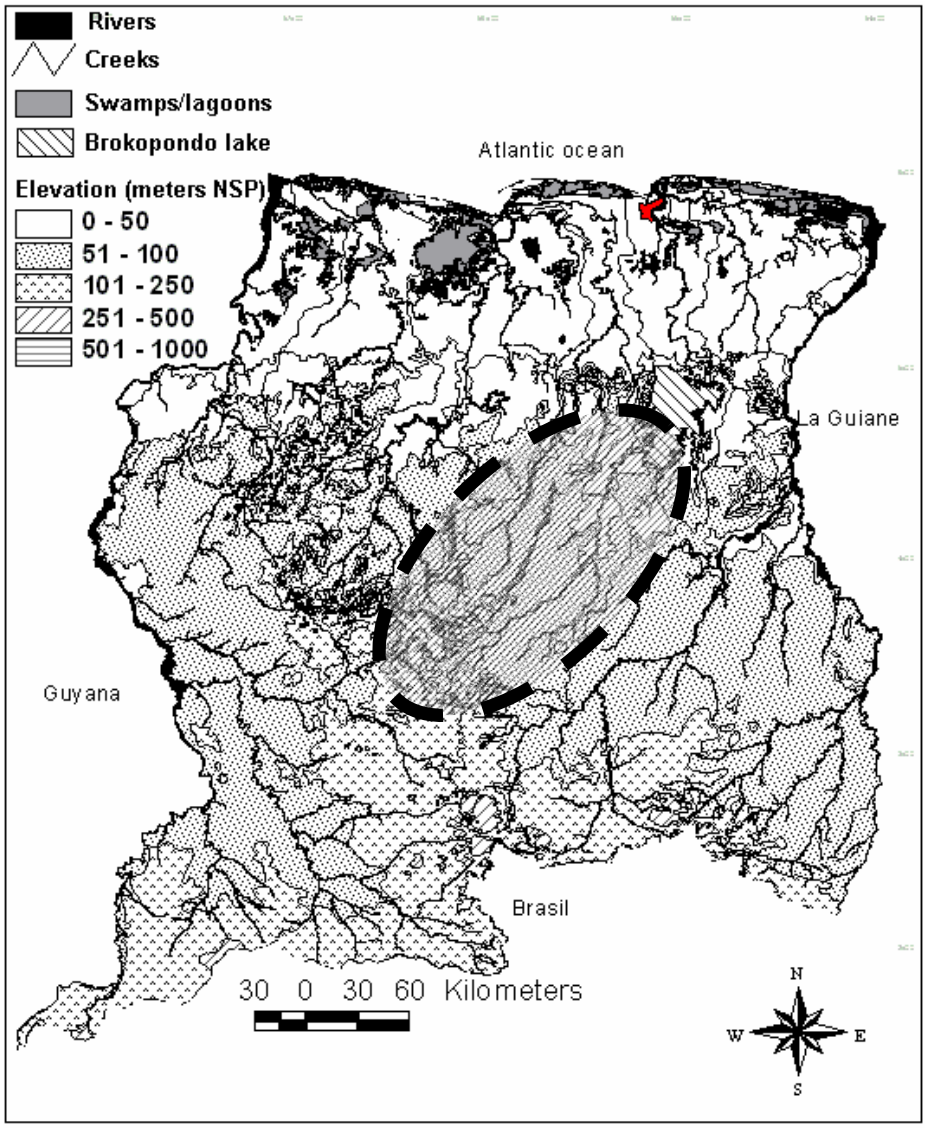
Rivers
Creeks
Swamps/lagoons
Brokopondo lake
Elevation (meters NSP)
0 - 50
51 - 100
101 - 250
251 - 500
501 - 1000
Atlantic ocean
La Guiane
Guyana
Brasil
30 0 30 60 Kilometers
N
W
E
S

(a)

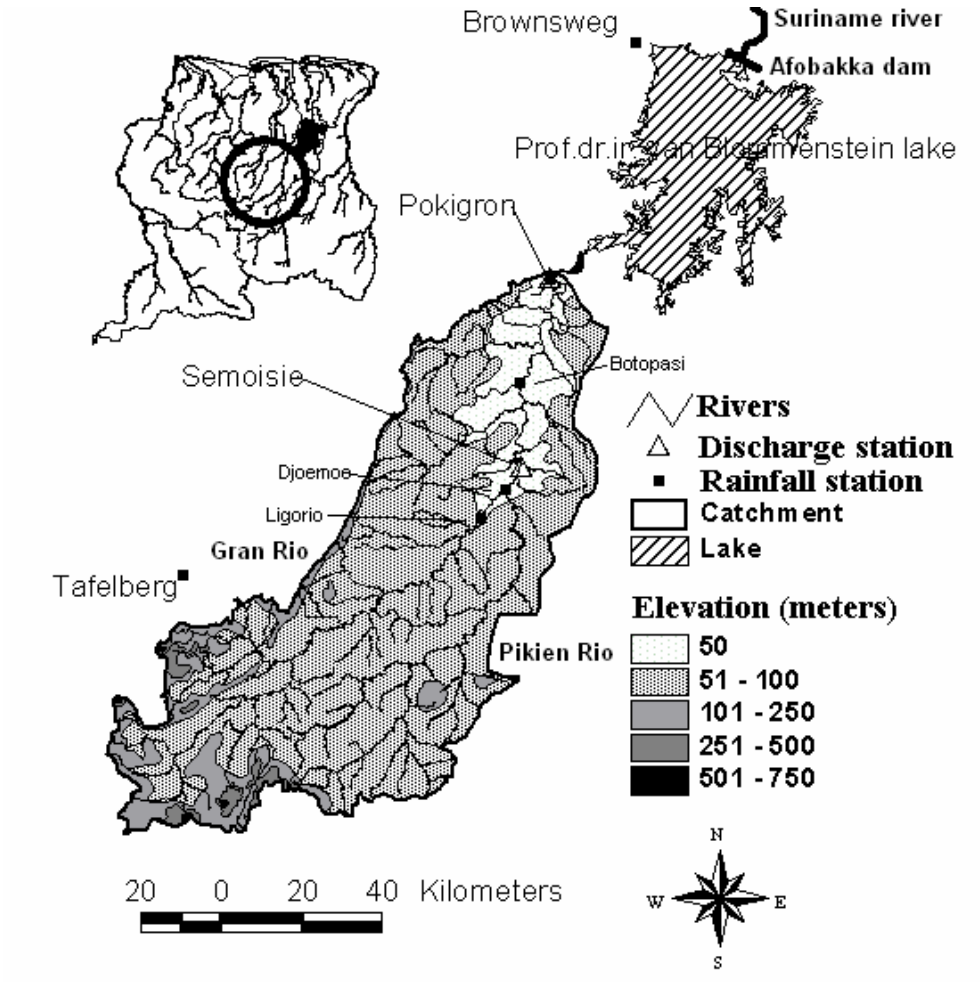

(b)

Figure 1.13: (a) The study area Suriname, (b) the Upper-Suriname river basin.

1.5 Research methodology

The methodology used in this research is schematically shown in Figure 1.14 and consists of mainly 5 components:

- Literature review
- Data selection and processing
- Selection of methods/techniques and models, and application
- Data analyses, processing of results and interpretation
- Conclusions and recommendations

The meteorological and hydrological observations are the most important input for this study. The Meteorological Service Suriname of the Ministry of Public Works maintains the network of meteorological stations in Suriname and the hydrological network is maintained by the Hydraulic Research Division of the Ministry of Public Works. In 1980 the meteorological network included about 183 rainfall stations including 26 climatologic stations and 8 synoptic stations, and was reduced to about 48 stations due to the war in the interior in 1986. The economic recession has also contributed to this condition. Out of this amount, only a few stations are located in the hinterland. Most of these stations have poor observations and since 2001, 11 stations have been operational again, but unfortunately the data series are also incomplete due to poor operation. Therefore it has been decided to use only precipitation, temperature and river discharge series, which are also the most common considered indicators for climate change. Other climate variable observations such as evaporation and wind speed are too short (< 10 years), contain also a lot of missing data and are also not up to date.

For this study, about 11 rainfall stations with daily data series were finally selected that contain sufficient and complete data series (1961-1985; 25 years), and that provide sufficient spatial coverage to characterize climate change and climate variability over Suriname. Some of these stations have more than 25 years of data, up to more than 100 years. These stations are more located in the northern part of Suriname. For temperature analyses, 7 stations were selected with data mainly from 1971-1985 (15 years). From the more than 50 river discharge stations installed between the 1950-1960s in different river basins, only four river discharge series with monthly data series (1961-1985; 25 years) were selected. The same reasons have resulted in the closure of all hydrological stations till today.

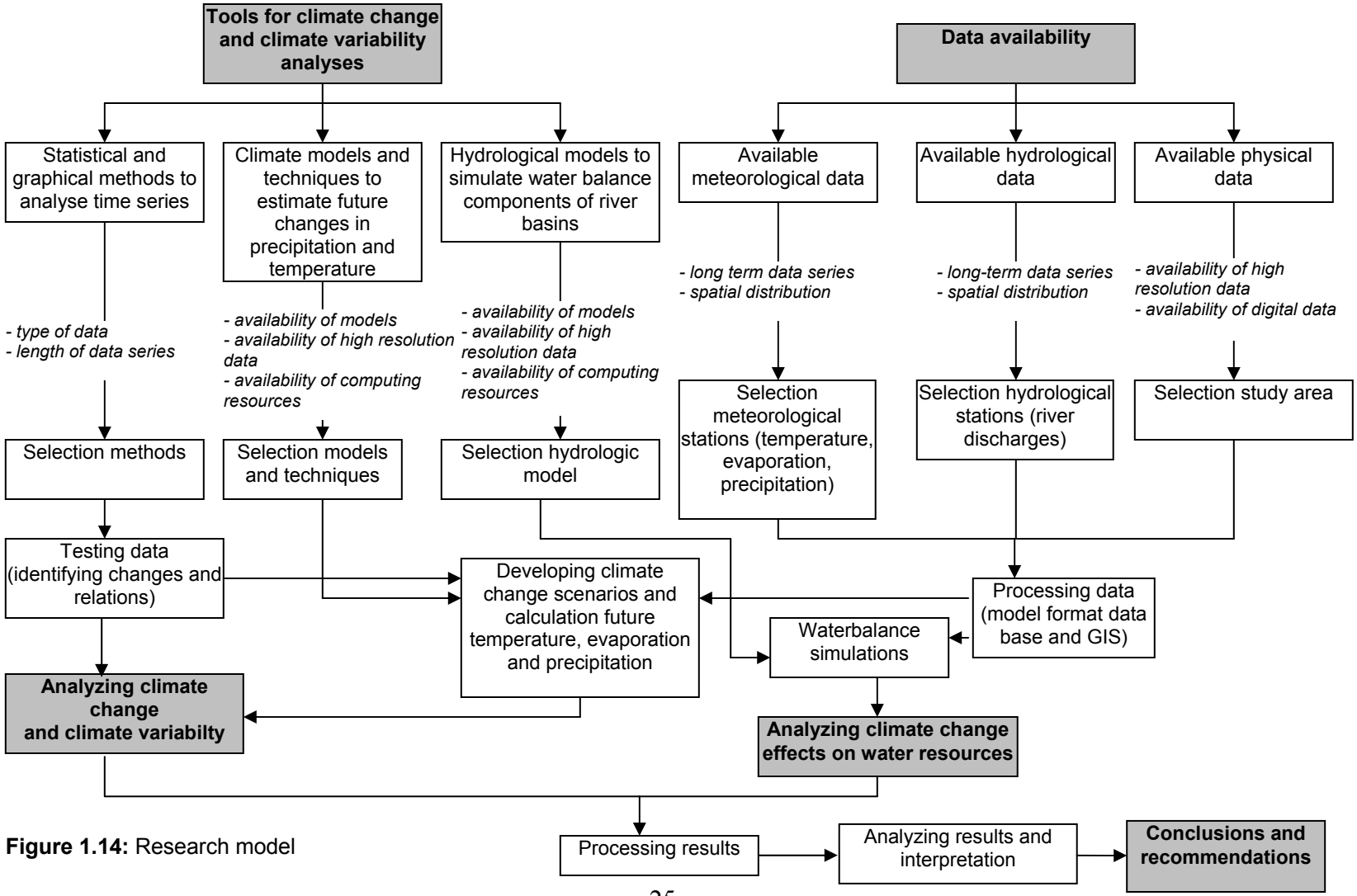

Figure 1.14: Research model

Data series that have gaps are completed using linear regression analyses between the nearest stations. Because of the above-mentioned data problems, climate analyses will only be performed on mean values and not on extreme values. The WMO (1988) advised to use the following minimum criteria for climate analysis: 50 years for precipitation and temperature data, and 30 years for all other data. Stations with 40 years or more of data can be used for both temporal and spatial variability. Stations with less than 40 years of data can only be used for spatial variability. Unfortunately, in this study we will not always be able to meet these requirements. Taking the shortcomings of the available observations and the requirements of the WMO into account, it is clear that the historical data will have an impact on the estimated future data by the climate and hydrological model. Therefore, the results obtained in this study should be considered as a first estimation.

Secondly, with regard to the selection of appropriate methods to analyse data and models for climate and hydrological analysis, there are a lot of literature sources available to perform this review. The selected temperature, precipitation and river discharge series will be used in this analysis. The statistical models used in this research are: MSExcel 2000, the Climate Predictability Tool v.5.04 (Retrieved June 10, 2005 from http://iri.columbia.edu/outreach/software/), Modstat statistical software v.2.04 (Knodt, 2003), AnClim software for time series analysis v.4.7.31 (Stipanek, 2003), XLStatistics workbook for data analysis v.5 (Carr, 2000) and the KNMI Climate Explorer (Retrieved August 10, 2005 from http://climexp.knmi.nl/). Most of these models were received free of charge for the purpose of this research. To generate climate scenarios, the Magicc/Scengen 4.1 model is used as the climate model. This model has been the primary model used by the Intergovernmental Panel on Climate Change (IPCC) to produce projections of future global mean air temperature. This model was also received free of charge for the purpose of this research. Although there are also a few RCM models are available from different institutions free of charge, we are unable to use them yet, because they require considerable computing resources (Bronstert et al., 2002; Chong-Yu, 1999; Giorgi and Mearns, 1991). For example, a 30 year period for an area of 5000 by 5000 km would take for one scenario, about 1.5 months to run on a super computer (36 processors), while on a Pentium IV PC (with minimum 60 GB disk space, 768 MB memory), this would take about 4.5 months. Other types of models such as the SDSM model was also applied to Suriname conditions, but no satisfactory results were obtained. This has probably to do with the shortness and quality of the data, the lack of sufficient upper air atmospheric variables and process formulations in the model. Therefore, these types of models will also not be used in this study. To model the response of river basins, the WetSpa hydrological model from the *Vrije Universiteit Brussels* is used in this research in combination with ArcView GIS 3.2. This model has been made fully available to our Department by the

promoter of this study. To study the effects of climate change on water resources, one river basin was chosen because of the amount of data required, processing time and computation time and resources.

1.6 Structure of the dissertation

Chapters 3 to 7 are a series of papers that are published and/or submitted to a journal and/or presented at an international conference. There may thus be repetition of theories and results in some chapters.

Chapter 2 provides a summary of statistical methods to detect climate change and climate variability, and models that can be used to estimate future changes in climate with respect to temperature and precipitation. The different advantages and disadvantages of these methods and models are also summarized in this chapter. A summary is also provided about methods to model water resources systems, with respect to river basins.

In chapter 3 statistical tests are used to analyse historical changes in the monthly and annual rainfall, temperature and river discharges in Suriname. A description of the different statistical tests is given here. Analyses of the effects of El Niño and La Niña on precipitation in Suriname are also provided. This chapter also analyses the relation between the anomalies in annual rainfall and river discharges and the anomalies in annual sea surface temperatures in the Atlantic and Pacific ocean. The effects of historical climate change and climate variability on water resources in Suriname is also analysed.

Chapter 4 gives insight into the different oceanic-atmospheric processes that influence precipitation in Suriname. Statistical tests are used to analyse the relationship between monthly rainfall anomalies and monthly sea surface temperatures in the Atlantic and Pacific ocean. Spatial variability of precipitation is also analysed in this chapter.

In chapter 5, the same statistical tests as in chapter 3 are used to analyse changes and variations in the historical river discharges, the Upper-Suriname river basin. The variability of monthly river discharges in relation with the sea surface temperatures in the Atlantic and Pacific ocean is also analysed.

Chapter 6 describes the methods of climate scenario construction for Suriname using the SCENGEN climate model. Observed and modelled precipitation and temperature are compared and future changes in these variables are estimated by a few global circulation models.

In chapter 7, the application of the WetSpa hydrological model in the Upper-Suriname river basin is presented. This model is used for two purposes. Firstly to estimate the historical water balance and river discharges for a large tropical basin with poor data, and secondly to estimate future changes in the water balance components under doubling of CO_2. A range of arbitrary changes in temperature and precipitation, and GCM scenarios are used to provide climate change scenarios to estimate future changes in the water resources in the study area.

Finally, in chapter 8, a summary of the main conclusions of this research and recommendations for future research in this study field are given.

2. METHODS AND MODELS TO ANALYSE CLIMATE CHANGE AND CHANGES IN WATER RESOURCES

Abstract

This chapter provides a literature review about the global causes and effects of climate change and variability in the last century, methods to analyse climate change and climate variability, and methods to model global climate change. The use of climate and hydrologic models to estimate the effects of climate change on water resources systems is also discussed. This review has shown that a lot of statistical methods exist in literature to detect spatial and temporal changes in climate variables, but there are no rules for selecting the best method. In general it may be concluded that the choice for a particular statistical method will mainly be dependent on the length of the data series and the purpose of the study. There are also different global and regional climate models available in literature and most of them are still in the process of development and contain still uncertainties in some processes. This influences the outputs of current and future changes in mainly temperature and precipitation. Therefore, one should use outputs of climate models only for sensitivity analyses. The huge requirements to run these climate models may limit the use in especially third world countries. However, some outputs of these climate models can easily be accessed on the internet and some climate models (e.g. regional climate models (RGM) can nowadays also be run on a personal computer. There are also a lot of hydrologic models available from different institutions, and subject to the type of the model and model input requirements, water balance components can easily be simulated. However, there is little experience with these models to simulate future water balance components under climate change conditions. It is finally concluded that a combination of available statistical methods, climate models and hydrologic models can be used to study future effects of global climate change on water resources, especially in countries with limited hydro-meteorological and physical data.

2.1 Introduction

To understand climate change may be complicated, as it involves not only complex processes and interactions within the atmosphere, but also environmental, economic, political, institutional, social en technological processes. The Intergovernmental Panel on Climate Change (IPCC), the United Nations Framework Convention on Climate Change (UNFCCC) and the World Meteorological Organization (WMO) have defined there own definition for climate change. In this research, climate change refers to a statistically significant variation in the mean state of the climate or its variability (trends or shift), persisting for a number of decades (WMO, 1988). Climate variability will be referred to as short-term processes such as the extremes and differences of monthly, seasonal and annual values (also called anomalies) from the climatically expected value. This definition is taken from the World Meteorological Organization (WMO, 1988). This chapter will provide more insight into the (a) methods to analyse climate change and climate variability, (b) methods to model global climate change and (c) methods to estimate the effects of climate change on surface water resources systems.

2.2 Methods for testing climate change and climate variability

Climate varies in space and time. Temporal variability is in general analysed by the temporal characteristics of climate parameters using statistical and graphical methods, while the spatial variability can be analysed by making maps of various parameters and their associated error (WMO, 1988). Meteorological time series (e.g. precipitation, temperature, evaporation) and hydrological time series (e.g. river discharges, water levels) may contain deterministic components (trend, shift, periodic changes) and stochastic components (seasonality) (Haan, 1977; Mamdouh et al., 1993). Figure 2.1 shows some of these components graphically. These components may be caused by changes in the environment such as climate change, land use changes (e.g. deforestation, urbanization), but also changes in instrumentations, observing practices and relocation. If the measured data are not influenced by human activities, but by natural activities, the data series are random (or inconsistent). In stationary time series (normal variability), the statistical properties (e.g. the mean, variance, standard deviation) do not change in time. Homogeneous time series do not have a trend or cycle effect (Mamdouh et al., 1993).

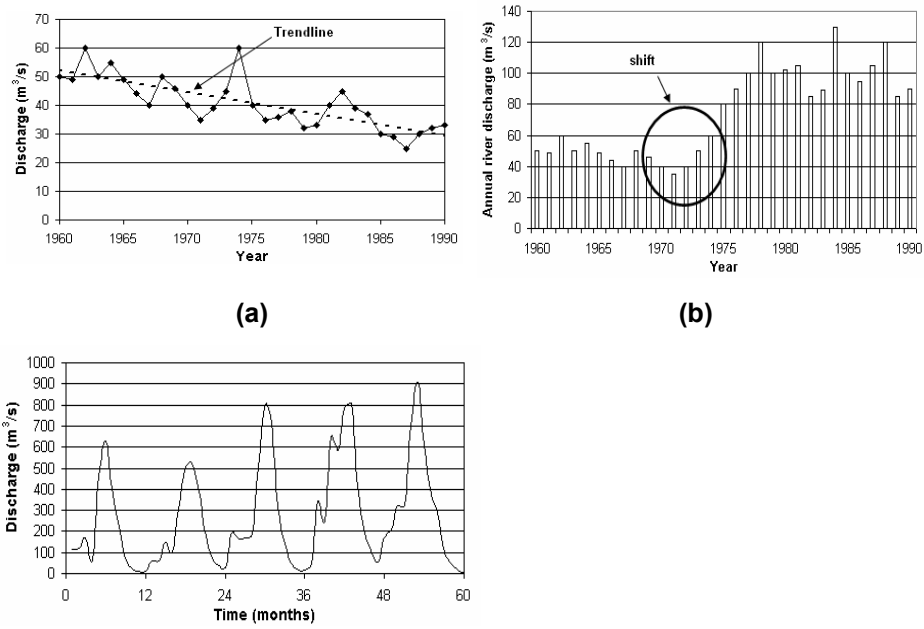

Figure 2.1: Fictitious time series showing (a) trend, (b) shift and (c) periodicity.

Figure 2.2 shows the procedure for determining climate change and climate variability in time series. In general, time series should first be separated in systematic and non-systematic variation (e.g. by the moving average filter). This should be preceded by a graphical analysis to assess the data (e.g. by plotting mean values or correlation coefficients in the form of frequency analysis or histograms). For non-systematic variation, compute the characteristics of the errors and also do a frequency analysis of the data to identify a potential distribution. Then apply e.g. the Kolmogorov-Smirnov test to check the assumed distribution. For the deterministic component, detect the shape of the trend from the graph (e.g. plot the annual mean values) and fit a least square function to it.

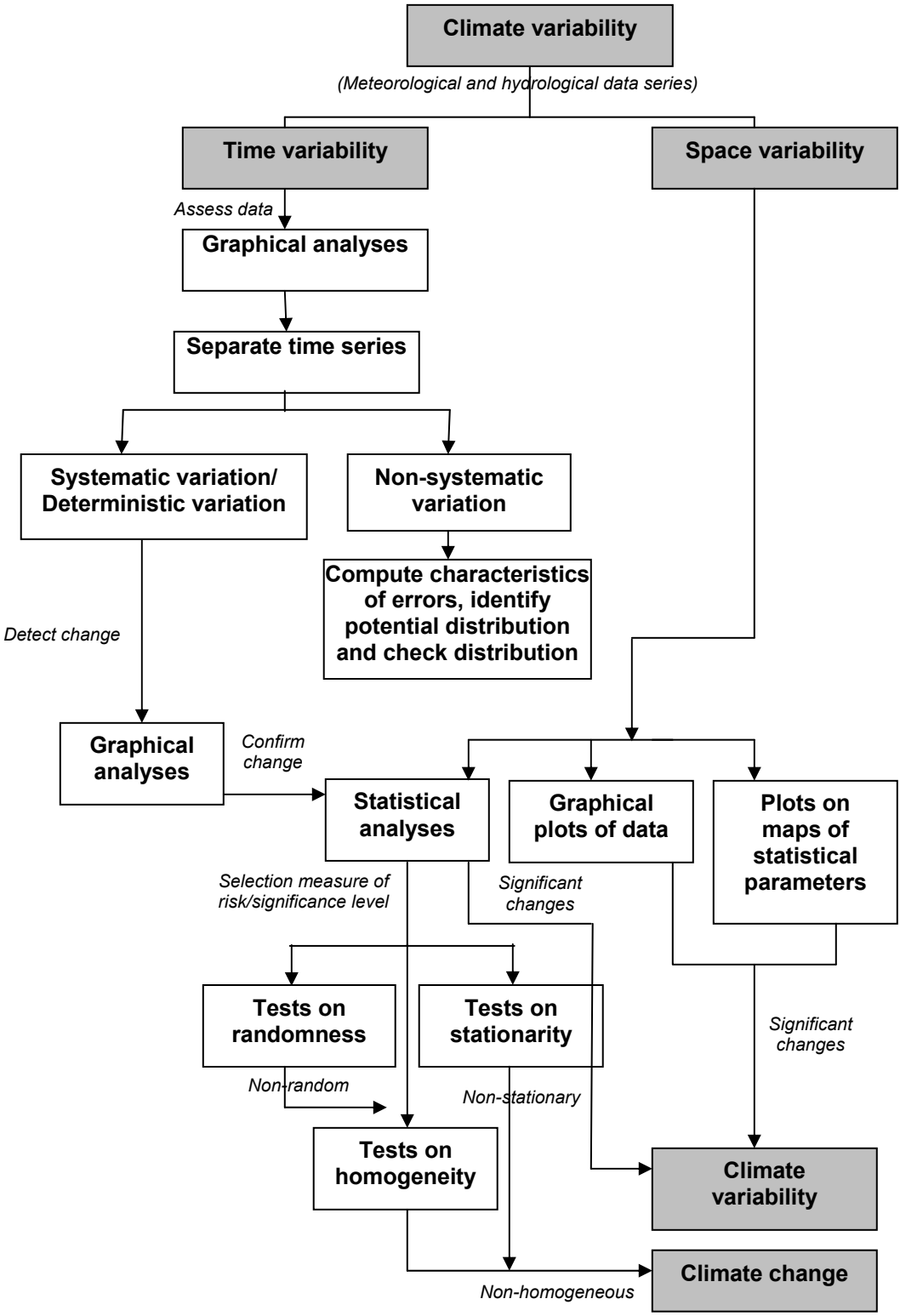

Figure 2.2: Schematic procedure for determining climate change and climate variability in meteorological and hydrological time series.

Statistical tests (parametric and non-parametric tests) are based on hypothesis testing, which includes the measure of risk or level of significance (e.g. 1%, 2.5%, 5% and 10%) and are used to confirm the amount of the change (McCuen, 2003). Some major advantages of non-parametric tests are: (a) they can be used for random variables measured on nominal and ordinary scale, while parametric tests can only be used for one of the scales, (b) they are less dependent on adequacy of the assumptions and the probabilities are usually exact, (c) they do not require a specific distribution of the data, while parametric tests require that the data follow a normal distribution, and (d) because small sample sizes are common, they are preferably used. The major disadvantages of non-parametric tests are: (a) they are based on ranks or counts and often result in tied values, which are more troublesome to deal with compared to parametric tests, (b) they are statically less powerful and give less quantitative information than parametric tests, and (c) in non-parametric tests it is also not possible to obtain critical values of exact levels of significance compared to parametric tests (Haan, 1977; Helsel and Hirsch, 1992; Jones et al*.,* 1996; McCuen, 2003; WMO, 1988). As most hydrological data series are positive skewed, non-parametric tests are well suited (Hirsch et al., 1992).

There is a range of methods in literature available to test randomness, stationariness and inhomogeneity of time series (Haan, 1977; Helsel and Hirsch, 1992; Hirsch et al., 1992; Mamdouh et al., 1993; McCuen, 2003). Some tests of randomness to measure monotonic increasing and decreasing trends in data are correlation analysis (e.g. the non-parametric Mann-Kendall linear correlation test, Spearman's linear correlation test, linear regression test, the parametric Pearson's linear correlation test, the Runs test, Von Neumann ratio test, serial correlation and double mass curve technique). Non-stationary in time series can be tested by the Kendall, Spearman, Pearson, Cox-Stuart and Run test (Haan, 1977; McCuen, 2003). Non-homogeneity should primarily be tested by graphical methods, followed by statistical tests such as the Mann-Kendall, Spearman, Pearson, Durban-Watson, t-test, Cumulative deviations, Run, and Cox-Stuart test. These powerful tests mainly check whether a significant change exists in the data and also the direction of the tendency (positive or negative trend). The Kendall's rank correlation coefficient is superior to the Spearman's rho correlation, because the large sample and rank approximations for the Spearman's correlation coefficient do not fit the distribution of the test statistics well for sample sizes smaller than 20. The Mann-Kendall and Spearman tests are less sensitive to outliers than the Pearson's test because they are based on ranks. They measure monotonic correlation between two continuous variables. The Pearson's test is computed using means and standard deviations and measures linear correlation. The Run test is based on the number of runs occurring in the data. A run is a set of observations above or below the mean of the observations (WMO, 1988). The serial

correlation test is a measure of common variation between adjacent values in a time series, but is however not very powerful for small samples (Haan, 1977; McCuen, 2003).

To test randomness against shift (or change point year) in the annual time series, different parametric and non-parametric tests are available such as the Standard Normal Homogeneity test of Alexandersson, the Craddock's test of Cumulative Deviations, the Worsley Likelihood ratio test, Kruskal-Wallis test and the parametric t-test. (Salas, 1992; WMO, 1988). The change point is the year where the slope of the first linear line changes with the second line. Basic assumption for the change point year tests is that the observations are independent and normally distributed. The Cumulative Deviations test works with anomalies and is easy to use. A disadvantage of the Standard Normal Homogeneity test is that the most probable years tend to occur near beginnings/ends of the series.

Trend and shifts can also be evaluated using filtering techniques on the annual values such as the moving filters. The moving average filter makes it easy to identify the form of the trend or period or cycle. This method does have some disadvantages. There are no rules for the choice of the smoothing interval and if the interval is not properly chosen, it is possible that all variation in the time series is eliminated. This technique is also not useful for short time series (McCuen, 2003). The statistical and graphical tests discussed in this chapter will be used for climate change analysis on precipitation, temperature and river discharges in chapter 3, 4 and 5.

2.3 Modelling of climate change

It may be easy to detect historical changes in hydro-meteorological time series, but making reliable projections of future changes in these variables may be more important. In the last 40 years, scientists have developed different techniques to estimate future changes in climate variables in temperature, precipitation, evaporation, soil moisture, runoff and sea level (Chong-Yu, 1999). The first method is the use of global circulation models (GCMs) on a large spatial scale (>10^4 km^2). These are three dimensional climate models that run on computers and are based on physical laws and physical empirical relationships. Since the development of GCMs in the 1960's, they have shown to be the most sophisticated method available till today (Chong-Yu, 1999; IPCC, 2001; IPCC-TGCIA, 1999; Hulme et al., 2000; Olivie, 1999; Santer et al., 1990; Wigley, 2003). Some of the leading GCMs are: the Had300 (UK Hadley Centre for Climate Prediction and Research - Europe), the ECH498 (German Climate Research Centre - Germany), the CCC199 (Canadian Centre for Climate Modelling and Analysis - Canada), the GFDL90 (US Geophysical Fluid Dynamics Laboratory - USA), the

CSI296 (Commonwealth Scientific and Research Organization - Australia), the GISS (Goddard Institute for Space Studies) and the CCSR96 (Japanese Centre for Climate Systems Research - Japan). The main disadvantages of GCM however are:

- Uncertainties in processes
  There is still a lot of uncertainty about the estimated climate variables especially precipitation. This is mainly caused by the deficiency of knowledge of physical-, chemical- and biological processes that produce climate, the uncertainty of future emissions of greenhouse gases (e.g. uncertainties in future population and economic growth, future technological development, deforestation rate, future agricultural development, future energy demand, future behaviour of the future climate system over large time scales), over- simplification of complex physical processes (such as oceans, sea ice, land-surface hydrology) and uncertainties on certain important phenomena such as cloud cover, water circulation of oceans, scale of motion in the ocean and the atmosphere.
- Spatial scale
  Due to the lack of geographical details (e.g. topography, land use, soil, parameters of the climate system), it is difficult to derive parameters on smaller scales and therefore GCMs cannot properly simulate the climate systems on smaller scales (10^{-2}-10^{4} km^2).
- Computation time
  The accuracy of a GCM partly depends on the spatial resolution of the grid and the length of the time step. Therefore a compromise must be made between the resolution desired and the computational facilities.

Because of the above-mentioned disadvantages, GCMs can only be considered for sensitivity analysis. It is therefore difficult to use GCM results for e.g. hydrological impact studies on river basin scale (10-100 km). To narrow the gaps between the GCMs ability and hydrology needs, four general techniques have been developed since the 1980's (Bronstert et al., 2002; Chong-Yu, 1999; IPCC-TGCIA, 1999; Giorgi, F. and Mearns, 1991; Mearns, 1999; Mearns et al., 2003). A summary of these techniques is given below:

- Statistical downscaling (SD)
  This technique simulates local surface variables based on large scale tropospheric variables through a statistical transfer function. Common procedures are weather-type methods (e.g. stochastic weather generators), regression-type methods (e.g. linear regression, artificial neural networks, principal components regression, canonical correlation analyses) and deterministic-type methods. Some two dimensional SD models are: the SDSM

statistical downscaling model of the Canadian Institute for Climate Studies CICS (U.S.A.), the CLIGEN weather generator of the Finnish Research Programme on Climate Change, the LARS-WG stochastic weather generator (U.K.) and the WGEN weather generator (U.S.A.) (Wilby and Dawson, 2001).

- Dynamical downscaling (DD)
  In this approach, a high resolution three dimensional regional climate model (RCM) is embedded in the GCM. RCM has become popular in the last 5-10 years, because of their high spatial resolution (20-50 km) and they can represent physical and dynamic processes in the climate system in a more realistic way, especially topographical forcing, land-sea and land use effects. Some RCM models are: the RegCM3 of the International Centre for theoretical Physics (Italy), the MM5 of National Center for Atmospheric Research (U.S.A.) and the PRECIS model of the Met Office (U.K.) (Arnell et al., 2003; Booij, 2002; Giorgi et al., 2001; Jones et al., 2004; Mearns et al., 1999)
  A main advantage of the downscaling techniques is that they are computationally inexpensive and provide information on a high resolution. The major disadvantage is that their basic assumption is often not verifiable e.g. the statistical relationship is the same under possible future climates. They also require high quality and long-term observations of surface and upper air climate variables (e.g. precipitation, pressure, wind speed, water vapour) (IPCC-TGCIA, 2003).
- Macro scale hydrological modelling (MHM).
  This technique uses a hydrological model for large basins (10^4 km^2) up till a continent.
- Hypothetical climate scenarios.
  These scenarios are plausible future climates. They are thus neither predictions nor forecasts of future conditions (IPCC-TGCIA, 1999; Jones at al, 2001; Mearns et al., 2003). They are developed from GCM results and used as input in a hydrological model. The historical time series can then be changed according to the climate change scenarios.
  For temperature this can be calculated as follows:

$$\left(T_{ij}\right)_1 = \left(T_{ij}\right)_0 + \Delta T_j \qquad \text{(Eq. 2.1)}$$

  where the subscript 0 and 1 refer to the scenario year 0 (present time series) and 1 (future time series under climate change conditions) respectively, T_{ij} is the temperature on day i of month j and ΔT_j is the monthly temperature increment. ΔT_j can be +1^{o}C, +2 ^{o}C, +3 ^{o}C.

  For precipitation this can be calculated as follows:

$$(P_{ij})_1 = (P_{ij})_0 \left[1 + \frac{\Delta P_j}{(P_j)_0} \right] \quad \text{(Eq. 2.2)}$$

where P_{ij} is the precipitation on day i of month j, P_j is the mean precipitation of month j and ΔP_j the monthly precipitation increment due to climate change conditions.

Most climate impact studies on water resources are based on GCM results and hypothetical scenarios, and to a lesser extend on RCM results, while the application of the other techniques is still in an experimental phase (Booij, 2002; Bronstert et al., 2002). The main advantage of GCMs currently is that their results are readily available and moreover, GCMs are considered to provide the best basis for the construction of climate change scenarios and to evaluate the effect of human activities on global climate. However, the different evaluation studies by the IPCC (2001) with regard to model performance between GCMs and RCMs, is that RCMs can reproduce average observations over regions of size 10^5-10^6 km^2 with errors generally below 2^{o}C and within 5% to 50% of observed precipitation, while GCMs have temperature biases generally below 4^{o}C and precipitation biases between -40% to 80% depending on the region and the model. The main uncertainty in future climate simulated by these types of climate models is thus mainly regarding precipitation. In chapter 6 and 7, GCM scenarios and hypothetical scenarios will be used to provide climate change scenarios (Robock et al., 1993; Whetton et al., 1993).

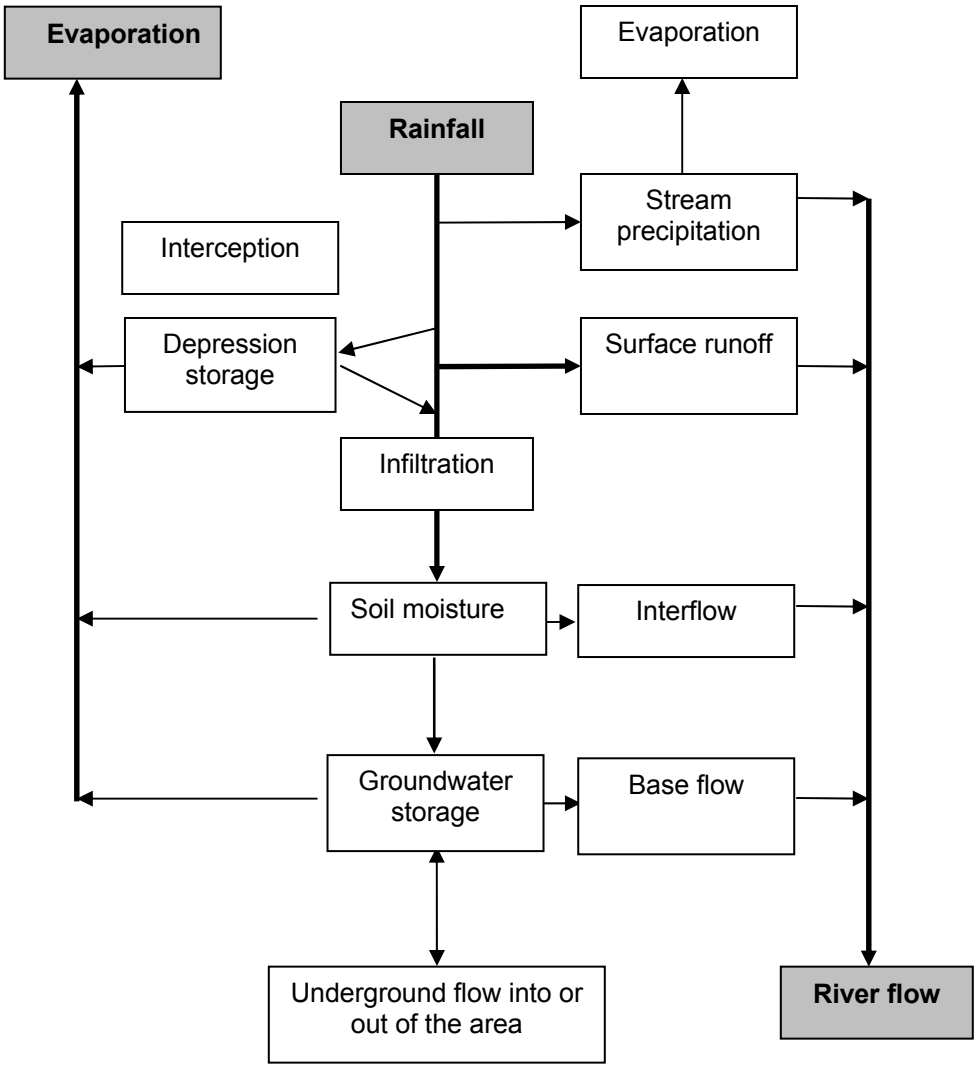

Figure 2.3: Schematic representation of the hydrological cycle on the land phase (Fekadu, 1999).

2.4 Modelling of water resources

In order to study the effects of a changing climate on water resources in e.g. a river basin, it is useful to use hydrological models. Since the mid 19th century, different hydrologic models have been developed (Gleick, 1987). Hydrologic models are based on the hydrologic cycle and consist of mathematical equations that describe the physical response of a river basin to climate inputs (e.g. precipitation, evaporation) and calculate for example

surface runoff, subsurface runoff, groundwater flow and infiltration. Figure 2.3 shows schematically the hydrological cycle of a river basin. As can be seen from this figure, precipitation that falls on the land surface is partly intercepted by vegetation, partly falls directly on rivers/streams/lakes and partly infiltrates into the soil. Precipitation that exceeds the interception capacity of the vegetation and infiltration capacity of the soil, starts the flow on land (surface runoff). Precipitation that has infiltrated may stay in the soil as soil moisture, move laterally as interflow or percolate further as groundwater recharge. The total runoff to a river consists thus of surface runoff, interflow and groundwater flow, and the total runoff returns to the ocean. This process goes on continuously.

The quantity of river flows, is besides precipitation, strongly affected by the physical characteristics of a river basin. Topographic features such as slopes have an important impact on runoff production. For example, if the slope length becomes shorter, a higher peak discharge will be reached. Soil constituents are important to the accurate modelling of runoff. Different soil types influence the infiltration and surface runoff. For example, sandy soils allow for more infiltration of precipitation than do heavier clay soils. Vegetation cover density affects mainly the surface runoff. For example, if the vegetation density increases, the infiltration increases, leading to a reduction in surface runoff. Different land use types causes different interception rates and also influences the surface runoff. Table 2.1 shows the most important variables that influence the main hydrological processes in a river basin. From this table it can thus be concluded that for modelling hydrological processes, detailed spatial information of the topography, soil and land use is important as is detailed temporal information on meteorological and hydrological data.

Nowadays there are many hydrological models available from different institutions and the Internet, and there are also different classifications for hydrological models (Booij, 2002; Maidment, 1993; Rientjes and Boekelman, 1998). The classification used in this thesis is based on the design of the models and consists of three groups: empirical, lumped/conceptual and physically-based models (Booij, 2002; WMO/UNESCO, 1997). Empirical models describe an output variable such as runoff in terms of input variables such as precipitation and evaporation, through a transform function, but without a prescription of the physical processes that occur. Lumped/conceptual models such as CLIRUN, WATBAL, Stanford watershed model, HBV model, PRMS-Precipitation Runoff Modelling System, represent the effective response of an entire basin, without attempting to characterize the spatial variability.

Table 2.1: Variables influencing the dominant hydrological processes in a river basin (Booij, 2002).

Variables	Processes						
	Precipitation	Actual evapotranspiration	Infiltration excess overland flow	Saturation excess over land flow	Subsurface storm flow	Subsurface flow	River flow
Precipitation	■	■	■	■	■	■	■
Temperature	■						
Potential evapotranspiration		■		■	■		■
Elevation	■	■	■	■	■		■
Land use		■	■	■	■		■
Soil texture		■	■	■	■	■	■
Macro pores					■		
Soil parent material			■			■	

Physically-based models such as the HSPF, HEC-1 and SHE, are able to represent the spatial variability of some of the important land surface characteristics such as elevation, vegetation, soil, and climatic parameters such as precipitation, evapotranspiration and temperature. Horizontal variability is modelled by representing the basin by individual sub-basins or grids and prescribing the hydrological characteristics of each basin or grid. Vertical variability is represented by vertical layers of the soil for each grid (Beven, 1989; Booij, 2002; Lui 2004).

Because of the many hydrologic models, the choice for such a model will depend on the appropriate mathematical processes formulation for the aim of the study, the appropriate spatial and temporal scale, and time and computation resources available (Chong-Yu-Xu, 1992).

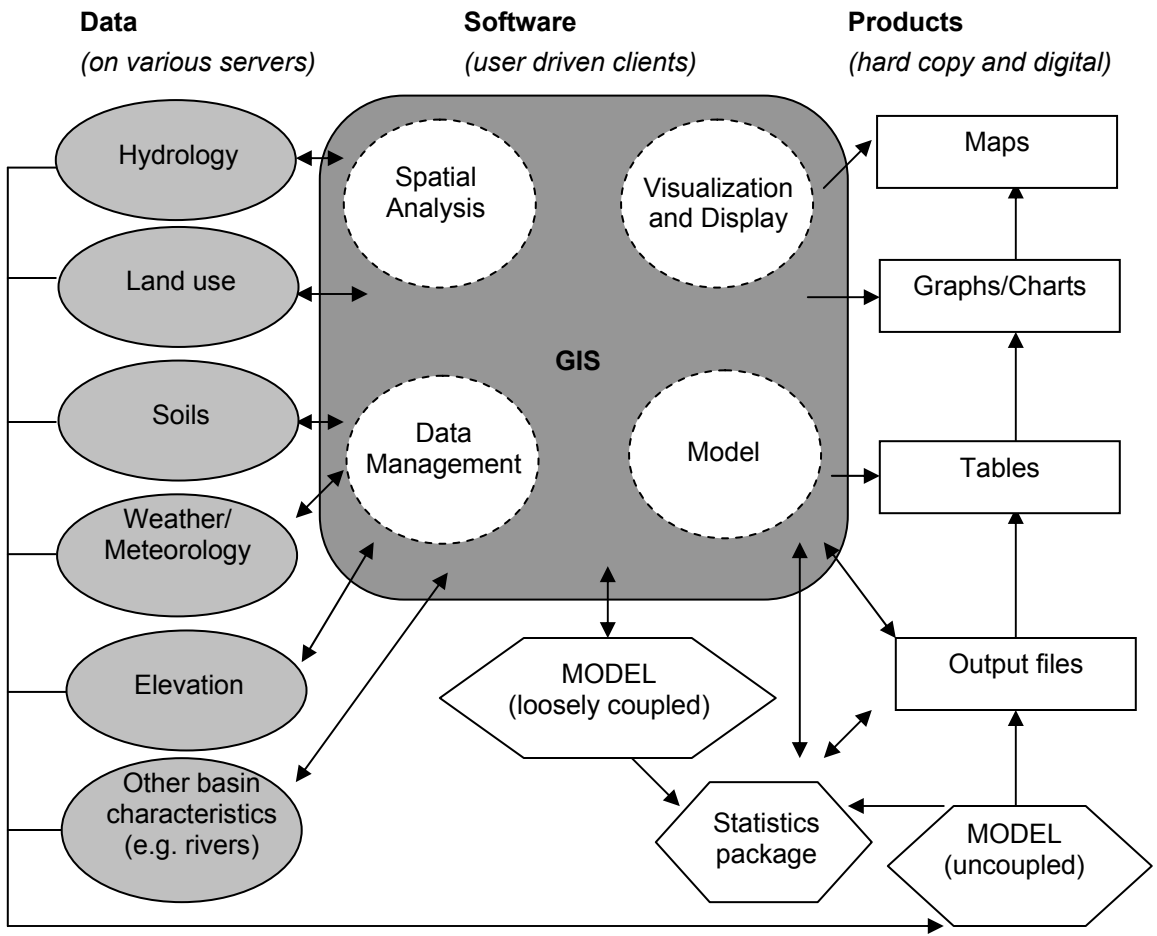

Figure 2.4: GIS-Hydrological modelling integration methods (after Liu, 2004).

There are however, just like with the climate models, also uncertainties introduced when using hydrologic modelling to study the response of a river basin. These are:

- Natural uncertainty (due to randomness and scale issues)
- Data uncertainty (due to errors in measurements, inadequacy of data)
- Model parameter uncertainty
- Model structure uncertainty (due to model incompleteness, model inaccuracy) (Booij, 2002)

Many hydrologic models nowadays can simulate the physical processes mathematically quit well and can also consider the spatial variation of model parameters. With the development of geographic information system techniques (GIS), hydrological models have become more physically based and distributed to account for the spatial heterogeneity of model parameters and processes at detail scale. As a result, the use of GIS in hydrological modelling has increased during recent years (Booij, 2002; Liu et al., 2003; 2004). Some integrated GIS-hydrological models are the TOPMODEL-Physical Based Runoff Production Model, the SHE model, IHDM-Institute of Hydrology Distributed Model, WATFLOOD-Waterloo Flood System, HBV-Hydrological Model System and the WetSPa model (Liu, Y., 2004). Fig. 2.4 shows the different inputs, processes and products that GIS software can perform with regard to hydrological modelling purposes.

Very few hydrologic modelling studies are known in the humid tropics. Because of the great variability in climate and land characteristics in these areas, it might be useful to use physically based distributed models (Andersen et al., 2001; Beven, 1989; 2000; Bormann, 2005; Campling et al., 2002; Molicova et al., 1997). In chapter 7, we will use the physically-based hydrological model WetSpa, from the Vrije Universiteit Brussels (Belgium), which has been made fully available by the promoter of this University to the University of Suriname, Department Infrastructure. This model has not yet been applied to tropical areas and large river basins with poor data.

2.5 Modelling of the impact of climate change on water resources

The impact of climate change on water resources (e.g. river basin) is usually assessed by defining climate scenarios for changes in climatic inputs (e.g. precipitation, temperature) to a hydrological model (IPCC, 2001). Climate scenarios can be calculated using different methods e.g. global circulation models (GCMs), regional climate models (RCMs), statistical downscaling techniques (SD), macro scale hydrological models (MHM) and hypothetical scenarios (Chong-Yu, 2000). Each of these methods has its own advantages

and disadvantages, and uncertainties and has already been discussed. There is also a variety of hydrological models available, each with its own characteristics such as data needs, time-spatial scale, modelled processes and uncertainties (Beven, 2000).

If we consider a river basin, the long-term average annual water balance can be presented by:

$$I_{(p)} = O_{(q,e,g)} \pm S_{(s)} \qquad \text{(Eq. 2.3)}$$

where "I" is the inflow in the system, "p" is the precipitation, "O" is the outflow in the system, "q" is the runoff, "e" is the evaporation, "g" is groundwater flow, "S" is storage in the system (change in soil moisture).

Precipitation and evaporation are climatic factors that are directly affected by climate change and this will cause different components of runoff including water resources to vary. Two situations may arise: "p" and "e" vary independently or "p" and "e" co-vary with climate.

In the last years, different studies have been performed in the field of climate change impact on water resources. Before the development of GCM (mid-1970s), most studies used hypothetical climate change scenarios, in combination with a hydrological model to assess the impact of climate change on water resources. For example, Bormann (2005) applied a lumped, conceptual UHP hydrological model to six river basins varying from 580 to 10,326 km^2 in the Queme river basin in tropical West-Africa and hypothetical scenarios based on SRES scenarios of the IPCC. The results show that a reduction in precipitation of 10% in the basin reduces the river discharge by about 35%. The UHP model has shown to be useful for tropical areas if physical data of the basin are available and rainfall data is scarce. About the same approach was also used in studies by Chiew et al. (1995), Gellens and Roulin (1998), Legesse et al. (2003), Nash and Gleick (1991), Niemann et al. (1994) and Yates (1994).

When GCMs became available, the results of these works were used as inputs in hydrological models. For example, in Guyana, the CGCM1 (Canadian Climate Center) and the HadCM2 model (Hadley Center) were used to study changes in precipitation, temperature, evaporation and water deficit (difference between precipitation and evaporation) for three time slices 1975-1995 (present), 2020-2040 ($2xCO_2$) and 2080-2100 ($3xCO_2$). The results show that under tripling of CO_2, the average temperature will rise with about 4.2^oC, evaporation will increase by about 3.3 mm/month, rainfall will decrease by about 21 mm/month and as a result, Guyana might experience large water deficits (22 mm/month) in the future. About the same approach

was also used in studies by Boorman and Sefton (1997), Demiraj et al. (2004) and Mimikou et al. (2000).

Meanwhile other techniques have also been used in recent years such as statistical downscaling and RCMs. For example, Menzel and Burger (2002) used a semi-distributed conceptual model HBV to simulate future changes in river discharges for the Mulde river basin (6,171 km^2) in Germany. A downscaling technique was used to temperature from the ECHAM4/OPYC3 GCM to local surface variables. The results show that by 2100, an increase in temperature will result in reduced precipitation and a decrease in river discharge in this basin. In southern Africa (23,000 km^2), the HadRM3H RCM was used to estimate changes in runoff. The results of 16 climate scenarios show that the average annual runoff will increase between 20% to 40% or even higher. The study, however, shows that the RCM model has overestimated rainfall and as a result produces too much runoff (Arnell et al., 2003).

From the above studies it can may be concluded that there are no appropriate methods to study the effects of climate change on water resources, but all the methods have shown their advantages in the studies. The obtained results were found satisfactory, but the authors warn that hydrological models are not designed to present future climates. So one should be careful taken when using the results. Whetton et al. (1993) has recommended to use more than one GCM in assessing climate change, because of the different predictions and variety in GCM scenarios and Robock et al. (1993) has advised also to use a range of hypothetical scenarios for climate impact studies on water resources. Gleick (1986, 1987) and Nemec and Schaake (1982) have concluded from different studies that simple water balance models are better to use because they are easier to use and require less computation compared to other types of hydrological models. They also proposes to use downscaling techniques or macro hydrological models to overcome the limitations of GCMs. This is also advised by Booij (2002). From the above recommendations and the available resources at our Department, it has therefore been decided to use GCMs and hypothetical climate scenarios and a distributed hydrological model for this research.

2.6 Conclusions

There is a variety of graphical and statistical methods available in literature to detect historical climate change, but each has its own purpose and limitation, and they are all based on hypothesis testing. The final results of the statistical output will mainly depend on the choice of a statistical test, the length of the data series and the significance level. The outputs of climate

variability analyses will in addition to climate change analyses also depend on the spatial distribution of observations. Global and regional climate models still have uncertainties in some processes, which influences to outputs of current and future changes in mainly temperature and precipitation. The main problem for river basin studies is still the spatial scale of global climate models. Other techniques such as downscaling techniques are easier to use, especially on a regional scale, but require also high resolution atmospheric and land surface data, which is mostly lacking, such as in Suriname. In case GCMs and RCMs are used, the outputs should only be used for sensitivity analyses. There are thus no appropriate methods to study regional effects of global climate change and it is also difficult to evaluate future climate change conditions on regional scale (river basin scale). However, many hydrologic models can very well simulate water balance components of river basins and can therefore also easily be used to simulate future water balance components under climate change conditions. However, hydrologic models (e.g. distributed models) also contain uncertainties in some hydrologic processes, and therefore, the final results using climate change time series should also be analysed with care.

Acknowledgements

I am thankful for the constructive and valuable review comments by Drs B. Tan, and C. Becker. Dipl.Met.

3. CHANGES IN SURINAME'S CLIMATE AND INFLUENCES ON WATER RESOURCES*

Abstract

This chapter highlights historical climate changes in long-term and short-term (1961-1985) rainfall, temperature and river discharge observations in Suriname and the impacts of these changes on surface water resources. Statistical tests are used to analyse the monthly and annual rainfall at 11 stations (1961-1985), the monthly and annual temperature at 6 stations (1971-1985) and the annual river discharges at 4 stations (1961-1985) in Suriname. Correlation analyses are used to study the relation between the annual rainfall (and discharge anomalies) and the annual sea surface temperature anomalies (SSTAs) in the Tropical North Atlantic (TNA), the Tropical South Atlantic (TSA) and the Tropical Pacific. Principal component analysis (PCA) and the Pearson's correlation coefficient (r) show that the annual rainfall anomalies are more or less uniform across Suriname. Linear trend analysis has shown that different trend (positive and negative) occur at different stations, in both monthly and annual rainfall. However, all the monthly and annual temperature time series indicate a warming trend. The difference in trend values in the annual rainfall and discharge may be caused by high spatial and temporal variability of rainfall and river discharges, the different statistical tests used and the shortness of the data series. Affects of El Niño events have shown that most months can become drier than normal, especially for stations along the coastal zone and in the centre of Suriname. In the eastern, western and southern parts of Suriname it is just the opposite. Affects of La Niña events in Suriname have shown that most months can become wetter than normal. The changes (trends) in annual river discharges are found to be closely related to the changes in annual rainfall. It is also found that the annual rainfall anomalies are stronger correlated to the SSTAs in the Atlantic region. Extreme SSTAs affect the inter-tropical convergence zone (ITCZ) and may result in years with rainfall excess and deficits, through delaying the movement of the ITCZ, and also during El Niño and La Niña events respectively. The historical changes in rainfall have shown to cause

* Part of this chapter has been published as: "Effects of global climate change and climate variability on Suriname's climate and water resources" in Interactie - Journal of the ADEK University of Suriname, 2005-7, pp 47-60, ADEK University of Suriname.

* Part of the results in this chapter has been presented as "Trends and variation in monthly rainfall and temperature in Suriname" at the Conference on Water Observation and Information System for Decision Support, 25-29 May 2004, Ohrid, FY Republic of Macedonia.

* Part of this chapter has been re-submitted as: "Changes in annual rainfall and river discharges in Suriname" to the International Journal of Climatic Change, 2007.

significant changes in surface water resources. Suriname's climate and freshwater resources are thus sensitive to long term and short changes in rainfall either by climate change (temperature increase) or climate variability (changes in SST), while freshwater resources in the coastal area of Suriname, are more sensitive to sea level rise. With the projected future increase in temperature, it is expected that freshwater resources will increase or decrease, resulting in more floods and droughts and finally human and economic damages. It is therefore recommend that it is better to include climate change and climate variability in future designs, planning and management of fresh water resources and water resources systems in Suriname. To get a better understanding of the impact of global climate change on Suriname's climate and fresh water resources, it is necessary that the responsible institutions in Suriname continue the collection of different hydro-meteorological variables. Further studies are also required for a better understanding of the influences of the Atlantic and Pacific climate processes on the rainfall and temperature in Suriname.

3.1 Introduction

It is only in recent years that trends and variation in extreme climate events such as heavy rainfall, prolonged dry periods, extreme hot days, large-scale floods and droughts, have received the world's attention which, due to global climate change, are expected to change in frequency as well as in magnitude and location (Jones, et al., 1996, McMichael and Haines, 1996; IPCC, 2001). In this way, global climate change may have serious negative impacts on the existing water resources leading to more economic losses and victims worldwide.

In the tropics, rainfall is the main source of fresh water resources. Long-term changes in parameters of climate (e.g. rainfall) will affect the water resources of various socio-economic sectors such as agriculture and livestock, hydropower generation, coastal ecosystems and water supply systems (e.g. reservoirs, aquifers). Rainfall variability is another important variable for designing and operating waterworks and hydraulic structures such as dikes/dams, sluices, canals, reservoirs, and for the planning and management of water resources systems e.g. irrigation/drainage schedules, spilling of water from reservoirs. Both of these parameters are of great importance to Suriname.

The rainfall pattern in Suriname is influenced by different oceanic-atmospheric processes such as: (a) the Intertropical Convergence Zone, (b) land-sea interactions, (c) land processes, (d) the El Niño-related sea surface temperature anomalies (ENSO-SST), and (e) the Tropical Atlantic Sea Surface Temperature anomalies (TA-SST) (Acevedo et al., 1999; Gable and Aubrey, 1990; Giannini et al., 2000; Rajagopolan et al., (undated); Rasmussen and Wallace, 1983; Robertson and Mechoso, 2002; Villwock, 1998; Wallace et al., 1994). Some of these processes are shown in Figure 1.8. Studies by Garzoli et al. (1999), Giannini et al. (2000), Marshall et al. (2001) and Villwock (1998) have shown that the climate variability in northeast South America (e.g. northeast Brazil), in particular rainfall, is more related to the SSTAs in the Tropical North Atlantic (TNA) region than to the Tropical South Atlantic (TSA) region and the Tropical Pacific. Rainfall variability in the Central American/Caribbean region appears to be more related to TNA SST fluctuations. When e.g. the SSTs in the TNA are warmer than normal, and the SSTs in the TSA colder than normal, the ITCZ is displaced northward during March-May. This causes an increase in rainfall in northeast South America. ENSO events have the strongest influences on rainfall such as in northern South America and may intensify the seasons e.g. by wetter or drier years than normal (Ambrizzi et al., 2005; Berlage, 1957; Martis et al., 2002; Rajagopolan et al., 1997; Ropelewski and Hapert, 1987, 1989, 1996; Wang, 2001). During the warm ENSO events, the SSTs

also increase in the TNA, reaching their maximum during December-February and March-May. During these periods, rainfall deficits are experienced in northeast South America such as in 1972-1973, 1982-1983 and 1997-1998. During La Niña events, SSTAs in the equatorial Pacific are negative and reach their peak between June-September. Rainfall excess is then experienced in northern South America during December-February and March-May such as in 1973-1974, 1975-1976 and 1988-1989 (Robertson and Mechoso, 2002; Turner, 2004; Wang, 2005).

In Suriname, the weather system is mainly determined by the north and southward (10^{o}N-0^{o}S) displacement of the Intertropical Convergence Zone (ITCZ) (Figure 3.1). During its passage, Suriname experiences heavy rain (early December-early February; April-mid-August), while dry seasons occur during its absence (February-early March; mid-August-December). The two rainy seasons contribute for 18 and 56% respectively to the annual rainfall in Suriname, while the two dry seasons contribute for 13 and 13% respectively to the annual rainfall in Suriname (Emanuels, 1968; SPS/OAS, 1988). For illustration purposes, the monthly rainfall distribution for the Cultuurtuin station is shown in Figure 3.2. The annual average rainfall distribution in Suriname for the period 1961-1985 is illustrated in Figure 1.9 showing the highest annual rainfall in the centre of Suriname (Tafelberg: approximately 2,850 mm) and the lowest in the north-western part of Suriname (Coronie and Nieuw-Nickerie: approximately 1,358 mm). From Figure 1.9 it appears thus that not only is the distribution of rainfall during the year not equal, but also the spatial distribution of rainfall. The average annual air temperature varies from 26^{o}C to 27.7^{o}C with daily maximum air temperatures varying from 33.7^{o}C to 37.5^{o}C. The average annual evaporation in Suriname varies from about 1600 mm to 1900 mm/year (Lenselink and van der Weert, 1970).

Although Suriname has experienced different periods of extreme climate events, little is still known about these historical changes in especially rainfall and the causes of these events. With the growing concern about the impacts of global climate change on especially freshwater resources, it may be important to understand the relation between the historical climate changes and water resources, but also the future changes. In this chapter long-term historical monthly rainfall and temperature data will be analysed with respect to climate change and climate variability (El Niño/La Niña events) and statistical analyses will be used to study the presence of changes (e.g. trends, shifts) in the historical annual rainfall, temperature and river discharge time series (1961-1985). The relationship between the annual rainfall and river discharge anomalies with the Atlantic and Pacific SSTAs will be analysed using correlation analyses.

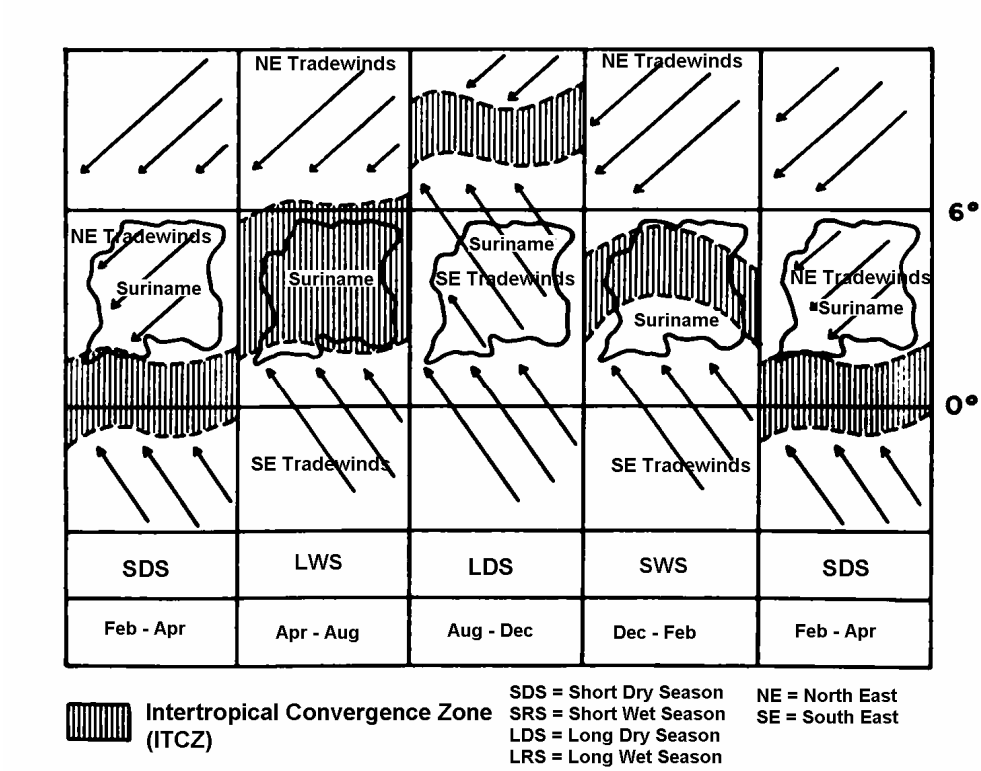

Figure 3.1: Movement of the Intertropical Convergence Zone (ITCZ) above Suriname (SPS/OAS, 1988).

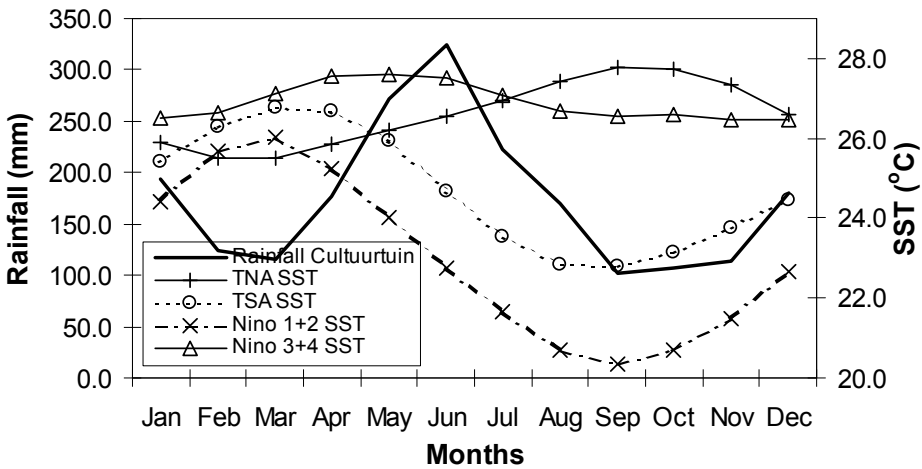

Figure 3.2: Observed monthly rainfall at Cultuurtuin (Paramaribo) and observed monthly SSTs in the TNA, TSA, and Niño 3+4 regions for the period of 1961-1985.

The relation between El Niño and La Niña events and the annual rainfall and river discharge anomalies will also be studied. Finally, the possible affects of climate changes on fresh water resources in Suriname will be discussed.

3.2 Data used

For this study, 11 rainfall stations were selected having sufficient data (> 25 years) and spatial coverage to characterize changes in annual rainfall, 4 river discharge stations (> 25 years) for 3 river basins and 6 temperature stations (> 15 years). Table 3.1 shows the characteristics of the different stations and Figure 3.3 the location of these stations. Due to the war in Suriname in 1986-1989, most of the hydro-meteorological stations in the interior were closed and therefore data is only available till 1985. Limited financial resources have also led to poor operation of stations in the northern part of Suriname. Daily observed meteorological data has been provided by the Suriname Meteorological Service and daily observed hydrological data has been provided by the Hydraulic Research Division, the Bureau for Hydroelectric Power Works and the Bauxite Institute Suriname/Suriname Aluminum Company LLC. Monthly observed SSTs (1961-1985) are adapted from the National Oceanic and Atmospheric Administration (NOAA-CIRES Climate Diagnostics Center, 2004) for the Tropical Northern Atlantic-TNA (5.5^{o}-23.5^{o}N, 15^{o}-57.5^{o}W), the Tropical Southern Atlantic-TSA (0^{o}-20^{o}S, 10^{o}E-30^{o}W) and the East Central Pacific ENSO-Niño 3+4 (5^{o}N-5^{o}S, 160^{o}E-150^{o}W). Figure 3.2 shows the observed monthly SSTs, Figure 3.4 shows the observed monthly SSTAs in the different regions. A positive anomaly indicates a warm SST in the ocean and a negative SST indicates a cooler ocean. Figure 3.5 shows the observed annual anomalies in rainfall and river discharges for the selected stations for the period of 1961-1985.

Table 3.1: Characteristics of (a) meteorological stations and (b) hydrological stations.

Station	Name and WMO name	Position	Altitude (m)	Precipitation data (period (years))	Temperature data (period (years))
1. Albina	803 KALBI - 81208	05.39N-54.03W	**	1915-1985 (71)	-
2. Brownsweg	64 BROW - *	05.01N-55.09W	490	1911-1986 (76)	-
3. Coeroeni	109 KCOER - 81253	03.22N-57.20W	165	1961-1985 (25)	1971-1986 (16)
4. Cultuurtuin	602 KCULT - 81201	05.50N-55.10W	**	1900-1999 (100)	1971-1999 (29)
5. Friendship Totness	301 FRIE - *	05.52N-56.20W	**	1904-1985 (82)	-
6. Groningen	501 GRON - *	05.47N-55.29W	**	1913-2001 (89)	-
7. Moengo	701 MOEN - 81206	05.37N-54.24W	**	1919-1985 (67)	-
8. Sipaliwini	112 SIPA - *	02.02N-56.07W	265	1961-1986 (26)	1971-1985 (15)
9. Stoelmanseiland	805 KSTOE - 81209	04.21N-54.25W	52	1959-1986 (28)	1971-1999 (29)
10. Tafelberg	513 KTAF - 81250	03.47N-56.09W	323	1959-1986 (28)	1971-1986 (16)
11. Nw-Nickerie	209 KNICK - 81202	05.56N-57.00W	**	1960-1999 (40)	1971-1986 (16)

* The stations without WMO number are rainfall stations
** indicates that the altitude of these stations is between 0-4 m above mean sea level.

(a)

Station	River/basin name	Position	Catchment upstream of station (km^2)	River discharge data (period (years))
1. Dramhosso	Saramacca	04.54N-55.34W	5,682	1960-1985 (26)
2. Langa Tabbetje	Marowijne	05.00N-54.31W	63,700	1952-1984 (33)
3. Semoisie	Upper Suriname	04.00N-55.50W	5,682	1952-1985 (34)
4. Pokigron	Upper Suriname	04.30N-55.22W	7,860	1952-1985 (34)

(b)

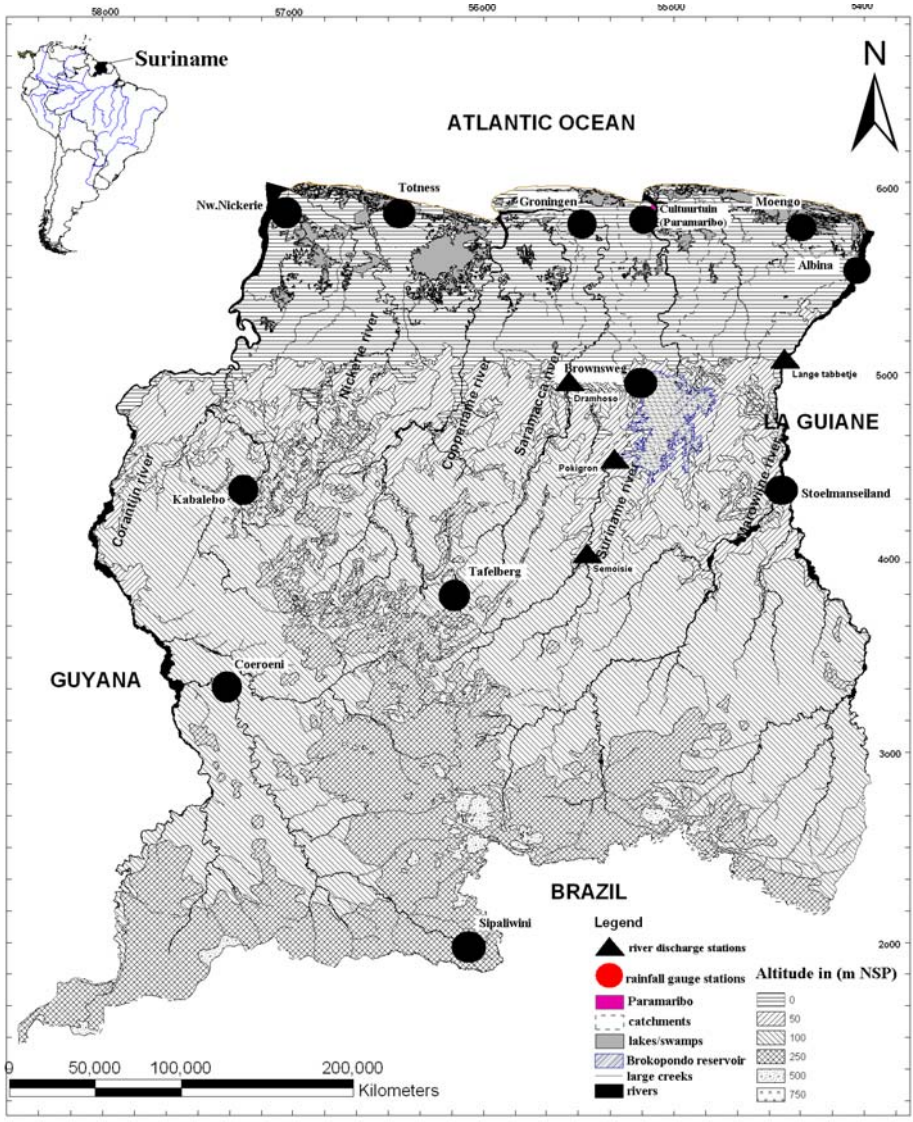

Figure 3.3: Location of the selected meteorological and hydrological stations in Suriname. Note: the circles show the location of the rainfall stations and the triangles show the river discharge stations.

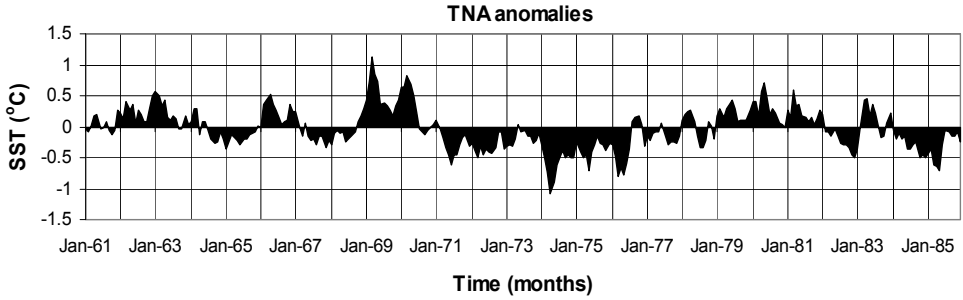

(a)

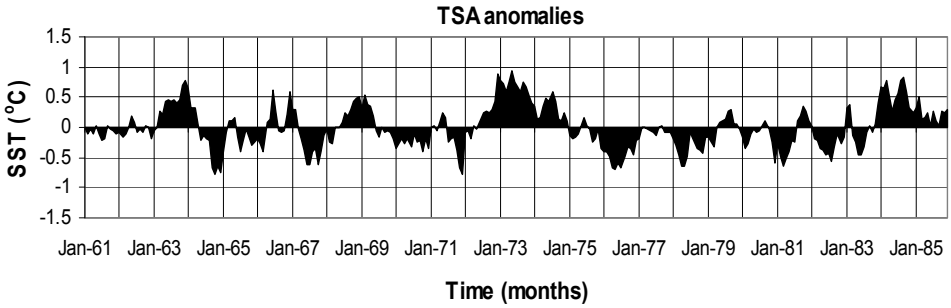

(b)

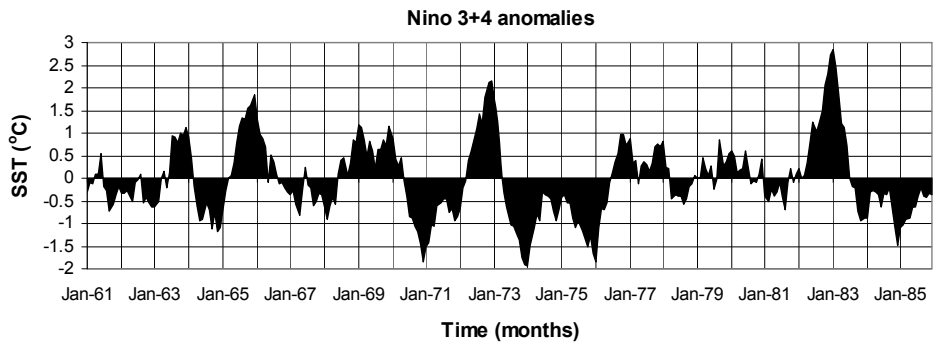

(c)

Figure 3.4: Time series of spatial mean SST anomalies with respect to 1961-1985 climatology in the (a) TNA region (5.5°-23.5 °N, 15°-57.5 °W), (b) TSA region (0°-20 °S, 10°E-30°W) and (c) Niño 3+4 region (5°N-5°S, 160°E-150°W).

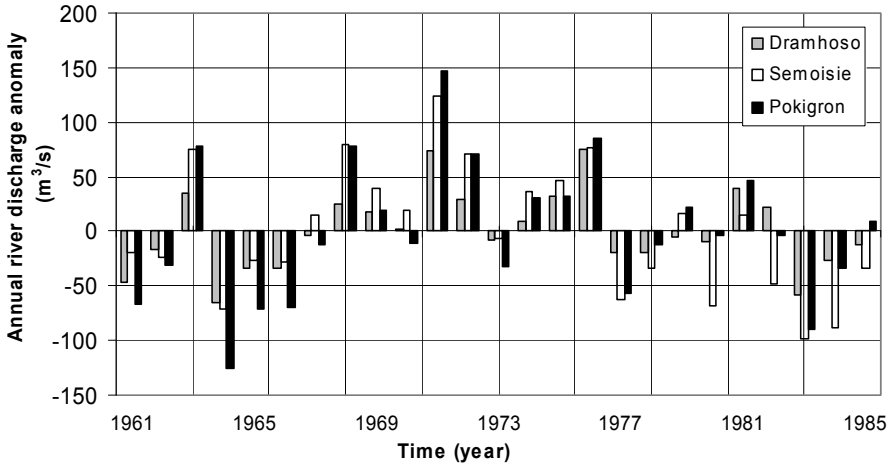
Annual river discharge anomaly (m3/s)
200
150
100
50
0
-50
-100
-150
1961
1965
1969
1973
1977
1981
1985
Time (year)
Dramhoso
Semoisie
Pokigron

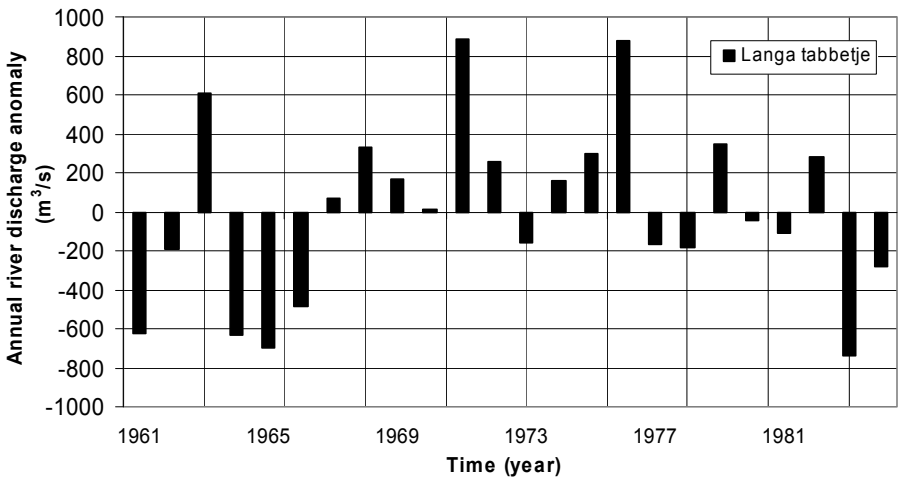
Annual river discharge anomaly (m3/s)
1000
800
600
400
200
0
-200
-400
-600
-800
-1000
1961
1965
1969
1973
1977
1981
Time (year)
Langa tabbetje

(a)

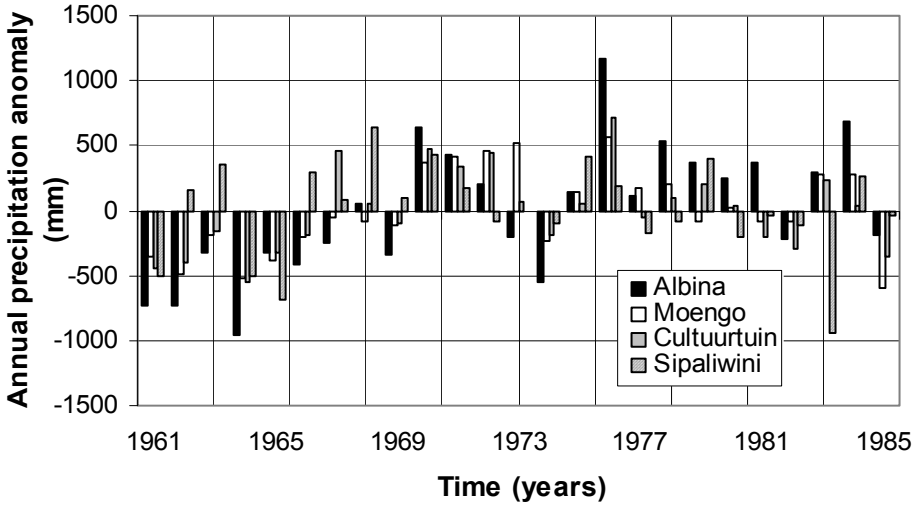
Annual precipitation anomaly (mm)
1500
1000
500
0
-500
-1000
-1500
1961
1965
1969
1973
1977
1981
1985
Time (years)
Albina
Moengo
Cultuurtuin
Sipaliwini

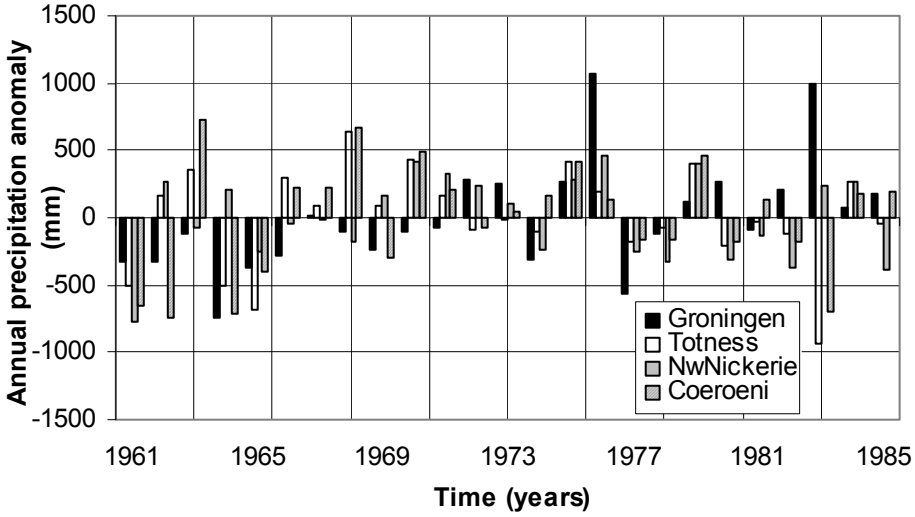
Annual precipitation anomaly (mm)
1500
1000
500
0
-500
-1000
-1500
1961
1965
1969
1973
1977
1981
1985
Time (years)
Groningen
Totness
NwNickerie
Coeroeni

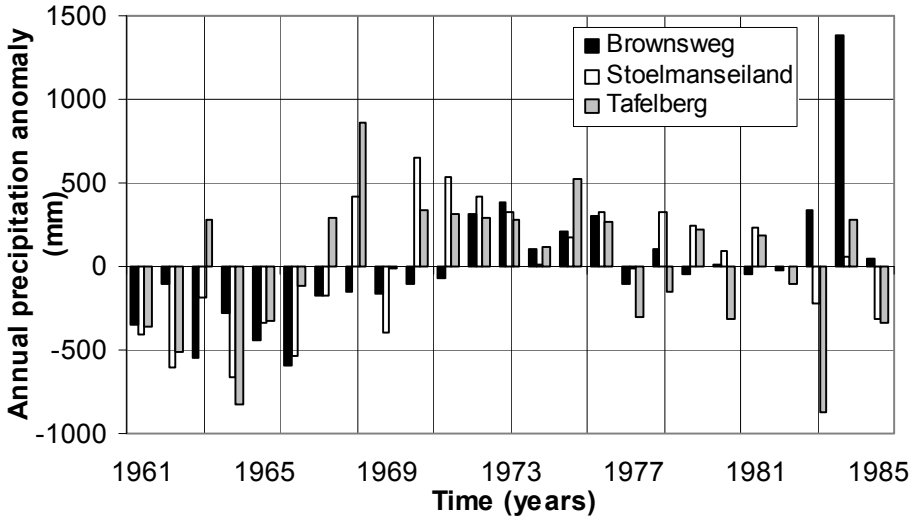

(b)

Figure 3.5: (a) Anomalies in annual river discharge and (b) anomalies in annual precipitation for the period 1961-1985 at the different stations.

3.3 Methodology

The complete monthly and annual time series are used to calculate the mean rainfall and temperature at the different stations, and linear regression analyses are used to identify negative or positive trends in these two variables. These time series are also used to analyse the impact of El Niño and La Niña climate variation by taking into account whether or not a month is wetter (W) or drier (D) than "normal" (which is the long-term annual average). The El Niño and La Niña years identified by Null (2002) and Couper-Johnston (2001) are used in this study (Retrieved April 10, 2003 from http://ggweather.com/enso/years.htm, http://conservewater.melbournewater.com.au/content/conserve/el_nino_years.htm). The common period 1961-1985 (25 years) is further used to identify spatial and temporal changes in the annual rainfall and river discharges. Because of the fact that the temperature time series are too short (15 years), they have been left out for further analysis (WMO, 1988). The mean $\bar{x}$, standard deviation s_x and variance S_x^2 are calculated as follows:

$$\bar{x} = \frac{\sum_{i=1}^{n} x_i}{n} \qquad \text{(Eq. 3.1)}$$

$$s_x = \sqrt{\frac{\sum (x_i - \bar{x})^2}{N}} \qquad \text{(Eq. 3.2)}$$

$$S_x{}^2 = \frac{1}{n-1}\sum \left(x_i - \bar{x}\right)^2 \quad (unbiased\ \ form) \qquad \text{(Eq. 3.3)}$$

where s is the ungrouped data series and n is the sample size.

In-homogeneity in the time series of annual precipitation and river discharges is tested by means of the Mann-Kendall, Spearman's and Regression test, the serial correlation coefficient, Run test and the Von Neumann ratio. The first three tests are based on the correlation coefficient ρ ($0 \leq \rho \leq 1$), which measures the strength between two continuous variables x_j and x_k. The hypothesis for these tests can be formulated as follows:
H_o: ρ = 0 (x_j and x_k are uncorrelated) and H_1: ρ ≠ 0 (x_j and x_k are correlated). Below a short description of these tests is given.

The **Mann-Kendall correlation coefficient τ or Mann-Kendall rank statistic (τ)** can be calculated as follows:

$$\tau = \frac{4P}{N(N-1)} - 1 \qquad \text{(Eq. 3.4)}$$

$$\text{with } P = \sum_{i=1}^{N-1} n_i \qquad \text{(Eq. 3.5)}$$

where n_i is the number of components with have got value greater than x_1 (or k_1), N is the number of components of the series (sample size).

For N>10, τ describes a Gauss normal distribution (x = 0, S_x^2 = (4N+10)/(9N(N-1)). The calculated value can be compared with the critical value:

$$(\tau)_t = 0 \pm t_g \sqrt{\frac{4N+10}{9N(N-1)}} \qquad \text{(Eq. 3.6)}$$

where t_g is the value of Gauss normal distribution with required significance level for a two-side test.

The decisions rule is as follows: if $z > z_\alpha$ or $< -z_\alpha$, the null hypothesis (H_o) is rejected, meaning that the data series contains a trend. α is the level of significance and $\pm z_\alpha$ is the critical value, which can be taken from literature (Helsel and Hirsch, 1992; McCuen, 2003).

The **Spearman's coefficient r_s or Spearman rank statistic r_S** can be calculated as follows:

$$r_s = 1 - \frac{6\sum_{i=1}^{N} d_i^{\,2}}{N(N^2-1)} \qquad \text{(Eq. 3.7)}$$

with $d_i = k_i - i$

where N is the sample size, d_i are the ranks.

For sample sizes of N > 8, the test statistic is given by:

$$t = r_s \sqrt{\frac{N-2}{1-r_s^{\,2}}} \qquad \text{(Eq. 3.8)}$$

The decision rule is as follows: if $t > t_\alpha$, H_o is rejected, meaning the trend is significant. t is the computated test criterion, t_α is the critical value of the Student t distribution with (N-2) degrees of freedom and α is the level of significance (Helsel and Hirsch, 1992; McCuen, 2003).

The **Pearson correlation coefficient R** can be calculated as follows:

$$R = \frac{\sum_{i=1}^{n-1} x_i x_{i+1} - \left(\sum_{i=1}^{n-1} x_i\right)\left(\sum_{i=2}^{n} x_i\right)/(n-1)}{\left[\frac{\left(\sum_{i=1}^{n-1} x_i^{\,2}\right) - \left(\sum_{i=1}^{n-1} x_i\right)}{n-1}\right]^{0.5} \left[\frac{\left(\sum_{i=2}^{n} - \left(\sum_{i=2}^{n} x_i\right)^2\right)}{n-1}\right]^{0.5}} \qquad \text{(Eq. 3.9)}$$

The significance of the Pearson R can be tested, using the following test statistic:

$$t = \frac{R}{\left((1-R^2)/(n-3)\right)^{0.5}} \qquad \text{(Eq. 3.10)}$$

where n is the sample size, t is the value of a statistic that has (n-3) degrees of freedom (t follows the Student's t distribution), $t_{v,\alpha}$ is the critical t value and can be obtained from tables in literature (Helsel and Hirsch, 1992; McCuen, 2003).

The decisions rule is as follows: if $t > t_{v,\alpha}$, H_o is rejected, meaning the trend is significant.

The **serial correlation coefficient r_1** can be expressed as:

$$r_1 = \frac{(N-1)\sum_{i=1}^{N-1} x_i x_{i+1} - (\sum_{i=1}^{N-1} x_i)(\sum_{i=2}^{N} x_i)}{\left[(N-1)\sum_{i=1}^{N-1} x_i^{\,2} - (\sum_{i=1}^{N-1} x_i)^2\right]^{1/2}\left[(N-1)\sum_{i=2}^{N} x_i^{\,2} - (\sum_{i=2}^{N} x_i)^2\right]^{1/2}} \quad \text{(Eq. 3.11)}$$

where N is the number of components of series (sample size), x_i is the value of the i-component of the observed series.

For distributions similar to the Gaussian distribution (for N > 40 we can accept expectations of normal distribution), we can use the following equation:

$$(r_{1)t} = \frac{-1 \pm t_g \sqrt{(N-2)}}{N-1} \quad \text{(Eq. 3.12)}$$

where t_g is the value of a standardized Gauss distribution for given significance level corresponding to a value r_1.

If $r_1 > r_{1t}$, the series are non-random and thus dependent of each other (for given significance level). In case the frequency distribution differs from the Gauss (normal) distribution, we can use the following critical value calculation equation:

$$(r_1)_t = \frac{(S_1^{\,2} - S_2) + t_g \sqrt{F(S)}}{N-1} \quad \text{(Eq. 3.13)}$$

with

$F(S)$

=

$$(N-1)(S_2^{\,2} - S_4) + \frac{N-1}{N-2}(S_1^{\,4} - 4S_1^{\,2}S_2 + 4S_1S_3 + S_2^{\,2} - 2S_4) - (S_1^{\,2} - S_2)^2$$

$S_p = \sum_{i=1}^{N} x_i^{\,p}$, p = 1, 2, 3, 4.

The hypothesis for the **Run test** can be formulated as follows: H_o: the data are randomly distributed and H_1: the data are not randomly distributed (non-homogenous). The test statistic is given by:

$$z = \frac{U - \overline{U} - 0.5}{S_u} \quad \text{(Eq. 3.14)}$$

where U is the number of runs, Ū is the mean, $[(2n_1n_2)/(n_1n_2)]+1$ and S_u^2 is the variance, $2n_1n_2(2n_1n_2-n_1-n_2)/(n_1+n_2)^2(n_1+n_2-1)$, n is the sample size, with

n_1 and n_2 number of outcomes x_1 and x_2, x_1 and x_2 are possible outcomes of a sample data ($n_1 + n_2 = n$).

The decisions rule is as follows: if $z \leq z_\alpha$, reject H_o, meaning that the data are non- random and there is real evidence of a trend. z is the computated value, z_α is the critical number of runs and can be taken from statistical tables in literature and α is the level of significance. For data samples where both n_1 or $n_2 < 20$, statistical tables from literature can be used (McCuen, 2003). For large sample sizes (n_1 and $n_2 > 20$), one can apply a Normal approximation $z \sim N(U, S_u^2)$ using the equations above (McCuen, 2003).

The **Von Neumann ratio** is defined as the ratio of the mean square (year to year) difference to the variable and can be given by:

$$V = \frac{N}{N-1} \frac{\sum_{i=1}^{N-1} (x_i - x_{i+1})^2}{\sum_{i=1}^{N} x_i^2 - \frac{1}{N} (\sum_{i=1}^{N} x_i)^2} \qquad \text{(Eq. 3.15)}$$

where N is the sample size, x_i is the value of the i-component of the observed series, V has got a Gauss normal distribution with expected value $2N/(N-1)$ and variance given approximately $4(N-2)/(N-1)^2$. The critical value is given by:

$$(V)_t = \frac{2N \pm 2t_g \sqrt{N-1}}{N-1} \qquad \text{(Eq. 3.16)}$$

where t_g is the value of Gauss normal distribution with significance level.

If the calculated value of test criterion $V < (V)_t$ we can reject H_0, meaning that the series is non-random.

The distribution of the population of a data series is tested by the **Kolmogorov-Smirnov test**. The Kolmogorov-Smirnov test valid for large sample sizes ($n \geq 20$), can be given by:

$$D = \max \left| P_1(X) - P_2(X) \right| \qquad \text{(Eq. 3.17)}$$

If the calculated maximum deviation D is greater or equal than the critical value of D_α, than H_o is rejected. For sample sizes ≤ 40, D_α can be obtained from literature (Haan, 1977; McCuen, 2000). D_α can be calculated, using the following equation:

$$D_\alpha = K \left(\frac{n_1 + n_2}{n_1 n_2} \right)^{0.5} \qquad \text{(Eq. 3.18)}$$

where K is a function of the level of significance.

To detect discontinuity in the data series, the Cumulative Deviation test, the Worsley Likelihood ratio test, the Linear Regression test and the Standard Normal Homogeneity test are used. The above tests will be executed using the following statistical programs: Modstat (Knodt, 2003), AnClim (Stipanek, 2003) and XLStatistics (Carr, 2000). Below, a summary of these tests is given.

The test statistic for the **Cumulative Deviation test** can be defined by the adjusted partial sums as follows:

$$Q = \max_{0<k<N} | S_k^{**} | \qquad \text{(Eq. 3.19a)}$$

with

$$S_0^{*} = 0 \quad \text{and} \quad S_k^{**} = S_k^{*}/D_Y, \; k = 0,...,n \qquad \text{(Eq. 3.19b)}$$

$$S_k^{*} = \sum_{i=1}^{k} (Y_i - \overline{Y}) , \; k = 1,...,n \qquad \text{(Eq. 3.19c)}$$

$$D_Y{}^2 = \sum_{i=1}^{n} (Y_i - \overline{Y})^2 / n \qquad \text{(Eq. 3.19d)}$$

where D_Y is the sample standard deviation, S_k^{**} is the standard partial sums, Y are the observations and $\overline{Y}$ is the mean of the observations.

For a homogeneous series, the values of S_k^{*} will oscillate around zero. If a break point is near K, than S_k^{*} reaches a maximum or minimum near k = K.

The test statistic for the **Worsley's likelihood ratio test** is:

$$W = \max_{0<k<n-1} | t_k | \qquad \text{(Eq. 3.20)}$$

where t_k is the test criterion of the Student *t*-test for test of difference in average between the first *k* and last (*n*-*k*) observations. If we know the location of the point of the change of *"m"*, we can use the Student *t*-test.

The test statistic for the **Standard Normal Homogeneity test** can be calculated as follows:

$$z_i = (q_i - \overline{q})/s_q \qquad \text{(Eq. 3.21)}$$

where $\overline{q}$ is arithmetic mean of q_i, s_q is standard deviation (with weight *n*-1), $z_i \in N(0,1)$.

The test statistic T_0 can be calculated, by comparing the mean of the first a-years of with that of the last n-a years, and well as follows:

$$T_0 = \max_{1\le a<n-1} \{T_a\} = \max_{1\le a<n-1} \{a\overline{z}_1^{2} + (n-a)\overline{z}_2^{2}\} \qquad \text{(Eq.3.22)}$$

with

$$\bar{z}_1 = \frac{1}{a}\sum_{i=1}^{a} z_i \ , (\bar{z}_1 \approx \mu_1) \qquad \text{(Eq. 3.23)}$$

$$\bar{z}_2 = \frac{1}{(n-a)}\sum_{i=a+1}^{n} z_i \ , (\bar{z}_2 \approx \mu_2) \qquad \text{(Eq. 3.24)}$$

If $T_o > T_{cr}$ than H_0 is rejected. T_{cr} can be obtained from literature tables.

For the classification of the spatial features of the annual cycle of rainfall (1961-1985) in Suriname, principal component analysis (PCA) of the annual rainfall anomalies is performed. PCA is calculated using the Climate Predictability Tool (v.5.04) of the International Research Institute for Climate Prediction IRI (http://iri.columbia.edu/outreach/software/). The PCA is a powerful tool to analyse pattern in data of high dimension (similarity, differences). The objective of PCA is to transfer "m" calculated variables into m uncorrelated components and this can be written as:

$$\underline{Z} = \underline{X}.\underline{A} \qquad \text{(Eq. 3.25)}$$

where $\underline{Z}$ is ($\underline{z}_1$, $\underline{z}_2$, …$\underline{z}_p$) and is a "m" by "n" matrix of "m" values of each of "n" components, $\underline{X}$ is the matrix of deviations from the mean and is a "m"x"n" matrix of "m" observations on "n" variables, $\underline{A}$ is ($\underline{a}_1$, $\underline{a}_2$,…$\underline{a}_p$) and A is a "n"x "n" matrix of coefficients defining the linear transformation.

To investigate the relationship between the annual rainfall and river discharge anomalies in Suriname with the SSTAs in the Atlantic and Pacific ocean, cross-correlation analyses are used. These analyses are carried out using the Anclim model. The cross correlation comes out from the simple linear correlation with Pearson correlation coefficient, but the data series are now shifted by some lag and the t-test is used to define the significance. The cross correlation coefficient $R_c(\tau)$ can be calculated using the following equation:

$$R_c(\tau) = \frac{\sum_{i=1}^{N-|\tau|} X_i Y_{i+\tau} - \frac{1}{N-|\tau|}\left(\sum_{i=1}^{N-|\tau|} X_i\right)\left(\sum_{i=\tau+1}^{N} Y_i\right)}{\left[\sum_{i=1}^{N-|\tau|} {X_i}^2 - \frac{1}{N-|\tau|}\left(\sum_{i=1}^{N-|\tau|} X_i\right)^2\right]^{0.5}\left[\sum_{i=1}^{N-|\tau|} {Y_i}^2 - \frac{1}{N-|\tau|}\left(\sum_{i=1+|\tau|}^{N} Y_i\right)^2\right]^{0.5}} \qquad \text{(Eq. 3.26)}$$

where X_i and Y_i are data series, N is the sample size, τ is the lag value (McCuen, 2003).

The test statistic for a two sided t-test with n_1+n_2-2 degrees of freedom can be given by:

$$\underline{t} = \frac{\overline{X}_1 - \overline{X}_2}{S_p(\frac{1}{n_1} + \frac{1}{n_2})} \quad \text{(Eq. 3.27)}$$

with

$$S_p{}^2 = \frac{(n_1 - 1)S_1{}^2 + (n_2 - 1)S_2{}^2}{n_1 + n_2 - 2} \quad \text{(Eq. 3.28)}$$

where X_1 and X_2 are the means of the samples from populations 1 and 2, n_1 and n_2 are the sample sizes, S_p is the square root of the variance, S_1 and S_2 are the variances of the samples.

H_o is rejected if $|t| > t_\alpha(n-1)$, α is the significance level of the test (McCuen, 2003).

For consistency and uniformity, all tests used will be performed at a 5% significance level (α), because of the availability of statistical tables. Because of the shortness of the data, the results presented here, should be used as an indication of climate variability and climate change on the rainfall and river discharges in Suriname.

3.4 Results and discussion

3.4.1 Changes in rainfall

Table 3.2a shows the calculated monthly average rainfall at different meteorological stations. The wettest month at all stations is May or June and the driest month is October. The monthly rainfall follows a sinusoidal curve, which expresses the four seasons. The monthly rainfall differs from location to location. For example, at the station Cultuurtuin the range (January to December) is between 103 mm to 324 mm, at Friendship-Totness 50 mm to 212 mm and at Tafelberg 56 mm to 428 mm. For the months of December to July, there is a great difference in monthly rainfall between the stations (130 mm to 225 mm), and for the months of August to November, there is a slight difference (3 mm to 7 mm).

Table 3.3 shows the trend in historical monthly rainfall and annual rainfall at the different meteorological stations for the complete time series. These results illustrate the absence of a clear trend in monthly and annual rainfall within the stations as well as between the stations. When the annual rainfall is increasing, it appears that monthly rainfall at most stations is increasing, especially in the months of March and April (short dry season), and in September and October (long dry season). This is illustrated by the high correlation rate between monthly rainfall and annual rainfall and by the high

coefficient of variation in those months. These values are higher for the months of March and April than for the months of September and October. These months are the transition months of the seasons. When the annual rainfall is decreasing, it appears that the monthly rainfall at most stations is also decreasing. This is especially true for January (short wet season), and July and August (long wet season). Some months indicate no significant trend. Months with highest slopes differ from station to station, for example Cultuurtuin: -1.07 mm/year in March; Sipaliwini: -3.76 mm/year in January; Tafelberg: +7.01 mm/year in April.

Table 3.2: (a) Observed average monthly rainfall (mm) and (b) average monthly temperature (^{o}C) at selected meteorological stations in Suriname.

Station (period; number of years)	Jan	Feb	Mar	Apr	May	Jun	Jul	Aug	Sept	Oct	Nov	Dec	ANNUAL
1. Albina (1915-1985; 71)	224	136	188	240	301	315	218	145	89	102	143	223	**2324**
2. Brownsweg (1911-1986; 76)	201	157	202	231	313	304	245	176	94	89	123	227	**2362**
3. Coeroeni (1961-1985; 25)	136	119	174	209	346	341	239	174	76	46	63	110	**2031**
4. Cultuurtuin (1900-1999; 100)	189	121	116	177	267	324	220	167	103	108	114	181	**2087**
5. Friendship-Totness (1904-1985; 82)	153	77	82	132	192	212	170	119	50	64	73	119	**1443**
6. Groningen (1913-2001; 89)	215	147	154	207	289	306	234	159	87	81	107	187	**2171**
7. Moengo (1919-1985; 67)	219	145	143	214	302	297	233	149	92	95	135	220	**2244**
8. Nieuw-Nickerie (1960-1999; 40)	152	95	97	163	229	267	225	153	82	51	74	159	**1748**
9. Sipaliwini (1961-1986; 26)	129	132	215	266	406	284	212	109	61	46	69	79	**2009**
10. Stoelmanseiland (1959-1986; 28)	231	171	239	248	350	311	252	165	87	83	130	219	**2486**
11. Tafelberg (1959-1986; 28)	286	212	270	340	428	382	315	172	81	56	95	213	**2852**

(a)

Station (period; number of years)	Jan	Feb	Mar	Apr	May	Jun	Jul	Aug	Sept	Oct	Nov	Dec	ANNUAL
1. Coeroeni (1971-1986; 16)	26.2	26.3	26.6	26.6	26.8	26.6	26.8	27.3	28.0	28.3	28.1	27.0	**27.0**
2. Cultuurtuin (1971-1999; 29)	26.5	26.7	27.0	27.1	27.0	26.7	27.0	27.7	28.0	28.0	27.6	26.7	**27.2**
3. Nieuw-Nickerie (1971-1986; 16)	26.5	26.6	26.9	27.1	27.0	26.9	27.0	27.6	27.9	27.9	27.6	26.9	**27.2**
4. Sipaliwini (1971-1985; 15)	26.0	26.1	26.2	26.3	26.3	26.4	26.3	26.8	27.6	28.1	27.8	26.9	**26.7**
5. Stoelmanseiland (1971-1999; 29)	26.0	26.1	26.5	26.6	26.6	26.4	26.7	27.5	28.2	28.4	27.8	26.4	**26.9**
6. Tafelberg (1971-1986; 16)	24.5	24.6	25.0	25.1	25.3	25.3	25.4	26.2	26.7	26.8	26.2	25.0	**25.5**

(b)

Table 3.3: Linear trends (mm/year) in monthly and annual average rainfall at different meteorological stations in Suriname from 1900-1961 and from 1985-1999. The value in the table represents the slope or trend. The positive sign (+) indicates a positive trend and the negative sign indicates a negative trend. Slopes with 0.00 values are very small slopes and are considered to be "no trend". The grey boxes indicate the highest slopes.

Station/Month (Period)	Jan	Feb	Maa	Apr	May	Jun	Jul	Aug	Sep	Oct	Nov	Dec	Annual	Location has become wetter/drier
1. Albina (1915-1985)	- 0.53	- 0.36	+ 0.40	+ 0.40	- 0.11	+ 0.71	- 0.00	+ 0.44	+ 0.33	+ 0.50	+ 0.46	- 0.47	+ 0.84	wetter
2. Brownsweg (1911-1986)	- 0.41	+ 0.44	+ 0.58	+ 0.30	- 0.16	- 0.38	- 0.08	+ 0.01	+ 0.50	+ 0.60	+ 0.62	+ 0.26	+ 3.34	wetter
3. Coeroeni (1961-1985)	- 1.25	- 2.32	+ 2.30	+ 6.96	+ 1.14	- 0.65	- 2.78	- 2.11	+ 2.23	+ 1.83	- 0.60	+ 2.28	+ 7.70	wetter
4. Cultuurtuin (1900-1999)	+ 0.13	- 0.44	- 1.07	- 0.99	- 0.45	+ 0.31	- 0.18	- 0.07	+ 0.30	+ 0.13	- 0.13	- 0.46	- 2.81	drier
5. Friendship-Totness (1904-1984)	- 0.84	- 0.55	- 1.67	- 0.42	- 0.52	- 0.75	- 0.92	- 0.07	- 0.08	+ 0.29	- 0.07	- 0.82	- 5.73	drier
6. Groningen (1913-2001)	- 0.31	+ 0.14	- 0.15	+ 0.19	+ 0.25	+ 0.99	- 0.21	+ 0.57	- 0.09	+ 0.45	+ 0.88	- 0.26	+ 2.50	wetter
7. Moengo (1919-1985)	- 0.79	+ 0.91	- 0.39	+ 0.04	- 0.50	- 0.56	- 0.62	- 0.11	+ 0.27	+ 0.30	+ 0.37	- 0.93	- 2.65	drier

8. Sipaliwini (1961-1985)	- 3.76	- 3.08	+ 2.43	+ 4.04	+ 0.49	- 6.34	+ 1.22	+ 2.56	+ 1.12	+ 0.21	- 1.18	- 0.57	+ 1.42	wetter
9. Stoelmanseiland (1959-1985)	- 0.04	+ 0.11	+ 3.93	+ 2.93	+ 0.24	- 0.86	+ 1.33	+ 2.95	+ 0.95	+ 3.81	+ 1.81	+ 2.58	+ 16.98	wetter
10. Tafelberg (1960-1985)	- 2.60	- 2.58	+ 0.27	+ 7.01	+ 3.71	- 4.01	- 2.50	- 1.26	+ 2.91	+ 1.27	- 1.17	+ 0.55	- 14.51	drier
11. Nieuw-Nickerie (1960-1999)	- 1.49	- 0.28	- 0.10	+ 0.44	- 1.17	+ 0.56	- 1.33	- 0.16	- 0.21	+ 0.25	+ 0.16	- 1.80	- 5.17	drier

Table 3.4: Maximum and minimum deviation in monthly rainfall during El Niño and La Niña years at different meteorological stations, reference to normal years. Note: LM is the number of months with a lower maximum rainfall than normal, HM is the number of months with a higher maximum rainfall than normal, Hm is the number of months with a higher minimum rainfall than normal. The value presented in the column "rainfall deviation" is taken as the highest value that occurred during the year.

Station	El Niño year				La Niña year			
	LM	Rainfall deviation (mm)	HM	Rainfall deviation (mm)	Hm	Rainfall deviation (mm)	HM	Rainfall deviation (mm)
1. Albina	9	-316	3	58	11	43	1	47
2. Brownsweg	10	-126	2	31	12	95	3	50
3. Coeroeni	6	-238	6	194	7	112	5	194
4. Cultuurtuin	8	-88	4	108	10	32	2	108
5. Friendship-Totness	10	-321	2	14	8	34	1	26
6. Groningen	4	-65	8	220	7	37	4	64
7. Kabalebo	4	-188	8	185	6	49	5	119
8. Moengo	9	-267	3	114	8	25	4	209
9. Sipaliwini	4	-51	8	139	6	19	10	139
10. Stoelmanseiland	4	-69	8	110	6	65	8	114
11. Tafelberg	7	-155	5	100	6	80	7	100
12. Nieuw-Nickerie	4	-41	8	218	7	24	6	218

Table 3.4 shows the monthly maximum and minimum rainfall deviations during El Niño and La Niña events at the different stations, reference to normal years. During the El Niño years, it was found that 6 of the 12 stations have low maximum rainfalls for 6 and more months during the year. With the exception of Tafelberg and Coeroeni, all these stations are located in the coastal zone. In these months, the maximum monthly rainfall at station Cultuurtuin is lower than normal by 88 mm, while at Friendship-Totness this value increases up to 321 mm. In most cases, the lowest maximum rainfall occurs in October and November (long dry season). Therefore, it may be concluded that the El Niño events cause wetter and drier months during the year of its occurrence, with respect to the maximum monthly rainfall. On the contrary, in the La Niña years, it was found that all 12 stations show a higher monthly minimum rainfall for 6 months or longer, reference to a normal year, and 4 of the 12 stations show a higher monthly maximum rainfall for 6 months or longer. The minimum monthly rainfall is about 34 mm (Friendship-Totness) to 126 mm (Nieuw-Nickerie) higher than normal. This means that, in the La Niña years, some months may be wetter in relation to the minimum rainfall and drier in relation to the maximum rainfall. It may be concluded that, in general, the La Niña events cause wetter months during the year with respect to the minimum monthly rainfall. Hence, it is difficult to provide a clear indication about the months that are affected as there is no clear distinction between stations in relation to El Niño and La Niña events.

At station Cultuurtuin, which is located in the city of Paramaribo and which is the most populated area of Suriname, it was found that the El Niño events caused lower maximum rainfall (-5 mm in May to -88 mm in November) than normal in most of the months in the period 1900-1999, except for January, February, July and September. In the period 1950-1999, La Niña events caused higher minimum rainfall (3 mm in February to 77 mm in December) than normal for most of the months, except for May and October. At station Nieuw-Nickerie, which is located in the largest and most important agricultural area of Suriname, El Niño events caused higher maximum rainfall than normal (6 mm in November to 218 mm in September) in most of the months in the period 1960-1999, except for the months of February, March, June, August and October, but La Niña events caused higher minimum rainfall (0 mm-126 mm in June) in most of the months, except for January, May, July, October and December. For illustration purposes, the anomalies in annual rainfall for station Cultuurtuin are shown in Figure 3.6. From the obtained results one can deduce that besides the ITCZ, El Niño and La Niña events also affect the annual rainfall in Suriname.

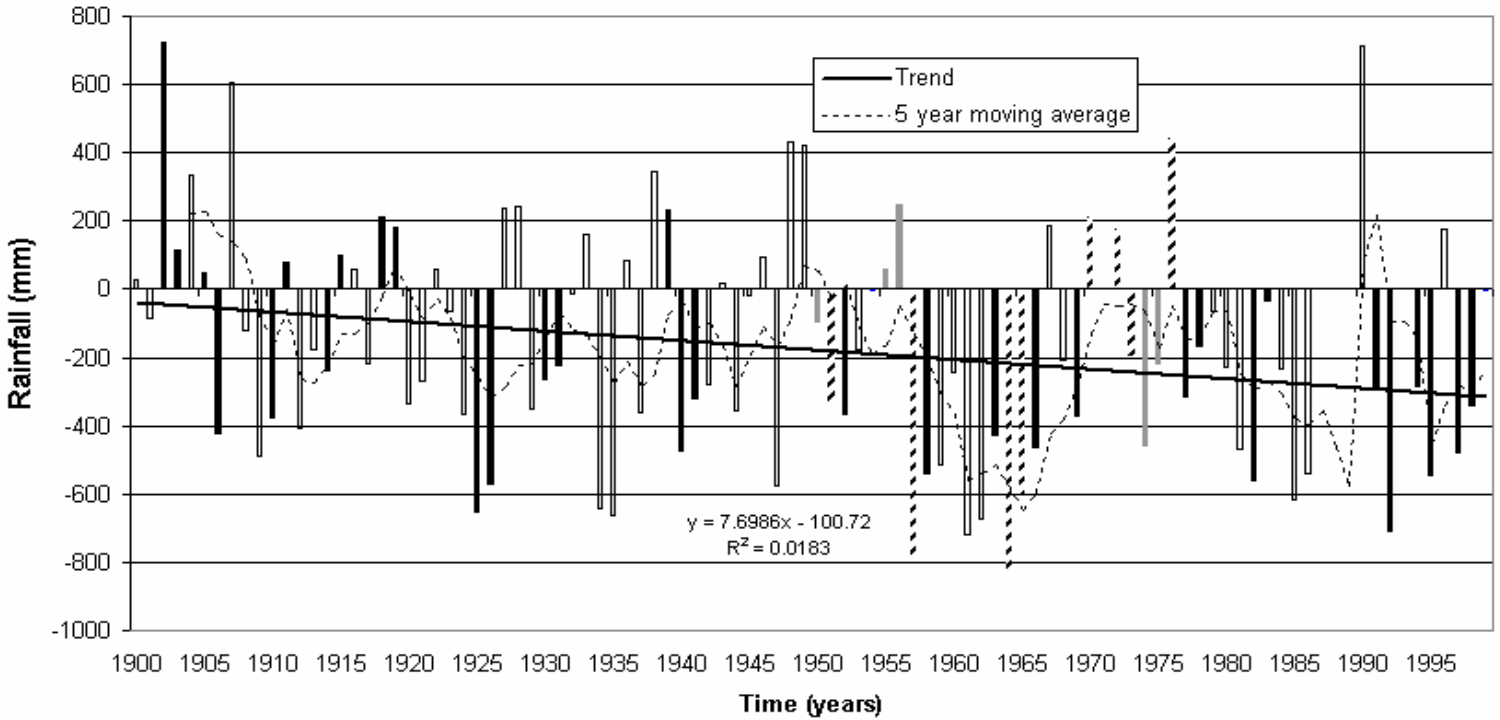

Figure 3.6: Anomalies in annual rainfall compared to normal years, during El Niño and La Niña years at station Cultuurtuin (1900-1999). Note: the black columns indicate El Niño years, the grey columns indicate La Niña years, the diagonally filled columns are both El Niño and La Niña years.

Figure 3.6 however indicates that the annual rainfall variations are not always extremely higher or lower than the long-term annual average rainfall. The results regarding drier conditions during El Niño years and those regarding wetter conditions during La Niña years do correspond with the studies found in literature (IPCC, 2001). It is clear that both El Niño and La Niña events may result in a decrease or increase in rainfall in Suriname, but it is also clear that other oceanic-atmospheric processes may also cause the same conditions in Suriname. With the rise of the SST in the world of 2-3^{o}C under doubling of CO_2 by 2100, the frequency and magnitude of El Niño and La Niña events may increase in many tropical areas (National Oceanic and Atmospheric Administration, undated). Since this change is directly linked to the ITCZ, the rainfall pattern in Suriname is expected to change significantly.

Table 3.5 shows the calculated annual rainfall and the linear rate of change (trend value) for the annual rainfall per station. The results show that the annual trend differs much throughout Suriname. Figure 3.7 shows the spatial change in the annual rainfall. The highest negative change (about 10 mm/year) has occurred in the centre of Suriname and the highest positive change in north-east Suriname (about 42 mm/year). This figure is based on the Mann-Kendall and Pearson tests, as these tests are much stronger than the general tests like the Runs, Von Neumann ratio and serial correlation test. For illustration purposes, the annual rainfall anomaly of the Cultuurtuin station is shown in Figure 3.9a.

The PCA and the Pearson's correlation coefficient ($0.47<r<0.83$) show that the annual rainfall anomalies tend to occur fairly uniformly across the whole country (Figure 3.8a). The first empirical orthogonal function (EOF) represents about 50% variance, which can be explained by the weak correlation at Brownsweg (0.47), Nieuw-Nickerie (0.55) and Groningen (0.57). Figure 3.8b shows the inter-annual variability with the temporal scores from which can be concluded that 1964 was the driest year and 1976 the wettest year during 1961-1985.

Table 3.5: Change in annual rainfall and river discharge for the period 1961-1985 at different gauge stations and the Kendall's τ, Pearson's r and Spearman's ρ correlation coefficient at a 95% reliability level. β_1 is the rate of change in the variable. p_α is the hypothesis test value.

Stations	Annual Rainfall (mm)	Change (mm) (%)	β_1	r (p_α)	τ (p_α)	ρ (p_α)
Rainfall station						
1. Albina	2354	1040 (44)	41.6	**0.60 (0.001)**	**0.46 (0.001)**	**0.65 (0.001)**
2. Brownsweg	2378	825 (35)	33.0	**0.61 (0.001)**	**0.46 (0.001)**	**0.64 (0.000)**
3. Coeroeni	2040	183 (9)	7.33	0.13 (0.529)	0.04 (0.766)	0.09 (0.668)
4. Cultuurtuin	2106	253 (12)	10.1	0.25 (0.112)	0.16 (0.254)	0.26 (0.210)
5. Groningen	2235	717 (33)	28.7	**0.50 (0.008)**	**0.42 (0.004)**	**0.58 (0.004)**
6. Nw-Nickerie	1759	65 (4)	2.61	0.06 (0.387)	-0.01 (0.963)	-0.01 (0.967)
7. Moengo	2270	362 (16)	14.5	0.32 (0.058)	0.27 (0.062)	0.35 (0.08)
8. Sipaliwini	2035	34 (2)	1.42	-0.04 (0.843)	-0.11 (0.455)	-0.11 (0.596)
9. Stoelmanseiland	2502	468 (19)	18.7	0.37 (0.033)	0.15 (0.304)	0.35 (0.091)
10. Tafelberg	2927	-245 (8)	-9.8	-0.20 (0.834)	-0.11 (0.455)	-0.15 (0.469)
11. Totness	1445	-130 (9)	-5.2	-0.14 (0.747)	-0.08 (0.575)	-0.13 (0.518)

Stations	Annual Rainfall (mm)	Change (mm) (%)	β_1	r (p_α)	τ (p_α)	ρ (p_α)
Discharge station						
1. Dramhosso	97	12 (12)	0.49	0.10 (0.318)	0.07 (0.607)	0.09 (0.668)
2. Langa Tabbetje	1635	175 (11)	7.00	0.11 (0.290)	0.06 (0.674)	0.11 (0.613)
3. Semoisie	146	-51 (35)	-2.05	-0.27 (0.906)	-0.213 (0.135)	-0.33 (0.107)
4. Pokigron	211	23 (11)	0.91	0.11 (0.306)	0.08 (0.543)	0.13 (0.555)

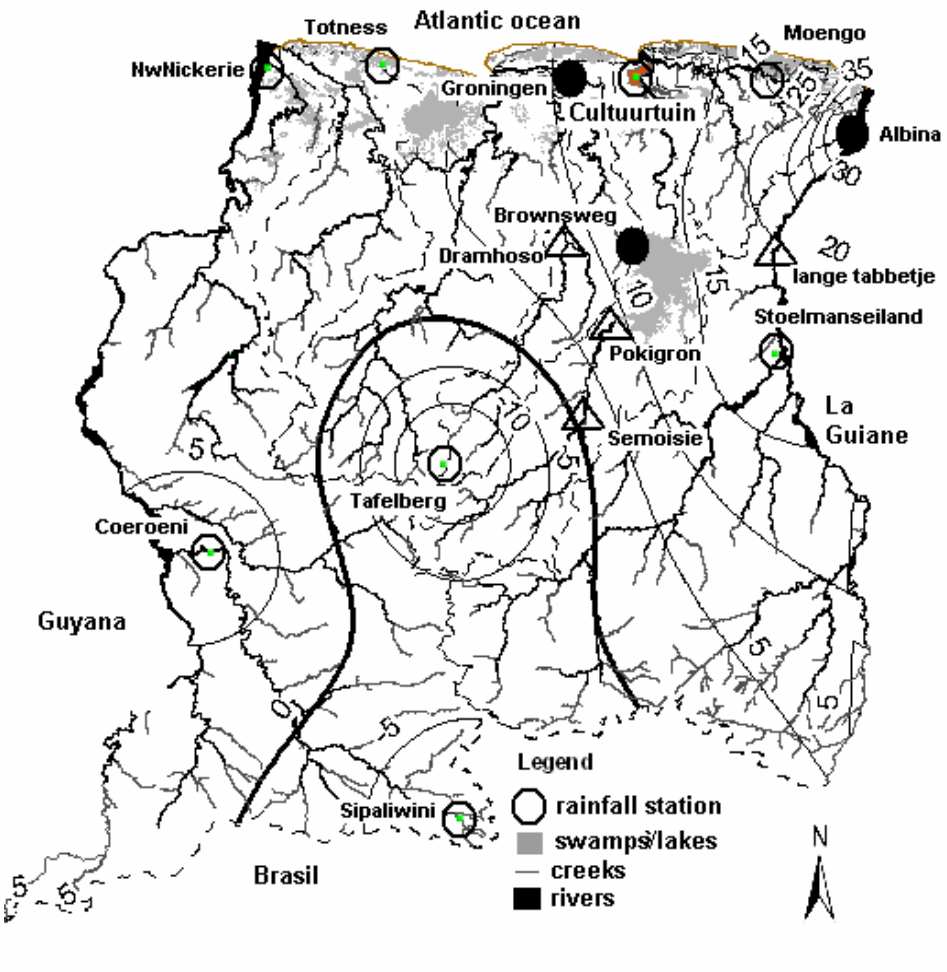

Figure 3.7: Contour map of trend of annual precipitation (mm/year) in Suriname, 1961-1985. Note: the circles (triangles) show the location of the rainfall (discharge) station. The solid black circle (triangle) indicates a significant trend (5% level of significance) and the void circles (triangles) indicate no significant change. The trends are based on the Kendall's and Pearson's tests.

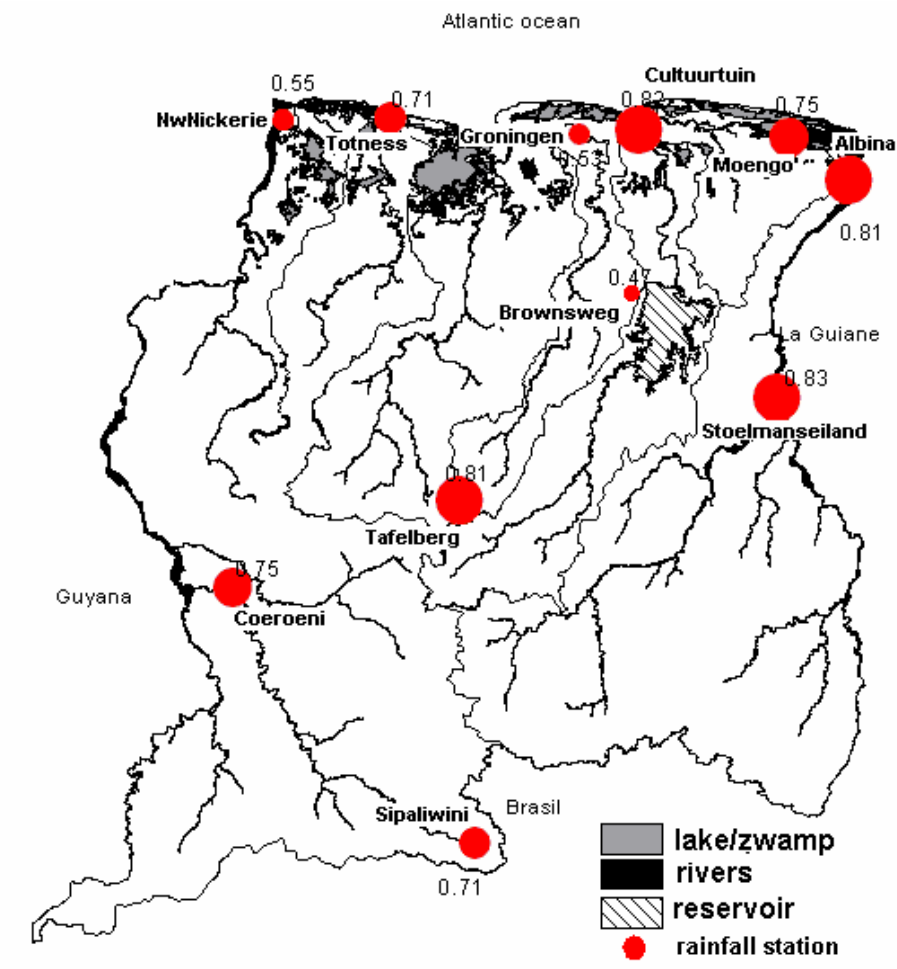
Atlantic ocean
0.55
NwNickerie
0.71
Totness
Groningen
Cultuurtuin
0.75
Albina
0.81
0.4
Brownsweg
La Guiane
0.83
Stoelmanseiland
0.81
Tafelberg
0.75
Coeroeni
Guyana
Sipaliwini
0.71
Brasil
lake/zwamp
rivers
reservoir
rainfall station

(a)

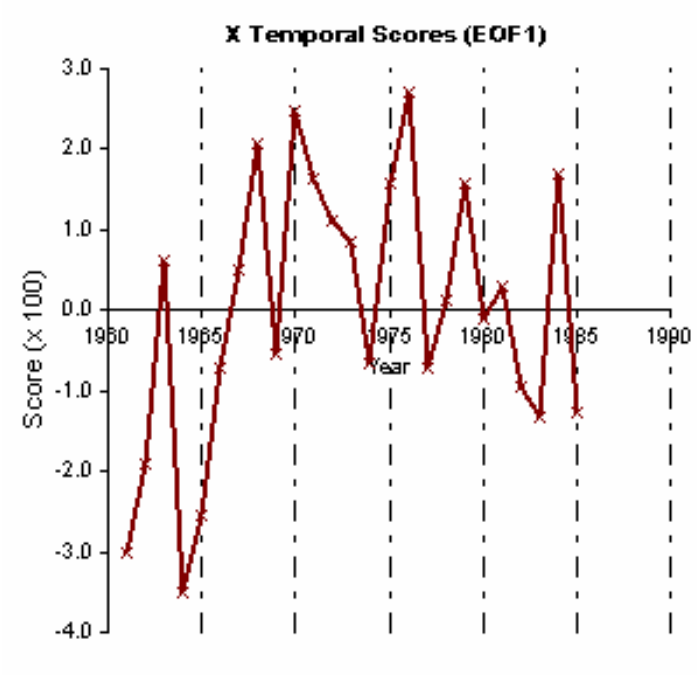

(b)

Figure 3.8: (a) Correlation of the annual rainfall between each rainfall station and the average of all the stations (Pearson's coefficient, 5% level of significance), (b) temporal scores (EOF 1). Note: the larger the circle, the higher the correlation.

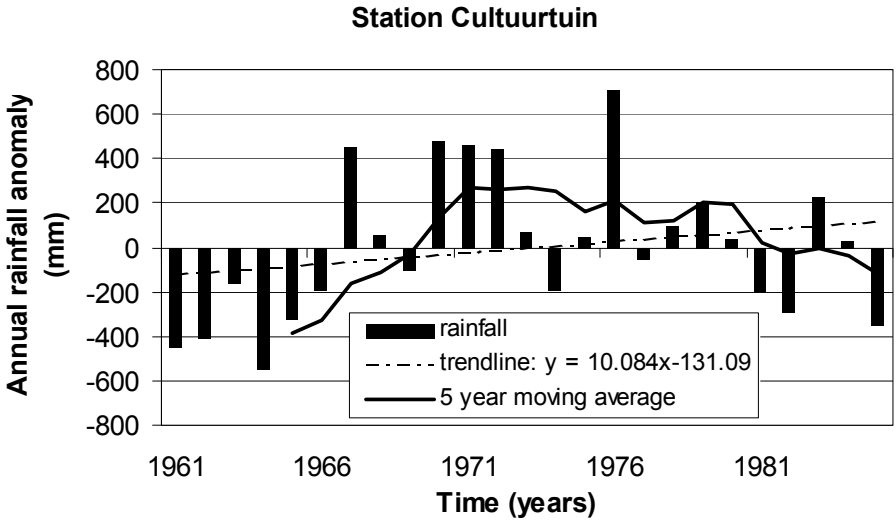

(a)

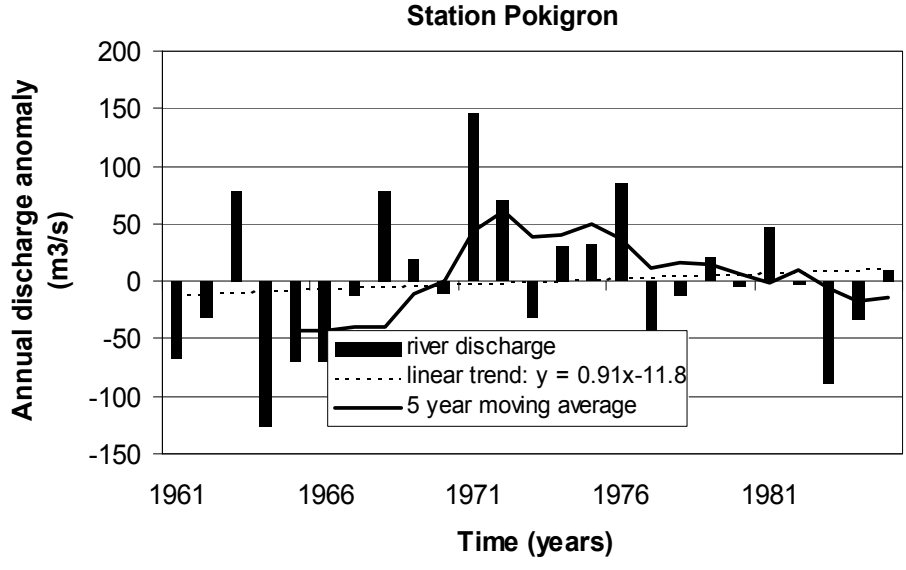

(b)

Figure 3.9: (a) Anomaly in annual rainfall at the Cultuurtuin station and (b) anomaly in annual river discharge at the Pokigron station for the period of 1961-1985.

Table 3.6: Results of the Runs test, serial correlation coefficient and the Von Neumann ratio for the annual rainfall and river discharge during 1961-1985.

Stations	Runs test	Serial correlation	Von Neumann Ratio
Rainfall station			
1.Albina	yes	**no**	**no**
2. Brownsweg	yes	**no**	**no**
3. Coeroeni	yes	yes	yes
4. Cultuurtuin	yes	**no**	**no**
5. Groningen	yes	yes	yes
6. Nw-Nickerie	yes	yes	**no**
7. Moengo	yes	**no**	**no**
8. Sipaliwini	yes	yes	yes
9. Stoelmanseiland	yes	yes	**no**
10. Tafelberg	yes	yes	yes
11. Totness	yes	yes	yes
Discharge station			
1. Dramhosso	yes	yes	yes
2. Langa Tabbetje	yes	yes	yes
3. Semoisie	yes	**no**	**no**
4. Pokigron	yes	yes	yes

Note: Confidence level is 95%; yes (no) indicates that the time series are (not) random.

Application of the Kolmogorov-Smirnov test has shown that the annual rainfall time series at all the stations show a normal variability (stationary). The results of the tests to detect discontinuity (change point) in the annual rainfall time series are shown in Table 3.6 and 3.7. From these results we can notice that at most rainfall stations, the Cumulative Deviation test, the Worsley Likelihood ratio test and the Standard Normal Homogeneity test find the same year of change per station, compared with the Linear Regression test. It is however noticed that the change point years are different for each station. The first three tests find change point years (shift) between 1962 and 1977, while the last test finds change point years between 1962 and 1984. Most of these years appear to be in the period between 1940-1980, which is the period when the global mean surface temperature was more or less stable. So it may be that global climate change is not the cause of the climatic shifts.

Table 3.7: Determination of the change point year in the time series of the annual rainfall and river discharge during 1961-1985 at different stations using the Linear Regression test (LRT), the Cumulative Deviation test (CDT), the Worsley Likelihood Ratio test (WLRT) and the Standard Normal Homogeneity test (SNHT) at a 95% confidence interval.

	First year of change			
Test / Stations	LRT	CDT	WLRT	SNHT
Rainfall station				
1. Albina	1975	1970	1970	1970
2. Brownsweg	1984	1970	1970	1970
3. Coeroeni	1968	1966	1963	1963
4. Cultuurtuin	1971	1967	1967	1967
5. Groningen	1983	1972	1972	1972
6. Nw-Nickerie	1962	1969	1962	1962
7. Moengo	1972	1970	1967	1967
8. Sipaliwini	1968	1966	1962	1966
9. Stoelmanseiland	1971	1970	1968	1968
10. Tafelberg	1967	1977	1977	1977
11. Totness	1969	1977	1977	1977
Discharge station				
1. Dramhosso	1971	1968	1967	1967
2. Langa Tabbetje	1971	1967	1967	1967
3. Semoisie	1971	1977	1977	1977
4. Pokigron	1971	1968	1967	1967

3.4.2 Changes in river discharges

The results of the different statistical tests applied to the annual river discharge series are shown in Table 3.5, 3.6 and 3.7. For illustration purposes, the annual river discharge anomaly of the Pokigron station (1961-1985) is shown in Figure 3.9b. The Mann-Kendall, Spearman's rank test and the Run test indicate that the time series at all four river discharge stations are random. Only the serial correlation coefficient and the Von Neumann ratio test indicate that the annual river discharge series at the Semoisie station has a significant (negative) linear trend. The highest positive trend is found at the Langa Tabbetje station (about 7 m^3/s.year) and the highest negative trend is found at the Semoisie station (about 2 m^3/s.year). The homogenization tests found different change point years (between 1967-1977) in the annual river discharge time series between the stations (Table 3.7).

3.4.3 Relation SSTAs-rainfall and SSTAs-river discharge anomalies

Based on the annual rainfall distribution map (Figure 1.9), we can see that rainfall in the centre of Suriname mainly determines the amount of river flows in the Pokigron, Semoisie and Dramhoso river basin. The linear correlation coefficient between the annual rainfall anomaly at Tafelberg with the annual river discharge anomaly at Semoisie and Pokigron is 0.84 ($p<0.05$) and 0.94 ($p<0.05$) for lag 0 respectively. The correlation between the annual rainfall anomaly at Tafelberg and the annual river discharge anomaly at Dramhoso is 0.62 ($p<0.05$), and the correlation between the annual rainfall anomaly at Stoelmanseiland and the annual river discharge anomaly at Langa Tabbetje is 0.57 ($p<0.05$). The negative change in the river flows at Semoisie of about 51% can therefore be explained by the decrease in annual rainfall (-245 mm (8%)) in the centre of Suriname (Tafelberg), which completely influences this catchment (Figure 3.7). The Dramhoso, Pokigron and Langa Tabbetje basins are more influenced by the positive change in the annual rainfall than by the negative change over the surface area (Figure 3.11).

Cross-correlation analyses between the annual rainfall and discharge anomalies with the SSTAs are shown in Table 3.8. The correlation between the annual TNA SSTAs and TSA SSTAs is 0.62 (for lag -4). It is also found that the Pacific El Niño influences both the TNA SSTAs ($r = -0.55$ for lag -1) and TSA SSTAs ($r = -0.55$ for lag -5). The results also show that there is a slightly stronger correlation between the annual rainfall anomalies and the SSTAs in the TSA region ($0.28<r<0.49$) compared to the SSTAs in the TNA region ($0.23<r<0.41$). The Niño 3+4 SSTAs shows much stronger correlations at some rainfall stations, compared with the TSA SST and TNA SSTAs, such as in Nieuw Nickerie ($r = 0.69$), Totness ($r = 0.40$) and Groningen ($r = 0.48$). The influence of ENSO events might explain the lowest annual rainfall in northwest Suriname. For example, the high SSTAs in the Niño 3+4 region in 1982-1983 (Figure 3.4c) explain the prolonged dry period from August 1982-February 1983 in northwest Suriname (Houben and Molenaar, undated; Mol et al., 2000). The results in Table 3.8 also show that the highest correlation between the river discharge anomalies and the SSTAs is obtained with the Niño 3+4 SSTAs ($0.56<r<0.63$). The correlation between the river discharge anomalies and the TNA and TSA SSTAs varies between 0.27-0.38 and 0.35-0.36 respectively.

Table 3.8: The highest cross-correlation coefficient c_k (with 95% confidence interval) between the annual SSTAs in the TNA, TSA and Niño 3+4 region with the annual rainfall anomalies and river discharge anomalies for the period 1961-1985.

Predictor	TNA SSTAs	TSA SSTAs	Niño 3+4 SSTAs
Rainfall station			
1. Albina	-0.41 (lag -1)	-0.44 (lag -4)	0.36 (lag -7)
2. Brownsweg	0.33 (lag 1)	0.49 (lag 1)	-0.34 (lag 0)
3. Coeroeni	-0.32 (lag 1)	-0.38 (lag -3)	-0.24 (lag 0)
4. Cultuurtuin	-0.31 (lag 1)	-0.39 (lag 5)	-0.27 (lag 4)
5. Groningen	0.35 (lag -1)	-0.34 (lag 2)	-0.48 (lag -5)
6. Nw-Nickerie	0.23 (lag -3)	-0.47 (lag 1)	0.69 (lag -7)
7. Moengo	0.31 (lag 1)	-0.51 (lag 1)	0.44 (lag -7)
8. Sipaliwini	0.28 (lag -5)	-0.49 (lag 5)	-0.40 (lag 5)
9. Stoelmanseiland	-0.23 (lag -1)	-0.49 (lag 4)	-0.43 (lag 3)
10. Tafelberg	0.32 (lag -2)	-0.34 (lag 4)	-0.37 (lag 0)
11. Totness	0.34 (lag -2)	-0.28 (lag 3)	-0.40 (lag 0)
River discharge station			
1. Dramhosso	0.34 (lag -2)	-0.36 (lag -4)	-0.62 (lag -1)
2. Langa Tabbetje	0.27 (lag -3)	0.36 (lag -6)	-0.63 (lag -1)
3. Semoisie	0.38 (lag -2)	-0.35 (lag 3)	-0.56 (lag -1)
4. Pokigron	-0.27 (lag -4)	-0.36 (lag 3)	-0.62 (lag -1)

Note: lag (k) = 0-12 years. The rainfall and discharge anomalies are taken as the first series and the SSTAs as the second time series. A positive lag indicates that the SSTAs are the leading index and a positive (negative) correlation indicates that large (small) rainfall (or discharge) anomalies are related to large SSTAs.

The difference in correlations between the rainfall anomalies, discharge anomalies and the Atlantic and Pacific SSTs anomalies may be explained by the high local variability in the annual time series per station, but perhaps also local influence of Atlantic and Pacific SSTs and local climate effects. In the analyses below only the Cultuurtuin and the Pokigron stations will be further taken into consideration. The results obtained for other rainfall stations are almost the same. Figure 3.4 shows that the annual SSTAs in the TNA region are prevailingly positive during 1961-1970 and prevailingly negative during 1971-1976. During 1977-1985, the TNA region is mostly warmer than normal and the TSA region mostly colder than normal. The rainfall and/or discharge deficit (Figure 3.5a and 3.5b) during 1961-1966 may be explained by the warmer than normal SSTs in the TNA region in those years. This may have caused the ITCZ to stay longer southwards of the equator especially during March-May (Ambrizzi et al., 2005). The El Niño

events in 1965/1966 might also have contributed to this fact. The driest year, 1964, may have been caused by the reverse impact of the strong La Niña event in this year, due to the absence of the ITCZ especially during March-May (Ambrizzi et al., 2005).

The rainfall excesses in the years 1970, 1971, 1972 and 1976, may have been caused by the warmer than normal SSTs in the TSA region and the colder than normal SSTs in the TNA region. This may have caused the ITCZ to stay longer above Suriname while moving to the north. The strong La Niña event in 1970/1971 and 1975/1976 and the reverse impact of the strong El Niño in 1972/1973 (Ambrizzi et al., 2005) may have also contributed to this fact. During these years, the Niño 3+4 region was also much cooler than normal. The decrease in rainfall in 1982-1983 and/or the river discharge in 1983 (Figure 3.5a and 3.5b), can be explained by the strong Niño 3+4 SSTAs in 1982.

The change point year in annual river flows at the Langa Tabbetje station (1967) is found to be close to that of the annual rainfall at Stoelmanseiland (1968, 1970) (Table 3.7). This is also the case for the river discharge at the Semoisie station and at the Tafelberg rainfall station. No clear relation has been found between the change point year in the rainfall series at Tafelberg and the discharge series at Pokigron and Dramhoso. The calculated change point years show to have been caused by the change from dry years to wet years (Figure 3.9). It may be concluded that the shifts are thus more related to the climate variability, in particular the SSTAs, in the tropical Atlantic and tropical Pacific.

3.4.4 Changes in temperature

Table 3.2b shows the calculated long-term average monthly temperature. Analysis shows that Tafelberg (350 m above NSP) has the lowest average monthly temperature during the year, and Cultuurtuin, Nieuw-Nickerie (both 1-2 m above NSP) and Kabalebo (150 m above NSP) the highest. The different temperature profiles throughout the year show a slight increase between January and July with no clear peaks, while in the same period the monthly temperature difference between the stations increases (0.5^{o}C to 1^{o}C). After July, a sharp increase in temperature occurs up to December. The hottest month appears to be October (long dry season). During this period, rainfall is at its lowest.

Results of long-term trends in monthly average and maximum temperature are presented in Table 3.9. From these results follows that nearly all months indicate a warmer trend. It should be noticed, however, that there are some

exceptions such as for station Coeroeni (May to September indicate a negative trend), Kabalebo and Stoelmanseiland. Furthermore, the highest slopes (trends) in average and maximum monthly temperature occur in different months for different meteorological stations. For station Coeroeni, this value equals 0.17^{o}C/year for the month of April. The monthly trend for station Cultuurtuin varies between 0.02^{o}C and 0.07^{o}C/year. The highest slopes for the average monthly temperature occurs in December (0.04^{o}C/year) and the maximum temperature in May and September (0.07^{o}C/year).

3.4.5 Changes in evaporation

Lack of sufficient and long-term data on evaporation in Suriname is the main reason that little is known about evaporation trends. Evapotranspiration is also not measured. If we take into consideration equation 2.1, we may conclude that a small change in rainfall or evapotranspiration will directly influence the water balance (e.g. river flows) in a river basin. It is generally known that evaporation increases with the increase in air temperature, air humidity, wind speed and cloudiness. Verhoog (1987) estimated that if the mean global temperature increases with 0.5^{o}C in the tropic-humid region, evapotranspiration will increase with about 2%, which is according to the theory used in GCMs. The IPCC has reported that a mean global temperature increase of 2^{o}C, increases potential evapotranspiration by up to 40% (if precipitation increases only 3-5%). These findings show how sensitive evaporation and evapotranspiration can be in relation to temperature. It is thus recommended to be careful when using temperature-evaporation relationships for estimation future changes in evaporation.

3.4.6 Sea level trends

The increase in the global mean temperature on Earth has resulted in an increase in the mean sea level due to warming of ocean water (expansion of salt water), melting of mountain glaciers and ice caps, melting of Greenland ice sheets and melting of Antarctic ice sheets (IPCC, 2007). Earth's observations before 1993 and satellite data after 1993 have shown that the total rate of sea level during 1993-2003 (about 3.1 mm/year) is higher that during 1961-2003 (about 1.8 mm/yr). Significant melting of ice in the Arctic region started in 1979, till today 2003, while significant melting of the Greenland ice cap started in 1992. It is believed that the global sea level rise has also increased water levels along the coast and in the estuarine rivers of Suriname.

Table 3.9: Linear trend (^{o}C/year) in monthly, average (ave), maximum (max) and annual temperature at different meteorological stations in Suriname from 1971 to 1985/1999. The value in the table represents the slope or trend (a). The positive sign (+) indicates a positive trend and the negative sign (-) indicates a negative trend. Slopes with 0.00 values are very small slopes and are considered to be "no trend". The grey boxes indicate the highest slopes.

Station\Month (Period)	Jan	Feb	Maa	Apr	May	Jun	Jul	Aug	Sep	Oct	Nov	Dec	Annual	Location has become warmer/ cooler
1. Coeroeni														
(1971-1985)	+	+	+	+	-	-	-	-	-	+	+	-	+	
average	0.01	0.03	0.04	0.04	0.01	0.00	0.03	0.02	0.01	0.00	0.02	0.02	0.00	warmer
	+	+	+	+	+	+	+	-	+	+	+	+	+	
maximum	0.02	0.08	0.10	0.17	0.06	0.04	0.08	0.02	0.01	0.02	0.07	0.03	0.06	
2. Cultuurtuin														
(1971-1999)	+	+	+	+	+	+	+	+	+	+	+	+	+	
average	0.03	0.03	0.03	0.03	0.02	0.03	0.03	0.02	0.02	0.03	0.02	0.04	0.03	warmer
	+	+	+	+	+	+	+	+	+	+	+	+	+	
maximum	0.06	0.05	0.07	0.06	0.06	0.03	0.03	0.03	0.07	0.02	0.06	0.05	0.04	
3. Sipaliwini														
(1971-1985)	+	+	+	+	+	+	+	+	+	+	+	+	+	
average	0.07	0.09	0.08	0.08	0.07	0.07	0.05	0.03	0.07	0.11	0.06	0.09	0.07	warmer
	+	+	+	+	+	+	+	-	+	+	+	+	+	
maximum	0.07	0.04	0.12	+0.04	0.09	0.05	0.06	0.04	0.08	0.07	0.04	0.04	0.04	

4. Stoelmanseiland (1971-1985)	+	+	+	+	+	+	+	-	+	+		-	+	
average	0.06	0.06	0.06	0.04	0.04	0.04	0.01	0.01	0.01	0.00	0.00	0.01	0.03	warmer
	+	+	+	-	+	+	+	-	-	+	+	+	+	
maximum	0.04	0.05	0.02	0.01	0.02	0.03	0.04	0.02	0.02	0.00	0.00	0.01	0.01	
5. Tafelberg (1971-1985)	+	+	+	+	+	+	+	-	+	+	+	+	+	warmer
average	0.05	0.04	0.04	0.03	0.03	0.02	0.02	0.00	0.01	0.00	0.02	0.01	0.02	
6. Nieuw-Nickerie (1971-1999)	+	+	+	+	+	+	+	+	+	+	+	+	+	warmer
average	0.02	0.02	0.02	0.03	0.02	0.02	0.03	0.02	0.03	0.02	0.01	0.02	0.01	

Estimation of SLR for Suriname was first given by Nedeco in 1968 and was about 1.1 mm a year for Suriname. Water level observations (1960-2004) in the Suriname river have shown that the mean water level along the coast of Suriname has increased with about 2.2 to 4.5 mm a year since 1960. Some observations in the Caribbean Region indicate that the relative SLR (a combination of the rise of sea water level and movement of land) is found to be about 5.3 mm to 9.3 mm a year since the 1950s. In Trinidad and Tobago, as well as in Guyana, the observed SLR in the period of 1951-1971 is 8 to 10 mm and 10.2 mm a year respectively (Gable et al., 1988). In Belem (north-east coast of South America), the relative annual sea level has increased with about 4 mm/year (1950-1985) (Mesquita, 2000). The estimated changes for the coast of Suriname are close to the one of Belem. If sea level rise increases linearly, it is expected that the coastal water levels will rise with about 50 cm, which is close to the predictions of Met Office-The Hadley Center (2003) and the IPCC (2007).

As most of the people live in the northern part of Suriname (flat area) and most economic activities of Suriname (e.g. infrastructure, agriculture areas, fisheries, industries) are also located in this area, a sea level rise of 1.0 m will cause flooding of the whole northern part of Suriname. Sea level rise may thus be much more important to consider at a short time scale (< 50 years) for Suriname than changes in e.g. rainfall. Different sea level rise scenarios and the impacts on the coastal area of Suriname have already intensively been studied and reported by Naipal and Amatali (1999b).

3.5 Impact of climate change and climate variability on the water resources in Suriname

3.5.1 Impact on surface water resources

Besides the gradual change in rainfall (1961-1985), it is more the extreme climate events that have affected surface fresh water resources (river basins, swamps) in Suriname, resulting in floods and droughts in different parts in Suriname. The drought of August 1997-February 1998 caused drying up of the fresh-brackish Bigi Pan lagoon and a high mortality of fresh and brackish water fish, the rice production was dropped in district Nickerie and there were severe shrinkage cracks in the asphalt pavement in the road section Wageningen-Henar bridge in district Nickerie. Another significant drought was in September 2004-January 2005, which resulted in food shortages in many villages in the interior of Suriname and closure of some of the turbine. This affected the hydro electricity production. The floods in April 2004, May 13-June 6, 2006 caused damage to many houses in the villages in the interior and the agriculture lands (food shortage) (Geijskens, 1943; Hollande, N., personal communication, October 1, 2004; Houben and Molenaar,

undated; Moksi Magazine, 2006; Mol et al., 2000; Scheltz, E., personal communication, September 5, 2004; United, 2006; Webster and Roebuck, 2001). Table 3.10 shows the years when some extreme events have occured in Suriname since 1821 and the possible causes of these events. This table shows that most events might have been caused by the influence of extreme SSTs in the Pacific ocean through the SST in the Atlantic ocean. As already explained, the ITCZ plays also plays an important role in wet and dry periods: warming sea surface temperature with low pressure systems in the Atlantic brings increased precipitation, while high pressure systems cause lower precipitation.

If under global climate change conditions, the variability in SSTs increases, it is expected that not only the ENSO and La Niña events will change, but also the behavior of the ITCZ. A lot of progress has been made in the last 20 years in modelling and predicting extreme events like ENSO, but it is still difficult to forecast ENSO and its global consequences (McPhaden, 2004). Reasons for these deficiencies are the lack of a good understanding of the causes of sea surface temperature (SST) anomalies, the physical processes of a coupled ocean-atmospheric perspective, and interactions of ENSO with the Pacific Decadal Oscillation (PDO) climate system. Rainfall may increase or decrease in Suriname and may also become intense. The occurrence of floods and droughts may increase, affecting not only the fresh water resources systems in both the coastal area and the interior of Suriname, but as already experienced also other sectors like infrastructure, agricultural production, fisheries and energy production (Figure 1.10). Because of the fact that it is not exactly known how much rainfall will change in Suriname due to global climate change, and how freshwater resources will change, it is necessary that different scenarios are analysed for different fresh water resources systems.

3.5.2 Impact on groundwater resources

Although groundwater resources systems are not included in this study, we will give a short summary of reported effects of sea level rise and estimated future impacts of global climate change on the groundwater resources in Suriname. Most of the aquifers in the coastal area of Suriname are confined and contain fresh (<250 mg Cl^-/l) to brackish (250-14,000 mg Cl^-/l) water, and are shallow to deep (10-500 m) (WMO/UNDP/Gov of Suriname, 1972). It can however been noticed from Figure 1.12 that sea water is penetrating slowly further into the freshwater part of these aquifers. The main reason for this is also over-pumping of wells over the last ten to twenty years in Paramaribo (van den Berg, 1997; van der Pol, 2002).

Table 3.10: Extreme events in Suriname (Geijskens, 1943; Hollande, N., personal communication, October 1, 2004; Houben and Molenaar, undated; Moksi Magazine, 2006; Mol et al., 2000; Scheltz, E., personal communication, September 5, 2004; United, 2006; Webster and Roebuck, 2001). The reasons stated in *italics* are estimates.

Date	Place	Event	Reason
1821	Central Suriname	Drought	-
1911	Central Suriname	Flood	-
1912-1913	Central Suriname	Drought	-
1924	Paramaribo	Flood	-
1925	Paramaribo	Flood	-
1925-1926	Central Suriname	Drought	*El Niño*
1938	Paramaribo	Flood	-
1938	Central Suriname	Drought	-
1939-1940	Central Suriname	Drought	*El Niño*
1945	Central Suriname	Flood	-
1948	Central Suriname	Flood	-
1950	Paramaribo	Flood	*La Niña*
1963	Central Suriname	Flood	*El Niño*
1964	Central Suriname	Drought	*La Niña*
Aug 1982-Feb 1983	North-west Suriname	Drought	El Niño
Feb 1993	Central Suriname (Upper Suriname river)	Drought	*El Niño*
Aug 1997-Feb 1998	North-west Suriname	Drought	El Niño
March 1999	Central Suriname (Upper-Suriname river)	Drought	*La Niña*
First half 2000	South-west Suriname (Kwamalasamutu-Coeroeni river, Upper-Suriname river)	Flood	*La Niña*
Jan 2001	Central Suriname (Upper-Suriname river)	Drought	*La Niña*

2003	North-west Suriname	Drought	*El Nino*
April 2004	Central Suriname (Gran Rio river, Upper-Suriname river)	Flood	-
Sept 2004	Paramaribo	Flood	Hurricane Ivan
Sept 2004-Jan 2005	Central Suriname (Upper-Suriname river)	Drought	*El Niño*
July 2005	Paramaribo	Flood	-
May 13-June 6 2006	Central Suriname (Upper-Suriname river, Tapanahony river, Coeroeni river)	Flood	Trough in the upper level of atmosphere in combination with ITCZ in lower atmosphere

Freshwater can still be found in the Savannah Belt area and in the Old Coastal Plain in Paramaribo and surroundings, while brackish water can be found in the Young Coastal Plain (Figure 1.12). It is expected that in Paramaribo, within a few years, most wells will produce water above the WHO limit of 250 mg Cl^-/l (van de Berg, 1997; Post, 1996). In West Suriname (Nickerie), groundwater modelling studies have estimated that, if extraction of groundwater increases, the chloride concentration will increase up to 500 mg/1 in the next 50 years (van Doorn, 2002). In East Suriname (Moengo/Wonoredjo), no increase is expected in chloride concentration in the next 30 years (van der Pol, 2002). The different locations are shown in Figure 1.11. Sea water intrusion due to future global sea level rise and over-pumping of coastal wells, may thus be more important to consider at short time scale (< 100 years) in Suriname than e.g. changes in rainfall (recharge). Although the lifetime of rainfall-recharge in the aquifers of Suriname is very high, it may be useful to study the sensitivity of recharge and water levels to the groundwater using groundwater modelling techniques.

3.6 Conclusions

Linear trend analysis in temperature has shown a warming trend in the monthly and annual temperature at all the 6 stations. If this trend continues, evaporation from open waters and evapotranspiration from vegetated surfaces will intensify and will affect rainfall patterns and fresh water resources.

Linear trend analyses in monthly rainfall have shown that, at most stations, especially the months of September and October (long dry season), and March and April (short dry season) have become wetter during the period 1961-1985, and the months of July and August (long wet season), and January (short wet season) have become drier during the same period. If this trend continues, future water resources planning and management need to be adjusted, especially for agricultural areas (e.g. rice culture) and reservoirs (hydropower). It was also found that the annual rainfall anomalies exhibited correlation with the Atlantic region (especially SSTAs in the TSA region). The SSTs influence the movement of the ITCZ and may cause rainfall excesses and deficits longer than the normal seasons. Not all extreme high and low rainfall events are caused by these events. Analyses of the affects of the El Niño, ENSO and La Niña events on rainfall have shown that these events are of much more importance than the historical linear changes. The historical changes in rainfall have already had major impacts on fresh water resources.

The statistical analyses (Mann-Kendall, Spearman's and Pearson's test) have shown that only at three stations (Albina, Brownsweg and Groningen), the annual rainfall are non-homogeneous (significant positive trend). These stations also show the highest annual rainfall. For homogeneity and

stationary, it was found that the Mann-Kendall, Spearman's and Pearson's test give more or less similar results, compared to the other tests. Based on the tests on the shift in data series, it was found that except for the Linear Regression test, the Standard Normal Homogeneity test of Alexandersson, the Craddock's test of Cumulative Deviations and the Worsley Likelihood ratio tests give almost the same results. Possible sources of the differences among the applied statistical methods are the limitation of long-term data sets, the limitations of the statistical test and the choice of a 5% risk level. This risk level may be high, since real non-homogeneities might too easily remain undetected at higher significance levels. The climate variability in Suriname may also be responsible for the conflicting trend characteristics in long-term (complete data series) and short-term (1961-1985) time series of the annual average rainfall. It should be mentioned that one must be careful in using the trend characteristics for Suriname such as the annual temperature and annual rainfall trends, especially those based on relatively short periods.

The historical changes in the annual rainfall and river discharges and the climatic shifts seem to be more related to the global decadal climate variability in the Atlantic and Pacific ocean and atmosphere, than to climate change. To improve our understanding of the climate change and climate variability processes in Suriname, collection of long-term high-quality (spatial and temporal) data on atmospheric and climate variables including sea and land surface temperature, evaporation, wind speed, sunshine, humidity, cloud cover, river flows, sea level, and river and ground water levels are needed for ongoing climate analyses by the competent authorities in Suriname. Further study is necessary as to the relationships between oceanic-atmospheric processes (e.g. ENSO, TAV, TNA) and climate variables (e.g. rainfall, temperature) in Suriname, especially the extremes of these atmospheric-ocean processes. Because of the threats and facts of global climate change and climate variability in Suriname, climate change scenarios should be developed, which can be based on historical trend analysis and climate model results. If global climate change will continue to increase in the future, it is expected that the variability in rainfall will increase and therefore also the fresh water resources. It is, therefore, recommended to incorporate impacts of climate change and climate variability in future development of water resources systems and planning and in the design of water works.

Acknowledgements

I am thankful for the constructive and valuable review comments by Drs B. Tan, Dr. J. Mol and C. Becker. Dipl.Met. I gratefully acknowledge the provision of software by Dr. R. Carr, Dr. R. Knodt and P. Stipanek and the

necessary data by the Meteorological Service Suriname (MDS) and the Center of Natural Resources and Assessment (CELOS). Three anonymous reviewers provided valuable comments that helped improve this chapter.

4. RAINFALL VARIABILITY IN SURINAME IN RELATION TO GLOBAL ATMOSPHERIC PROCESSES*

Abstract

Spatial correlations in the annual rainfall anomalies are analysed using principal component analyses (PCA). Cross correlation analysis and composites are used to measure the influence of sea surface temperatures anomalies (SSTAs) in the tropical Atlantic and tropical Pacific Ocean with the seasonal rainfall in Suriname. It is shown that the spatial and time variability in rainfall is mainly determined by the meridional movement of the Inter-tropical Convergence Zone (ITCZ). It occurs that the rainfall anomalies are fairly uniform throughout the country. The strongest correlation between the December-January rainfall (short wet season) at station Cultuurtuin is found with the SSTAs in the Pacific region and is about $c_{lag\ 1}^{\text{Niño 1+2}} = 0.59$. In the March-May rainfall (beginning long wet season) there is a lagged correlation with the SSTAs in the Pacific region ($c_{lag\ 3}^{\text{Niño 1+2}} = 0.59$). The June-August rainfall (end part of long wet season) shows the highest correlation with SSTAs in the TSA region and is about c = -0.52 for lag 0. In the September-November long dry season there is also a lagged correlation with the TSA SSTAs of about $c_{lag\ 3} = 0.66$. The different correlations and predictors can be used for seasonal rainfall predictions.

* This chapter has been published as: “Rainfall variability in Suriname and its relationship with the Tropical Pacific ENSO SST anomalies and the Atlantic SST anomalies”, International Journal of Climatology 26, 2006.

* A summary of this chapter has also been published as: “Variability of rainfall in Suriname and the relation with ENSO-SST and TA-SST”, Advances in Geosciences 6, 77-82, 2006.

4.1 Introduction

In addition to topography, land-sea interactions and land processes, climate variability in north and northeast South America is also linked to oceanic and atmospheric processes in the Tropical Atlantic (TA) and the Tropical Pacific. The most important phenomena on inter-annual to decadal time scale in this region are the Pacific El Niño-Southern Oscillation (ENSO), the Atlantic zonal equatorial mode (or the "Tropical Atlantic Niño") and the Tropical Atlantic Meridional Gradient (TAMG) (or the "Tropical Atlantic dipole index") (Berlage, 1957; Giannini et al., 2000; Marshall et al., 2001; Martis et al., 2002; Rajagopolan et al., 1997; Robertson and Mechoso, 2002; Villwock, 1998; Wang, 2001, 2005). The above phenomena are caused by the variability in sea surface temperatures (SSTs). The anomalies in sea level pressure and winds are the leading factors in determining the anomalies in SSTs (Ambrizzi et al., 2005). The different mechanisms are schematically shown in Figure 3.1. Garzoli et al. (1999), Giannini et al. (2000), Marshall et al. (2001) and Villwock (1998) have shown that the rainfall in northern South America is more related to the SSTAs in the Tropical North Atlantic (TNA) than to the Tropical South Atlantic (TSA) and the Tropical Pacific ENSO.

The Pacific ENSO is one of the well-known phenomena that may cause floods and droughts in different parts of the tropics (30^{o}N-30^{o}S). It generally starts in March/April, reaches its peak between December and February and declines in March of the following year. The ENSO affect the TA through the Walker and Hadley circulation. The Walker circulation consists of air rising in the eastern Pacific, diverges eastward and sinks in the equatorial Atlantic and returns to the west. During the Hadley circulation, ascending air from South America moves from the Tropical North Atlantic, descends in the equatorial Atlantic and flows southward to South America. When the SSTAs in the equatorial Pacific are positive (warm phase), the SSTs north of the equator becomes warmer than the south of the equator and with a lag of 4-5 months. The Pacific Walker cell and the Atlantic Hadley circulations are then stronger and weaker respectively and this leads to a weakening of the northeast trade winds in the TNA and less surface evaporation (Ambrizzi et al., 2005; Marshall et al., 2001). The maximum SSTs in the TNA are reached during December-February and March-May (Marshall et al., 2001, Rajagopolan et al., 1997; Ropelewski and Hapert, 1987, 1989, 1996; Wang, 2001). During these periods, rainfall below normal is experienced in northern South America. During La Niña events, SSTAs in the equatorial Pacific are negative (cold phase). La Niña events reach their peak between June and September. Above normal precipitation is experienced during December-February and March-May in northern South America (Acevedo et al., 1999; Obasi, 1999; Turner, 2004).

The Atlantic Niño is similar but weaker than the Pacific Niño. Most warm events of the Atlantic Niño (e.g. 1963, 1968, 1973, 1981, 1984, and 1987) occurred in August-September and a few in December-February (Wang, 2005). During these events, the Atlantic Walker circulation is weakened and the easterly trade winds in the western Atlantic decrease. The Hadley circulation is strengthened and SSTs increase in the equatorial western Atlantic. Wang (2001, 2005) defined the Tropical Atlantic dipole and showed that it is correlated with the north-south displacement of the ITCZ (Wang, 2005). When the Tropical Atlantic dipole becomes strongly positive (negative), rainfall decreases (increases) during December-February (Ambrizzi et al., 2005).

In Suriname little is known about the different oceanic-atmospheric processes that determine rainfall. Understanding these processes may be useful for estimating future impacts of climate change on rainfall and water resources. In this chapter, an attempt is made to analyse the variability of the rainfall in Suriname and the relationship with the Atlantic and Pacific SSTs.

4.2 Data and methods

Twelve rainfall gauge stations distributed throughout Suriname that contain sufficient data are used to characterize the climate variability across Suriname (Figure 3.3). The meteorological data is provided by the Meteorological Service Suriname. For the classification of the spatial features of the annual cycle of rainfall (1961-1985) in Suriname, principal component analysis (PCA) of the annual rainfall anomalies is performed. PCA is calculated using the Climate Predictability Tool (v.5.04) of the International Research Institute for Climate Prediction IRI (http://iri.columbia.edu/outreach/software/). The PCA method is widely used to identify patterns of variability among large datasets of time series. This method has already been explained in chapter 3 (equation 3.25).

To investigate the relationship between the rainfall anomalies in Suriname and the Atlantic and Pacific SSTAs on inter-annual scale, cross correlation analyses and composites are used. The cross correlation equations are given in chapter 3. These analyses are carried out on a seasonal scale (December-February DJF; March-May MAM; June-August JJA; September-November SON), using the Anclim model (Stipanek, 2003) and the KNMI Climate Explorer (http://climexp.knmi.nl/).

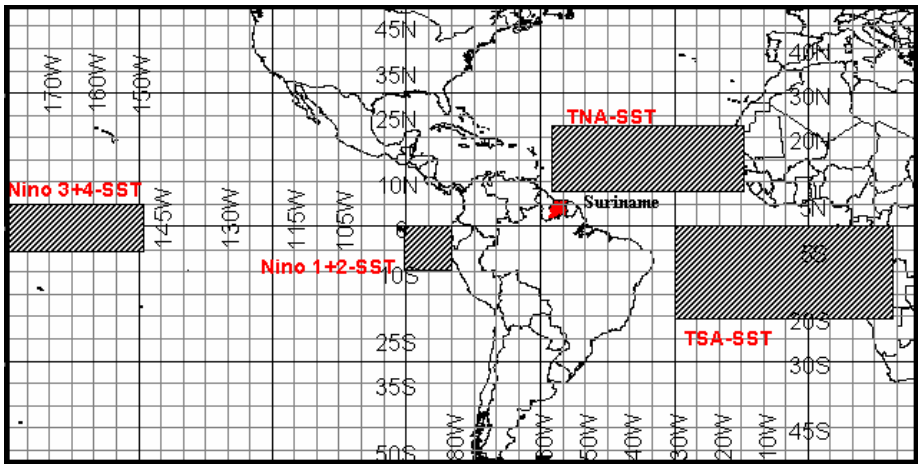

Figure 4.1: Sea surface temperature (SST) area indices for the Tropical Northern Atlantic (TNA), the Tropical Southern Atlantic (TSA), the Extreme Eastern Tropical Pacific /ENSO SST (Pacific Niño 1+2) and the East Central Pacific/ENSO SST (Pacific Niño 3.4) (NOAA-CIRES Climate Diagnostics Center, 2004).

Monthly observed SSTs (1950-2003) are adapted from the National Oceanic and Atmospheric Administration (NOAA-CIRES Climate Diagnostics Center, 2004) for the Tropical northern Atlantic-TNA (5.5^{o}-23.5^{o}N, 15^{o}-57.5^{o}W), the Tropical southern Atlantic-TSA (0^{o}-20^{o}S, 10^{o}E-30^{o}W), the Extreme Eastern Tropical Pacific ENSO-Niño 1+2 (0^{o}-10^{o}S, 90^{o}-80^{o}W) and East Central Pacific ENSO-Niño 3+4 (5^{o}N-5^{o}S, 160^{o}E-150^{o}W). The monthly Atlantic Niño SSTAs (3^{o}S-3^{o}N, 20^{o}W-0^{o}) and SSTAs in the Tropical Atlantic ("dipole index") are obtained from Dr. Wang, C. (NOAA-CIRES). The Atlantic dipole is defined as the difference between the SSTAs in the TNA (5.5^{o}-23.5^{o}N, 15^{o}-57.5^{o}W) and the SST anomalies in the TSA (0^{o}-20^{o}S, 10^{o}E-30^{o}W) (Wang, 2001). The different SSTs areas are shown in Figure 4.1. Reanalyses of fields (1961-1985) from the National Center for Environmental Prediction - National Center for Atmospheric Research (NCEP-NCAR) are also used to investigate the correlation (r) between seasonal rainfall and SSTs. For the uniformity and availability of statistical tables, all statistical tests in this study are performed at a 5% significance level.

4.3 Results and discussion

4.3.1 Variability of rainfall

Figure 1.9 shows the distribution of the annual precipitation (1961-1985) based on the twelve rainfall stations. A main feature of the precipitation distribution is that the annual precipitation is the highest in the centre of Suriname (about 2800 mm) and the lowest in the low-lying areas (north-west Suriname: about 1650 mm). Figure 3.7 shows that a decrease in annual precipitation occurs in the center and southwest of Suriname (5-15 mm/year). Northeast Suriname shows the strongest increasing trend (10-43 mm/year). Three stations in this area show a significantly positive trend in this area. Figure 4.2a shows the average seasonal total precipitation and Figure 4.2b the seasonal trends for DJF, MAM, JJA and SON. These results indicate that the season rainfall distribution has the same pattern as the annual rainfall distribution. Significant trends were only found in the MAM rainfall at station Cultuurtuin, Albina, Moengo, Groningen, Brownsweg and Coeroeni. This is due to the steep increase in rainfall during February-March. A decrease (increase) in seasonal rainfall during 1961-1985 is observed in east (west) Suriname during DJF and JJA. During MAM and SON positive trends are observed throughout Suriname.

The PCA results (Figure 4.3a) show that the annual rainfall anomalies tend to occur fairly uniform across the whole country (positive loadings between 0.16 and 0.34, and about similar weights at most stations). The first principal component, represents 51% of the total variance in the data, which can be explained by the low spatial loading at Brownsweg (0.16), Nieuw-Nickerie (0.21) and Groningen (0.19). Figure 4.3b shows the inter-annual variability with the temporal scores from which can be concluded that 1964 was a very dry year and 1976 a very wet year. In the next paragraph the seasonal spatial variability of rainfall will be discussed further.

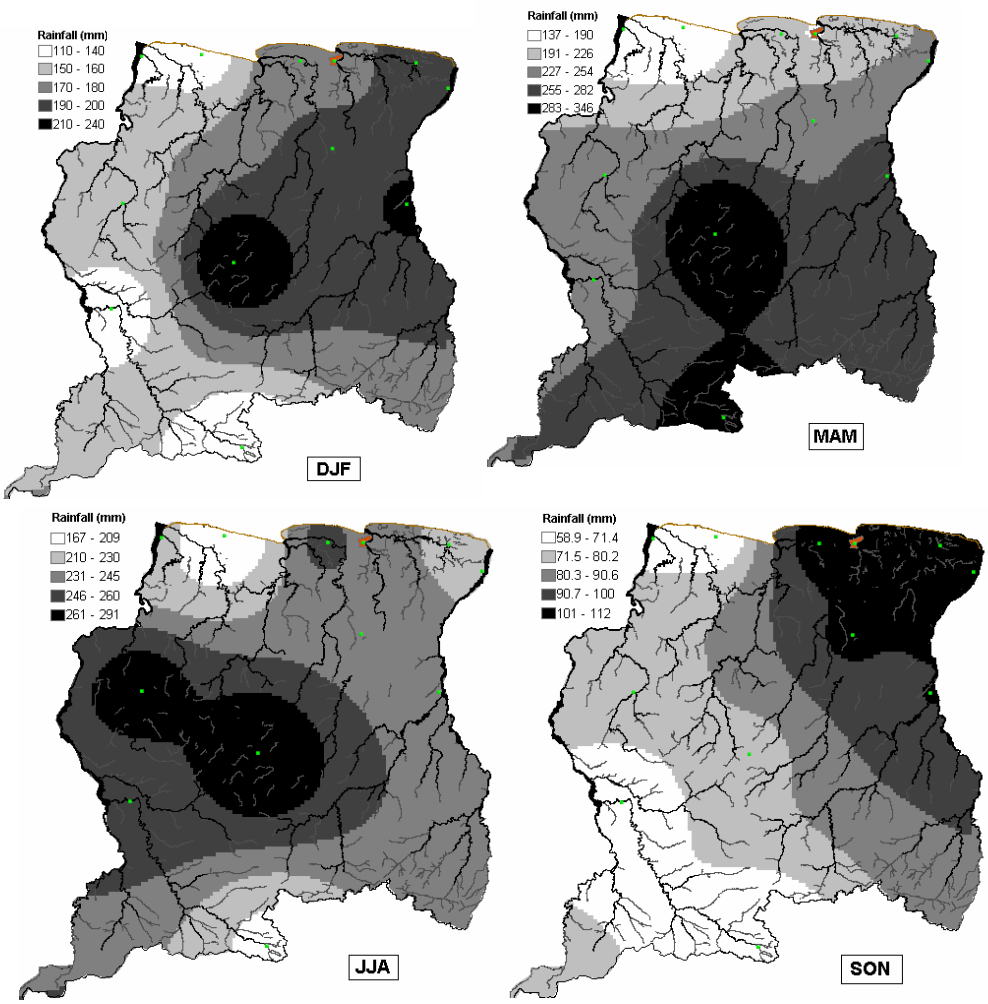
Rainfall (mm)
110 - 140
150 - 160
170 - 180
190 - 200
210 - 240
DJF
Rainfall (mm)
137 - 190
191 - 226
227 - 254
255 - 282
283 - 346
MAM
Rainfall (mm)
167 - 209
210 - 230
231 - 245
246 - 260
261 - 291
JJA
Rainfall (mm)
58.9 - 71.4
71.5 - 80.2
80.3 - 90.6
90.7 - 100
101 - 112
SON

(a)

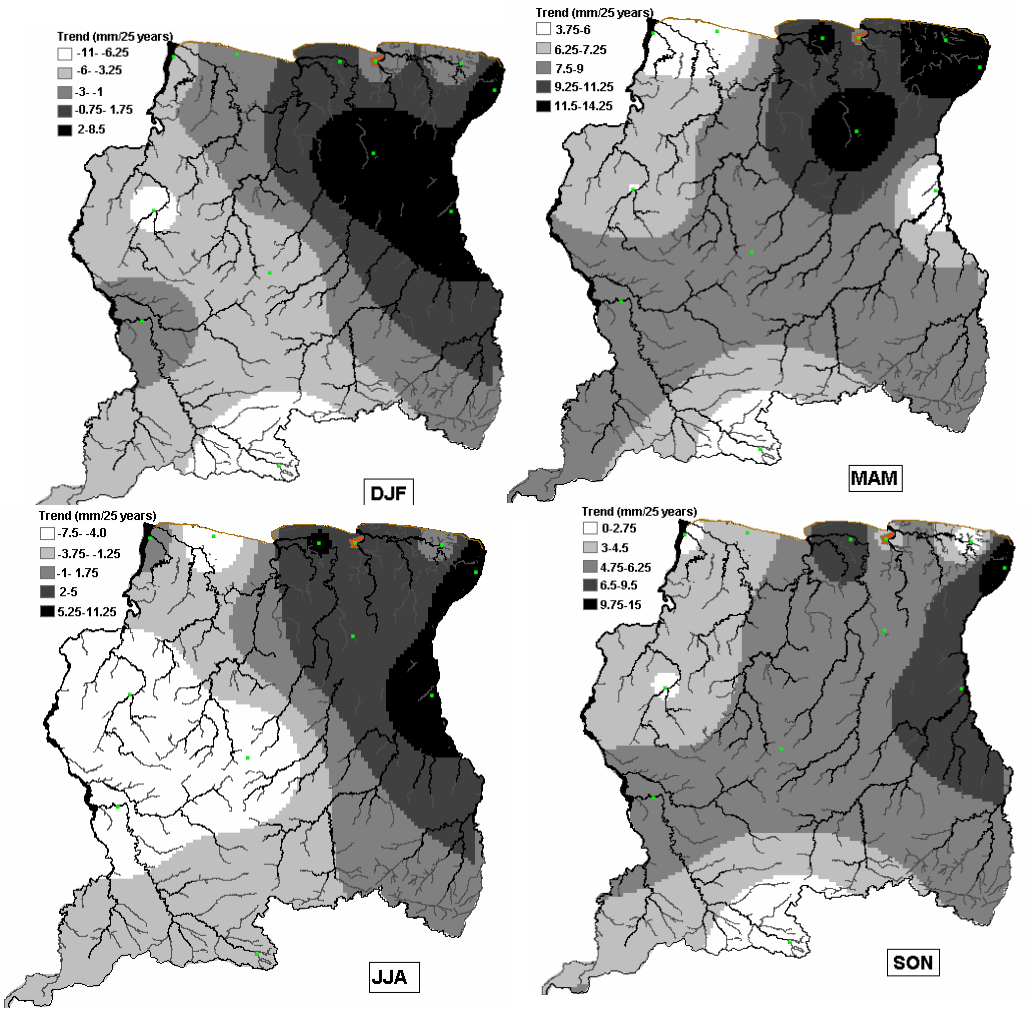

(b)

Figure 4.2: (a) Average seasonal total precipitation (mm) in Suriname, 1961-1985 during December-February (DJF), March-May (MAM), June-August (JJA) and September-November (SON), (b) trend in seasonal precipitation (25 mm/years) during DJF, MAM, JJA, SON. Significant trends at 5% level are found in the MAM rainfall at station Cultuurtuin, Albina, Moengo, Groningen, Brownsweg and Coeroeni.

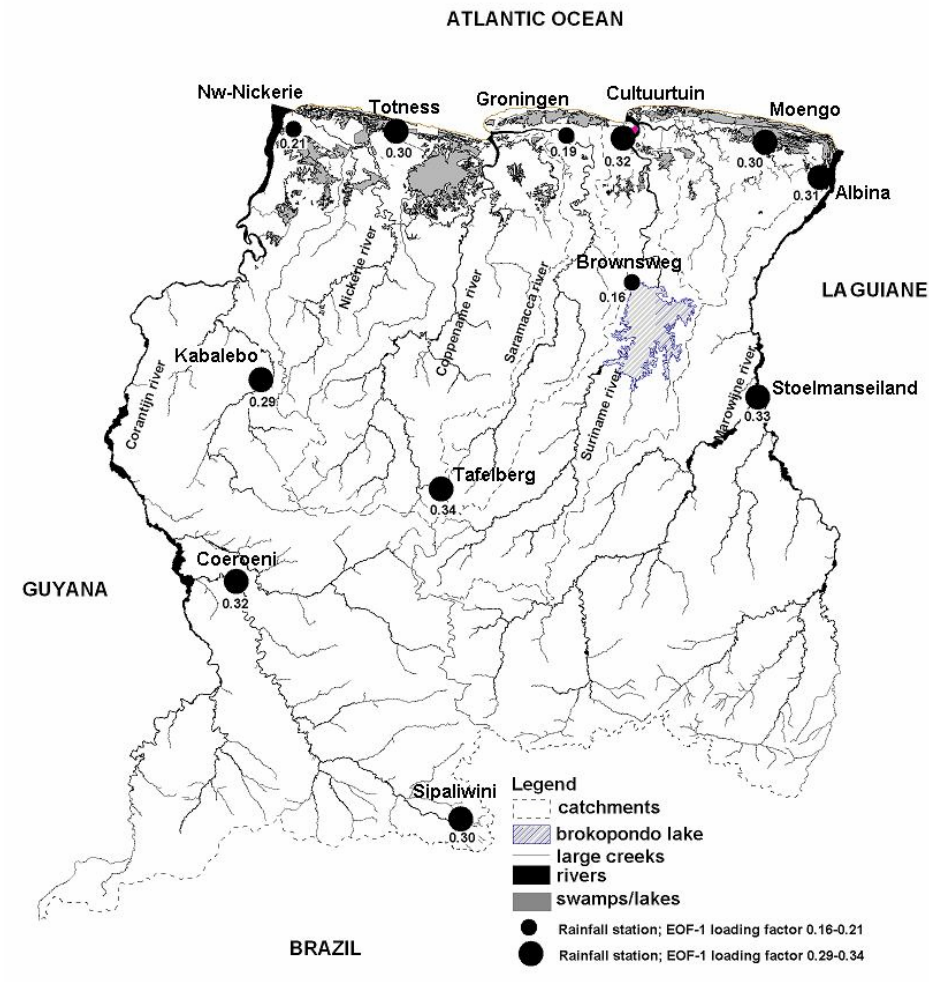
ATLANTIC OCEAN
Nw-Nickerie
Totness
Groningen
Cultuurtuin
Moengo
Albina
0.21
0.30
0.19
0.32
0.30
0.31
Nickerie river
Coppename river
Saramacca river
Brownsweg
0.16
LA GUIANE
Kabalebo
0.29
Corantijn river
Suriname river
Marowijne river
Stoelmanseiland
0.33
Tafelberg
0.34
GUYANA
Coeroeni
0.32
Sipaliwini
0.30
BRAZIL
Legend
catchments
brokopondo lake
large creeks
rivers
swamps/lakes
Rainfall station; EOF-1 loading factor 0.16-0.21
Rainfall station; EOF-1 loading factor 0.29-0.34

(a)

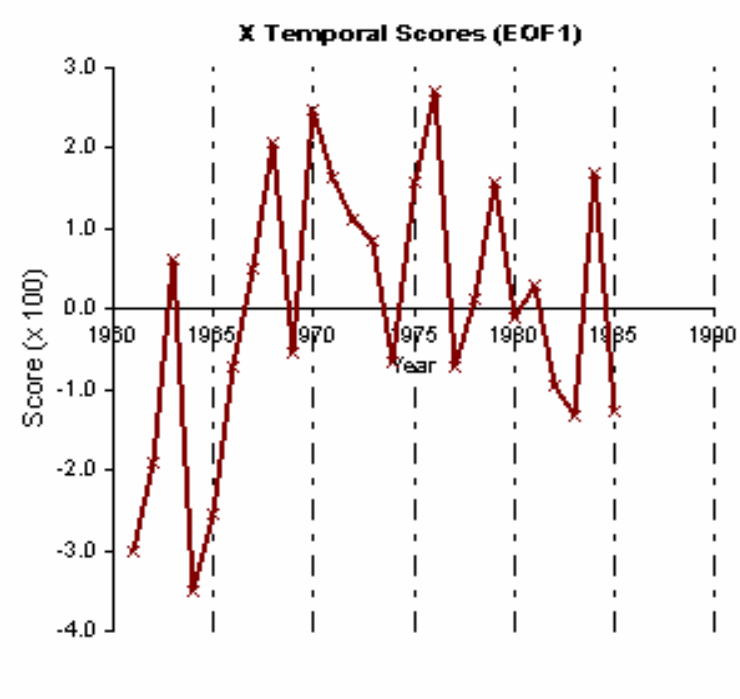

(b)

Figure 4.3: (a) Spatial loadings (EOF-1) of the annual rainfall anomalies at 12 rainfall stations, (b) temporal scores (EOF-1).

4.3.2 Relationship between rainfall anomalies and Atlantic and Pacific SSTAs

Figure 3.2 shows the observed monthly SSTs in the Atlantic and Pacific regions and the monthly observed rainfall at station Cultuurtuin. The monthly rainfall shows a seasonal cycle, which is caused by the meridional movement of the ITCZ (Emanuels, 1968). Most of the other rainfall stations also show a similar seasonal rainfall pattern. The monthly rainfall is the highest in May-June and the lowest in October-September.

Figure 4.4 shows the lagged correlation (Pearson's coefficient) of the DJF, MAM, JJA and SON precipitation anomalies at station Cultuurtuin with the SSTAs in the TNA, TSA, Niño 1+2, Niño 3+4, Atlantic Niño and the TA dipole region. Because of the fact that all the rainfall stations show similar results, only station Cultuurtuin will be used further in this study. During December-February (the short wet season), the TNA is less warm than normal and the TSA is warmer than normal.

North-easterly trade winds north of the equator are strengthened, while the south-easterly trade winds south of the equator are weakened (Villwock, 1998; Webster, 2005). In DJF, the precipitation anomalies show a much stronger correlation with the SSTAs in the Niño 1+2 region ($c_{lag\ 3}$ = -0.63), followed by the Tropical Atlantic Niño region ($c_{lag\ 0}$ = -0.36) and the TA region ($c_{lag\ 0}$ = -0.32). A positive lag indicates that the SSTAs is the leading index and a positive (negative) correlation indicates that large (small) precipitation anomalies are related with large SSTAs. Correlations with the SSTAs in the TNA region ($c_{lag\ 11\text{-}12}$ = 0.23) and the SSTAs in the TSA region ($c_{lag\ 3}$ = -0.24) are lower (Figure 4.4 (a), (b), (f)). During DJF, the ITCZ has a small rainfall belt and is displaced southward of Suriname and causes a reduction in precipitation across Suriname (Figure 4.4b) that reaches its peak during February-March. February-March is the short dry season. During April-mid August (the long wet season) the TNA (TSA) becomes warmer (colder) than normal indicating a northward movement of the ITCZ. Oceanic air rises over the TNA warm water, easterly trade winds from the Atlantic Ocean are weakened north of the equator and easterly trade winds south of the equator increase. The southeasterly trade winds also bring the tropical heat sources of the Amazon to Suriname. Evaporation increases over the TNA and as a result precipitation increases over northern South America. During this period, the ITCZ has a rainfall belt that is twice the rainfall belt during DJF and hardly covers whole of Suriname. The extension of this season to about 4 months, compared to the small wet season, is due to the fact that during May-July, the equatorial air mass from the Amazon region moves in northerly direction and clashes with the relief of the country (near Tafelberg), but also with the northeast trade winds. This causes the ITCZ movement above Suriname to become slower. This explains the high rainfall in the centre of Suriname (Figure 4.4b).

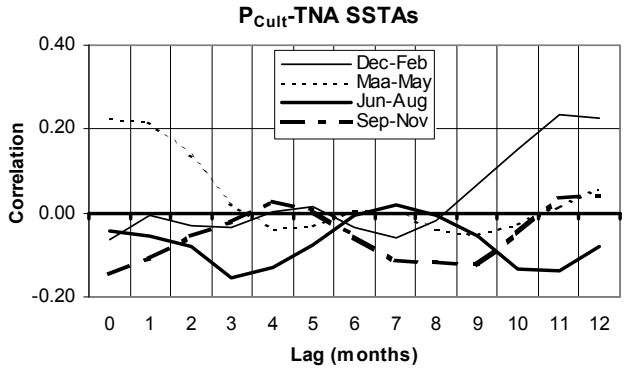
P_{Cult}-TNA SSTAs
Dec-Feb
Maa-May
Jun-Aug
Sep-Nov
Correlation
0.40
0.20
0.00
-0.20
0 1 2 3 4 5 6 7 8 9 10 11 12
Lag (months)

(a)

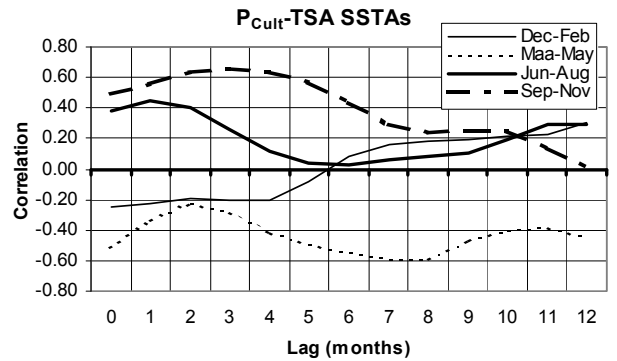
P_{Cult}-TSA SSTAs
Dec-Feb
Maa-May
Jun-Aug
Sep-Nov
Correlation
0.80
0.60
0.40
0.20
0.00
-0.20
-0.40
-0.60
-0.80
0 1 2 3 4 5 6 7 8 9 10 11 12
Lag (months)

(b)

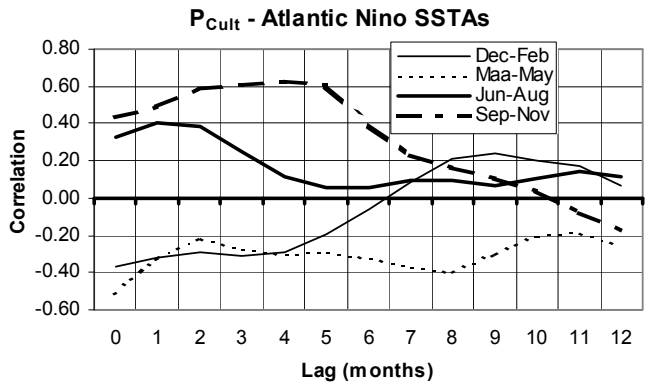
P_{Cult} - Atlantic Nino SSTAs
Dec-Feb
Maa-May
Jun-Aug
Sep-Nov
Correlation
0.80
0.60
0.40
0.20
0.00
-0.20
-0.40
-0.60
0 1 2 3 4 5 6 7 8 9 10 11 12
Lag (months)

(c)

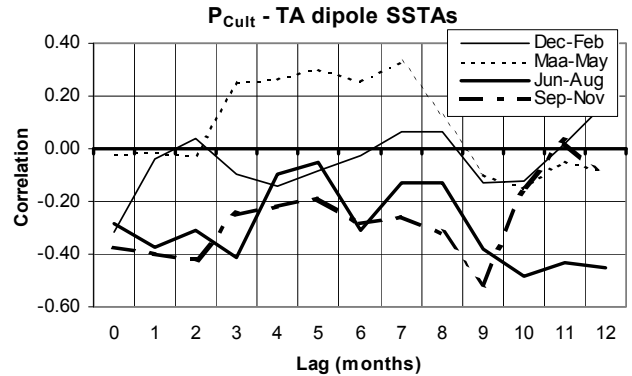
P_{Cult} - TA dipole SSTAs
Dec-Feb
Maa-May
Jun-Aug
Sep-Nov
Correlation
0.40
0.20
0.00
-0.20
-0.40
-0.60
0 1 2 3 4 5 6 7 8 9 10 11 12
Lag (months)

(d)

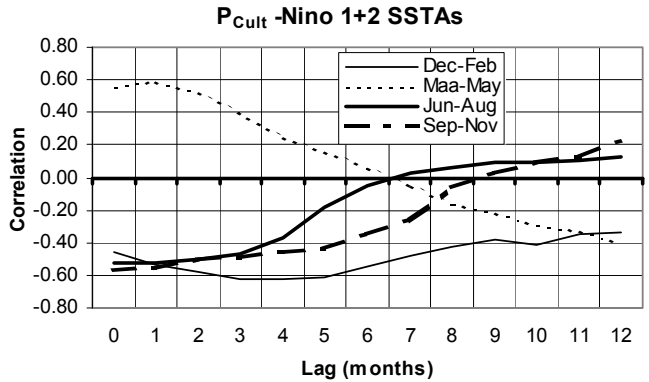

(e)

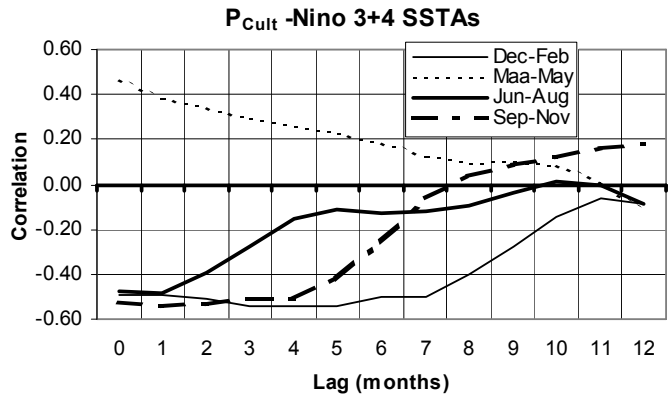

(f)

Figure 4.4: Lag correlation coefficient of the precipitation anomalies (1961-1985) at station Cultuurtuin for December-February (DJF), March-May (MAM), June-August (JJA) and September-November (SON) with the (a) TNA SSTAs, (b) TSA SSTAs, (c) Niño 1+2 SSTAs, (d) Niño 3+4 SSTAs, (e) Atlantic Niño SSTAs and (f) Tropical Atlantic dipole SSTAs. Note: lag positive, SSTAs leading index.

Table 4.1: The highest cross correlation coefficient c_k (with 95% confidence interval) (a) between the monthly time series of SSTAs in the TNA, TSA, Niño 1+2 and Niño 3+4 region (1961-1985) and (b) the highest lag correlation coefficient of the monthly SSTAs for the December-February (DJF), March-May (MAM), June-August (JJA) and September-November (SON) period for the same regions (1961-1985). Note: lag 0-12 months.

Predictor	TNA SSTAs	TSA SSTAs	Niño 1+2 SSTAs	Niño 3+4 SSTAs
TNA SSTAs	1.00	-0.12 (lag 11)	0.25 (lag -5)	0.49 (lag -4)
TSA SSTAs		1.00	-0.29 (lag 9)	-0.40 (lag 12)
Niño 1+2 SSTAs			1.00	0.67 (lag 1)
Niño 3+4 SSTAs				1.00

(a)

Predictor / Period	DJF	MAM	JJA	SON
c_k(TNA-TSA SSTAs)	-0.30 (lag 11)	-0.40 (lag 10)	-0.17 (lag 12)	-0.43 (lag 8)
c_k(TNA-Niño 1+2 SSTAs)	0.17 (lag 3)	0.54 (lag 5)	0.56 (lag 7)	0.19 (lag 1)
c_k(TNA-Niño 3+4 SSTAs)	0.40 (lag 9)	0.72 (lag 4)	0.69 (lag 4)	0.33 (lag 6)
c_k(TSA-Niño 1+2 SSTAs)	0.44 (lag 4)	0.44 (lag 8)	0.44 (lag 12)	0.32 (lag 12)
c_k(TSA-Niño 3+4 SSTAs)	0.36 (lag 9)	0.22 (lag 12)	0.38 (lag 1)	-0.13 (lag 4)
c_k(Niño 1+2-Niño 3+4 SSTAs)	0.89 (lag 0)	0.62 (lag 0)	0.69 (lag 1)	0.87 (lag 1)

(b)

During the beginning of the long wet season (MAM), the Niño 1+2, TSA and the Tropical Atlantic Niño SSTAs all show a strong correlation with the rainfall anomalies in the same order of magnitude of about $c_{lag\ 1}{}^{Niño1+2} = 0.59$, $c_{lag\ 0}{}^{TSA} = -0.52$ and $c_{lag\ 0}{}^{Atlantic\ Niño} = -0.52$, than with the TNA SSTAs ($c_{lag\ 0} = 0.23$) and the TA dipole SSTAs ($c_{lag\ 7} = 0.33$) (Figure 4.4). During JJA, the SSTAs in both the TA dipole and TSA region show a stronger correlation with the rainfall anomalies than in the other regions of $c_{lag\ 10} = -0.49$ and $c_{lag\ 0} = -0.52$ respectively.

From mid-August to November (the long dry season), the SSTs in the TNA (TSA) are the highest (lowest) and the precipitation maximum has passed over Suriname and is found north (5^oN-10^oN) above the Atlantic Ocean (Webster, 2005). During this period, the trade winds south of the equator increase surface winds and cause surface evaporative cooling and, as a result, less rainfall above Suriname. The rainfall anomalies show the largest positive correlation with the SSTAs in the TSA region ($c_{lag\ 3}$ = 0.66) and the Atlantic Niño region ($c_{lag\ 4}$ = 0.63) than in the other regions.

Cross correlation analyses have shown (Table 4.1) that the Pacific Niño 3+4 SSTAs show a stronger correlation with the TNA SSTAs during all the seasons compared to the Niño 1+2 SST. The highest correlation is reached in MAM and is 0.72 for k = 4 months. In the TSA region, the Niño 1+2 SST is slightly stronger correlated with the SST than the Niño 3+4 SST. The highest correlation (c_k = 0.44) is obtained when the Niño 1+2 SSTAs lead the TSA SSTAs by 4, 8 and 12 months in DJF, MAM and JJA respectively. Similar results were also found by Wang (2001) and Marshall et al. (2001).

4.4 Conclusions

Analysis of spatial variability of rainfall (1961-1985) has shown that a medium to high correlation exists in the annual rainfall variability (1961-1985) between the different stations. A decreasing trend in annual precipitation occurs in central and southwest Suriname (maximum -14.5 mm/year), while a rising trend is observed in the other areas of Suriname. The highest negative trend is in northeast Suriname and is about 42.7 mm/year. The highest rainfall occurs at all the stations in May-June and the lowest rainfall in October-September. Statistical analyses of rainfall in Suriname show that rainfall correlate well with SSTAs in the TNA, TSA, Niño 1+2, Niño 3+4, Atlantic Niño and the TA dipole region. Based on station Cultuurtuin, the highest correlation (ck = -0.63) between the DJF rainfall (short wet season) is found with the Pacific SSTAs in the Niño 1+2 region three months earlier.

The MAM rainfall anomaly (beginning long wet season) correlates with the TA SSTAs ($c_{lag\ 0}^{\ TSA}$ = -0.52; $c_{lag\ 0}^{\ Atlantic\ Niño}$ = -0.52) as well as with the Pacific SSTAs ($c_{lag\ 1}^{\ Niño\ 1+2}$ = 0.59). The highest correlation between the JJA rainfall (long wet season) and the SSTAs is reached in the TSA region and is about c = -0.52 for lag 0. Finally, the long dry season (SON) is more strongerly correlated with the TSA SSTAs ($c_{lag\ 3}$ = 0.66).

For all seasons it is found that the rainfall is also medium to highly correlated with the Pacific SSTAs, which indicates that El Niño events may cause rainfall below or above normal (drought conditions). The knowledge of rainfall variability and processes responsible for this variability, among other things,

is used to provide scenarios that can be used for water resources planning and design of hydraulic works. At present, forecasting the Atlantic climate variability and the Pacific ENSO with respect to rainfall need to be further examined. More research is needed to advance our understanding of the tropical oceanic and atmospheric processes, the interactions and the mechanisms of variability in Suriname and surrounding countries.

Acknowledgements

I would like to thank Chunzai Wang, Giannini Alessandra and Geert van Oldenborgh for their cooperation. Three anonymous reviewers provided valuable comments that helped improve this chapter.

.

5. CHANGES AND VARIATION IN THE DISCHARGE REGIME OF THE UPPER-SURINAME RIVER*

Abstract

Long-term changes and variability in river flows in the tropical Upper-Suriname River Basin in Suriname (2^{o}-6^{o} Northern Length, 54^{o}-58^{o} Western Length) are analysed including the relation to sea surface temperatures (SSTs) in the tropical Atlantic and Pacific Ocean. For variability analyses, lag correlation analyses and statistical properties of the data series are used. Long term changes are analysed using parametric and non-parametric statistical techniques. The analyses are performed for the period 1952-1985. The results show that both river discharge series at Semoisie and Pokigron are non-stationary and have a negative trend. The negative annual rainfall trend in the centre of Suriname may be responsible for the negative trend in the annual river discharges in the basin. The highest correlation is obtained when the Tropical North Atlantic (TNA) SSTs lags the monthly discharges at Pokigron by 3-4 months (c = 0.7) and when the Tropical South Atlantic (TSA) SSTs lags the discharges by 4 months (c = -0.7). c is the Pearson's coefficient. From the analyses also follows that the high (low) monthly flows, from April-August (September-March) are associated with increasing (decreasing) SSTs in the TNA and with decreasing (increasing) SSTs in the TSA. The results also reveal that years with low (high) discharges are more related to warmer (colder) SSTs during the year in the TNA region and a southward displacement of the Inter-tropical Convergence Zone (ITCZ). However, the Pacific El Niño events (La Niña) may also be responsible for low (high) flow years in this basin.

* This chapter has been published as a research article: "Changes and variation in the discharge regime of the Upper-Suriname River Basin and its relationship with the tropical Pacific and Atlantic SST anomalies", Journal of Hydrological Processes, DOI: 10.1002/hyp.6733, 2007.

5.1 Introduction

Hydrological processes of watersheds such as surface runoff and evapotranspiration are sensitive to changes in land use and climate change (Maidment, 1993). The Intergovernmental Panel on Climate Change (IPCC, 2001) has shown that global climate change in the last century has resulted in an increase in the earth's average surface air and sea temperature by about 0.3°C to 0.6°C. This change has affected the global hydrological cycle, primarily rainfall and runoff. (IPCC, 2001; Jones et al., 1996; Lozan et al., 1998; McMichael et al., 1996; Solomon et al., 1987; Tamara et al., 1999; WMO/UNESCO, 1997). Extreme climate and weather events have in the last 10 years been responsible for about 90% of all disasters on earth such as floods, extreme droughts and hurricanes and have affected different socio-economic sectors and the environment e.g. infrastructure, agriculture, fisheries and health (Kundzewicz, 2000; Ross and Lott, 2000, 2004). Both long-term and short-term changes in climate may thus also affect water resources.

In the northern and northeastern part of South America, rainfall is mainly influenced by the Tropical Atlantic Sea Surface Temperature (SST) through the Walker and Hadley circulation (Ambrizzzi et al., 2005). The Walker circulation consists of air rising in the eastern Pacific, diverges eastward and sinks in the equatorial Atlantic and returns to the west. During the Hadley circulation, ascending air from South America moves from the Tropical North Atlantic (TNA) region (5.5°-23.5° Northern Length, 15°-57.5° Western Length), descends in the equatorial Atlantic and flows southward to South America (Wang, 2001). Rainfall in northern South America is also influenced by the Pacific El Niño-Southern Oscillation (ENSO) related SST anomalies (SSTAs), the Atlantic zonal equatorial mode (the "Atlantic Niño") and the Tropical Atlantic Meridional Gradient (TAMG) (or Tropical Atlantic dipole index) (Wang, 2001; Wang, 2005). SSTA is defined as the difference between the observed value and the long term mean of all the observations and will further be discussed in paragraph 5.2. Some of these processes are schematically shown in Figure 1.8.

The Pacific ENSO is one of the well-known phenomena that may cause floods and droughts in different parts of the tropics (30° Southern Length - 30° Northern Length). Some significant El Niño events occurred in the periods of 1957-1958, 1965-1966, 1982-1983, 1986-1987, 1997-1998. During these events, the SSTAs in the equatorial Pacific are positive (warm phase). The Pacific Walker cell and the Atlantic Hadley circulations are stronger and weaker respectively. This leads to a weakening of the northeasterly trade winds in the TNA and less surface evaporation in the TNA region (Marshall et al., 2001). As a result, SST increases in the TNA,

with a lag of 4-5 months, reaching its maximum in the periods of December-February and March-May. In these periods, rainfall below normal is experienced in northern South America (Marshall et al., 2001, Rajagopolan et al., 1997, Ropelewski and Hapert, 1987, 1989, 1996) and Wang (2001). During La Niña events, SSTAs in the equatorial Pacific are negative (cold phase). La Niña events reach their peak between June-September. Precipitation above normal is experienced in the periods December-February and March-May in northern South America (Acevedo et al., 1999; Robertson and Mechoso, 2002; Obasi, 1999; Turner, 2004; Wang, 2005).

The Atlantic Niño is similar but weaker than the Pacific Niño. Most warm events of the Atlantic Niño (e.g. 1963, 1968, 1973, 1981, 1984, 1987) occurred in August-September and a few in December-February (Wang, 2005). During these events, the Atlantic Walker circulation is weakened and the easterly trade winds in the western Atlantic decrease. The Hadley circulation is strengthened and SSTs increase in the equatorial western Atlantic.

The Tropical Atlantic Meridional SST Gradient is calculated as the Tropical North Atlantic SSTs minus the Tropical South Atlantic SSTs, and is correlated with the north-south displacement of the Inter-tropical Convergence Zone (ITCZ) (Ambrizzi et al., 2005; Wang, 2005). When the gradient is strongly positive, air rises over the TNA and moves southward and causes less precipitation over northern South America, especially during December-February. When the gradient becomes strongly negative, rainfall increases over this area.

Recent studies by Garzoli et al. (1999), Giannini et al. (2000), Marshall et al. (2001) and Villwock (1998) have shown that the rainfall in northern South America is more related to the SSTAs in the TNA than the Tropical South Atlantic (TSA) and the tropical Pacific ENSO. SSTs warmer than normal in the TNA and colder than normal in the TSA correspond with weaker (stronger) than normal northeasterly (southeasterly) trade winds in the TNA and a northward displacement in the ITCZ during March-May. This causes an increase in rainfall in this region.

In Suriname (2^{o}-6^{o} Northern Length, 54^{o}-58^{o} Western Length), the high temporal and spatial variability of rainfall determines the hydrological regime of rivers. Prolonged dry periods, due to the remote influence of ENSO, were experienced in north-west Suriname in 1925/1926, 1939/1940, August-November 1982, December 1982-February 1983 and 1997/1998 (Houben and Molenaar, undated; Mol et al., 2000; Webster and Roebuck, 2001). The drought of 1997/1998 was also experienced in the neighbouring countries Guyana and northeastern Brazil. In the last 25 years, the variable rainfall has

affected the proper operation of the Prof. Dr. Ir. van Blommenstein reservoir in Suriname that is being used for hydropower generation. This reservoir receives its water from the Upper-Suriname River catchments (Figure 1.13b) and has a drainage area of about 7,860 km^2. During at least four periods, the lake inflows were reduced significantly: 1987/1988 (18 months), March 1999, January 2001 and September 2004-January 2005. Some of these periods may be linked to the warm phase of the Atlantic Niño. Because of the importance of this reservoir for the economy of Suriname, a better understanding of the climate - river discharge behavior in the Upper-Suriname River Basin is required. In this study statistical methods will be used to analyse long term changes and variation in the river discharges in this basin and the influence of the Pacific and Atlantic sea surface temperature on the river discharge.

5.2 Data and methodology

5.2.1 Data

The largest available data sets (1952-1985) used in this study are the monthly river discharges of station Semoisie (drainage area of about 5,682 km^2) and Pokigron (drainage area of about 7,860 km^2). Figure 1.13b shows the locations of these stations. The river discharge series are provided by the Hydraulic Research Division (WLA), the Bureau for Hydroelectric Power Works (BWKW) and the monthly inflows (1911-2001) in the van Blommenstein reservoir by the Bauxite Institute Suriname/Suriname Aluminum Company LLC. The observed time series of monthly and annual mean river discharges at Semoisie (Q_{sem}) and Pokigron (Q_{pok}) are graphically shown in Figures 5.1 and 5.2 respectively. Within these catchments, a few rainfall gauge stations are available, but the observed data are insufficient to be considered for climate change and climate variability analysis. The two closest rainfall stations with sufficient data are Brownsweg (490 m Normaal Surinaams Peil - NSP) and Tafelberg (323 m NSP) (Figure 1.13b). The observed monthly rainfall (1961-1985) of these stations is shown in Figure 5.3. The meteorological data is issued by the Meteorological Service Suriname (MDS). A summary of the hydrological characteristics of the Upper-Suriname River catchments is presented in Table 5.1.

Monthly observed SSTs (1950-2003) are adapted from the National Oceanic and Atmospheric Administration (NOAA-CIRES Climate Diagnostics Center, 2004) for the Tropical Northern Atlantic-TNA (5.5^o-23.5^{o}N, 15^o-57.5^{o}W), the Tropical Southern Atlantic-TSA (0^o-20^{o}S, 10^{o}E-30^{o}W), the Extreme Eastern Tropical Pacific ENSO-Niño 1+2 (0^o-10^{o}S, 90^o-80^{o}W) and East Central Pacific ENSO-Niño 3+4 (5^{o}N-5^{o}S, 160^{o}E-150^{o}W).

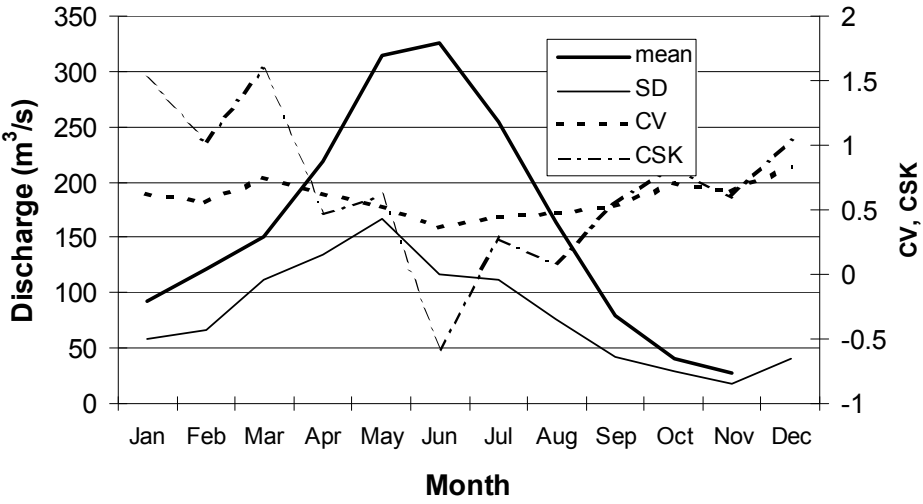

(a)

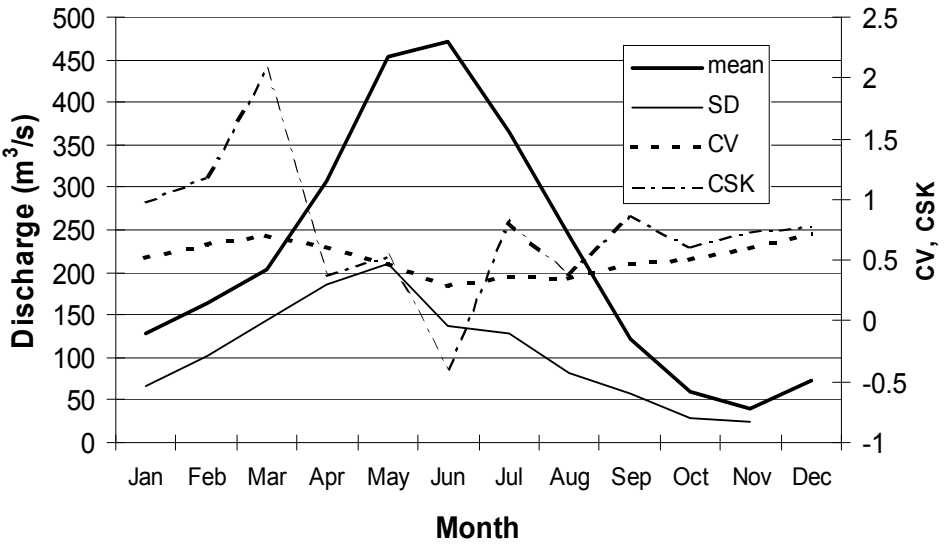

(b)

Figure 5.1: Observed monthly mean river discharges of the Upper-Suriname River including Standard Deviation (SD), Coefficient of Variation (CV) and Coefficient of Skewness (CSK) at (a) Semoisie and (b) Pokigron (1952-1985). The equations used for CV and CSK are taken from Mamdouh et al. (1993).

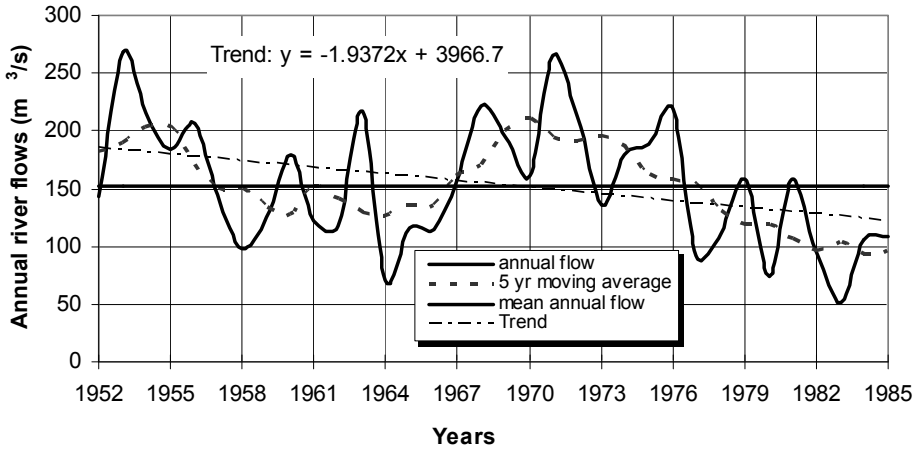

(a)

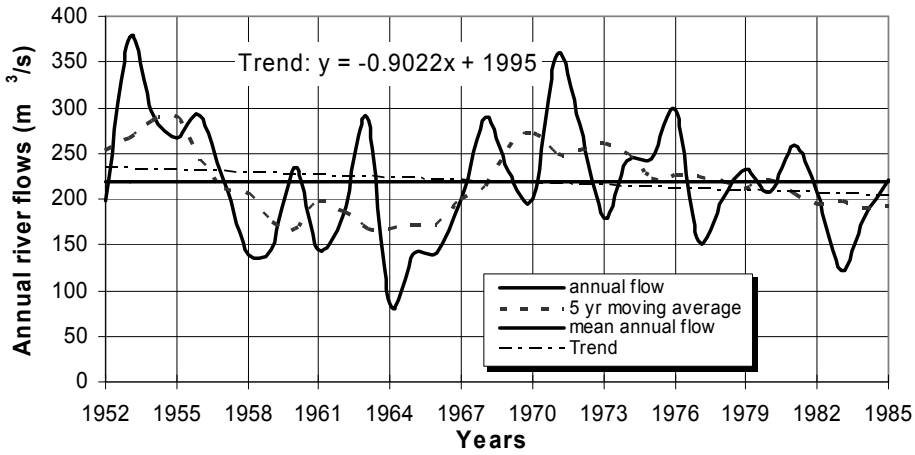

(b)

Figure 5.2: Time series of observed annual mean river discharges (m^3/s) in the Upper-Suriname River catchment at station (a) Semoisie and (b) Pokigron during a 34 years period (1952-1985). Note: thick dotted line is the five-year moving running average and the thin linear dotted line is the trend line.

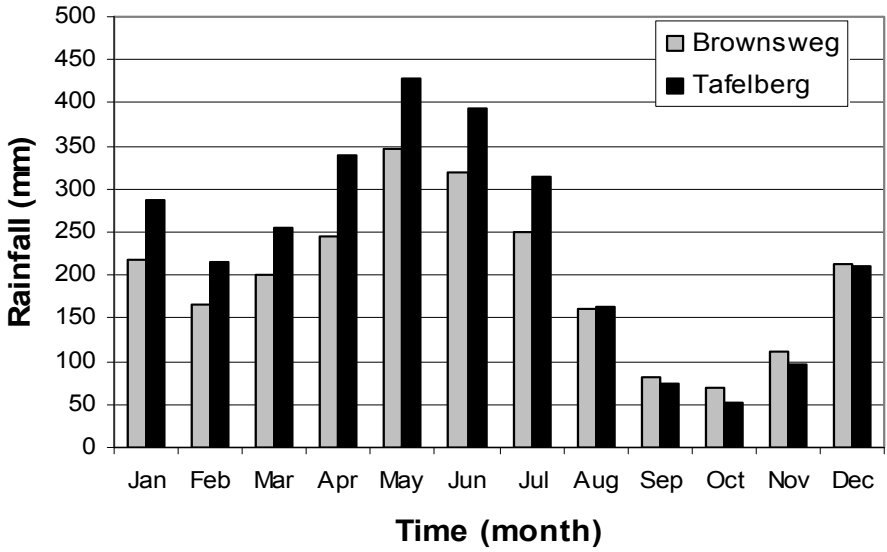

Figure 5.3: Time series of observed monthly mean rainfall (mm) at station Brownsweg and Tafelberg during a 25 years period (1961-1985).

Table 5.1 Hydrological characteristics of the Upper-Suriname River Basin.

Discharge Station	Semoisie	Pokigron
Catchment area upstream of station (km^2)	5,682	7,860
Elevation stations (m NSP)	94	78
River length (km)	160	235
Mean annual discharge (m^3/s)*	153	219
Average maximum annual discharge (m^3/s)*	268	377
Average minimum annual discharge (m^3/s)*	51	86
Annual flow depth (mm)	850	879
Annual rainfall (mm)**	2,700	2,600
Runoff coefficient (-)	0.31	0.34
Annual evaporation (mm)**	1,825	1,850

* The calculations are based on annual time series of 34 years (1952-1985) for both stations.

** Source: Nurmohamed and Naipal (2004), Lenselink and van der Weert (1970).

The monthly Atlantic Niño SSTAs (3°S-3°N, 20°W-0°) and SSTAs in the Tropical Atlantic ("dipole index") are obtained from Dr. Wang, C. (NOAA). The locations of the SST areas are shown in Figure 4.1. The SST anomaly is obtained by subtracting the annual (monthly) climatologies (for 12 months) for each data series for the individual annual (monthly) data.

Figure 5.4 shows the SSTAs for the different regions for the period 1952-1985. Figure 5.4a shows that the annual SSTAs in the TNA region are prevailingly positive during 1961-1970 and prevailingly negative during 1971-1976. During 1977-1985, the TNA region is mostly warmer than normal and the TSA region mostly colder than normal (Figure 5.4b). A warm TNA and cold TSA region indicate that trade winds in the TNA region are weakened and strengthened in TSA region. The ITCZ is shifted northwards of Suriname, reducing precipitation above Suriname. Figure 6.5c and 6.5d show the SSTAs in the Pacific ocean. During this 33 years period since 1952, there were about 4 strong warm events (El Niño), for example in 1957-1958, 1965-1966, 1972-1973 and 1982-1983. During this period, one can also notice a few strong cold events (La Niña), for example in 1955-1956, 1970-1971, 1973-1974 and 1975-1976. Figure 5.4e shows the SSTAs in the tropical Atlantic ocean and from this figure we can see that about 5 extreme warm events (SSTAs > 0.7°C) occurred during 1952-1985, for example in July 1963, January 1973, August 1981. Figure 5.4f shows that the TNA-TSA SSTA gradient is mainly positive for 1952-1970 and 1976-1983, and prevailingly negative during 1971-1975.

5.2.2 Methodology

Most of the methods chosen are widely used in similar studies and have been recommended by the WMO (1988). The goodness-of-fit test (the Chi-square test and the Kolmogorov-Smirnov test) is applied to test if the monthly and annual river discharges (1952-1985) follow a normal distribution. The test statistic for the Chi-square goodness of fit test can be calculated from the relationship:

$$\chi_c^2 = \frac{\sum_{i=1}^{k} (O_i - E_i)^2}{E_i} \qquad \text{(Eq. 5.1)}$$

where k is the number of class intervals, Q_i and E_i are the observed and the expected number of observations in the i^{th} class interval respectively, χ_c^2 is the Chi-square distribution with k-p-1 degrees of freedom, where p is the number of parameters estimated from the data (McCuen, 2000).

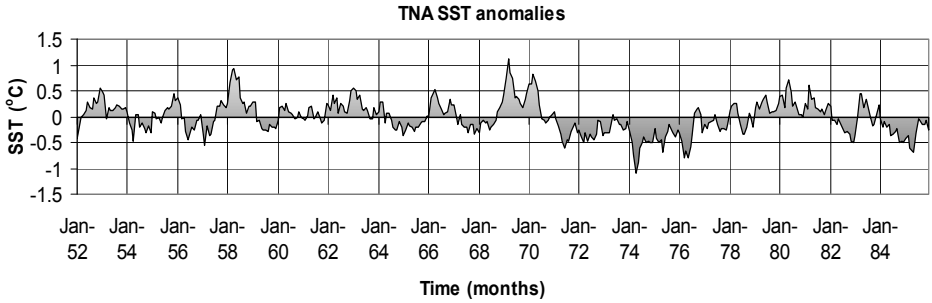
TNA SST anomalies
SST (°C)
1.5
1
0.5
0
-0.5
-1
-1.5
Jan-52 Jan-54 Jan-56 Jan-58 Jan-60 Jan-62 Jan-64 Jan-66 Jan-68 Jan-70 Jan-72 Jan-74 Jan-76 Jan-78 Jan-80 Jan-82 Jan-84
Time (months)

(a)

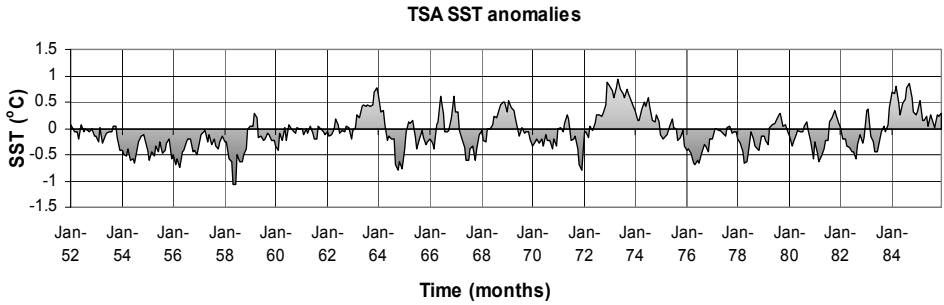
TSA SST anomalies
SST (°C)
1.5
1
0.5
0
-0.5
-1
-1.5
Jan-52 Jan-54 Jan-56 Jan-58 Jan-60 Jan-62 Jan-64 Jan-66 Jan-68 Jan-70 Jan-72 Jan-74 Jan-76 Jan-78 Jan-80 Jan-82 Jan-84
Time (months)

(b)

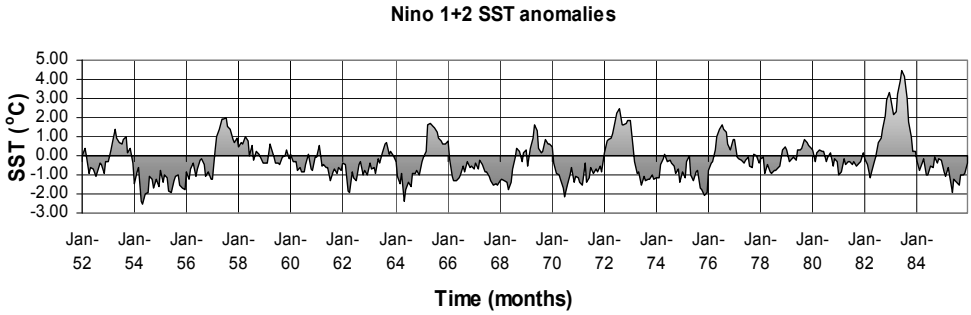
Nino 1+2 SST anomalies
SST (°C)
5.00
4.00
3.00
2.00
1.00
0.00
-1.00
-2.00
-3.00
Jan-52 Jan-54 Jan-56 Jan-58 Jan-60 Jan-62 Jan-64 Jan-66 Jan-68 Jan-70 Jan-72 Jan-74 Jan-76 Jan-78 Jan-80 Jan-82 Jan-84
Time (months)

(c)

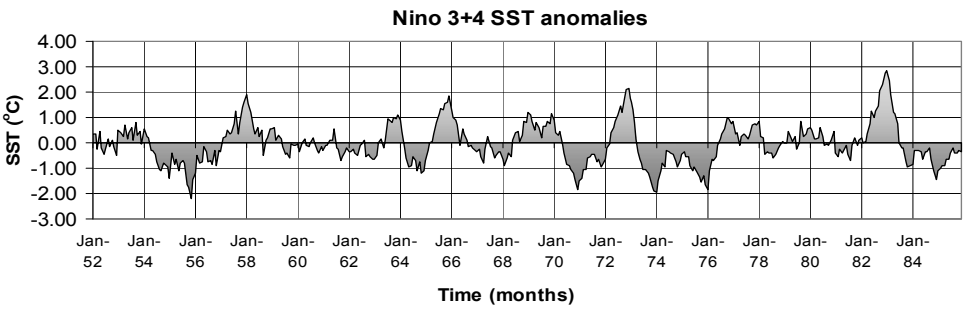
Nino 3+4 SST anomalies
SST (°C)
4.00
3.00
2.00
1.00
0.00
-1.00
-2.00
-3.00
Jan-52 Jan-54 Jan-56 Jan-58 Jan-60 Jan-62 Jan-64 Jan-66 Jan-68 Jan-70 Jan-72 Jan-74 Jan-76 Jan-78 Jan-80 Jan-82 Jan-84
Time (months)

(d)

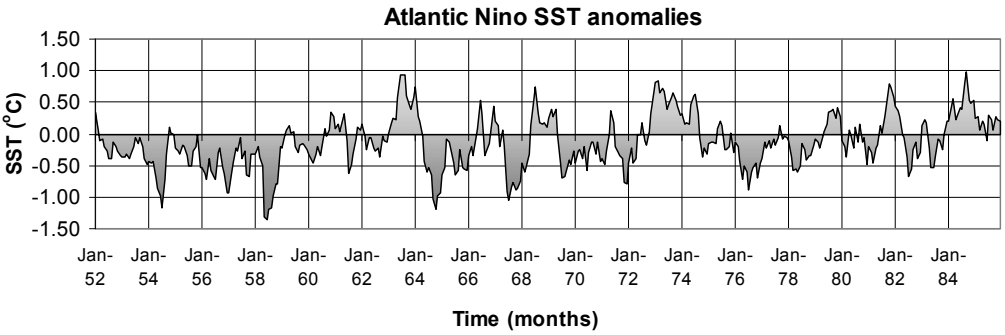

(e)

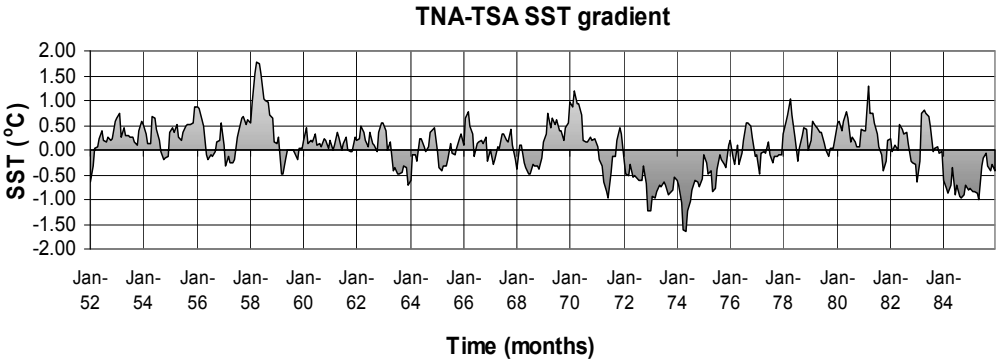

(f)

Figure 5.4: Time series of (a) SSTAs in the TNA region (5.5°-23.5°N, 15°-57.5°W), (b) SSTAs in the TSA region (0°-20°S, 10°E-30°W), (c) SSTAs in the Niño 1+2 region (0°-10°S, 90°-80°W), (d) SSTAs in the Niño 3+4 region (5°N-5°S, 160°E-150°W), (e) SSTAs in the Atlantic Niño region (3°S-3°N, 20°W-0°), (f) SSTAs in the TA region = TNA-TSA SST (TNA: 5°-25°N, 55°-15°W; TSA: 0-20°S, 30°W-10°E).

The null hypothesis is rejected if $X_c^2 > X^2_{1\text{-}a,\ k\text{-}p\text{-}1}$. The test statistic for the Kolmogorov-Smirnov test is given in chapter 3, equation 3.17 and 3.18.

Temporal variability of the river discharges in the Upper-Suriname River Basin is studied by using statistical parameters (for example the mean, coefficient of variation, coefficient of skewness) (WMO, 1988).

The formula for the mean $\bar{x}$ and standard deviation s_x, for an ungrouped data serie x with n values, are given in equation 5.2 and 5.3 respectively:

$$\bar{x} = \frac{\sum_{i=1}^{n} x_i}{n} \quad \text{(Eq. 5.2)}$$

$$s_x = \sqrt{\frac{\sum (x_i - \bar{x})^2}{N}} \quad \text{(Eq. 5.3)}$$

The coefficient of variation CV and coefficient of skewness CSK are calculated using the following equations:

$$Cv = \frac{S_x}{\bar{x}} \quad \text{(Eq. 5.4)}$$

$$CSK = \frac{n^2}{(n-1)(n-2)} \frac{\frac{1}{n}\sum_j f_j (X_j - \overline{X})^3}{\frac{1}{n}\sum_j f_j (X_j - \overline{X}^2)^{1.5}} \quad \text{(Eq. 5.5)}$$

where S_x is the standard deviation, x is the original sample mean, f is the absolute frequency, X is the grouped sample and X is the mean of the group sample (Mamdouh et al., 1993).

For detecting climate change of hydrological time series (randomness, stationary and homogeneity) different parametric and non-parametric statistical tests from the literature are used (Haan, 1977; Helsel and Hirsch, 1992; Mamdouh et al., 1993; McCuen, 2003; WMO, 1988). If the measured data are not influenced by human activities, but natural activities, the data series are random (or inconsistent). In stationary time series (normal variability), the statistical properties (e.g. the mean, variance, standard deviation) do not change in time. Homogeneous time series do not have a trend or cycle effect (Mamdouh et al., 1993).

General tests for randomness are carried out by using the serial correlation coefficient and the Von Neumann ratio test (equation 3.15). The Student's t-test (for shift in the mean) and the F-test (for shift in the variance) are used to test non- stationary of the annual river discharges (equation 3.27 and 3.28). For a two tailed F test, the F ratio is calculated as follows:

$$F = S_l^2 / S_s^2 \quad \text{(Eq. 5.6)}$$

where n_l and n_s are the sample sizes and S is the sample variance. If the calculated F ratio is less than the critical F ratio, than H_o ($\sigma_1^2 = \sigma_2^2$) is rejected. The critical F ratio can be obtained from literature (McCuen, 2000). For this purpose, the data series are divided into two equal series: 1952-1968 (17 years) and 1969-1985 (17 years).

To identify if a deterministic component (trend, shift) exists in the observed annual river discharges, auto/serial correlation analysis (equation 3.11) is used and to test randomness against shift (break point year) in the annual river flows, the Standard Normal Homogeneity test of Alexandersson (SNHT), the Craddock's test of Cumulative Deviations (CDT), the Worsley Likelihood ratio test (WLRT) and the T test are used. These equations are given in chapter 3, equation 3.16…3.28. To detect monotonic increasing or decreasing trends in the monthly and annual time series, the non-parametric Mann-Kendall, Spearman's and Pearson's tests are used (equations 3.4 to 3.10) and the river discharges are also evaluated using a filtering technique (the moving average filter). A five-year wavelength is used as it is less sensitive than a ten-year wavelength. The moving mean can be given by the following equation:

$$x_m = \frac{x_1 + x_2 + \ldots x_n}{N}, \frac{x_2 + x_3 + \ldots x_{n+1}}{N}, \frac{x_3 + x_4 + \ldots x_{n+2}}{N} \ldots \qquad \text{(Eq. 5.7)}$$

where x_i is the variable (rainfall) for year i and N is the total number of years.

The interannual relationship between the observed monthly river discharges and the observed monthly Atlantic and Pacific SSTs is studied using lagged correlation analyses. These analyses are carried out on a monthly and seasonal scale using the Anclim model (Stipanek, 2003) and the KNMI Climate Explorer (Retrieved August 10, 2005 from http://climexp.knmi.nl/). In addition, high and low river discharges are analysed and compared to the El Niño and La Niña events according to Null (2003), Turner (2004) and the International Research Institute - IRI (Retrieved August 10, 2005 from http://iri.columbia.edu/outreach/software/). In this study, a high river flow year is defined if $x \geq \bar{x} + STDEV$ (68% confidence limit) and a low river flow year if $x \geq \bar{x} - STDEV$, where x is the river discharge, $\bar{x}$ is the long-term mean and STDEV is the standard deviation.

For the uniformity and availability of statistical tables, all tests used are performed at a 5% significance level and calculated using the Modstat (Knodt, 2003), AnClim (Stipanek, 2003), XLStatistics (Carr, 2000) statistical programs.

Table 5.2: Results of different statistical tests on the river discharges at Semoisie and Pokigron (1952-1985) at a 5% level of significance

Statistical characteristics	Type of data	River discharge at Semoisie	River discharge at Pokigron	Tests
Normal distributed *(goodness-of-fit test)*	monthly, annual	yes (except March, October/December)	yes (except March, October/December)	Chi-square test and Kolmogorov-Smirnov tests
Independent *(deterministic component)*	annual	no	yes	Autocorrelation analyses
Random *(general test of randomness)*	monthly, annual	no (except December)	yes (except March)	Serial correlation coefficient and Von Neumann ratio test
Non-stationary *(shift in mean/variance)*	annual	no	no	F test and the Student's t test
Linear trend *(significant)*	annual	yes	no	Mann-Kendall, Spearman's, and Pearson's tests
Random *(jump/shift)*	annual	yes (1977)	no	Cumulative Deviation test, Worsley Likelihood ratio test, T test and Standard Normal Homogeneity test of Alexandersson

5.3 Results and discussion

5.3.1 Analysis of long-term changes in the river discharges

The annual river discharge series (1952-1985) at Semoisie and Pokigron show a linear Pearson's correlation coefficient (c) of 0.89 and the monthly river discharge series show a linear Pearson's correlation of 0.94. A significantly high correlation ($c = 0.97$, $p<0.05$) is found between the annual discharge at Pokigron and the van Blommenstein lake inflows for the period 1952-1985.

Both the Chi-square and Kolmogorov-Smirov tests show that the annual river discharge series (1952-1985) at station Semoisie and Pokigron are normally distributed and the F test and Student's t test have shown that the annual river discharge series at both stations are non-stationary. The Mann-Kendall, Spearman's and Pearson's tests have shown that the annual discharge series at Semoisie and Pokigron show a negative linear trend. During 1952-1985 (33 years), a reduction of about 62.7 m^3/s is observed at Semosie (trend value is 1.9 $m^3\ s^{-1}\ year^{-1}$; $p = 0.04$) and at Pokigron a reduction of about 29.7 m^3/s is observed during the same period (trend value is 0.9 $m^3\ s^{-1}\ year^{-1}$; $p = 0.44$). The different statistical tests results are presented in Table 5.2. The difference in the river discharge trend value may be caused by the variation in the rainfall distribution over the study area (Figure 1.9) and the difference in annual rainfall trends in the centre of Suriname. A recent study by Nurmohamed and Naipal (2004) has shown that the annual rainfall at Tafelberg (south-west of the basin) shows a negative trend of 14.5 mm $year^{-1}$ ($p = 0.10$) and the annual rainfall at Brownsweg (north of the basin) shows a positive trend of 33.2 mm $year^{-1}$ ($p = 0.35$) for the period 1961-1985.

The annual river flows at Semoisie and Pokigron (Figures 5.2a and 5.2b) show periods with an increasing and a decreasing linear trend. Based on the results of the moving average, four periods can be distinguished at Semoisie: a decrease in the period of 1953-1958, a leveling off in 1958-1965, an increase between 1964 and 1971, and a decrease after 1971. The same method shows three main periods in the time series at Pokigron (Figure 5.2b): a steep decrease during 1952-1964, a slow increase in the period 1964-1971 and a slow decrease after 1971. The steepest decrease in annual river flow at Semoisie was noticeable in the period 1975-1983 and was about -79.0 m^3/s (about 52% of the long-term annual mean river discharge), while at Pokigron this was the case in the period of 1953-1958 and was about -92.7 m^3/s (about 42% of the long-term annual mean river discharge). The oscillations in annual time series of about 15 years might be attributed to the natural oscillation of the global atmospheric-ocean system and/or solar variability (Chiew et al., 2005). In the first period (Semoisie: 1953-1958; Pokigron: 1952-1964), the SSTs in the TSA, Niño 1+2, Niño 3+4 and Atlantic

Niño region (Figure 5.4) are predominantly negative (higher than -0.5°C), while the TNA-TSA gradient is predominantly positive (about 0.5°C). The decrease in discharge during this period may be related to the "strong" cooling effect of the Pacific SST and the Atlantic Niño SST on the warm waters in the TNA, which cause less air to rise and a decrease in precipitation in the study area. The increase in discharge in the period of 1965-1970 may be related to the "strong" positive SST anomaly in the TNA (higher than 0.5°C), especially during 1969-1970. A warm TNA causes surface air to rise, easterly trade winds in the TNA to weaken, the water vapor to condense resulting in an increase in precipitation or river discharge in the study area. For the decrease in discharge after 1971 at Pokigron, a possible explanation may be found in the strong negative TNA-TSA gradient (lower than -0.5°C), especially during 1971-1976. The statistical analyses have shown (Table 5.2) that only the annual river discharge series at Semoisie show a shift in 1977. This may have been caused by the change from dry years to wet years (Figure 5.2). It may be concluded that the shifts are thus more related to the climate variability, in particular the SSTAs, in the tropical Atlantic and tropical Pacific. In the next sections, more analyses will be performed to understand the discharge behavior.

5.3.2 River discharge variability and sea surface temperature relationship

The annual cycle of the discharge at Semoisie and Pokigron (Figure 5.1) is characterized by a maximum in May-June and a minimum in October-November. The monthly discharge follows almost the same seasonal pattern as the monthly rainfall at the nearby rainfall stations (Figure 5.3). Figure 5.1 also shows the high interannual discharge variability as the monthly standard deviation is always greater than 50% of the mean monthly discharge. The highest coefficient of variation (CV) at both stations are both in March (0.72-0.75) and December (0.72-0.83). This has to do with the sudden increase in rainfall or river discharge in these months. Because of the high consistency of Q_{pok} with Q_{sem} and the lake inflows, only the time series at Pokigron will be considered in the further analyses.

Figure 5.5 shows the monthly observed SST for the four regions including the monthly discharge at Pokigron (Q_{pok}) for the period 1952-1985. This figure shows that the TNA SSTs are higher than the TSA SSTs except in February-April. SST in the TNA (TSA) is warmest in September (March) and coldest in March (September). The lagged correlation analyses (Pearson's coefficient) have shown that the maximum (minimum) flows are related to high (low) SSTs in the TNA region and TSA region.

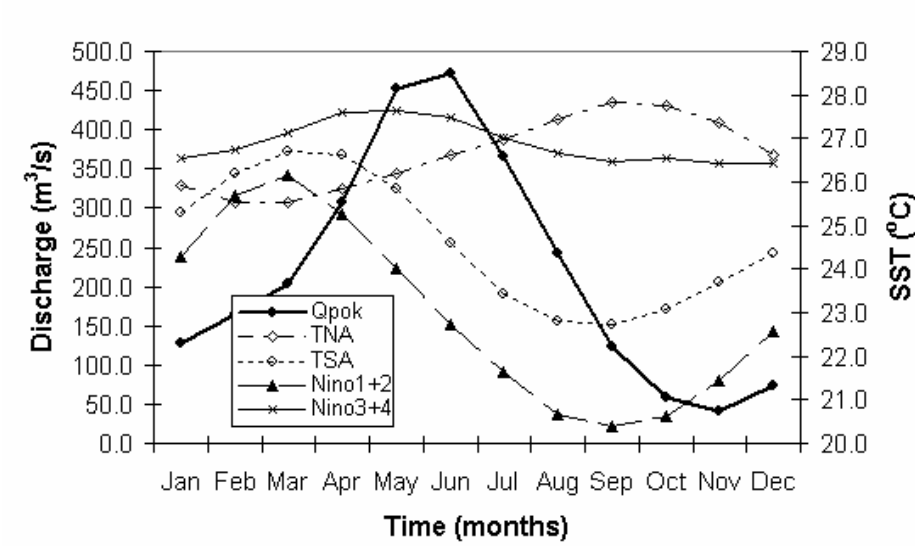

Figure 5.5: Monthly variation of observed SST in the TNA, TSA, Niño 1+2 and Niño 3+4 regions, and the monthly observed discharge at Pokigron for the period 1952-1985.

The lagged relationship between the seasonal SSTAs in the TNA, TSA, Niño 1+2, Niño 3+4 region and the river discharge anomalies at Pokigron is graphically shown in Figure 5.6. A positive lag indicates that the SSTAs are the leading index and a positive (negative) correlation indicates that large (small) river discharge anomalies are related with large SSTAs**.**

The river discharge anomaly is calculated as a three months average divided by the long-term mean of the time series (1952-1985). From these results, it seems that the discharge in the Upper-Suriname River Basin is more strongly correlated with the Pacific SSTAs in December-February (DJF) (c is -0.63 with Niño 1+2 SSTAs for lag is 8 months), June-August (JJA) (c is -0.73 with Niño 3+4 SSTAs for lag is 5 months) and September-November (SON) (c is -0.65 with Niño 3+4 SSTAs for lag is 4 months). In March-May (MAM), the discharge in the Upper-Suriname River Basin is slightly stronger correlated with the SSTAs in the TSA region (c is -0.46 for lag is 2 months) than with the Pacific SSTAs.

Table 5.3 shows the highest cross correlation coefficients between the observed monthly SSTs, and between the monthly SSTAs in the different regions. The results show that the Pacific El Niño influences the TA SST. The Niño 3+4 SST shows a stronger correlation with the TNA SST in all the seasons compared to the Niño 1+2 SST.

Table 5.3: The highest lagged cross correlation coefficient c_k (with 95% confidence interval; k = 0-12 months) (a) between the monthly SSTAs in the TNA, TSA, Niño 1+2 and Niño 3+4 region and (b) the highest lag correlation coefficient of the monthly SSTAs for the December-February (DJF), March-May (MAM), June-August (JJA) and September-November (SON) period for the same regions. Note: the SSTAs in the first column of Table 5.3a are taken as the first series and the SSTAs in the first row as the second time series. In Table 5.3b, the first SSTAs are taken as the first series and the second SSTAs as the second series. A positive lag indicates that the second series is the leading index.

Predictor	TNA STAs	TSA SSTAs	Niño 1+2 SSTAs	Niño 3+4 SSTAs
TNA SSTAs	1.00	-0.13 (lag 1)	0.26 (lag -5)	0.46 (lag -5)
TSA SSTAs		1.00	-0.21 (lag 12)	-0.27 (lag 12)
Niño 1+2 SSTAs			1.00	0.68 (lag 1)
Niño 3+4 SSTAs				1.00

(a)

Predictor \ Period	DJF	MAM	JJA	SON
c_k(TNA-TSA SSTAs)	-0.34 (lag 12)	-0.29 (lag 9)	-0.15 (lag2-3)	-0.45 (lag 9)
c_k(TNA-Niño 1+2 SSTAs)	0.19 (lag 3)	0.50 (lag 5-6)	0.48 (lag 6-7)	0.22 (lag 4)
c_k(TNA-Niño 3+4 SSTAs)	0.41 (lag 8)	0.68 (lag 3-4)	0.66 (lag 4)	0.38 (lag 6)
c_k(TSA-Niño 1+2 SSTAs)	0.44 (lag 4)	0.19 (lag 7-8)	-0.27 (lag 1)	0.14 (lag 12)
c_k(TSA-Niño 3+4 SSTAs)	0.37 (lag 5-6)	-0.14 (lag 4)	-0.30 (lag 1)	0.11 (lag 2
c_k(Niño 1+2-Niño 3+4 SSTAs)	0.85 (lag 0)	0.66 (lag 0)	0.70 (lag 1)	0.87 (lag 1)

(b)

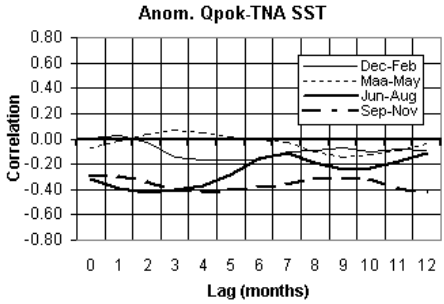

(a)

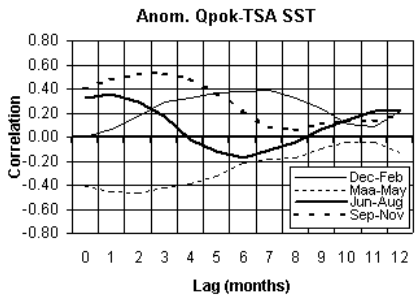

(b)

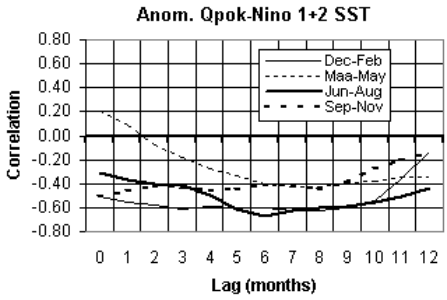

(c)

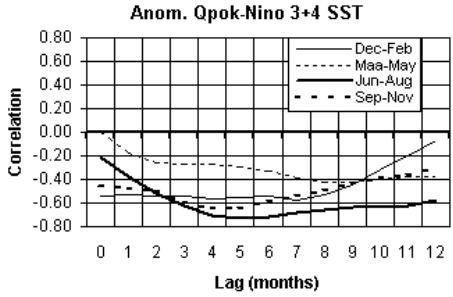

(d)

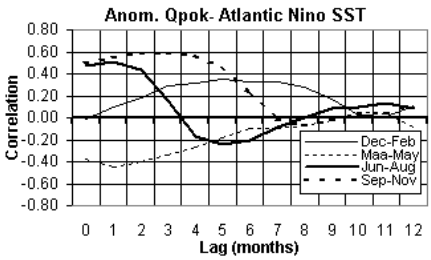

(e)

Figure 5.6: Lag correlation coefficient of the river discharge anomalies for December-February (DJF), March-May (MAM), June-August (JJA) and September-November (SON) with the (a) TNA SSTAs, (b) TSA SSTAs, (c) Niño 1+2 SSTAs, (d) Niño 3+4 SSTAs, (e) Atlantic Niño SSTAs for the period of 1952-1985.

The highest correlation (c is 0.66-0.68) is obtained when the Niño 3+4 SST leads the TNA SST by 3-4 months in March-May and June-August. In the TSA region, the Niño 1+2 SST shows a slightly stronger correlation with the TSA SST compared to the Niño 3+4 SST. A high correlation is also found between the December-February TSA SST and the Niño 3+4 SST 5-6 months earlier and is about 0.37. During DJF, the TSA SSTAs show a much higher correlation (c is 0.39 for lag is 7 months) with the discharge anomalies than the TNA SSTAs (c is -0.17 for lag is 6 months) (Figures 5.6).

During December-April, the TNA region becomes cold and the TSA region warm (Figure 5.5). Northeasterly trade winds north of the equator are strengthened, while the southeasterly trade winds south of the equator are weakened (Villwock, 1998; Webster, 2005). The ITCZ is displaced southward of Suriname causing a reduction in precipitation including river discharge, mainly during February-April (Figure 5.5). During MAM, the TSA SSTAs also show a much higher correlation (c is -0.46 for lag is 1 month) with the discharge anomalies than the TNA SSTAs (c is -0.07 for lag is 0 month). In this period, oceanic air rises over the TNA warm water region, easterly trade winds from the sea are weakened north of the equator and evaporation increases over the TNA region. Easterly trade winds south of the equator increase and bring the tropical heat sources of the Amazon over Suriname. The ITCZ is displaced northwards of Suriname and precipitation increases over northern South America. During JJA, both northeasterly and southeasterly trade winds are strong and while the ITCZ travels from the south of Suriname to the north, it also collides with the geographical relief of the country (near Tafelberg) as well with the trade winds. The movement of ITCZ over Suriname becomes slower and causes the wet season to extend. In this period the ITCZ is present over almost all of Suriname. Both TNA (c is -0.42 for lag is 2 months) and TSA SSTAs (c = 0.35 for lag is 1 month) show a high correlation with the discharge anomalies. During SON, the ITCZ has already passed over Suriname and is found to the north above the Atlantic Ocean. The TSA region is cold. In this period, the trades south of the equator increase surface winds and cause evaporative cooling resulting in less rainfall over Suriname. The TSA SSTA show a stronger correlation (c is 0.53 for lag is 3 months) with the discharge anomalies than the TNA SSTAs (c is -0.42 for lag is 4 months).

When comparing low flow years (1958, 1959, 1961, 1964, 1965, 1966, 1977, 1983) and high flow years (1953, 1954, 1956, 1968, 1971, 1976) at Pokigron with the annual Atlantic and Pacific SSTs, and the Atlantic Niño index, no clear relation is found. However, during low flow years, the SSTAs in the TNA region (Figure 5.4a) are predominantly positive, except in 1959, 1964, 1965 and 1977, while during high flow years, SSTAs in the TNA region are predominantly negative, except in 1953. SSTAs in the TSA region (Figure

5.4b) for low and high flow years are almost all negative, except in 1966 and 1968. Four of the eight low years (1958, 1965, 1977, 1983) correspond with El Niño events and three of the six high flow years (1956, 1971, 1976) correspond with La Niña events. According to Ambrizzi et al. (2005), the decrease in rainfall (or discharge) during some of the El Niño events in the northern and northeastern part of South America, especially during DJF and MAM, is related to the strong Walker and Hadley circulation. Figure 5.6 shows that the Niño 3+4 SSTAs have a much stronger correlation than other SSTs with the Q_{pok} anomalies during DJF (c is 0.54-0.57 with Niño 3+4 SSTAs for lag is 0-7 months) and during JJA (c is –0.63- -0.73 with Niño 3+4 SSTAs for lag is 3-12 months). It is also found that most of the Q_{pok} anomalies of the eight low flow years coincide with positive Niño 3+4 SSTAs for DJF, MAM, JJA, SON (for lag –5 months), while only the years 1961 and 1965 show negative Niño 3+4 SSTAs for MMA and JJA. That fact that only positive indexes are found during the whole year may be related to the fact that ENSO events generally starts in March/April and reach their peak between December and February and decline in March of the next year. Most of the Q_{pok} anomalies of the six high flow years coincide with negative Niño 3+4 SSTAs for all seasons (for lag -9 months). The years 1953 and 1954 show a positive Niño 3+4 SSTAs in JJA, SON and DJF, MMA and JJA respectively. A similar pattern is also found for the Q_{pok} anomalies in MAM (for lag 7-12 months). This clearly shows that the amount of precipitation or discharge during DJF, MAM and JJA can be reduced due to El Niño events and, therefore, extend the long dry season.

5.4 Conclusions

The relationship between the discharges in the Upper-Suriname River Basin and the SSTs in the tropical Atlantic (TNA, TSA, Atlantic Niño) and Pacific Atlantic (Niño 1+2, Niño 3+4) are analysed in the period 1952-1985. Insight is gained in the short-term changes and variation in the discharge regime. The hydrological regime of the study basin is characterized by a high variation in monthly and annual river discharges, which is mainly caused by the variation in SSTs in the Atlantic ocean including the ITCZ. Statistical analyses have shown that the annual discharge in the Upper-Suriname River Basin is characterized by a negative trend, which is believed to have been caused by the negative rainfall trend in the centre of Suriname. However, this trend may also have been influenced simply by the shortness of the data series.

The annual cycle of the river discharges are linked to the anomalously warm/cold SSTAs in the tropical north/south Atlantic. Some of the low flow years were found to be related to a warmer TNA during the year and some high flow years were found to be related to a colder TNA during the year. Some low flow years may also have been caused by the absence of the

ITCZ (southward displacement), longer than normal during the year, but also El Niño events. In the last case, the river discharges are influenced by the Pacific SSTs through the tropical Atlantic variability, especially in December-February by the Niño 1+2 SSTAs and in June-August and September-November by the Niño 3+4 SSTAs. Some high flow years may have been caused by La Niña events.

It is expected that further global warming in the tropical Atlantic and Pacific ocean, will increase the SSTs, and El Niño-like conditions and, therefore, high river flows (floods) and low flows (including prolonged dry periods) in the Upper-Suriname River Basin (IPCC, 2001). Because of the fact that the river discharge behavior in this basin is not fully understood, further research is required in determining the role of the oceanic-atmospheric processes on the rainfall in Suriname in order to better understand the inter-annual changes of discharges in the river basin.

Acknowledgements

I acknowledge the valuable review comments of two anonymous reviewers.

6. SCENARIOS FOR FUTURE CLIMATE CHANGE*

Abstract

This chapter describes one way of developing climate change scenarios for temperature and precipitation for three time horizons (year 2020, 2050 and 2080), using results of five atmospheric-ocean global circulation models (AOGCMs). The GCM (CCSR96, CSI296, ECH498, HAD300, GFDL90) results are taken from the MAGICC/SCENGEN climate model and are available at a grid scale of about 250 km. The results show that there is a high correlation (Pearson's correlation coefficient of 0.97) between the monthly observed temperature data and the modeled GCM baseline data. In case of precipitation data, a correlation coefficient of 0.99 was found. The five GCMs follow the seasonal pattern of the temperature well, while only the CCSR96 model follows the precipitation pattern well. The climate change scenarios for Suriname, based on the average of the outputs of 5 GCMs, indicate an increase in mean annual temperature up to 2.6^{o}C in 2080, compared to 1961-1990 and for the annual precipitation, a decrease of 4.7% in 2080, compared to 1981-2000. Precipitation is expected to increase during January-April and to decrease during May-December. The future increase in mean temperature in Suriname may lead to an increase in evapotranspiration and, correspondingly, changes in future precipitation. There are also clear indications that the wet and dry seasons in Suriname will change in duration and shift.

* This chapter has been published as: "Development of scenarios for future climate change in Suriname", Journal of Universidad Catolica Boliviana San Pablo, ACTA NOVA, Vol. 3, No. 3, December 2006.

6.1 Introduction

In the last century, the amount of heat trapped in the earth atmosphere has increased due to the increased emission of greenhouse gases and has resulted in changes in the global climate. According to the IPCC (2001), the global average surface temperature has increased over the 20th century by 0.6^{o}C. In the northern subtropical areas (10^{o}-30^{o}N), precipitation has decreased rather than increased. One of the important consequences of global climate change is the change in the hydrological cycle, especially in precipitation, evapotranspiration, soil moisture, infiltration, surface and groundwater runoff (IPCC, 2001; Tamara et al., 1999).

The most convincing methods for studying the effects of the increasing concentrations of carbon dioxide (CO_2) and other greenhouse gases on the earth's climate are atmospheric-oceanic global circulation models (AOGCMs). There are generally three approaches that may be applied for predicting future climate change: (a) incremental scenarios, (b) spatial-temporal analog scenarios and (c) climate model-based scenarios. The advantages and disadvantages of these approaches are extensively described in literature (IPCC, 2001; IPCC-TGCIA, 1999; Jones et al., 2001; Feenstra and Short, 1996). For regional impacts of climate change, finer scale information (scales of 100 km or finer) can be derived indirectly from GCM outputs by using three main methods: (a) statistical downscaling, (b) dynamic downscaling and (c) direct GCMs or regional climate models (RCMs). These methods and their (dis)advantages are also extensively described in literature (Arnell et al., 2003; Giorgi et al., 2001; IPCC, 2001; IPCC-TGCIA, 1999; Jones, 2004; Mearns et al., 2001, 2003). Figure 6.1 shows a schematic procedure for constructing climate scenarios for use in impact assessment (IPCC, 2001; Jones et al., 2004).

To date, there have been a few studies about climate change impact in Suriname. In the country climate change study of 1999, future scenarios for sea level rise were developed. It was concluded that both the man-made and natural systems of the coastal area are vulnerable when the sea level rises up to 1.0 m (Naipal and Amatali, 1999b). Nurmohamed and Naipal (2004) have analysed precipitation and temperature time series (1900-1990) and identified significant positive and negative trends (5% level of significance) at some stations, mostly located in the coastal area. In order to assess the effects of future climate change on water resources and to take appropriate measures, it is important to know if the precipitation and/or the interannual variability of precipitation will increase or decrease or if the rain and dry season will shift, extend or shorten as a consequence of global warming.

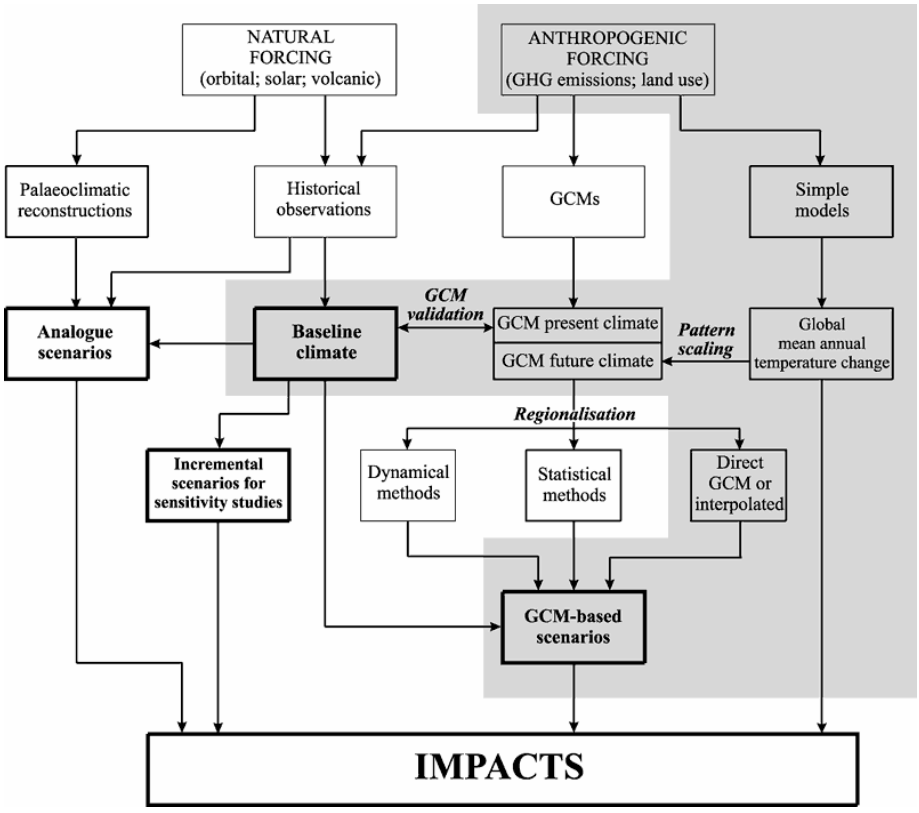

Figure 6.1: Procedure for constructing climate scenarios for use in impact assessment (IPCC, 2001; Jones et al., 2001)

The objective of this study is to generate future climate change scenarios on a monthly time scale for the mean precipitation and temperature for Suriname using the output of atmospheric-ocean global circulations models (AOGCMs) approach. Because of the large spatial resolution of the GCMs, scenarios on monthly time scale can be accepted for large study areas.

6.2 Study area and data

The study area covers the whole of Suriname (Figure 6.2). Observed baseline precipitation data, with spatial resolution of 2.5°, is taken from the Climate prediction Centre (Retrieved June 10, 2005 from http://www.cgd.ucar.edu/cas/catalog/surface/precip/arkin.html) and observed baseline temperature data, with spatial resolution of 0.5°, is taken from the Climatic Research Unit (CRU) (Retrieved June 10, 2005 from http://www.cru.uea.ac.uk/cru/data/hrg.htm).

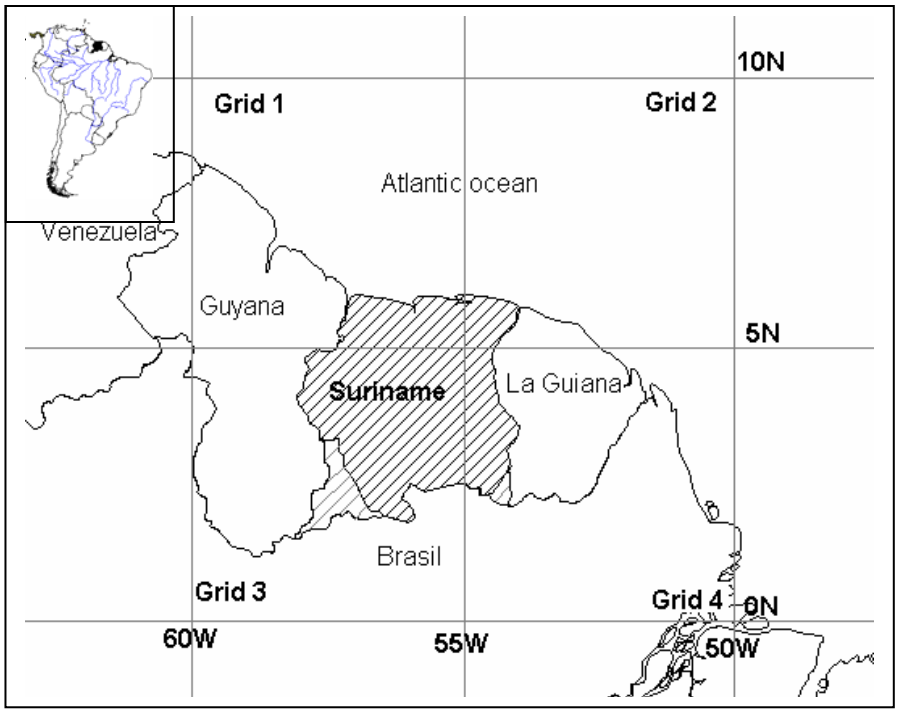

Figure 6.2: Selected grid cells in and around the study area Suriname for five AO-GCMs.

These data are normalized to a grid of 5^{o} latitude by 5^{o} longitude, and the output data in the MAGICC/SCENGEN model are presented at this scale. For comparison purposes, 12 monthly observed precipitation time series (1961-1985) and 7 temperature time series (1971-1985) for selected stations scattered across Suriname were taken from the Meteorological Service Suriname (MDS). The arithmetic mean of the stations is used to represent the average monthly precipitation and temperature for Suriname.

Table 6.1: Characteristics of the five AOGCMs (Retrieved June 10, 2005 from www.grida.no/climate/ipcc_tar/wg1/316.htm#tab81, http://cera-www.dkrz.de/IPCC_DDC/SRES/index.html, http://www-pcmdi.llnl.gov/projects/cmip/overview_ms/table1.html).

Model	Acronym	Center/Country	Atmospheric resolution (^{o} latitude x ^{o} longitude) and number of vertical layers
HadCM3	HAD300	UK Meteorological Office - UK	2.5 x 3.75 (19)
GFDL_R15	GFDL90	Geophysical Fluid Dynamics Laboratory – USA	2.25 x 3.75 (14)
CCSR/NIES	CCSR96	Center for Climate System Research (CCSR) and National Institute for Environmental Studies (NIES) - Japan	5.6 x 5.6 (20)
CSIRO	CSI296	Australia's Commonwealth Scientific and Industrial Research Organization - Australia	3.2 x 5.6 (9)
ECHAM4	ECH498	Max Planck Institute for Meteorology - Germany	5.6 x 5.6 (19)

6.3 Methods

The scenarios for future climate change in Suriname were developed using the MAGICC/SCENGEN model version 4.1 (Model for the Assessment of Greenhouse Gas Induced Climate Change) (Wigley, 2003). MAGICC has been the primary model used by the Intergovernmental Panel on Climate Change (IPCC) and produces projections of future global mean temperature and sea level rise. The global mean temperatures from MAGICC are used to drive SCENGEN, which produces spatial patterns of change in climate variables e.g. precipitation, temperature. The model structure of MAGICC/SCENGEN is given in Figure 6.3. Five recent AOGCMs from different international institutions across the world are selected to simulate the spatial patterns of future climate change. These are: Had300, ECH498, GFDL90, CSI296 and CCSR96. The precipitation and temperature outputs from the original GCM are in SCENGEN interpolated to 5^{o}x5^{o} grids (about 550 km). Figure 6.2 shows the selected grids for Suriname. Table 6.1 shows some characteristics of the AOGCMs. The mean of all the Special Report Emission Scenarios – SRES (P50) is used as the emission scenario (Jones et al., 2004). It should be mentioned that there are a few models that can be used to produce these scenarios such as MESSAGE (MES), IMAGE (IMA), MiniCam (MIN).

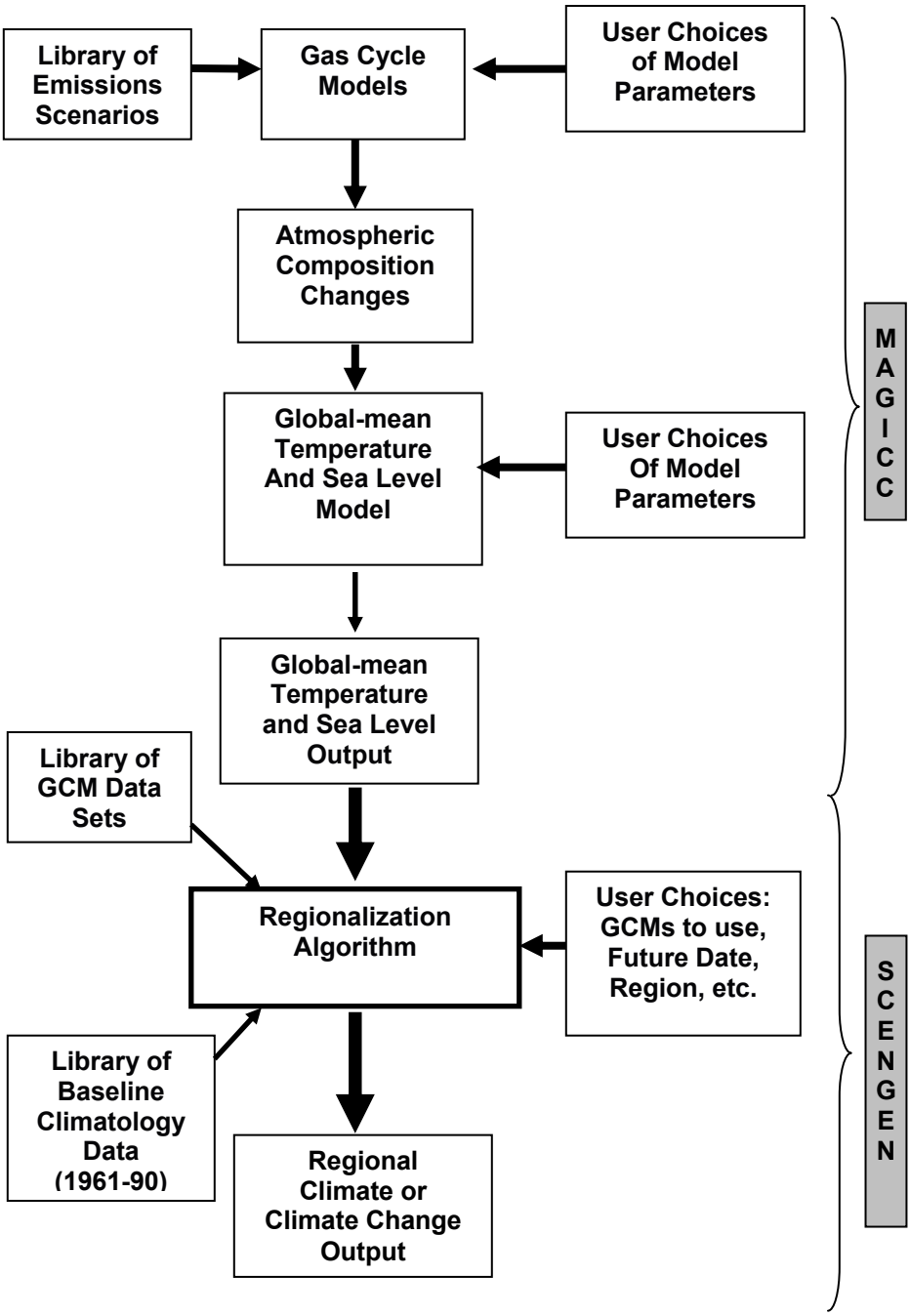

Figure 6.3: Model structure of the MAGICC/SCENGEN model (Wigley, 2003)

For constructing the climate change scenarios for Suriname, the procedure from the IPCC-TGCIA (1999) was followed:

- Run the GCM for Suriname.
- Compare GCMs results with the observed data.
- Select GCMs that best approximate the observed baseline data to construct climate change scenarios.
- Define patterns of change for these GCMs experiments as the difference or ratios between 2 x CO_2 and 1 x CO_2 simulation for temperature and precipitation respectively.
- Combine these changes with the baseline data set by adding the difference for temperature and the ratios for changes of precipitation to the baseline data to obtain the scenario.

Three time slices (2005-2035, 2035-2065, 2065-2095) have been selected to generate scenarios of change in mean temperature with reference to the 1961-1990 baseline data set, and mean precipitation with reference to the 1981-2000 baseline data set. It is assumed that the long-term mean of the baseline data set does not significantly differ from the observed data set in Suriname. We will also assume that the spatial and temporal pattern are constant, but that only the magnitude will change.

6.4 Results and discussion

6.4.1 Observed and modeled precipitation and temperature

Figures 6.4a and 6.4b show the measured precipitation (1961-1985) and temperature data (1971-1985) across Suriname together with the modeled baseline precipitation (1981-2000) and temperature (1961-1990) data for the individual AOGCMs and the average of the AOGCMs. The Pearson's correlation coefficient (r) (at 95% confidence interval) between the monthly measured temperature data in Suriname and the average of the monthly observed baseline data by the five GCMs is about 0.97. The Pearson's correlation between the measured temperature data and modeled baseline GCM temperature data is 0.75 for CCSR96, 0.83 for CSI296, 0.66 for ECH498, 0.79 for HAD300 and 0.86 for GFDL90. For the monthly temperature pattern, the CSI296 and the GFDL90 underestimate the modeled observed data, while the other models overestimate the modeled observed data.

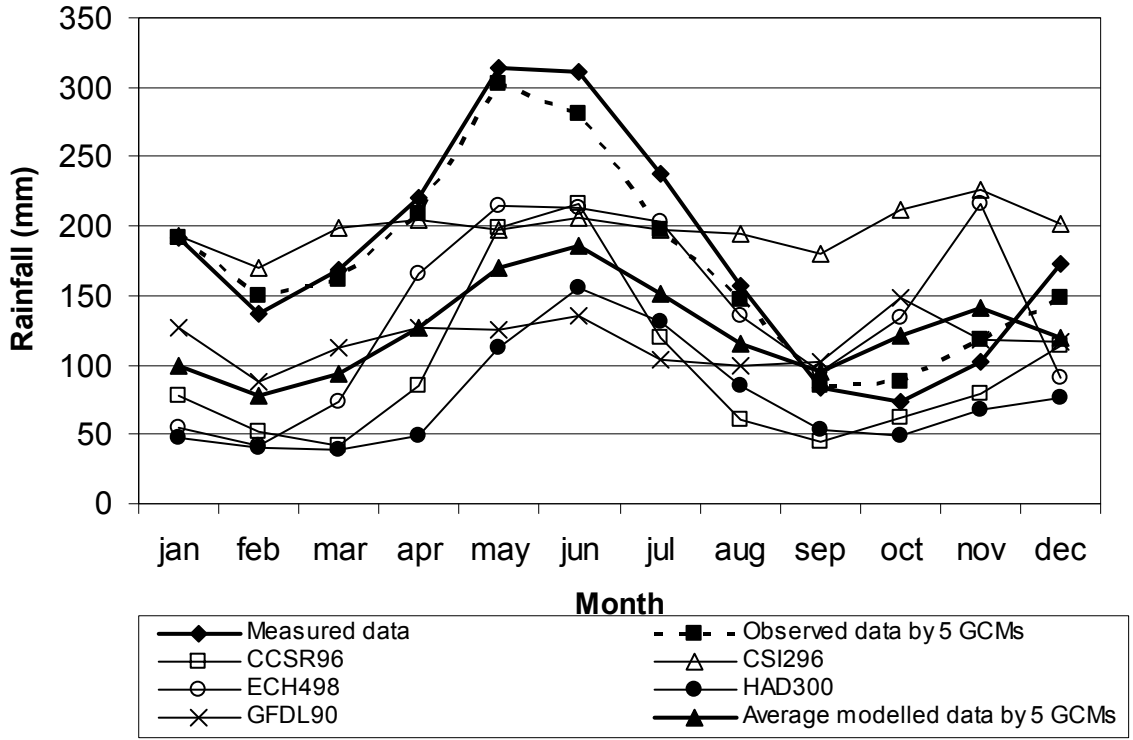
350
300
250
200
150
100
50
0
Rainfall (mm)
jan
feb
mar
apr
may
jun
jul
aug
sep
oct
nov
dec
Month
Measured data
Observed data by 5 GCMs
CCSR96
CSI296
ECH498
HAD300
GFDL90
Average modelled data by 5 GCMs

(a)

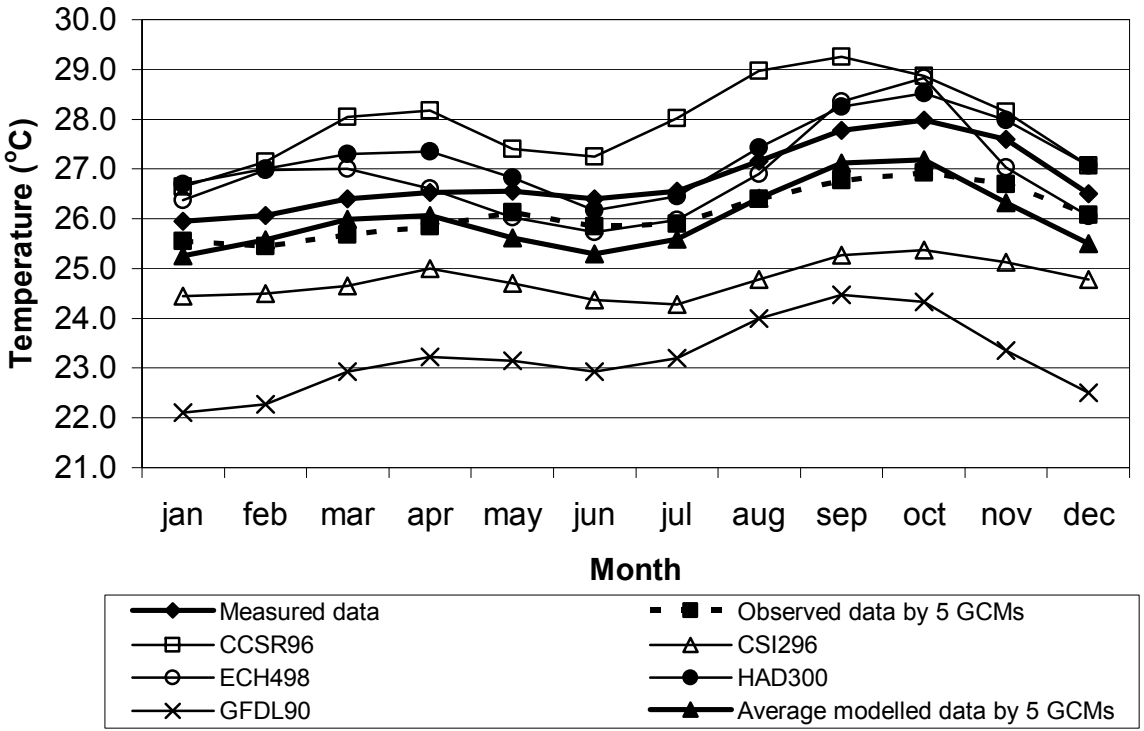

(b)

Figure 6.4: (a) Average observed baseline precipitation (1981-2000) from five AOGCMs, modeled data for individual GCMs and measured data (1961-1985) from selected stations in Suriname, (b) average observed baseline temperature (1961-1990) from five AOGCMs, modeled data for individual GCMs and measured data (1971-1985) from selected stations in Suriname.

The monthly Pearson's correlation coefficient between the measured precipitation in Suriname and the average of the monthly baseline precipitation data by the five GCMs is about 0.99. The correlation between the measured precipitation data and modeled baseline GCM precipitation data is 0.85 for CCSR96, 0.02 for CSI296, 0.47 for ECH498, 0.66 for HAD300 and 0.23 for GFDL90. All five GCMs, except for the CSI296 model, underestimate the modeled observed precipitation data. The model that best fits the observed temperature data is the GFDL90 GCM and the model that best fits the observed precipitation data is the CCSR96 GCM. For calculation of the climate change scenarios for temperature and precipitation, the average of the future changes of the five GCMs will be used, because of the high correlation and this also gives a better presentation of regional anthropogenic climate change than the pattern derived from any single GCM (Hulme, 2000).

6.4.2 Scenarios of future precipitation and temperature change

Figures 6.4a and 6.4b show the monthly average precipitation and temperature changes corresponding to the P50 global emission scenario for the years 2020, 2050 and 2080 for Suriname. These results are thus the average of grid points 1 to 4 (Figure 6.2). The seasonal and monthly changes are shown in Tables 6.2 and 6.3 respectively. According to the GCM results, we may draw the conclusion that the highest monthly increase in temperature (Figure 6.5a) is expected in August with 1^{o}C by 2020, 2.3^{o}C by 2050 and 3.5^{o}C by 2080 and the lowest increase in monthly temperature is expected in March with about 0.4^{o}C by 2020, 1^{o}C by 2050 and 2^{o}C by 2080. The annual temperature is expected to increase from 0.6^{o}C in 2020 to 2.6^{o}C in 2080.

The highest monthly precipitation increase (Figure 6.5b) is estimated to occur in March and is about 22.5 mm (13%) by 2020, 48.1 mm (29%) by 2050 and 50.4 mm (30%) by 2080. All percentages are reference to the measured data. The highest decrease in precipitation is expected in August for 2020 and 2050 and is about 20.2 mm (13%) and 38 mm (24%) respectively. For 2080, the highest decrease occurs in June and is about 45 mm (15%). The annual precipitation is expected to decrease with 4.1 mm in 2020 (< 1%) to 102.6 mm (4.7%) in 2080.

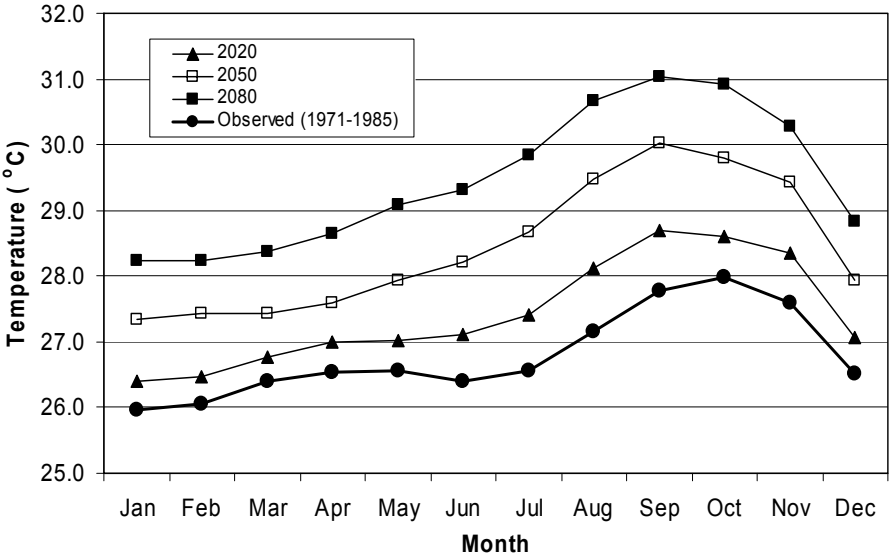

(a)

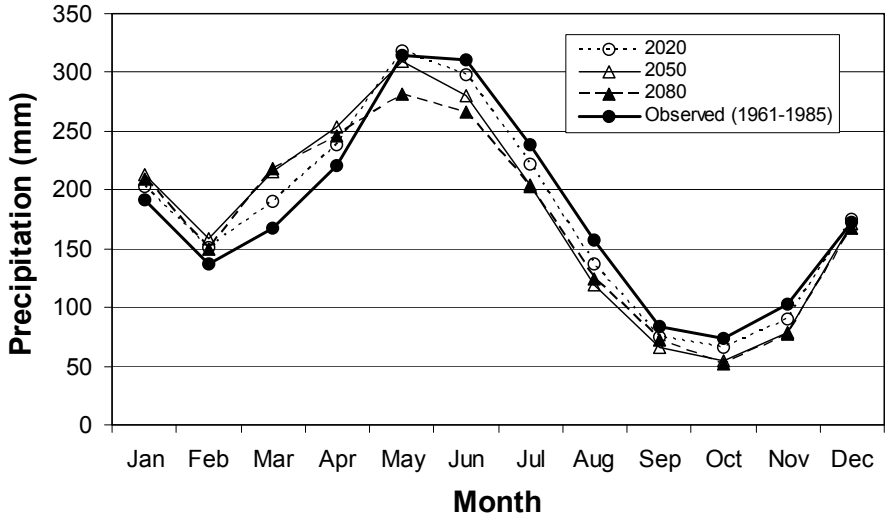

(b)

Figure 6.5: (a) Future monthly average temperature in Suriname, reference to the measured temperature data (1971-1985), (b) future monthly average precipitation in Suriname, reference to the measured precipitation data (1961-1985). The P50 emission scenario for the years 2020, 2050 and 2080 is used and the average outputs of five AOGCMs.

Table 6.2: Projections of seasonal and annual changes in temperature (°C) and precipitation (mm) across Suriname according to the P50 emission scenario, using average experiments results of five AOGCMs.

Period*	SWS	SDS	LWS	LDS	Annual
Temperature change (°C)					
2020	0.6	0.4	0.5 to 1.0	0.8 to 1.0	0.6
2050	1.4	1.0 to 1.4	1.1 to 2.3	1.8 to 2.3	1.6
2080	2.3	2 to 2.2	2.1 to 3.5	2.7 to 3.3	2.6
Precipitation change (mm/month)					
2020	2.3 to 11.6	14.7 to 22.5	-20.2 to 18	-12.8 to 20.2	-4.1 (< -1%)
2050	-1.5 to 21.7	21.7 to 48.1	-4.6 to -38.0	-23.3 to 38.0	-44.4 (-2%)
2080	-6.2 to 17.8	13.3 to 50.4	-32.6 to 25.5	-25.5 to -32.6	-102.6 (-4.7%)

* In general, the following seasons can be identified for Suriname: short wet season (SWS): December - January; long wet season (LWS): April – mid-August); short dry season (SDS): February - March; long dry season (LDS): mid-August - December.

Table 6.3: Projections of monthly changes in temperature (°C) and precipitation (mm) across Suriname according to the P50 emission scenario using average experiments results of five AOGCMs.

Period*	Jan	Feb	Maa	Apr	May	Jun	Jul	Aug	Sep	Oct	Nov	Dec
Temperature change (°C)												
2020	0.4	0.4	0.4	0.5	0.5	0.7	0.9	1.0	0.9	0.6	0.8	0.6
2050	1.4	1.4	1.0	1.1	1.4	1.8	2.1	2.3	2.3	1.8	1.8	1.4
2080	2.3	2.2	2.0	2.1	2.5	2.9	3.3	3.5	3.3	3.0	2.7	2.3
Precipitation change (mm/month)												
2020	11.6	14.7	22.5	18.0	4.6	-12.8	-15.5	-20.2	-9.0	-7.8	-12.8	2.3
2050	21.7	21.7	48.1	33.0	-4.6	-30.8	-33.3	-38.0	-18.0	-19.4	-23.3	-1.5
2080	17.8	13.3	50.4	25.5	-32.6	-45.0	-34.9	-32.6	-11.3	-21.7	-25.5	-6.2

With regard to future precipitation changes, it may be concluded that the short wet season (December - January) and the short dry season (February - March) will become wetter. The long wet season (April – mid-August) and the long dry season (mid-August - December) will become slightly drier (Figure 6.5b). Figure 6.5b also shows that the four seasons in Suriname will change in duration and shift. The mean monthly rainfall will decrease from 181 mm to 172 mm. The short dry season will become shorter with about 1 month, the long wet season will be extended with about 0.5 month and the long dry season will also be extended with about 0.5 month.

Because of the many uncertainties in the developing climate scenarios from GCMs related to future emissions, GCM selection, resolution, assumptions for model parameters (Arnell et al., 2003; Giorgi et al., 2001; IPCC-TGCIA, 1999; Jones et al., 2004; Mearns et al., 2003), the future temperature and precipitation changes presented in Tables 6.2 and 6.3 should be considered average scenarios across Suriname. The scenarios calculated for Suriname are thus the average over the four grids (Figure 6.2). From the scenarios, with respect to temperature, the long dry season in Suriname may well become the warmest in the future compared to the other seasons. The expected increase in mean temperature will tend to increase evapotranspiration everywhere and reduce precipitation and, hence, lower water resources proportionally.

6.5 Conclusions

Under doubling of carbon dioxide (CO_2) in the atmosphere, the monthly and annual mean temperature is expected to rise in Suriname. The mean precipitation is expected to increase during January to April, and to decrease in May to December. The expected warmer temperatures will most likely increase evapotranspiration. In addition, the changes in other climate parameters such as cloudiness, wind and humidity could further affect evapotranspiration. The individual GCMs also indicate that precipitation in Suriname will decrease in general. Because water resources essentially depend on the difference between precipitation and evapotranspiration, the impact on water resources could be even greater. There is also a growing risk of drier periods than normal during May-December and wetter periods than normal during January-April, and this will put pressure on water resources systems. It is clear that water management measures will need to be taken in the future to cope with these problems. It should be mentioned that because of the limitations of current GCMs e.g. the low resolution, it is better to use regional climate models (RCMs) to formulate climate scenarios for Suriname. They capture climate variations better due to topography, soils, and vegetation as well as extreme events and have a high resolution (about 25-50 km). The results in this study should therefore be considered as plausible changes in future precipitation and temperature for Suriname.

Because of the scale of the GCMs, no indication can be given about the frequency and magnitude of daily rainfall events and temperature in Suriname.

Acknowledgements

Meteorological data have been provided by the Meteorological Service Suriname. The provision of the MAGICC/SCENGEN model 4.1 from the National Center for Atmospheric Research (NCAR-USA) and the assistance of Dr. T. Wigley are gratefully acknowledged. Two anonymous reviewers provided valuable comments.

7. MODELLING HYDROLOGICAL RESPONSE OF THE UPPER-SURINAME RIVER BASIN TO CLIMATE CHANGE*

Abstract

The goal of this chapter is to assess the impact of future climate change on the hydrological regime of the tropical Upper-Suriname river basin (7,860 km^2) located in Suriname. GCM-based climate scenarios from the MAGICC/SCENGEN model and 14 hypothetical climate scenarios are used to examine potential changes in water balance components in the study area. A physically-based distributed hydrological model, WetSpa, and Geographic Information Systems (GIS) are used to simulate the historical and future hydrological conditions. The evaluation results indicate that the model has a relatively high confidence (model bias C1 is 0.046 and the model determinant coefficient C2 is 0.833) and can give a fair representation of the river flow hydrographs at a daily scale (Nash Sutcliffe coefficient C3 is 0.622). The results indicate that an obvious increase in the annual temperature (1.8^{o}C and 3.2^{o}C by 2050 and 2080 respectively) in the study area is accompanied with a clear tendency in reduced precipitation during January-March and August-December, and an increased tendency during April-July. The sensitivity analyses of water balance components under temperature and precipitation change (GCM scenarios for 2050, 2080) show that by 2080, the annual river discharge will drop 35%. When using hypothetical climate scenarios (T+2^{o}C, T+4^{o}C and P$\pm$10%, $\pm$30%, $\pm$50%), calculations show that the annual river discharge will increase with maximally 75% for the scenario T+2^{o}C P+50% and will decrease with maximally 87.5% for the scenario T+2^{o}C P-50%. The results are indications of potential impacts of climate change on water resources in the Upper- Suriname river basin, but true predictive skills require a significant improvement in the ability of global climate models to predictive changes in regional climate variability. The WetSpa model has proven to be useful for hydrological modelling studies where availability of physical catchment characteristics and hydroclimatic data is scarce.

---

* This chapter has been published as: "Modelling hydrological response of the Upper-Suriname river basin to climate change by the WetSpa model", Journal of Spatial Hydrology, Vol. 7, No. 1 Spring 2007.

* Part of this chapter has been published as: "Hydrologic modeling of the Upper Suriname River basin using WetSpa and ArcView GIS", Journal of Spatial Hydrology, Vol. 6, No. 1 Spring 2006.

7.1 Introduction

The increase in global mean surface air temperature by about 0.6°C ± 0.2°C over the late 20th century has affected the global hydrological cycle (Glen, 2004). According to climate models, the global surface temperature is likely to rise by about 1.5-3.5°C by the end of 2100. A simple increase in temperature will increase evaporation and enable the atmosphere to transport higher amounts of water vapor. Therefore, it is assumed that rainfall and runoff will be accelerated. Long-term changes in precipitation on earth will affect water resources and, consequently different socio-economic sectors such as hydropower generation, drinking water supply, irrigation, ecosystems, forests and wetlands.

Predicting long-term climate change impacts on water resources using hydrological modelling and climate modelling is still a very intricate task. Currently, global circulation models (GCMs) are the most powerful climate models to predict changes in hydrometeorological variables (e.g. cloud cover, evaporation, temperature, precipitation, soil moisture) due to increasing levels of atmospheric greenhouse gases (Bronstert et al., 2002; Gleick, 1986; IPCC, 2001; IPCC-TGCIA, 1999). However, the outputs of the GCMs may not be used directly for climate impact analyses at basin scale due to the coarse resolution (about 300 km) and the fact that local climate (e.g. precipitation) and/or hydrological processes are still not well reproduced in time and space by the GCMs. Therefore, the results of GCMs can only be used for sensitivity analyses. The use of hypothetical climate change scenarios can also be considered as an option to study future hydrological changes (Niemann et al. 1994; Robock et al., 1993).

Hydrological models, using geographic information systems (GIS) techniques, are nowadays a powerful tool to understand current and future hydrological changes of a river basin (Boorman and Sefton, 1997; Gleick, 1986; Perrin et al., 2001). GIS techniques allow us to handle the spatial varied data in digital form and to derive basin parameters (e.g. slope, flow direction). There are a few classifications for hydrological models and they are somewhat arbitrary (Beven, 2000; Booij, 2002; Maidment 1992; Perrin et al. 2001). In general, hydrological models can be classified in empirical, conceptual and physically based spatial distributed models. Some conceptual models are the Stanford watershed model (Crawford and Linsley, 1966), the HBV model (Bergstrom and Forsman, 1973) and the PRMS model (Leavesley et al., 1983). Some physically based spatial distributed models are the IHDM model (Calver and Woord, 1995), the TOPMODEL (Beven and Kirkby, 1979), the MIKE-SHE model (Refsgaard and Storm, 1995), the HBV model (Lindstrom et al., 1997) and the SWAT model (Arnold et al., 1998). The main differences between the first two and the third group of models are

that the empirical and conceptual models take no or very little account of the spatial distribution of physical data of the basin (e.g. soil, land use, topography) nor of the spatial variation of the climate (e.g. precipitation, evaporation), they have very few parameters to optimize, are easier to operate and require less data than the distributed models.

It has been shown that distributed hydrological models for (large tropical) catchments have important application to the prediction of the effect of climate change (Andersen et al., 2001; Bormann, 2005; Campling et al., 2002; Gleick, 1986; Roulin, 1998; Legesse et al., 2003; Liu, 1999; 2004; Menzel and Burger, 2002; Molicova et al., 1997; Perrin et al., 2001). For example, Legesse et al. (2003) applied a physical distributed precipitation-runoff model, PRMS, to the Ketar river basin (3,220 km^2) in Ethiopia and arbitrary climate scenarios. This study shows that a 10% change in daily rainfall results in a decrease in annual runoff of about 30%. The model has shown to produce relatively good results for an area with poor data. The main conclusions from many of the above case studies are that the predicted climate change impacts are influenced by the model performance and the lack of spatial detail in GCMs, which makes it difficult to reflect the inhomogeneous spatial pattern in precipitation and evapotranspiration. The model performance is mainly influenced by the inadequacy of the model structure, errors in data, the lack of high resolution topographic, soil and land use maps, the lack of sufficient rainfall stations and measurements of potential evapotranspiration, and information on soil hydraulic processes.

In the tropical part of South America, the climate is mainly characterized by a large inter annual to decadal variability in rainfall and river discharges caused by the variability in sea surface temperature in the Atlantic and Pacific ocean (Ambrizzi et al., 2005; Giannini et al., 2000; Marshall et al., 2001; Martis et al., 2002; Rajagopolan et al., 1997; Wang, 2001, 2005). In Suriname (2^o-6^o Northern Length, 54^o-58^o Western Length), the sensitivity to short term climatic fluctuations can be illustrated by prolonged dry (drought) and wet periods (heavy rainfall, floods). Some recent prolonged dry periods were in (a) north-west Suriname during August-November 1982, December 1982-February 1983, August 1997-February 1998, and (b) in central Suriname during September 2004-January 2005 (Houben and Molenaar, undated; Mol et al., 2000). Some recent floods were experienced in (a) south-west and central Suriname during the first half of 2000, April 2004 and May-June 2006 and (b) northern Suriname (Paramaribo) during September 2004 and July-August 2005 (Hollande, N., personal communication, October 1, 2004; Scheltz, E., personal communication, September 5, 2004).

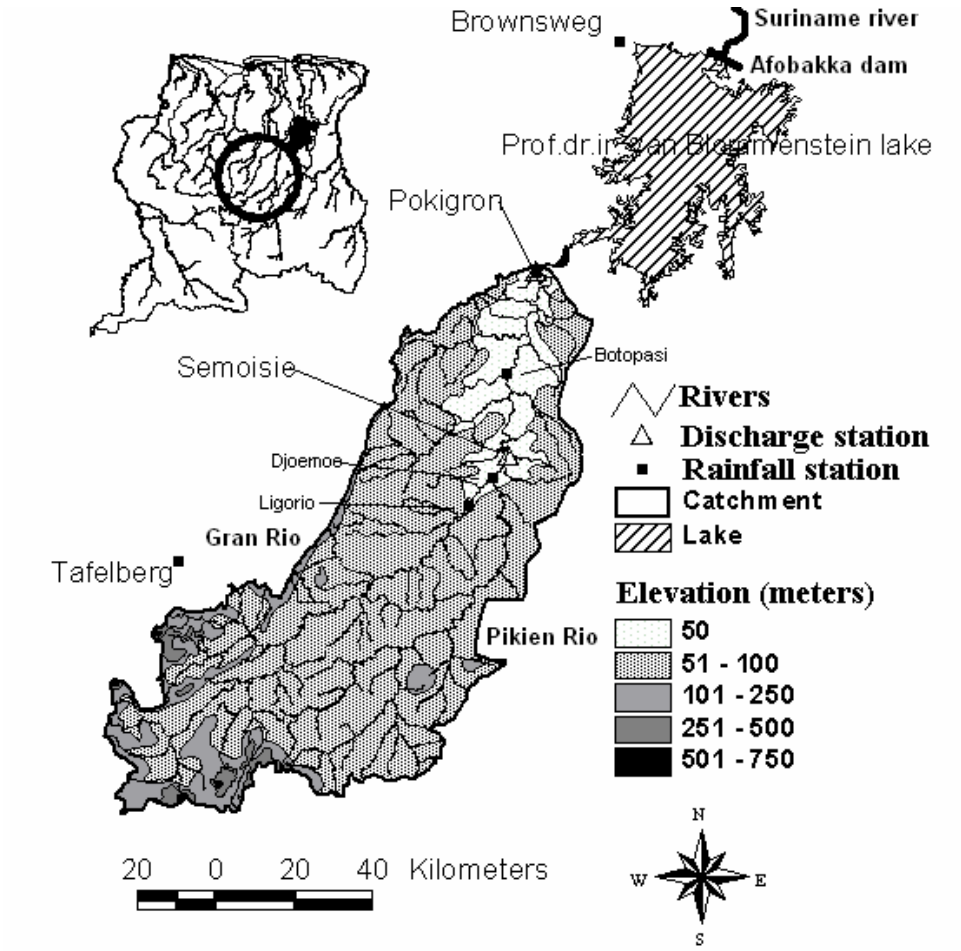

Figure 7.1: The Upper-Suriname river basin and network of hydro-meteorological stations.

One of the sensitive areas in Suriname is the Upper-Suriname river basin (Fig. 7.1), which is the main source of water for the Prof. Dr. Ir. van Blommenstein reservoir. This artificial reservoir is used for hydropower generation (189 Megawatts) for industrial and domestic purposes, and is therefore very important to the economy of Suriname. This reservoir has also been affected by prolonged dry periods such as the recent one in September 2004-January 2005. The continuing increase in global temperature on earth (IPCC, 2001), makes it necessary also to understand how river flows and/or water balances of river basins may change due to long-term climate changes as it will impact different economic sectors and also the management of water resources. The goal of this paper is therefore to understand how water resources in the Upper-Suriname river basin (Suriname) might change due to

future climate change by using a hydrological model and climate change scenarios.

7.2 Study area and data used

7.2.1 Selected catchment

The Upper-Suriname River basin is situated in Suriname and has a total drainage area of about 7,860 km^2 up till Pokigron (Figure 7.1). The topography varies from 75 m to 809 m above mean sea level. The natural vegetation comprises high tropical dense forest. The different soil types in this basin are: sand (1.6%), silt (5.5%), silt clay loam (48.2%), clay loam (27.9%) and clay (16.8%). Un to now, no significant changes in land use have been observed in this area. The basin is characterized by a tropical humid climate with a substantial seasonal variation. Figure 7.2 shows plots of the mean monthly values of precipitation, estimated pan evaporation, estimated potential evapotranspiration and river discharge in the basin. These values are arithmetic mean of the variables of the stations, as shown in Figure 7.1. The highest average precipitation is observed in May and is about 386 mm and the lowest average precipitation is observed in October and is about 58 mm (Nurmohamed and Naipal, 2004). The monthly pan evaporation in the study area varies from 93 mm in January to 138 mm in October (Lenselink and van der Weert, 1970). The highest discharge is reached in June and is about 495 m^3/s and the lowest discharge is about 34 m^3/s in November. The annual precipitation in this area is about 2,300 mm for the lower part of the basin and increases to 2,800 mm for the upper part of the basin. The annual pan evaporation is around 1,850 mm. The annual discharge at Pokigron (1952-1985) is about 219 m^3/s.

7.2.2 Data collection

Daily and monthly series of six rainfall stations (1961-1983) in or close to the study area (station Brownsweg, Pokigron, Botopasi, Djoemoe, Ligorio and Tafelberg) were obtained from the Meteorological Service Suriname. Records of mean daily river discharge (1952-1985) at two stations (Pokigron and Semoisie) were obtained from the Hydraulic Research Division Suriname and the Bureau for Hydroelectric Power Works. Only these stations were found suitable for use in this study in terms of data length and continuity. The network of these stations is shown in Figure 7.1. Pan evaporation (Eo) data is very scarce in this area. Therefore, pan evaporation data (1975-1983) at Pokigron has been interpolated from station Coeroeni (at about 233 km) and Sipaliwini (at about 216 km) and pan evaporation data at Semoisie has been interpolated from station Stoelmanseiland (at about 120 km).

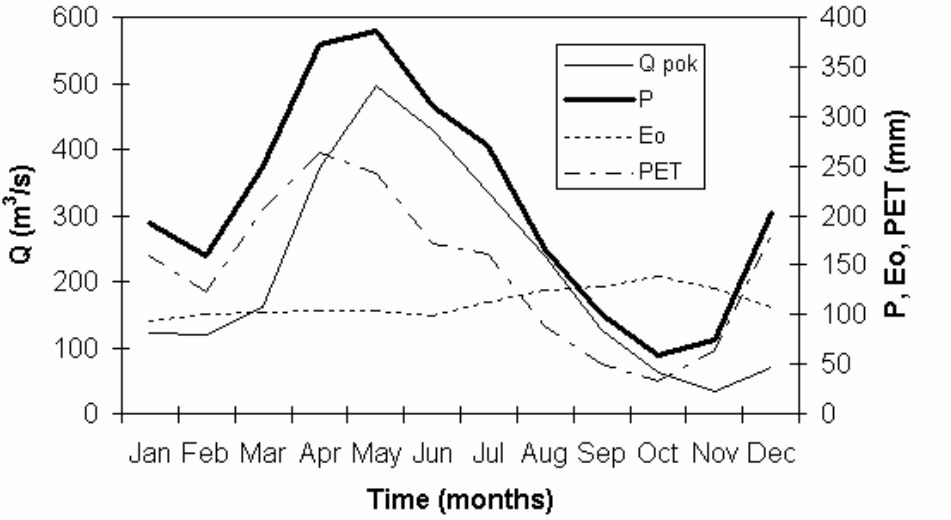

Figure 7.2: Mean monthly precipitation (P), pan evaporation (Eo), potential evapotranspiration (PET) and river discharge (Q_{pok}) in the Upper-Suriname River basin.

Although these stations are very far, they are the closest stations to the study area with mostly complete daily observed data. The actual evapotranspiration (ET) is estimated from the long-term water balance in this basin, ET = Q-P, with ET = k*Eo, where Q is the river discharge, P is the precipitation, Eo is the pan evaporation, k is a monthly factor. The years 1975-1983 were finally selected because they have sufficient daily data to use for hydrological modelling purposes.

To complete missing data of precipitation and discharge, linear interpolating is applied. The linear correlation coefficient (Pearson) between the monthly rainfall data of the stations ranges from 0.51 to 0.82. The river flows at Semoisie and Pokigron show a high consistency with a cross correlation coefficient of 0.95 for lag 0 and 0.71 for lag 1 month. A topographic map with river network of 1:100,000 (50 m interval) from year 1963, a soil map of 1:100,000 from 1963 and a land use map of 1:100,000 from 1963 were obtained from the Center of Natural Resources and Assessment (Narena). Observed baseline precipitation and temperature data used in the GCMs were taken from the Climatic Research Unit global 0.5 x 0.5^{o} 1961-1990 climate archives.

7.3 Methodology

In this paragraph, the WetSpa model is first described, followed by the way the input data has been processed. In the last section, an explanation is given on how the different climate change scenarios have been constructed.

7.3.1 Description of the WetSpa model

WetSpa is a continuous, distributed, physically-based hydrological model with variable time step (hourly or daily). This model is developed by the Vrije Universiteit Brussel, Belgium (Liu and De Smedt 2004) and has been applied to small and medium catchments (34-1,176 km^2) in Belgium, Luxembourg, Slovakia and Hungary. Liu et al. (1999, 2004) and Seifu (2003) have shown that the model is suitable for simulation of spatial distribution of hydrological processes and analysis of land use changes and climate change impacts of hydrological processes. The hydrological processes are summarized in Table 7.1 and the model structure is shown in Figure 7.3.

Table 7.1: Main hydrological processes and components per grid cell and equations of the WetSpa model (Liu, 2004)

Process	Equation	Approach
Basin water balance	$P = RT+ET+\Delta SS+\Delta SG$	-
Precipitation P	$P = \sum_{t=0}^{T} \sum_{i=1}^{N_w} P_i(t) / N_w$ (mm)	-
Total runoff RT	$RT = \sum_{t=0}^{T} \sum_{i=1}^{N_w} \left[RS_i(t) + RI_i(t)\right] / N_w + \sum_{t=0}^{T} \sum_{s=1}^{N_r} \frac{QG_s(t)}{A_s} / N_w$ (mm)	-
Overland flow RS_i	$RS_i(t) = PE_i(t)\left[1 - \exp\left(-\frac{PE_i}{SD_{i,0}}\right)\right]$ (mm)	Linear diffusive wave approximation (Miler and Cunge, 1975)
Interflow or subsurface runoff RI_i	$RI_i(t) = \frac{c_s D_i S_i K\left[\theta_i(t)\right]\Delta t}{W_i}$ (mm)	Darcy's Law and kinematic approximation
Groundwater outflow $QG_s(t)$	$QG_s(t) = Kg\left[SG_s(t)/1000\right]^2$ (mm)	Non-linear reservoir method (Wittenberg and Sivapalan, 1999)
Groundwater balance $SG_s(t)$	$SG_s(t) = SG_s(t-1) + \frac{\sum_{i=1}^{N_s}\left(RG_i(t)\right)A_i}{A_s} - EG_s(t) - \frac{QG_s(t)\Delta t}{1000 A_s}$ (mm)	-
Percolation RG_i	$RG_i(t) = K_i(\theta_i(t))\Delta t = K_{i,s}\left(\frac{\theta_i(t) - \theta_{i,r}}{\theta_{i,s} - \theta_{i,r}}\right)^{(2+3B)/B} \Delta t$ (mm)	Darcy's law and Brooks and Corey relationship (Brooks and Corey, 1966; Eagleson, 1978)

Evapotranspiration ET	$ET = \sum_{t=0}^{T} \sum_{i=1}^{N_w} \left[EI_i(t) + ED_i(t) + ES_i(t) \right] / N_w + \sum_{t=0}^{T} \sum_{s=1}^{N_r} EG_i(t) / N_w$ (mm)	-
Change in soil moisture ΔSS	$\Delta SS = \sum_{t=1}^{N_w} D_i \left[\theta_i(T) - \theta_i(0) \right] / N_w$ (mm)	-
Change in groundwater storage ΔSG	$\Delta SG = \sum_{s=1}^{N_w} \left[SG_s(T) - SG_s(0) \right] / N_r$ (mm)	-

Abbreviations: T is the simulation period (s), N_w is the number of cells over the basin, $RI_i(t)$ is interflow out of a cell over time interval Δt (day) (mm), c_s is a scaling parameter, D_i is the root depth (mm), S_i is the cell slope (m/m), $K(\theta_i)t$ is the effective hydraulic conductivity (mm/hour), W is the cell width (mm), Kg is the non-linear groundwater flow recession coefficient (m/s), $SG_s(t)$ groundwater storage of a sub-catchment at time t (mm), c_v is the vegetation coefficient, $\theta_{i,f}$ is the soil moisture content at field capacity (m^3/m^3), $\theta_{i,w}$ is the soil moisture content at plant wilting point (m^3/m^3), $ES_i(t)$ is the actual evapotranspiration (mm), EDi(t) is cell evaporation (mm), EP is the daily potential evaporation (mm), EI_i (t) is the evaporation from the cell interception storage (mm), t is the time step, A_i is the cell area (m^2), A_s is the sub basin area (m^2), $QG_s(t)$ is the groundwater discharge (m^3/s), EG_i (t) is the average evapotranspiration from groundwater storage of the sub basin (mm), c_r is the runoff coefficient, θ is the soil moisture content (m^3/m^3), θ_s is the soil porosity (m^3/m^3), K_s is the saturated hydraulic conductivity, θ_r is the residual soil moisture content (m^3/m^3), B is the cell pore size distribution index, Nr is the number of sub-catchments, $\theta_i(T)$ and $\theta_i(0)$ is the cell soil moisture constant at time T and time 0 (m^3/m^3).

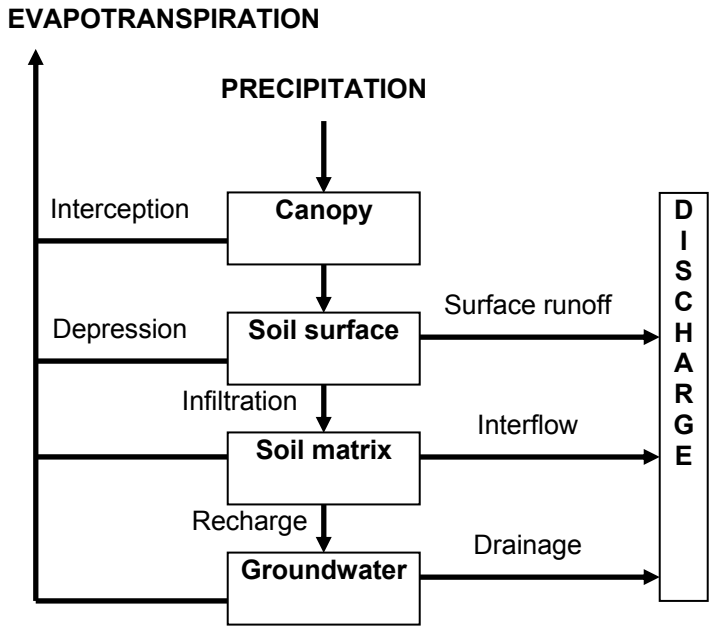

Figure 7.3: Schematic representation of the different components of the WetSpa model at a pixel cell level (Liu and De Smedt, 2004)

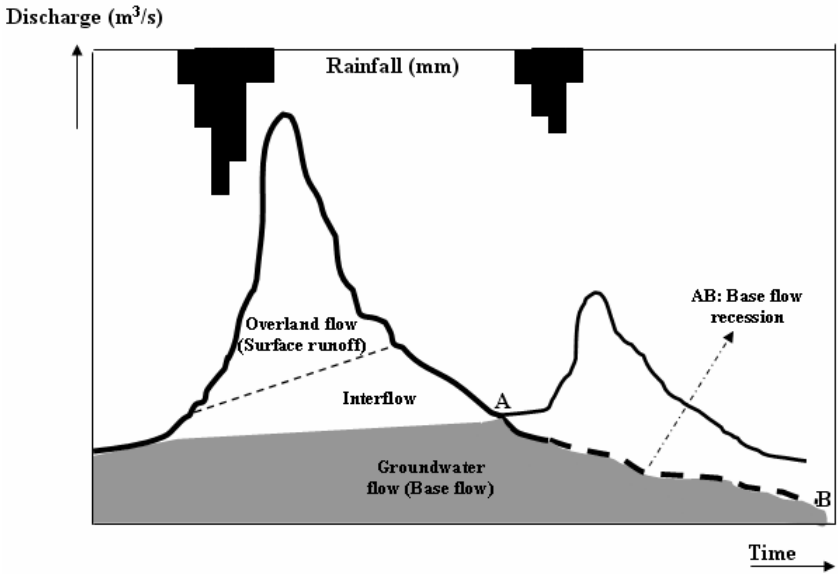

Figure 7.4: Idealized hydrograph and components of the river flow during two rainfall events.

Table 7.2: Global input parameters in WetSpa (Liu, 2004)

Parameter	Name	Unit	Range (best value)	Method of estimation
ki	interflow scaling factor	-	1-10	ratio of horizontal and vertical hydraulic conductivity; calibration recession curve observed and computed hydrograph
Kg	groundwater flow recession coefficient	-	< 0.01 or ki	calibration of observed and computed low flow hydrographs
K_ss	initial soil moisture	mm	-	calibration
go	initial groundwater storage in depth	mm	-	calibration of observed and computed low flows for initial phase
G_max	maximum groundwater storage in depth	mm	-	calibration
K_ep	correction factor for potential evapotranspiration	-	~ 1.0	calibration of water balance simulation
K_run	the surface runoff exponent	-	1-3	calibration from observations
P_max	maximum rainfall intensity	mm/day	-	from observations

The main input data in the WetSpa model are spatial data (elevation, river network, land use and soil type), and hydrological and weather data (precipitation, evapotranspiration, discharges). For calibration of the model, nine global input parameters (Table 7.2) can be used for tropical areas. Most of the parameters are found through calibration. The main outputs of the WetSpa model are river flow hydrographs for the entire basin and subbasins (e.g. surface runoff, interflow, groundwater flow), water balance and spatial distributed hydrological characteristics for the entire basin at each time step (e.g. runoff, soil moisture, groundwater recharge, infiltration rates) (Liu et al.,

2004; Seifu 2003). Some the components of the river flow are schematically shown in Figure 7.4.

The calibration period (January 1978 to December 1981) and the validation period (January 1982 to December 1983) are selected for modelling analyses with a model initialization period set to 1975-1977. To determine how well the observed hydrographs are reproduced by the model, five model efficiencies (C1, C2, C3, C4, C5) are used (Table 7.3) and a visual inspection of the joint plots of the daily/monthly simulated and observed hydrographs is used to judge the ability of the model to simulate seasonal variability and extreme conditions. The global input parameters are adjusted till a satisfactory performance of the model is obtained.

7.3.2 Data processing

From the topographic contour map, a 10 m elevation contour map with grid size 50 m (slope factor 0.5, threshold factor 1.0) was first created from a 50 m elevation contour map using the ArcView Contour Gridder extension. Different resolution digital elevation models (DEM) were created (50 m, 100 m, 200 m, 500 m) using the TOPOGRID function in Arc/Info. From visual comparison of the actual river network and the generated river network and because of computation time and computer memory, the 100 m DEM was accepted for further model simulation. From the DEM, the following physical parameters for each grid cell were created by ArcView: stream orders and network, slope of overland flow and river channels, flow direction, flow accumulation, sub-watersheds based on stream links and the hydraulic radius according to a flood frequency of 2 years.

The soil information was first reclassified according to the 12 U.S. Department of Agriculture soil texture classes (USDA) used in WetSpa and then also converted to a 100 m grid map. From the soil map, different maps of physical properties such as porosity, hydraulic conductivity, residual moisture, pore index field capacity, wilting point were created using the default parameters characterizing the soil of the study area (Table 7.4). The land use information was also converted into six land use classes used in WetSpa and then converted to a 100 m grid. From this map, different maps of physical properties were calculated such as root depth, Manning's coefficient and interception capacity using the default parameters characterizing the land use of the study area (Table 7.5). Based on the combination of DEM, soil and land use map, the potential runoff coefficient and depression capacity maps were created. The flow routing parameters were calculated using ArcView GIS using the slope, hydraulic radius and manning coefficient maps.

Table 7.3: Evaluation criteria for the model performance.

Criteria	Description	Range (best value)	Source
$C1 = \frac{\sum_{i=1}^{N} Qs_i - Qo_i}{\sum_{i=1}^{N} Qo_i}$	Model bias for evaluating the ability to reproduce water balance	0	Liu, 2004
$C2 = \frac{\sum_{i=1}^{N} \left(Qs_i - \overline{Qo}\right)^2}{\sum_{i=1}^{N} \left(Qo_i - \overline{Qo}\right)^2}$	Determinant coefficient representing the simulation variance (model confidence)	0-1 (1)	Liu, 2004
$C3 = 1 - \frac{\sum_{i=1}^{N} \left(Qs_i - Qo_i\right)^2}{\sum_{i=1}^{N} \left(Qo_i - \overline{Qo}\right)^2}$	Model efficiency for evaluating the ability of reproducing river flows	< 1 (1)	Nash and Sutcliffe, 1970
$C4 = 1 - \frac{\sum_{i=1}^{N} [\ln Qs_i - \ln Qo_i]^2}{\sum_{i=1}^{N} [\ln Qo_i - \ln \overline{Qo}]^2}$	Model efficiency for evaluating the ability of reproducing low flows	< 1 (1)	Smatkhin et al., 1998

$C5 = 1 - \frac{\sum_{i=1}^{N}(Qs_i + \overline{Qo})(Qs_i - Qo_i)^2}{\sum_{i=1}^{N}(Qo_i + \overline{Qo})(Qo_i - \overline{Qo})^2}$	Model efficiency for evaluating the ability of reproducing high flows	< 1 (1)	Guex, 2001; USACE, 1998

Abbreviations: Qs_i is the simulated river flow at time step i (m^3/s), Qo_i is the observed river flow at time step i (m^3/s), N is the number of time steps, $\overline{Qo}$ is the mean observed river flows.

Table 7.4: Default parameters characterizing the soil in the study area (Liu and De Smedt, 2004)

Texture class	Hydraulic conductivity (mm/h)	Porosity (m^3/m^3)	Field capacity (m^3/m^3)	Wilting point (m^3/m^3)	Residual moisture (m^3/m^3)	Pore size distribution index
Clay loam	1.51	0.464	0.310	0.187	0.075	8.32
Sand	208.80	0.437	0.062	0.024	0.020	3.39
Silt clay loam	4.32	0.398	0.244	0.136	0.068	7.20
Clay	0.60	0.475	0.378	0.251	0.090	12.13
Silt	6.84	0.482	0.258	0.126	0.015	3.71

Table 7.5: Default parameters characterizing the land use in the study area (Liu and De Smedt, 2004)

Land use class	Vegetated fraction (%)	Leaf area index	Root depth (m)	Manning's coefficient ($m^{-1/3}$ s)	Interception capacity (mm)
Evergreen broad leaf tree	90	5-6	1.5	0.60	0.15-2.00
Tall grass	80	0.5-6.0	1.0	0.40	0.10-1.50

From the results we can conclude that the average potential runoff coefficient is mainly between 0.2 and 0.4, while in the hilly area (south east part of the study area) values of up to 0.7 are reached. This is due to the steeper slopes in the hilly area. The point rainfall data of six stations were used to create areal rainfall distribution, using the ArcView Thiessen polygon extension. For potential evapotranspiration, a Thiessen polygon map was also created based on time series at two locations.

The WetSpa model was finally run using observed daily rainfall, potential evapotranspiration and the derived physical parameters from digital elevation, land use and soil maps in ArcView GIS for both the semi-distributed and fully distributed model. In WetSpa, the fully distributed model operates on cell scale and a variable time step and the semi-distributed model on small subwatershed scale.

7.3.3 Climate change scenarios

The MAGICC/SCENGEN climate model has been the primary model used by the Intergovernmental Panel on Climate Change (IPCC) and is therefore also used in this study to develop GCM based climate change scenarios. The following GCMs have been selected for this study: Had300 (UK Hadley Centre for Climate Prediction and Research, Europe), ECH498 (German Climate Research Centre, Germany), GFDL90 (US Geophysical Fluid Dynamics Laboratory, USA), CSI296 (Commonwealth Scientific and Ind. Research Organization, Australia) and CCSR96 (Japanese Centre for Climate Systems Research, Japan) (Retrieved June 5, 2005 from http://www-pcmdi.llnl.gov/projects/cmip/overview_ms/table1.html and http://www.grida.no/climate/ipcc_tar/wg1/316.htm#tab81). A study by Nurmohamed and Naipal (2004) has shown that the GCMs, although with a spatial resolution of 550 km, represent the seasonal variation in temperature and precipitation in Suriname reasonably well. The GCMs are used to simulate the average monthly change in temperature and precipitation for two time frames 2035-2064 (2050) and 2065-2094 (2080). The daily change is calculated by dividing the monthly change by 30 days. The daily temperature and precipitation changes for year 2050 and 2080 have been added to the 9 years of daily observed data (1975-1983) (IPCC-TGCIA, 1999; Hulme et al., 2000; Wigley, 2003). These future data time series are used as inputs in the WetSpa model to simulate future changes in water resources in the study area. The average of the outputs of the GCMs is used to present future climate change for the study area, rather than outputs of a single GCM (Hulme et al., 2000). We will assume that the spatial and temporal pattern is constant, but only the magnitude will change. We should however remark that the periods of the observed data series in the study

area (1975-1983) and the period of the baseline GCM data series (temperature: 1961-1990; precipitation: 1981-2000) are different.

Because of the already mentioned limitations of GCMs (paragraph chapter 2), we will also use hypothetical scenarios. This method is adopted from Gellens and Roulin (1998) and is widely used. Changes in temperature of $+2^{o}C$ and $+4^{o}C$ and/or precipitation changes of $\pm$10%, $\pm$30% and $\pm$50% are adopted as scenarios. Such kind of scenarios have also been used by Booij (2002, 2005), Boorman et al. (1997), Bormann (2005) and Bronstert et al., (2002). Compared to the GCM scenarios, the changes are here applied uniformly to the entire historical daily data series in the study area: future temperature data time series are created by adding to each historical daily observed temperature value, a change of $+2^{o}C$ or $+4^{o}C$, and future precipitation data time series are created by adding to each historical daily observed precipitation value, a change of $\pm$10% or $\pm$30% or $\pm$50%. Based on a linear relationship between the observed actual evaporation and the observed temperature in the study area, the future evapotranspiration is estimated using the future temperature (Wigley, 2003). The future change in temperature is used to estimate the future change in evapotranspiration. It is simply assumed that evaporation changes linearly with temperature (Wigley, 2003). The WetSpa model is finally set up to run the GCM scenario years 2050 and 2080 and a total of 14 hypothetical scenarios. Precipitation and evapotranspiration data for the period 1975-1983 represent current climate conditions ($1xCO_2$ concentration), and the GCM and hypothetical scenarios represent climate change conditions ($2xCO_2$ concentration).

7.4 Results and analyses

7.4.1 Calibration and validation results of the WetSpa model

A manual calibration is used, starting with a first estimation of ki, Kg, K_ss, K_ep, go and G_max, using the methods and/or ranges mentioned in Table 7.2. The model is re-run (about 75 runs) to obtain a good match between the observed and simulated river flow hydrographs. The judgment is based on numerical evaluation of the results. The following optimum global parameters were found and are used for further analyses: ki = 1.0, Kg = 0.01, K_ss = 1.0, K_ep = 1.0, go = 30 mm, G_max = 400 mm, K_run = 1.5 and P_max = 300 mm/day. It was shown that the model performance is mainly affected by the global input parameters (the interflow scaling factor, the groundwater flow recession coefficient, the initial soil moisture and the initial groundwater storage).

Table 7.6: Model performance for the calibration/validation period (1975-1983) for the Upper-Suriname River basin at station Pokigron. C1 to C5 are the model evaluation criteria.

Model	Model evaluation				
Semi-distributed model	**C1**	**C2**	**C3**	**C4**	**C5**
Calibration (1978-1981)	-0.011	0.839	0.543	0.555	0.643
Validation (1982-1983)	0.194	0.875	0.768	0.633	0.850
Total (1978-1983)	0.046	0.833	0.622	0.609	0.715
Fully distributed model					
Calibration (1978-1981)	-0.219	0.726	0.552	0.493	0.585
Validation (1982-1983)	-0.029	0.794	0.779	0.779	0.804
Total (1978-1983)	-0.166	0.727	0.631	0.659	0.662

Table 7.6 shows the comparison in model evaluation criteria for the semi-distributed and fully distributed model. It is found that the most sensitive global input parameters are ki, Kg, K_ss and go. From the results, we can also see that the semi-distributed model produces slightly better evaluation results than the fully distributed model. The calibration and validation results show that there is a reasonably moderate agreement between the measured and simulated river flows during this period. WetSpa reproduces the observed water balance (1978-1983) with 4.6% overestimation, the Nash-Sutcliffe model efficiency for reproducing the river flows is about 62% and the ability to reproduce low and high flows is 62% and 71% respectively. The model confidence is 83%.

Figure 7.5 shows a typical calibration result for year 1982 corresponding to the chosen global input parameters. From this result we can clearly see that the model has simulated the seasonal and inter-annual variability in river discharge in the basin very well. The increase in river flow can be explained by the heavy rainfall events and the increase in base flow (interflow and groundwater flow) during January - mid-June. The decrease in flow after mid-June can be explained by the decrease in rainfall events and the base flow.

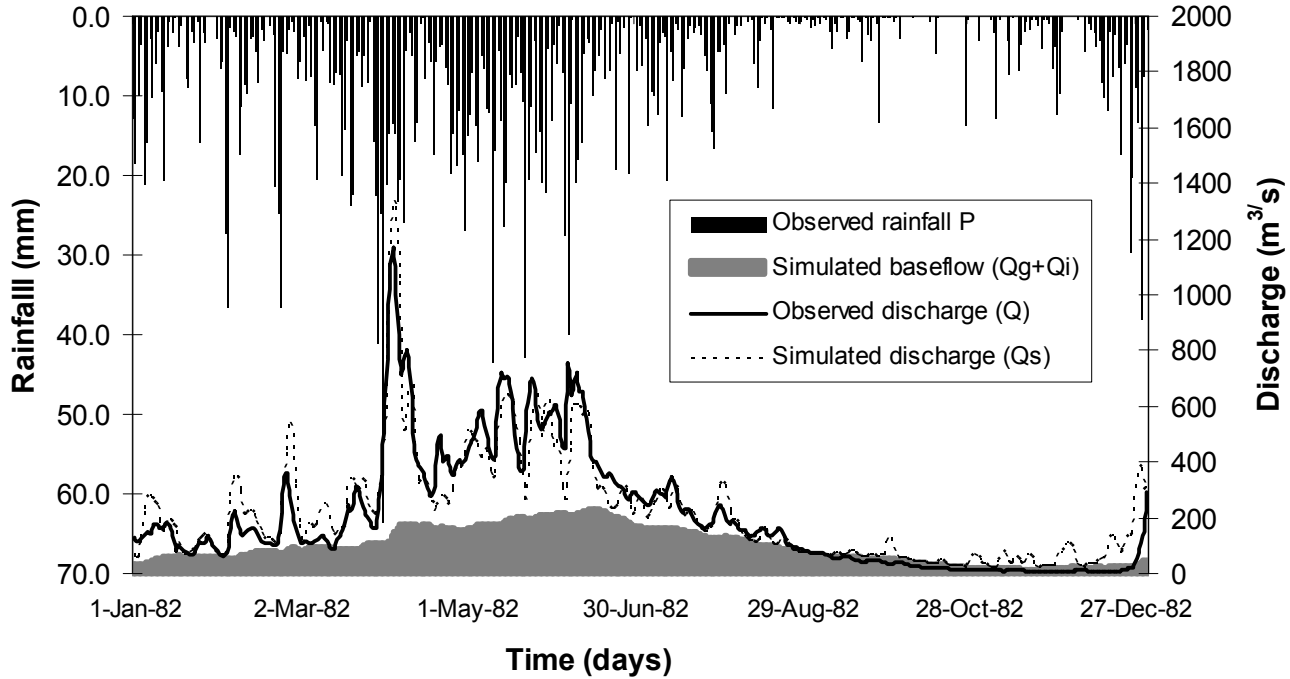

Figure 7.5: Mean daily observed and simulated river discharge and simulated base flow at Pokigron for 1982 (semi-distributed model).

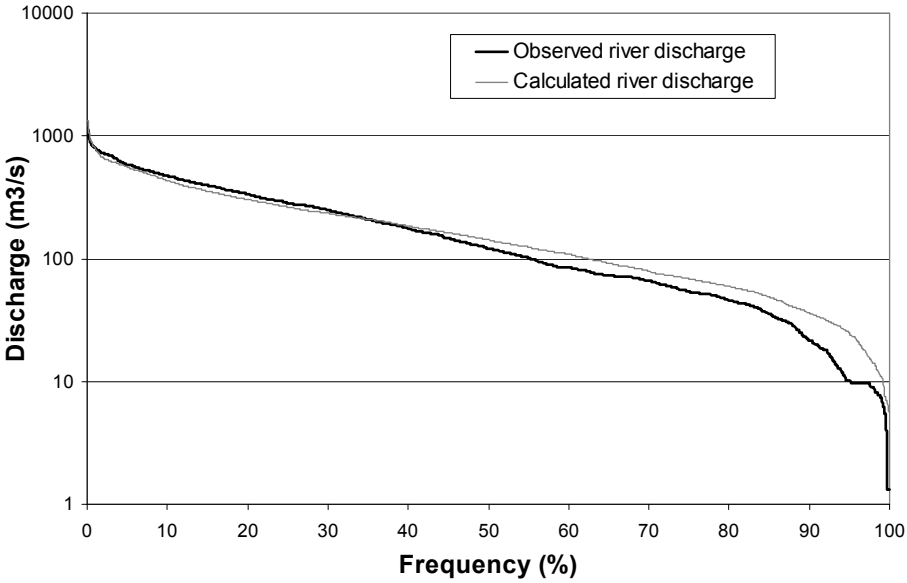

Figure 7.6: Comparison of the ranked value of the daily observed and simulated mean flows at Pokigron (1978-1983)

Table 7.7: Observed and simulated total water balance of the Upper-Suriname river basin for the period 1978-1983.

Component	Observed (mm)	Percentage of P (%)	Simulated (mm)	Percentage of P (%)
Precipitation	14173	**100**	14052	**100**
Interception			1162	8.3
Infiltration			9453	67.3
Actual evapotranspiration	9237	**65.2**	8528	**60.7**
Percolation			5053	35.9
Surface runoff			2667	19.1
Interflow			112	0.8
Groundwater flow			2177	13.9
Total runoff	4736	**33.4**	4956	**35.3**
Soil moisture difference			-28	-0.2
Groundwater storage			-51	-0.3

Analyses of the ranked value of the observed and simulated flows indicate that there are some obvious deviations for low flows (Q < 160 m^3/s) and for high flows (Q > 220 m^3/s) (Fig. 7.6). The error for small flows is up to 436%, especially for flows smaller than 30 m^3/s and for large flows up to 23%. The large errors for small flows are caused by lack of observations, especially during the dry seasons (September-November). The errors for large flows may be caused by the use of daily observations, which cannot accurately capture storm events causing floods. The shortness of the data series may also have affected the calibration results. The lack of other measurements of

the hydrological processes (e.g. groundwater flow, infiltration) makes it also difficult to estimate the base flow recession coefficient, the surface runoff coefficient and the maximum groundwater storage, and may also contribute to the large errors in low flows and high flows respectively. The deviations between the observed and simulated flows may further be caused by the lack of a good representation of the meteorological conditions in the study area. The spatialization of point rainfall and evaporation data may also affect the quality of the hydrological simulation. Rainfall and evaporation stations are very scarce and the stations are generally located along the river. Other reasons are deficiency of model structure (Liu, 2004), low resolution and errors in the elevation, soil and land use maps, and the default input parameters used in the model.

Table 7.7 summarizes the observed and simulated water balance for the period of 1978-1983. It is evident that the observed and simulated precipitation and total runoff water balance components do not differ much from each other. The simulated water balance shows that the total runoff of the Upper-Suriname River basin is composed of 57% surface runoff and 43% base flow (groundwater flow and interflow). The seasonal water balance analyses show that when the river discharge increases in the Upper-Suriname river during December-February and March-May (wet season), the amount of surface runoff is about 60% and base flow about 40% of the total runoff and does not change significantly during both periods. When the discharge decreases, base flow dominates during June-August and September-November (long dry season) and is about 67% and 74% of the total runoff respectively. Surface runoff is about 33% and 26% of the total runoff during June-August and September-November respectively. It is also concluded from the results that during the low flow period, the model evaluation results are the lowest.

7.4.2 Climate change scenarios simulation

Figure 7.7 shows the mean observed precipitation (1975-1983) and the modeled baseline precipitation (1981-2000) for the current climate and the future monthly precipitation from the GCM outputs (2050, 2080) for the study area. The Pearson's correlation coefficient (r) between the observed and modeled baseline monthly time series is 0.91 ($p < 0.05$), from which we can conclude that the GCM follows the seasonal pattern well. Two 30-year periods, namely 2035-2065 (2050) and 2070-2099 (2080) are used to estimate the future climate. The observed annual precipitation (1978-1983) in the study area is 2,388 mm and the modeled annual baseline precipitation (1981-2000) is 1,915 mm.

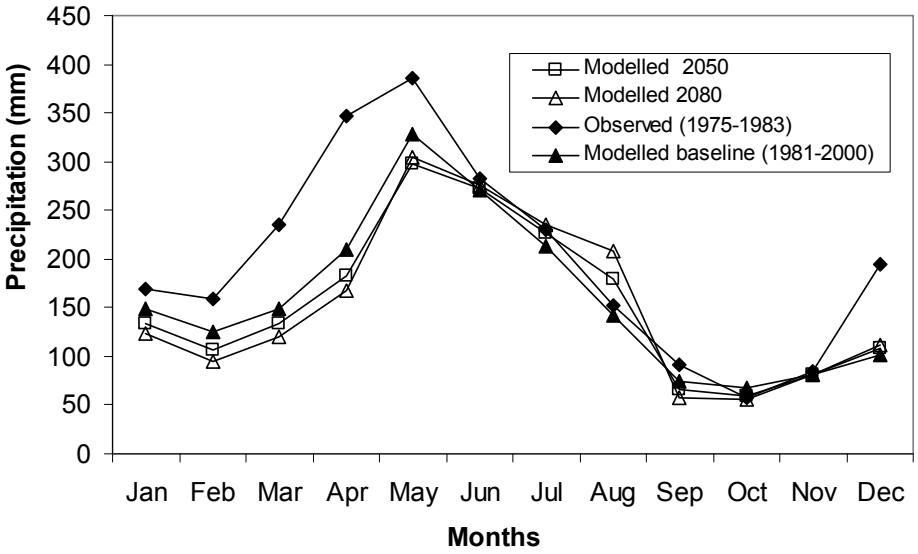

Figure 7.7: Observed precipitation (1975-1983) in the Upper-Suriname river basin, modeled observed baseline precipitation (1981-2000) and simulated future precipitation (2050, 2080) predicted by GCMs climate scenarios.

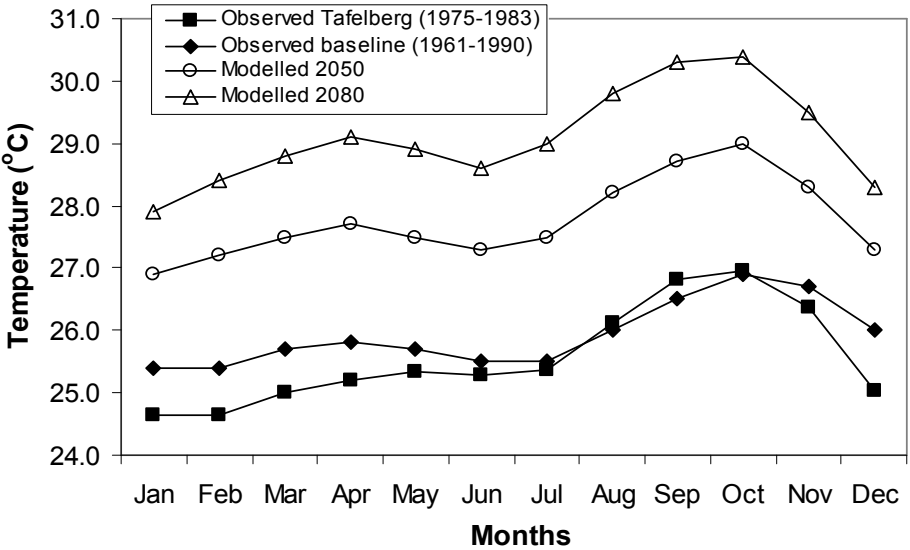

Figure 7.8: Observed temperature (1973-1985) near the Upper-Suriname river basin (station Tafelberg), modeled observed baseline temperature (1961-1990) and simulated future temperature (2050, 2080) predicted by GCMs climate scenarios.

This is a difference of about 20%. It should be remarked that the modeled precipitation is valid for a much bigger area than the Upper-Suriname river basin. Grid 3 of Figure 6.2 is used only for this purpose.

The GCMs predict a decrease in precipitation during January-June with a maximum difference of 31.0 mm/month (8%) during May and a decrease of about 9 mm/month during September-October. By 2050, an increase is predicted during July-August with a maximum difference of 37.2 mm/month (24.2%) in August and 6.2 mm/month in December. The same pattern is found for 2080 but with higher values: a decrease in precipitation during January-June with a maximum difference of 43.4 mm/month (12.6%) in April and a decrease of about 12.4-18.6 mm/month during September-October. During July-August, precipitation is expected to increase with a maximum difference of 65.1 mm/month (42.5%) in August and 9.3 mm/month in December. The annual precipitation in the basin will slightly decrease with about 68 mm (2.8%) in 2050 and 78.6 mm (3.3%) in 2080.

Figure 7.8 shows the mean observed temperature (1975-1983) for station Tafelberg and the modeled baseline temperature (1961-1990) from the five GCMs for the study area. The seasonal pattern of monthly temperature is also well simulated by the GCMs ($r = 0.90$; $p < 0.05$). The observed annual temperature (1978-1983) in the study area is 25.6^{o}C and the modeled annual baseline temperature (1961-1990) is 25.9^{o}C. This is a difference of 0.3°C. The annual temperature in the study area is predicted to increase with 1.8^{o}C and 3.2^{o}C by 2050 and 2080 respectively. This figure also shows the predicted mean monthly temperature corresponding to the years 2050 and 2080. The GCMs predict an increase in mean temperature during all the months with a maximum of 2.2^{o}C in September/October by 2050 and 3.8^{o}C in September/October by 2080.

From the predicted changes in temperature (Figure 7.8), the future changes in pan evaporation are calculated. The annual pan evaporation in the study area is estimated to increase with about 1,048 mm (78%) by 2080 (if temperature increases by 3.2^{o}C). The historical monthly temperature series from the GCMs and the evaporation series at Pokigron and Semoisie have a correlation coefficient of 0.92 ($p < 0.05$) and 0.87 ($p < 0.05$) respectively. Figure 7.9 shows the mean observed evaporation in the study area and the mean evaporation for 2050 and 2080. The highest increase in evaporation is estimated to be in September and is 2.6 and 4.3 mm/day by 2050 and 2080 respectively. Evapotranspiration is calculated, using a simple linear temperature-evaporation relationship and the water balance equation 2.1.

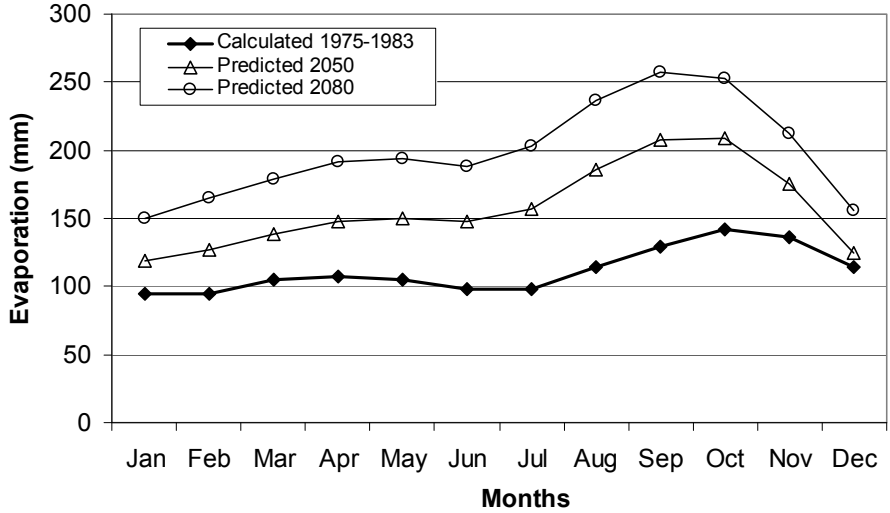

Figure 7.9: Estimated pan evaporation (1975-1983) in the Upper-Suriname river basin and estimated future pan evaporation (GCM scenarios: 2050, 2080).

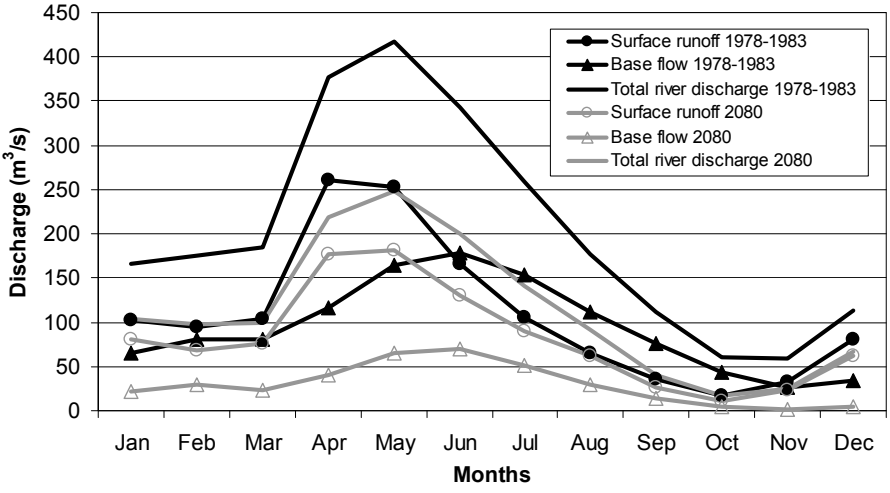

Figure 7.10: Mean monthly values of river discharge, surface runoff and base flow of the Upper-Suriname river basin for the period 1978-1983 and the future period 2080 (GCM scenarios).

Table 7.8: (a) Total annual water balance components for the current (1978-1983) and future periods (GCM scenarios for 2050, 2080), (b) change in mean monthly precipitation, total river discharge, surface runoff and base flow for future periods (GCM scenarios for 2050, 2080). The values in brackets are percentages referring to the 1978-1983 period. P is precipitation, Qt is total river discharge, Qs is surface runoff and Qb is base flow.

Component \ Period	1978-1983	2050	2080
Precipitation (mm)	14,052	15,734 (12%)	13,963 (-0.6%)
Actual evapotranspiration (mm)	8,528	9,171 (8%)	9,929 (17%)
Total river discharge (mm)	4,956	3,733 (-24%)	3,230 (-35%)
Surface runoff (mm)	2,667	2,269 (-15%)	2,169 (-19%)
Base flow (mm)	2,289	1,385 (-40%)	1001 (-56%)
Difference in soil and groundwater storage (mm)	568	2830	804

(a)

Period	2050				2080			
Component	P (mm)	Qt (m^3/s)	Qs (m^3/s)	Qb (m^3/s)	P (mm)	Qt (m^3/s)	Qs (m^3/s)	Qb (m^3/s)
Jan	-15.5 (9)	-60 (36)	-32 (31)	-28 (43)	-24.8 (15)	-63 (38)	-20 (20)	-43 (66)
Feb	-19.6 (12)	-64 (37)	-23 (24)	-41 (51)	-34.1 (22)	-77 (44)	-26 (28)	-51 (63)
Mar	-15.5 (7)	-58 (32)	-17 (17)	-40 (49)	-27.9 (12)	-85 (46)	-28 (27)	-57 (70)
Apr	-27 (8)	-96 (25)	-51 (20)	-46 (40)	-43.4 (13)	-159 (42)	-84 (32)	-75 (65)
May	-31 (8)	-109 (26)	-51 (20)	-58 (35)	-24.8 (6)	-170 (41)	-70 (42)	-99 (60)
Jun	3 (1)	-87 (25)	-22 (13)	-65 (37)	6.2 (2)	-142 (41)	-35 (21)	-108 (61)
Jul	12.4 (5)	-73 (28)	-9 (9)	-64 (42)	21.7 (9)	-117 (45)	-16 (15)	-102 (67)
Aug	37.2 (24)	-62 (35)	-6 (9)	-55 (49)	65.1 (43)	-86 (49)	-4 (6)	-83 (74)
Sep	-9 (10)	-50 (45)	-5 (14)	-45 (59)	-18.6 (20)	-70 (63)	-9 (26)	-62 (82)
Oct	-9.3 (16)	-34 (57)	-4 (24)	-30 (70)	-12.4 (22)	-43 (72)	-5 (29)	-38 (88)
Nov	0 (0)	-27 (47)	-7 (22)	-20 (77)	0 (0)	-33 (57)	-9 (28)	-24 (92)
Dec	6.2 (3)	-33 (29)	-12 (15)	-22 (65)	9.3 (5)	-47 (41)	-18 (24)	-29 (85)

(b)

Table 7.9: Changes in annual water balance components in percentage for future periods caused by the following hypothetical scenarios (a) T+2°C P±10%, P±30%, P±50% and (b) T+4°C P±10%, P±30%, P±50%. The future values are given in percentages reference to the 1978-1983 period. T is the temperature and P is the precipitation.

Component \ Period	T+2°C, P-50%	T+2°C, P-30%	T+2°C, P-10%	T+2°C, P+0%	T+2°C, P+10%	T+2°C, P+30%	T+2°C, P+50%
Actual evapotranspiration	-32	-13.2	2.4	9.3	16	27.8	38.6
Total river discharge	-84	-61.2	-32	-16	0.9	36.8	75
Surface runoff	-76.5	-53.4	-24	-7.3	11.4	54.7	104.1
Base flow	-93.1	-71.8	-44.1	-30.1	-16.1	9.7	33.5

(a)

Component \ Period	T+4°C, P-50%	T+4°C, P-30%	T+4°C, P-10%	T+4°C, P+0%	T+4°C, P+10%	T+4°C, P+30%	T+4°C, P+50%
Actual evapotranspiration	-29.9	-8.4	9.3	17	24.3	37.3	48.9
Total river discharge	-87.5	-69.3	-43.8	-29.3	-13.5	20.5	57
Surface runoff	-78.8	-57.1	-29.7	-13.9	3.9	44.9	92.1
Base flow	-97.8	-84.3	-62.4	-50.1	-37.5	-13.2	9.5

(b)

The actual annual evapotranspiration in the study area is predicted to increase with 643 mm (8%) and 1401 mm (17%) by 2050 and 2080 respectively. The changes in evapotranspiration are in the same order of magnitude as reported by Verhoog (1987).

7.4.3 Climate change impact on the Upper-Suriname river basin

Table 7.8a shows the annual water balance components for the 1978-1983 period and for the future periods 2050 and 2080 based on GCM results. The results indicate that for the GCM climate scenario year 2050, a 12% increase in mean annual precipitation and an 8% increase in mean annual evapotranspiration results in a reduction of the mean annual river discharge in the Upper-Suriname river by 24%, compared to the 1978-1983 period. From the obtained results, we can conclude that a small change in the mean annual temperature (1.8^{o}C and 3.2^{o}C for 2050 and 2080 respectively) has a significant impact on the river discharge.

The annual river discharge components change as follows: surface runoff decreases by 15% and base flow decreases by 40%. The monthly base flow and surface runoff reduction varies between 35% to 77% and 9% to 31% respectively. It is also found that for the GCM scenario year 2080, a decrease of 0.6% in mean annual precipitation and an increase in mean annual evapotranspiration of 17% result in a decrease of 35% in the mean annual river discharge. Surface runoff decreases by 19% and base flow decreases by 56%. The monthly base flow and surface runoff reduction vary between 60% to 92% and 6% to 42% respectively. The decrease in river discharge can be explained by the fact that evaporation from the soil and transpiration from plants increases. The impact of climate change on the different runoff components of the Upper-Suriname river basin for the GCM scenarios year 2080, simulated with the WetSpa model, is graphically presented in Figure 7.10. From these plots we can also see that during January-June (wet season), surface runoff is the main source of the total river discharge, while during July-November (dry season) base flow is mainly contributing to the river discharge. This is also shown in Table 7.8b.

Table 7.9 shows the changes in annual water balance components caused by hypothetical climate scenarios. The hypothetical scenarios show that a 2^{o}C and 4^{o}C increase in temperature and no change in precipitation, cause a decrease in the total annual river discharge of 16% and 29.3% respectively. Surface runoff decreases by about 7.3% and 13.9% respectively and base flow decreases by about 30.1% and 50% respectively. The results are quite close to the WetSpa simulations using the GCM predictions for 2050 (~ T+2^{o}C) and 2080 (~ T+4^{o}C) respectively (Table 7.8a and 7.9). When precipitation is increased up till 50%, the WetSpa model simulates an increase in annual river discharge up till 75% and 57% for T+2^{o}C and T+4^{o}C

respectively. Surface runoff and base flow also increase (Table 7.9). The fact that the estimated river discharge for T+4°C is lower than for T+2°C may be caused by the higher evapotranspiration. When precipitation is decreased up to 50%, the annual river discharge decreases up to 84% and 87.5% for T+2°C and T+4°C respectively. Surface runoff and base flow also decrease. The difference in hydrologic simulation results may be caused by the amount of changes generated from the GCM results and hypothetical scenarios, and the calculation method of the future scenarios. Hypothetical scenarios are found to give a good view of how water balance components may change under different climate change conditions. GCM outputs however may give more realistic climate change results, because the outputs are based on climate modelling results using observed climatological data. Taking the above limitations into account, the values presented in Table 7.8 and 7.9 give only an order of magnitude of a response to a hypothetical change in temperature and precipitation due to climate change.

Both types of climate scenarios have shown that the Upper-Suriname river basin is sensitive to climate change. Such large annual and monthly changes in the water balance may result in extreme events such as flooding and drought. The most dramatic case is for T+2°C. If the river discharge in the Upper-Suriname river decrease, this will also have significant impact on hydropower generation in the future. The decrease in surface runoff and base flow will also have its impact on the vegetation cover (tropical forest might change into dry forest) and in turn again affect the amount of water resources. If river discharges increase, this will cause water levels to rise, resulting in flooding of the river banks and changes in the morphology of rivers. It should, however, be noticed that an increase in surface air temperature will not only affect precipitation and evapotranspiration, but factors such as solar radiation, wind, cloudiness and vegetation cover may also affect the basin hydrology.

7.5 Discussion and conclusions

The hydrological simulation of the GCM scenario years 2050 and 2080 indicates that the annual river discharge in the Upper-Suriname river basin will decrease in magnitude (maximum 35%). This decrease may change vegetation cover in time and in turn again affect the discharge in the Upper Suriname river. When applying hypothetical scenarios (T+2°C, T+4°C and P+10%, 30% and 50%), the WetSpa model simulates an increase in annual river discharges in the river basin of maximum 75%, and for T+2°C, T+4°C and P-10%, -30% and -50%, the river discharge is predicted to decrease with maximally 87.5%. The results obtained by both methods, do differ much from each other. Hypothetical climate change scenarios however give a better indication of how hydrological processes might change due to gradual

changes in temperature. The difference in simulated water balance components based on GCM and hypothetical scenarios may be explained by the application of the type of scenarios (e.g. uniform change in temperature in the case of hypothetical scenarios, limitations of GCM models). Therefore, the simulated runoff values in this study give only an order of magnitude of plausible changes. Uncertainties in the simulated future water balance components can also be caused by the model performance of the WetSpa model. This could be increased by using field parameters instead of literature values, longer historical data series for calibration and more hydrological observations (e.g. base flow) for calibration of the WetSpa model. The uncertainty of river discharge prediction for hydrological modelling using climate change scenarios, is also caused by the fact that precipitation patterns from a coarse gridded GCM are uncertain. Besides the many uncertainties in GCMs, the uncertainties in the climate scenarios may also cause deviations in the predictions (Giorgi et al., 2001; Mearns et al., 2003). It is therefore advised to use downscaling techniques and regional climate models in future studies (Menzel and Burger, 2002). Regional scenarios of future climate can be used to study the “true” impacts of climate change on the river discharge in the Upper-Suriname river basin. Another uncertainty in the obtained results is the lack of knowledge about the future change in evapotranspiration. As little is known about the ability of the WetSpa model to simulate future changes in water balance components under climate change conditions, it would also be useful to apply more hydrological models to this study area for the same purpose. Future work on the impact of climate change should also be extended by the consideration of changes in land cover due to the interaction between climate change and changes in vegetation composition. This study has shown that the estimated changes in runoff may be significant enough to be considered for future impact analyses e.g. flood studies and effect on hydropower generation.

Acknowledgements

Sincere thanks to Dr. Y. B. Liu (Vrije Universiteit Brussels, Belgium) for the provision of the WetSpa model and the National Center for Atmospheric Research (NCAR- USA) for the provision of the MAGICC/SCENGEN model 4.1. I acknowledge the valuable review comments of three anonymous reviewers.

8. CONCLUSIONS AND RECOMMENDATIONS

8.1 General

The main objective of this PhD research is to investigate the impact of global climate change and variability on water resources in Suriname. Historical meteorological and hydrological data in Suriname are analysed with respect to climate change and climate variability, using statistical tests and graphical analyses. Outputs from global circulation models are taken from the Magicc/Scengen climate model 4.1 and are used to estimate future changes in temperature and precipitation in Suriname under global climate change conditions. The WetSpa hydrological model is finally used to estimate plausible changes in water resources in the Upper-Suriname river basin (case study area) under these conditions. The conclusions and limitations of this research will be given in paragraph 8.2 and the recommendations for future research in paragraph 8.3.

8.2 Conclusions and limitations

The literature review has shown that there are many statistical tests available to test randomness, stationariness and inhomogeneity of data series, there is no univocal method to analyse climate change. Literature review has also shown that climate change analysis, based on statistical tests are sensitive to mainly the length of data series, outliers and level of significance, and there is also no appropriate rule for selecting a statistical test.

To model climate in a particular area (e.g. precipitation), literature has shown that nowadays there are different methods available such as GCMs, RCMs, downscaling techniques and hypothetical climate scenarios, but the choice can be based on the available resources (e.g. long-term data series, research time, computer resources, financial resources). On the other hand, except for the GCMs, all the other techniques are still in an experimental phase. The main disadvantage of the GCMs is, however, that they cannot provide climate information on a small scale (e.g. 10^{-2}-10^{4} km^2).

Modelling water resources is quite easier than modelling climate since there are many hydrological models available and for climate change in river basins, simple water balance models are already suitable. Depending on the purpose (e.g. processes to model), the spatial scale and time scale, selection of a hydrological model might become a difficult task. Another problem with sophisticated models is just like in climate models the uncertainties, but perhaps more importantly, the fact that hydrological models have in principle not been designed yet to make future estimations of hydrological processes.

Literature has finally also shown that, because there are no univocal methods yet to study the effects of climate change on water resources, care should be taken when making future estimations in hydro-climatological variables using climate and hydrological models. It is therefore recommended to use more than one method.

Historical data analyses of precipitation have shown that both positive and negative annual trends occur in Suriname, depending on the location of the meteorological stations and the length of the observations. The time series used in this study varied from 25 years (1961-1985) up to 100 years (1900-1999). Linear trends in historical annual precipitation vary from -15 mm/year, in the centre of Suriname to 43 mm/year in the north-east of Suriname, during the period 1961-1985. This change corresponds with about -8% to 44% respectively. The majority of the rainfall stations (9) indicate a positive trend and 2 stations a negative trend. Three stations indicate a significant positive trend at a 95% confidence level and they are located in the north-east of Suriname. No significant trend in monthly rainfall were found. No consistent trends between the precipitation stations was found, with respect to monthly and annual precipitation. The changes in precipitation are close to the estimations of the IPCC (2001), but with the difference that the IPCC only estimates an increase in precipitation in and close to Suriname, which may be caused by the longer time series they have used. Statistical analyses have also shown high and low temporal scores (-3.5 to 2.7) in the annual rainfall in Suriname, which indicates that the inter-annual variability varies a lot. The variation in spatial loadings between 0.16 and 0.34 also indicates also a large spatial variability in annual rainfall in Suriname. The difference in trend and the time-spatial variability are caused by the high variability in rainfall between the stations, but may perhaps also be caused by the shortness of data series.

The positive linear trend in the historical annual temperature in Suriname (0.1^{o}C to 1^{o}C during the period 1971-1985 (15 years)) is in agreement with the estimations made by the IPCC (2001) and WMO (2001) in and close to Suriname. Nearly all months at the different meteorological stations indicate a warmer trend.

The historical annual river discharges (1961-1985) in the interior of Suriname also show no significant trend at a 95% confidence level. Three stations have shown a positive trend and one station (Semoisie) a negative linear trend. The trends vary from -2 m^3/s.year (-35%) to 7 m^3/s.year (11%). The negative trend in annual river discharges in the centre of Suriname may have been caused by the observed negative trend in annual precipitation in the centre of Suriname, but may also be just an artifact of the shortness of the data series.

The application of different parametric and non-parametric statistical tests to identify deterministic and stochastic components in the data series have shown to be very useful in getting reliable results, except in the case of identifying shifts in data series. Besides these reasons, the choice of the significance level (5%) and the equations used in the statistical tests may also have influenced the final results. The high variability in precipitation per station and between stations, and the shortness of observations make it difficult to identify shifts in hydro-climatic variables and the possible reasons. Shifts should be detected at the same time at all stations. Because of the above-mentioned reasons, but most importantly the shortness of precipitation, temperature and river discharge observations (< 50 years), the obtained results may not fully be representative for climate change studies (e.g. trends). These results are indications and should therefore be used with care.

The seasonal anomalies in precipitation and river discharge in Suriname was found to correlate well with sea surface temperature anomalies (SSTAs) in the Pacific and Atlantic ocean. The analyses have also shown that El Niño events in the Pacific ocean also influence the climate in Suriname, especially precipitation during December-May, while large SSTAs in the tropical Atlantic ocean may be responsible for the large inter-annual variations in precipitation especially during June-August (the long wet season) and September-November (the long dry season). Similar results were also obtained for the river discharge anomalies in the Upper-Suriname river basin and the SSTA in the Pacific and Atlantic ocean.

Rainfall deficit and low flow years (drought conditions) may have been caused by warmer than normal SSTs in the tropical North Atlantic ocean, which resulted in the ITCZ staying longer southwards of Suriname, especially during August-November, but also by the El Niño events (e.g. 1965-1966) and reverse impacts of La Niña events (e.g. 1964). Rainfall excess and high flow years (flood conditions) may have been caused by warmer than normal SSTs in the tropical South Atlantic ocean, which resulted in the ITCZ staying longer above Suriname, especially during June-August, but also by La Niña events (e.g. 1970-1971) and the reverse impacts of El Niño events (e.g. 1972-1973). It could however not clearly be shown which months during the year are significantly affected during these events, due to the shortness of the data series and the high inter-annual and spatial variability in precipitation in Suriname. No clear explanation could be found of the causes of wet/dry years in Suriname, including prolonged wet/dry seasons, either in precipitation and river discharge observations. This has to do with the different complex oceanic-atmospheric processes that interact with the climate, in particular precipitation in Suriname. The historical changes in the

annual precipitation and river discharge may thus be related to global decadal climate variability in the Atlantic and Pacific ocean and the atmosphere, caused by global climate change.

Estimating future changes in temperature and precipitation for throughout Suriname by 5 global circulation models (CCSR96, CSI296, ECH498, HAD300, GFDL90) have shown that most GCMs produced the seasonal pattern of temperature well (Pearson's correlation coefficient (r) varies from 0.66-0.86). Only one GCM (CCSR96) produces the precipitation pattern well (r is about 0.85). The GCMs indicate that under doubling of CO_2, the mean annual temperature will increase in Suriname up to 2.6^{o}C by 2080. The highest monthly temperature increase will be in August with 3.5^{o}C by 2080. The mean annual precipitation is expected to decrease with maximally 4.7% (103 mm) by 2080. These magnitudes in trends are also reported in IPCC reports. On a monthly scale, precipitation is expected to increase between January-April, with maximally 30% (50 mm) in March by 2080, and decrease between May-December with maximally 15% (45 mm) in June by 2080. These future changes will cause the short wet season and short dry season to become wetter, while the long wet and long dry season may become drier. If such changes take place, measures will have to be taken for water resources users regarding the management of water resources and sufficient sources of water resources will need to be identified for the future. However, the results from the GCMs and the predictions for Suriname should also be used with care, because of the limitations of GCMs and some assumptions made in this study. For example, the observed baseline period in the GCMs is slightly different than the observed data in Suriname, the average of four grids from the SCENGEN (5^{o}x5^{o}) model that cover Suriname is used to present future changes in temperature and precipitation and the results of the 5 GCMs differ much from each other, especially in the case of precipitation. Besides these limitations, GCM are not able to take into account e.g. orgraphic effects, effects of vegetation cover and soil, and land sea interactions. GCMs also do not produce evapotranspiration results. Therefore, future precipitation and temperature changes can only be used as sensitivity analyses for regional climate changes. The impacts of regional water resources (e.g. river basin scale) will also include uncertainties when using GCM results.

The distributed hydrological model WetSpa has shown to simulate river discharge and water balance (1978-1983) of the Upper-Suriname river basin quite well. The ability to reproduce water balance, represented by the model bias C1, was about 0.046. The low Nash-Sutcliffe coefficient for the mean river flows (0.622), low river flows (0.715) and high river flows (0.609) may be caused by the small amount of observations of precipitation and river discharges, and the use of large scale maps (1:100.000) of elevation, land

use and soil. Other factors may be the limitations of the WetSpa model (e.g. simplified literature equations of runoff, rather than physical based equations), a less dense spatial distribution of the meteorological stations used in the WetSpa model, the choice of the interpolation method, the use of literature values for model parameters of land use and soil (e.g. hydraulic conductivity, field capacity), choice of grid size and a manual calibration. Because of the high efficiency (C1) to reproduce water balance components, this model was further used to estimate future changes in these components in the Upper-Suriname river basin.

Under global climate change conditions (doubling of CO_2 by 2100), the WetSpa model shows that the annual river discharge will decrease in magnitude with about 45% by 2080 (when temperature increases 3.2^{o}C and precipitation decreases with 0.6%). Hypothetical climate change scenarios indicate, however that when the temperature increases 2^{o}C and the precipitation increases from 0% to 50%, the river discharge changes from -16% to 75% (actual evapotranspiration increases from 9% to 39%). When precipitation changes from 0% to -50%, the river discharge changes with -16% to -84% (actual evapotranspiration decreases from 9% to 32%). When the temperature increases 4^{o}C and precipitation increases from 0 to 50%, the river discharge changes with -29.3% to 57% (actual evapotranspiration increases from 17% to 49%) and when precipitation decreases from 0 to 50%, the river discharge changes with -29.3% to -87.5% (actual evapotranspiration decreases from 17% to 30%). As a result of these changes, monthly river discharges and other water balance components (e.g. subsurface runoff, base flow) also change and may result in more frequent drought and/or floods in the future in this area.

It can be concluded that there is quite a difference when using GCM based and hypothetical based climate scenarios in the WetSpa model for estimating water balance components in the Upper-Suriname river basin. These differences are also caused by the limitation of GCM models (paragraph 2.3), the differences in application of these two types of climate scenarios (chapter 5) and the ability of the WetSpa model to simulate future water balance components. The results however seem to be consistent. When temperature increases, evapotranspiration increases and when precipitation decreases, evapotranspiration also decreases due to the fact that less water is available to evaporate. The predicted changes in potential evapotranspiration for Suriname are close to literature values as reported in paragraph 3.4.5.

It has been shown that if the estimated changes in water balance components occur under global climate change, water resources will significantly change. If precipitation increases, floods may occur more frequently and/or longer and if precipitation decreases, drought conditions

may increase. The seasonal changes in river discharges may thus be greater and perhaps of much more importance than the annual changes. Under such conditions, there will be a need to set up management rules in the future with respect to the design of hydraulic works and the distribution of water resources e.g. for agricultural use. Flood/drought warning systems and food security programs will be highly necessary. No analysis could however be performed on extreme flows, because of the shortness of the historical observations (1978-1983).

This study has shown that it is quite difficult to estimate future changes in water resources, as there is still a lot of uncertainty in future changes in precipitation. But other effects should also be taken into account e.g. if the temperature rises, vegetation cover also changes and this should again be changed in the input data of the hydrological model. The lack of observed evapotranspiration data in this area, as one of the major input data in the WetSpa model, also introduces an uncertainty in the historical and future water balance estimation. Because of the very poor data on many meteorological variables, a simple linear relationship between temperature and evaporation outside the study area was used, to estimate evapotranspiration. This study has shown that a small change in precipitation and/or evapotranspiration causes a large change in runoff components in the Upper-Suriname river basin.

8.3 Recommendations for future research

This research is one of the first one studying the effects of climate change on water resources in Suriname. The methods of historical analysis, model selection, choice of climate scenarios and hydrological modelling were found satisfactory and could therefore be applied to other areas in Suriname. However, the limitation in available meteorological and hydrological observations, the differences in climate models and the limitations of the hydrological model, have influenced the obtained results and therefore also the uncertainty in future sensitivity analyses on water resources in the Upper-Suriname river basin. Therefore the following recommendations are suggested for future research:

- To get more reliable results for climate change studies in Suriname, it is necessary to continue and expand the collection of high-quality meteorological data (e.g. temperature, evaporation, wind) and hydrological data (e.g. base flow, groundwater levels, sea water levels), and increase the number of measurement stations throughout Suriname. This research has shown that besides temperature, precipitation and river discharges, it is necessary to collect more variables to increase our understanding on climate

processes in Suriname. These data will be useful for model calibration and verification, and weather forecasting purposes. Long-term and high-quality observations will also improve the detection of changes in climate and the understanding of possible causes. It is also recommended to analyse historical maximum and minimum values of meteorological and hydrological observations, and frequencies of extreme values.

- To apply more than one statistical technique for the detection of climate change and variability on only long-term meteorological and hydrological observations (> 50 years) using also more than one risk value.

- To improve our understanding of the influence of oceanic-atmospheric processes and other climate mechanism in the (sub)tropical region (e.g. Pacific Decadal Oscillation, South Atlantic Convergence Zone) on the climate of Suriname, including prolonged wet and dry periods and extreme events. Advanced statistical techniques should also be considered to be used and more climate variables e.g. for the analyses of wet/dry periods, influence of El Niño on precipitation in Suriname. The influence of land-sea interactions on the coastal climate and land processes in the interior of Suriname need to be studied in detail.

- To apply more global circulation models (GCMs) for Suriname and for different climate variables (e.g. evaporation, soil moisture, surface runoff rate) in order to get a better comparison of plausible climate changes for Suriname.

- To apply more types of climate change scenarios for Suriname to get a wide range of plausible changes in precipitation, temperature and other climate variables. It is recommended to use existing regional climate models (RCMs) and downscaling techniques to future GCM based climate scenarios. These methods can produce climate information at smaller spatial scales, while they can be used for water resources studies at river basin scale. The application of these methods can only be successful if there are long-term and high-quality surface and upper air climatological data series.

- To improve the WetSpa model evaluation results, with respect to low and high river flows. It is recommended to use field parameters for land use and soil (e.g. runoff coefficient, Manning's coefficient, soil moisture) in the model, different grid sizes, other interpolation methods (e.g. Kriging), a denser hydroclimatological network for

model calibration. However, the estimation of values of parameters from the field may cost a lot (field trips, laboratory experiments).

- To develop an appropriate method for the estimation of evapotranspiration for areas in Suriname with poor climatological data.

- To fill in gaps in historical and future observations in especially rainfall, it is recommend to develop a weather generator.

- It is also recommended to study the effects of land use changes due to increased temperatures. With a distributed hydrological model this can easily be done. The relation between temperature increase and land use and evapotranspiration should be analysed, as little is known about this.

- It is finally recommended that for the design of hydraulic structures (e.g. dams) for water resources systems (e.g. reservoirs, irrigation), not only historical river discharges should be taken into account, but also plausible changes in river discharge due to global climate change and climate variability. It is therefore necessary to develop water resources design criteria for river basins in Suriname. It may also be useful to develop early flood/drought warning systems in river basins in order to reduce socio-economic losses and losses of lives.

BIBLIOGRAPHY

Acevedo, M., McGregor, K. et al.,1999. *Relations of climate variability in Venezuela to tropical Pacific SST anomalies*, 10th Symposium on Global Change Studies, America Meteorological Society, preprints, pp. 81-84. Annual Meeting, Dallas, TX.

Ambrizzi, T., de Souza, E. B. and Pulwarty, R. S., 2005. The Hadley and Walker regional circulations and associated ENSO impacts on South American seasonal rainfall, In: *The Hadley Circulation: present, past and future*, Diaz, H.F. and Bradley, R.S. (eds), pp. 203-231. Kluwer Academic Publishers, the Netherlands.

Andersen, J., Refsgaard, J.C., Jensen, K.H., 2001. *Distributed hydrological modelling of the Senegal River Basin – model construction and validation*, pp. 200-214. Journal of Hydrology, 247.

Arnell, N.W., Hudson, D.A. and Jones, R.G. , 2003. *Climate change scenarios from a regional climate model: estimating change in runoff in southern Africa*, Journal of Geophysical Research, Vol. 108, no. D16, 4519.

Arnold, J.G., Srinivasan, R., Muttiah, R.S., Willieam, J.R., 1998. *Large area hydrological modeling and assessment, Part I: Model development*. J. Am. Water Resour. Ass. 34 (1), pp. 73-89.

Bergstrom, S., Forsman, A., 1973. *Development of a conceptual deterministic rainfall-runoff model.* Nord Hydrol. 4, pp. 147-170.

Berlage, H.P., 1957. *Fluctuations of the general atmospheric circulation of more than one year, their nature and prognostisc value*, pp. 152. Koninklijk Nederlands Meteorologisch Instituut, Mededelingen en Verhandelingen 69.

Beven, K., 1989. *Changing ideas in hydrology – the case of physically based models*, pp. 157-172. Journal of Hydrology 105.

Beven, K. J., Kirkby, M.J., 1979. *A physical based variable contributing area model of basin hydrology*. Hydrol. Sci. Bull 24 (1), pp. 43-69.

Beven, K. J., 2000. *Precipitation-runoff modelling*. John Willey and Sons Ltd, England.

Booij, M.J., 2002. *Appropriate modelling of climate change impacts of river flooding*. Ph.D. Thesis, Universiteit Twente, the Netherlands.

Booij, M.J., 2005. *Impact of climate change on river flooding assessed with different spatial model resolutions.* Journal of Hydrology, 303, pp. 176-198.

Bormann, H., 2005. *Regional hydrological modeling in Benin (West Africa): Uncertainty issues versus scenarios of expected future environmental change*, pp. 472-484. Physics and Chemistry of the Earth, 30.

Boorman, D.B. and Sefton, C.E.M., 1997. *Recognizing the uncertainties in the quantification of the effects of climate change on hydrological response*, pp. 415-434. Climate Change 35.

Bronstert, A.Niehoff, D. and Burger, G., 2002. *Effects of climate and land use change on storm runoff generation: present knowledge and modeling capabilities*, pp. 209-529. Hydrol. Process. 16.

Brooks, R.H., Corey, A.T., 1966. *Properties of porous media affecting fluid flow*, J. Irrig. Drain. Amer. Soc. Civil. Eng. IR2, pp. 61-88.

Berlage, H.P., 1957. *Fluctuations of the general atmospheric circulation of more than one year, their nature and prognostic value*, Koninklijk Nederlands Meteorologisch Instituut, Mededelingen en Verhandelingen 69. pp. 152. the Netherlands.

Calver, A., Wood, W.L., 1995. The institute for hydrology distributed model, In: *Computer model of watershed hydrology*, V.P. Singh (ed), Water Resources Publications, Littleton, Colo.

Campling, P., Gobin, Q., Beven, K., Feyen, J., 2002. *Rainfall-runoff modeling of a humid tropical catchment: the TOPMODEL approach*, pp. 231-253. Hydrological Processes, 16, 231-253.

Carr, R., 2000. XLStatistics 5.71. *XLent Works* [http://www.deakin.edu.au/~rodneyc/xlstats.htm], Australia.

Chiew, F.H.S., Whetoon, P.H., McMahon, T.A. and Pittock, A.B., 1995. *Simulation of the impacts of climate change on runoff and soil moisture in Australian catchments*, pp. 121-147, Journal of Hydrology 167.

Chong-Yu-Xu, 1999. *Climate change and hydrologic models: a review of existing gaps and recent research developments*, pp. 369-382. Water Recourses Management 13.

Chong-Yu-Xu, 1992. *Monthly water balance models in different climatic regions* (PhD thesis), pp. 50-53. Vrije Universiteit Brussels, Belgium.

Crawford, N.H., Linsley, R.K., 1966. *Digital simulation in hydrology-Stanford watershed model IV*. Tech.Rep. 39, Standford University, Standford.

Demiraj, E., Mucaj, L, and Bicja, M., 2004. *Climate change and the expected impact in water resources in Albania*, Balwois Conference 2004, Macedonia, 25-29 May 2004.

Dooge, J. and Kuusistito et al., 1998. *Climate and Water – A 1998 Perspective* (The Second International Conference on Climate and Water), pp. 1-16. Finland.

Eagleson, P.S., 1978. *Climate, soil, and vegetation, a simplified model of soil moisture movement in liquid phase*, Water Resour. Res. 14(5), pp. 722-730.

Emanuels, J., 1968. *Klassificatie der seizoenen*, serie 2 no 6, Meteorologische Dienst, pp. 1-14. Ministerie van Bouwwerk, Verkeer en Waterstaat, Suriname.

Fekadu, M., 1999. *Conceptual rainfall-runoff models for different time steps, with special consideration for semi-arid and arid catchments* (PhD thesis), pp. 11-33. Vrije Universiteit Brussels, Belgium.

Feenstra, J. and Short, M., 1996. *Handbook on Methods for Climate Change Impact Assessment and Adaptation Strategies*, Draft Version 3, pp. 1.1-4.36. United Nations Environment Programme (UNDP) and Institute for Environmental Studies, Vrije Universiteit Amsterdam, the Netherlands.

Fung, L. , 1993. *Climate Change in Suriname*, pp. 1-6. Ministry of Public Work, Suriname.

Gable, F. and Aubrey, D., 1990. *Potential Impact of Contemporary Changing Climate on Caribbean Coastlines*, pp. 35-67. Ocean and Shoreline Management 13, England.

Garzoli, Z., Enfield, D., Reverdin G, Mitchum G, Weisberg R, Chang P, Carton J., 1999. COSTA, *Climate observing system for the tropical Atlantic*, Workshop Miami, May 4-7, 1999. Retrieved July 16, 2004 from http://www.aoml.noaa.gov/phod/COSTA/.

Gellens, D. and Roulin, E., 1998. *Stream flow response of Belgian catchments to IPCC climate change scenarios,* pp. 242-258. Journal of Hydrology 210.

Geijskens, D., 1943. *De visserij in het district Nickerie*, pp. 31. Publication of the Surinamese Ministry of Agriculture, Paramaribo, Suriname.

Giorgi, F. and Mearns, L., 1991. *Approaches to the simulation of regional climate change*. A review. pp. 191-216, Rev. Geophys. 29.

Giorgi, F., Hewitson, B., Christensen, J., Hulme, M., Von Storch, H., Whetton, P., Jones, R., Mearns, L. and Fu, C., 2001. Regional Climate Information: Evaluation and Projections (chapter 10), pp. 585-629. In: J.Houghton et al. (Editors), *Climate Change 2001: The Scientific Basis, Contribution of Working I to the Third Assessment Report of the IPCC*, Cambridge U. Press.

Gianninni, A., Kushnir, Y. and Cane, M., 2000. *Interannual variability of Caribbean rainfall, ENSO and the Atlantic Ocean*, pp. 297-311. J. Climate 13.

Glen, B., 2004. *Introduction to climate change*, Inc. Retrieved July 16, 2004 from http://www.climateark.org/vital/intro.asp.

Gleick, P.H., 1986. *Methods for evaluating the regional hydrological impacts of global climatic changes*, pp. 97-116. Journal of Hydrology 88.

Gleick, P.H., 1987. *The development and testing of a water balance model for climate impact assessment: modeling the Sacramento basin*, pp. 1049-1061. Water resources research, vol. 23, no. 6.

Guex, F., 2001. *Modelisation hydrologique dans le basin versant de l'Alzette (Luxembourg), regionalization des parameters d'un modele global*, Travail pratique de Diplome, Ecole Polytecnique Federale de Laussanne 67.

Groen, K.,1998. Hydrogeological investigations in Suriname, In: Wong, T. et al.: *The history of earth sciences in Suriname,* pp.129-174. Kon. Ned. Akad. Wet and Ned. Inst. Toegep. Geowet. TNO.

Groen, K., 2002. *The Effects of Transgressions and Regressions on Coastal and Offshore Groundwater, A case study of Suriname and generic studies into groundwater flow systems, salinity patterns and paleogroundwater* (PhD thesis), pp. 1-191.Vrije Universiteit Amsterdam, the Netherlands.

Haan, C., 1977. *Statistical Methods in Hydrology*, pp. 128-311. The Lowa State University Press, USA.

Helsel, D. and Hirsch, R., 1992. *Statistical methods in water resources*, pp. 208-352. Studies in Environmental Science 49, Elsevier Publication Publishers BV, the Netherlands.

Hirsch, R.M., Helsel, D.R., Cohn, T.A and Gilroy, E.J., 1992. Statistical analyses of hydrological data, In: *Handbook of Hydrology*, Maidment, D. R (Eds), pp. 17.14-17.51. McGrawHill Inc, United States of America.

Hulme, M., Wigley, T.M.L., Barrow, E.M., Raper, S.C.B., Centella, A., Smith, S.J., Chipanshi, A.C., 2000. *Using a Climate Scenario Generator for Vulnerability and AdaptationAssessments: MAGICC and SCENGEN Version 2.4.Workbook*, Climatic Research Unit, Norwich UK.

Hammond, D. and ter Steege, H., 1998. *Propensity for fire in Guianan rainforest*, pp. 944-947. Conservation Biology 12.

Hassel, K. and Miller, J., 1999. *Delaware river water resources and climate change*, pp. 1-9. Rutgers University, New Jersey.

Houben, L. and Molenaar, A., undated. *Rehabilitation of the East-West Road Connection, causes and repair methods of road cracks in recently rehabilitated road stretch and advice on technical specifications for a planned new road* (draft), pp. 1-16. Delft University of Technology, the Netherlands.

IPCC, 2001. *Climate change 2001: The Scientific Basis. Contribution of Working Group I to the Third Assessment Report of the Intergovernmental Panel on Climate Change* (Watson, R., Houghton, J., Ding, Y., Griggs, J., Noguer, M., van der Linden, P., Dai, X. Maskell, K., Johnson, C. (Editors), Cambridge University Press, United Kingdom.

IPCC-TGCIA, 1999. *Guidelines on the Use of Scenario Data for Climate Impact and Adaptation Assessment. Version 1*. Prepared by Carter, T.R., M. Hulme, M. Lal, Intergovernmental Panel on Climate Change, Task Group on Scenarios for Climate Impact Assessment. Technical report.

Intergovernmental Panel on Climate Change (IPCC), 2007. *Climate Change 2007: The Physical Science Basis, Contribution of working group I to the fourth assessment report of the IPCC*, Alley, R., Berntsen, T. et al. (eds). pp. 1-18. IPCC, Switzerland.

IPCC Data Distribution Centre, undated. Retrieved July 16, 2004 from http://ipccddc.cru.uea.ac.uk/cru_data/visualisation/visual_index.html.

IPCC-TGCIA., 1999. *Guidelines on the Use of Scenario Data for Climate Impact and Adaptation Assessment. Version 1*, pp. 1- 69. Prepared by Carter, T.R., M. Hulme, and M. Lal, Intergovernmental Panel on Climate Change, Task Group on Scenarios for Climate Impact Assessment.

IPCC, 2001. *Climate change 2001: The Scientific Basis. Contribution of Working Group I to the Third Assessment Report of the Intergovernmental Panel on Climate Change*, pp. 1-98. (Eds. Watson, R., Houghton, J., Ding, Y., Griggs, J., Noguer, M., van der Linden, P., Dai, X. Maskell, K. and Johnson, C.), Cambridge University Press, United Kingdom.

Jones, J., Changming, L., Ming-Ko, W. and Hsiang-T., 1996. *Regional Hydrological response to Climate Change*, pp. 1-423. The Netherlands.

Jones, R.G., Noguer, M., Hassel, D.C., Hudson, D., Wilson, S.S., Jenkins, G.J. and Mitchell, J.F.B., 2004. *Generating high resolution climate change scenarios using PRECIS*, pp. 1-40. Met Office Hadley Centre, Exeter, UK.

Jones, R.N., Leemans, R., Mearns, L., Nakicenovic, N., Pittock, A., Semenov, S. and Skea J. , 2001. *Developing and applying scenarios* (chapter 3), pp. 147-181. In: Climate Change 2001: The Scientific Basis, Contribution of Working I to the Third Assessment Report of the IPCC (Houghton, J. et al. (eds)), Cambridge U. Press.

Keeling, C. and Whorf, T., 2004. *Atmospheric CO_2 concentrations (ppmv) derived from in situ air samples collected at Mauna Loa Observatory*, Hawaii. Retrieved August 8, 2004 from http://cdiac.esd.ornl.gov/ftp/maunaloa-co2/maunaloa.co2.

Knodt, R., 2003. *MODSTAT software and manual*, Bellingham, USA.

Kundzewicz, Z., 2000. *Coping with hydrological extremes*, pp. 66-75. International Water Resources Association, Water International, vol 25, number 1.

Leavesley, G.H., Lichty, R.W., Troutman, B.M., Saindon, L.G., 1983. *Precipitation-runoff modeling system.* User manual. USGS waterresources investigation report 83-4238, USGS, Denver.

Legesse, D., Vallet-Coulomb, C. and Gasse, F., 2003. *Hydrological response of a catchment to climate and land use changes in Tropical Africa: a case study South Central Ethiopia*, pp. 67-85. Journal of Hydrology, 275.

Lenselink, K. and van der Weert, R., 1970. *Estimating free water evaporation in Suriname*, pp. 70-79. *Surinaamse landbouw*, Suriname.

Lindstrom, G., Johansson, B., Persson, M. Gardelin, M. and Bergstrom, S., 1997. *Development and test of the distributed HBV-96 hydrological model.* J. Hydrol. 201, pp. 272-288.

Liu, Y., 1999. *GIS-based spatially distributed hydrological modeling of the Barebeek catchment*. M.Sc. Thesis, Vrije Universiteit Brussels, Belgium.

Liu, Y.B. and De Smedt, F., 2004. *WetSpa extension, a GIS based hydrologic model for flood prediction and watershed management*. Technical report, Vrije Universiteit Brussels, Belgium.

Liu, Y.B, Gebremeskel, S., De Smedt, F., Hoffman, L and Pfister, L., 2003. *A diffusive approach for flow routing in GIS based food modeling*. pp. 91-106, J. Hydrol, 283.

Liu, Y., 2004. *Development and application of a GIS based hydrological model for flood prediction and watershed management*. Ph.D. Thesis, Vrije Universiteit Brussels, Belgium.

Lozan, J., Grassl, H., Hupfer, P., 1998. *Climate of the 21st Century: Changes and Risks*, pp. 5-448. Germany.

Maidment, D.R., 1992. Hydrology. In: *Handbook of Hydrology*, Maidment, D. R (Eds), pp. 1.1 – 23.1. McGrawHill Inc, United States of America.

Martis, A., van Oldenburg, G.J and Burgers, G., 2002. *Predicting rainfall in the Dutch Caribbean – more than El Nino?*, pp. 1219-1234. Int. J. Climatol. 22.

Mamdouh, S., Oorschot van , H. and De Lange, S., 1993. *Statistical Analysis in Water Resources Engineering,* pp. 1-390. Rotterdam, the Netherlands.

Marshall, J., Kushnir, Y., Battisti, D., Change, P., Czaja, A., Dickson, R., Hurrel, J., McCartney, M., Saravanan, R. and Visbeck, M., 2001. *North Atlantic Climate Variability: phenomena, impacts and mechanism,* pp. 1863-1898. Int. J. Climatol. 21.

Mastny, L., 2000. *Melting of Earth's ice cover reaches new high*. Retrieved August 8, 2004 from http://www.anti-corporate.com/meltingice.htm.

McCuen, R., 2003. *Modeling Hydrologic Change*, pp. 135-288. Lewis Publishers CRC Press LLC, USA.

McMichael, A., Haines, A., Epstein, P.R., 1996. *Climate Change and Human Health*, pp. 1-40; 123-174. WMO/WHO/UNEP, London.

McPhaden, M., 2004. *Evolution of the 2002/03 El Nino*, pp. 677-695. Bulletin of the American Meteorological Society, vol 85, nr 5.

Mearns, L.O., 1999. *Comparison of climate change scenarios generated from regional climate model experiments and statistical downscaling*. pp. 6603-21, J.Geophys. Res.104.

Mearns, L.O., Giorgi, F., Whetton, P., Pabon, D., Hulme, M. and Lal, M., 2003. *Guidelines for use of climate scenarios developed from regional climate model experiments*, DDC of IPCC TGCIA (final version), pp. 1-38.

Mearns, L., Hulme, M, Carter, T., Leemans, R., Lal, M., Whetton, P., Hay, L., Jones, R., Katz, R., Kittel, T., Smith, J. and Wilby, R., 2001. Climate scenario development (chapter 13), pp. 585-629. In: *Climate Change 2001: The Scientific Basis, Contribution of Working I to the Third Assessment Report of the IPCC* (Houghton, J. et al. (eds)), Cambridge U. Press.

Meehl, G.A., W.M. Washington, C.A. Ammann, J.M. Arblaster, T.M.L. Wigleym and C. Tebaldi., 2004. *Combinations of Natural and Anthropogenic Forcings in Twentieth-Century Climate,* pp. 3721-3727. Journal of Climate 17.

Menzel, L. and Burger, G., 2002. *Climate change scenarios and runoff response in the Mulde catchment* (Southern Elbe, Germany), pp. 53-64. Journal of Hydrology, 267.

Met Office-The Hadley Centre, 2003. Retrieved 16-07-2004 from http://www.metoffice.com/research/hadleycentre/models/modeldata/HadCM2_IS92a_map_SL_ann_19601990_20702100.gif.

Mesquita, A., 2000. *Sea level variations along the Brazilian coast: a short review*. Brazilian Symposium on sandy beaches, pp. 15.

Miller, W.A., Cunge, J.A., 1975. Simplified equations of unsteady flow, In: *Unsteady flow in open channels*, Mahmood, K. and Yevjevich, V. (ed). Water Resources Publications, Fort Collins, CO.

Mimikou, M.A., Baltas, E., Varanou, E. and Pantazis, K., 2000. *Regional Impacts of Climate Change on Water Resources quantity and quality indicator*, pp. 95-109. Journal of Hydrology 234.

Molicova, H., Grimaldi, M.m Bonell, M., Hubert, P., 1997. *Using topmodel towards identifying and modeling the hydrological patterns within a headwater, humid, tropical catchment*, pp. 1169-1196. Hydrological Processes, 11.

Mol, J., Resida, D., Ramlal, J. and Becker, C., 2000. *Effects of El Niño-related drought on freshwater and brackish water fishes in Suriname, South America*, pp. 429-440. Environmental Biology of Fishes 59, Kluwer Academic Publishers, the Netherlands.

Naipal, S. and Amatali, M., 1999 (a). *Project Country Study Climate Change Suriname Water Resources* (Technical report 4), pp. 4-76. Ministry of Public Works, Suriname and Institute for Environmental Studies, Netherlands.

Naipal, S. and Amatali, M., 1999 (b). *Project Country Study Climate Change Suriname and First Steps Towards Coastal Zone Management*, pp. 4-83. Ministry of Public Works, Suriname and Institute for Environmental Studies, Netherlands.

National Institute for Environment and Development, 2005. *First National Communication to the United Nations Framework Convention on Climate Change*, NIMOS, pp. 34-44.

National Oceanic and Atmospheric Administration (NOAA), undated*, PFEL Climate and Marine Fisheries.* Retrieved July 16 2004 from http://www.pfel.noaa.gov/research/climatemarine/cmfclimate/cmfcc5.html.

Nash, L.L. and Gleick, P.H., 1991. *Sensitivity of stream flow in the Colorado basin to climatic changes*, pp. 221-241. Journal of Hydrology, 125.

Nash, J.E., Sutcliffe, J.V., 1970. *River flow forecasting through conceptual model*, J.Hydrol. 10, pp. 282-290.

Nemec, J. and Schaake, J., 1982. *Sensitivity of water resources systems to climate variation*, pp. 327-343. Hydrological Sciences Journal, 27.

NEAA – Netherlands Environmental Assessment Agency, 2007. *Hyde 1700-2000*. Retrieved August 8, 2004 from www.mnp.nl/hyde/.

Niemanm J., Strzepek, K., Yates, D., 1994. *Impacts of spatial and temporal data on a climate change assessment of Blue river Nile*, WP 94-44, IIASA, Laxenburg, Austria.

NOAA-CIRES Climate Diagnostics Center, 2004. *Climate Indices: Monthly Atmospheric and Ocean Time Series*. Retrieved August 7, 2004 from http://www.cdc.noaa.gov/ClimateIndices/

Null, J., 2003. *El Niño and La Niña Years: A consensus list*. Retrieved August 8, 2004 from http://ggweather.com/enso/years/htm.

Nurmohamed, R., 1998. *Een methode voor systematisch onderzoek naar het micro-miniwaterkracht potentieel in het binnenland van Suriname*. (B.Sc. Thesis), Faculteit der Technologische Wetenschappen, Universiteit van Suriname, Suriname.

Nurmohamed, R., 2002. *The Impact of Climate Change on the Rainfall Distribution in Suriname*, in 5th International Inter-Guianas Conference on "Building Capacity to Meet the Emerging Challenges in the Guianas", Georgetown, Guyana, October, 23 - 25, 2002 (*in publ*).

Nurmohamed, R. and Naipal, S., 2004. *Trends and Variation in Monthly Rainfall and Temperature in Suriname,* in Proceedings BALWOIS Conference on Water Observation and Information System for Decision Support, pp. 3. Ohrid, FY Republic of Macedonia , 25-29 May 2000.

Obasi, G., 1999. *The 1997-1998 EL Niño event: a Scientific and Technical Retrospective*, pp. 1-96. WMO/UNECSO/UNEP/ICSU, Switzerland.

Perrin, C., Michel, C. and Andreassian, V., 2001. *Does a large number of parameters enhance model performance? Comparative assessment of common catchment model structures on 429 catchments*, pp. 275-301. Journal of Hydrology, 242.

Polsbroek, A., 2004. *"… en Suriname loopt onder water." So what?",* De Ware Tijd, Compas, 9th volume, No 34, 28 August 2004. Suriname.

Post, V., 1996. *Modeling of the paleo hydrologic situation in the coastal plain of Suriname*, pp. 1-53.Vrije Universiteit Amsterdam, the Netherlands.

Rajagopolan, B., Kushir, Y., Tourre, Y and Cane, M. (1997). *Temporal Variability of North Atlantic Oscillation and Tropical Atlantic SST*, Lamont-Doherty Earth Observatory of Columbia University, New York.

Rasmussen, E.M., Dickinson, R.E., Kutzbach, J.E. and Cleaveland, M.K., 1992. Climatology, pp.2.1-2.33. In: *Handbook of Hydrology*, Maidment, D. R (Eds), McGrawHill Inc, United States of America.

Rasmussen, J. and Wallace, J., 1983. *Meteorological aspects of the 1982-83 El Niño/Southern Oscillation Episode,* pp. 104-127. Science, 222.

Rientjes, T.H.M. and Boekelman, R.H., 1998. *Hydrological models (CThe 443),* pp. 1-63, TUDelft, the Netherlands.

Robock, A., Turco, R.P., Harwell, M.A., Ackerman, T.P., Andressen, R., Chang, H.S., Sivakumar, V.K., 1993. *Use of general circulation model output in the creation of climate change scenarios for impact analyses*, Climate Change 23, pp. 293-335.

Robertson, A and Mechoso, C., 2002. *Links between the American Ocean and the South American Climate Variability*, CLIVAR Exchanges No 25.

Ropelewski, C.F. and Halpert, M.S., 1987. *Global and regional precipitation patterns associated with the El Niño/Southern Oscillation*, pp. 1606-1626. Mon. Wea. Rev, 115.

Ropelewski, C.F. and Halpert, M.S., 1989. *Precipitation patterns associated with the high index phase of the Southern Oscillation*, pp. 268-284. J. Climate, 2.

Ropelewski, C.F. and Halpert, M.S., 1996. *Quantifying Southern Oscillation-precipitation relationships,* pp. 1043-1059. J. Climate, 9.

Ross, T. and Lott, N., 2000. *A climatology of recent extreme weather and climate events, Technical Report No 2000-02*, National Climatic Data Center, Asheville, USA.

Ross, T. and Lott, N., 2004. *Worldwide Weather and Climate Events*. Retrieved August 8, 2004 from http://www.ncdc.noaa.gov/oa/reports/weather-events.html

Salas, J.D., 1992. Analyses and modelling of hydrological time series. In: *Handbook of Hydrology*, Maidment, D. R (Eds), pp. 19.119.20. McGrawHill Inc, United States of America.

Santer, B.D., Wigley, T.M.L., Schlesinger, M.E. and Mitchell, J.F.B., 1990. *Developing Climate Scenarios from Equilibrium GCM Results.* pp. 29, Max-Planck-Institut für Meteorologie Report No. 47, Hamburg, Germany.

Seifu, G., 2003. *Modeling the effect of climate and land-use changes on the hydrological processes: an integrated GIS and distributed modeling approach*. Ph.D. Thesis, Vrije Universiteit Brussels, Belgium.

Solomon, S., Beran, M. and Hogg, W., 1987. *The influence of climate change and climate variability on the hydrological regime and water resources*, pp. 1-619, IAHS Publ. 168, IAHS Press, Oxfordshine, UK.

SPS/OAS, 1988. *Suriname Planatlas*, National Planning Office of Suriname and Organization of American States, Washington D.C.

Stipanek, P., 2003. *AnClim v4.6.23 – Software for time series analysis*, Dept. of Geography, Fac. of Natural Sciences, MU, Brno. 1.47MB

Tamara, S. L., Sundquist, E. T., Schwartz, S. E., Hall, D.K., Fellows, J.D. and Killeen, T.L., 1999. *Climate Change and Greenhouse Gases*, pp. 453-463. America Geophysical Union, EOS vol 80, no 39.

Tans, P., 2007. *NOAA/ESRL*. Retrieved March 27, 2007 from www.esrl.noaa.gov/gmd/ccgg/trends.

Turner, J., 2004. *The El Niño-Southern Oscillation and Antarctica*, pp. 1-31. Int. J. of Climate, 24.

Van de Berg, M., 1997. *Grondwaterbeheersing van de A-zand aquifer* (BSc thesis), pp. 1-56. Universiteit van Suriname.

Van der Pol, H., 2002. *Geohydrologisch onderzoek in Moengo en Wonoredjo, Suriname,* (stageverslag), pp. 1-28. Vrije Universiteit Amsterdam, the Netherlands.

Van Doorn, A., 2002. *Geohydrologische studie van Nieuw-Nickerie mbt het ontwerp van een nieuwe drinkwaterplaats* (stageverslag), pp. 1-25. Vrije Universiteit Amsterdam, the Netherlands.

Verhoog, F., 1987. Impact of climate change on the morphology of river basins, pp. 315-326. In: Solomon, S., Beram, M. et al., *The influence of Climate Change and Climate Variability on the Hydrological regime and Water Resources*, IAHS publications, No 168, Washington, USA.

Villwock, A., 1998. *Clivar Initial Implementation Plan*. Retrieved March 27, 2004 from www.clivar.com/publications/othre_pubs/iplan/iip/pd2.htm.

Wallace, J., Vogel, S. et al., 1994. *Impacts of El Niño and benefits of El Niño Prediction*. Retrieved July 16, 2004 from http://www.pmel.noaa.gov/tao/elnino/report/el-nino-report.html, National Oceanic and Atmospheric Administration (NOAA).

Wang, C., 2001. *Atlantic climate variability and its associated atmospheric circulation cells*, pp. 1516-1536. Int. J. of Climate 15.

Wang, C., 2005. ENSO, Atlantic climate variability, and the Walker and Hadley circulations, In: *The Hadley Circulation: present, past and future*, Diaz, H.F. and Bradley, R.S. (eds), pp. 173-202. Kluwer Academic Publishers, the Netherlands.

Watson, R., Zinyowera, M et al., undated. *IPCC Special Report on The Regional Impacts of Climate Change, An Assessment of Vulnerability*. Retrieved July 16, 2004 from http://www.grida.no/climate/ipcc/regional/500.htm.

Webster, P. J., 2005. The elementary Hadley circulation, In: *The Hadley Circulation: present, past and future,* Diaz, H.F. and Bradley, R.S. (eds), pp. 9-60. Kluwer Academic Publishers, The Netherlands.

Webster, T. and Roebuck, L., 2001. *Water Resources Assessment of Suriname*, pp. 1-50. US Army Corps of Engineers, United States.

Wigley, T., 2003. *MAGICC/SCENGEN 4.1 Software and manual*, pp. 1-24. NCAR, Boulder, CO, USA.

Wilby, R. and Dawson, C., 2001. *Using SDSM - A decision support tool for the assessment of regional climate change impacts*. pp.1-64, Department of Geography, King's College London, Strand, UK.

Wittenberg, H., Sivapalan, M., 1999. *Watershed groundwater balance estimation using stream flow recession analysis and base flow separation*, J. Hydrol 219, pp. 20-33.

WMO/UNESCO, 1997. *Water Resources Assessment – Handbook for Review of National Capabilities.* pp. 1-113, United States of America.

WMO/UNDP/Gov of Suriname, 1972. *Public Water Supplies and Sewerage Project – Water Resources – Vol. III (hydrogeological and hydrological studies),* pp. 1-112. New York.

WMO, 2001. *WMO statement of the status of the global climate in 2000, WMO-no.920*, World Meteorological Organization, Switzerland.

World Meteorological Organization WMO, 1988. *Analyzing long time series of hydrological data with respect to climate variability,* (WCAP-3), pp. 1-12.

Whetton, P.H., Fowler, A.M., Haycock, M.R. and Pittock, A.B.,1993. *Implications of climate change due to enhanced greenhouse effect on floods and droughts in Australia*, Clim. Change 25, 289.

USACE, 1998. *HEC-1 Flood Hydrograph Package: user's manual*, US Army Corps of Engineers, Davis, CA.

Yates, D., 1994. *WatBal – An integrated water balance model for climate impact assessment of river basin runoff*, WP-94-64, pp. 1-28. IIASA, Austria.

Yusoff, I., Hiscock, K. et al., 2000. *Simulation of the impacts of climate change on groundwater resources in eastern England*, pp. 319-338. Special Publication 193-Geological Society, London.